

**TUMOUR IMMUNE MICROENVIRONMENT,
GENOMEWIDE COPY NUMBER ABERRATIONS AND
THEIR INTERACTIONS IN MALIGNANT PLEURAL
MESOTHELIOMA**

Bibhusal Thapa

ORCID ID: 0000-0003-0978-6671

Submitted in total fulfilment of the requirements of

the degree of

Doctor of Philosophy

October 2017

Olivia Newton-John Cancer Research Institute

And

Department of Medicine, Austin Health

The University of Melbourne,

Melbourne, Australia.

Produced on archival quality paper

Abstract:

Malignant pleural mesothelioma (MPM) is a rare but deadly malignancy. Despite predictions, worldwide incidences have not significantly diminished and available therapeutic modalities have failed to improve outcomes. There are some indications that immune based therapies and targeted therapies may hold promise but suitable phenotypes have been hard to identify. This thesis describes investigations we conducted into the tumour immune microenvironment, the copy number aberrations (CNAs) and the interaction between the two in MPM.

The findings presented in this thesis elucidate the complexity of the tumour immune microenvironment in MPM. We establish MPM to be immunogenic but also demonstrate that the immune characteristics vary amongst tumours mostly with tumour histological subtype. We reveal sarcomatoid MPMs to be associated with high lymphocytic infiltration but also greater expression of immune checkpoint receptors and their ligands. In addition, we also exhibit the prognostic implications associated with some of these markers.

The genome wide copy number analyses described in this thesis disclose that although copy number aberrations are the commoner of genomic alterations in MPM, their extent and pattern vary amongst tumours. We describe their clinical and pathological associations. We confirm most previously described prominent CNAs but more importantly uncover new ones which may be important in MPM prognostication and therapeutics. We find that greater degree of genomic instability confers a worse prognosis in MPM independent of histology but neither degree of genomic instability nor any specific CNA correlates with the immunological milieu.

Our findings contribute towards the understanding and development of potential prognostic and predictive markers for immunotherapy in MPM. Further, they also reveal potential targets for development of targeted therapies in this disease where none was thought feasible.

Declaration

This is to certify that

i. The thesis comprises only my original work towards the PhD except where indicated in the Preface

ii. Due acknowledgement has been made in the text to all other materials used

iii. The thesis is fewer than 100,000 words in length, exclusive of tables, bibliography and appendices

Bibhusal Thapa

Preface

Dr. Paul Boutros and colleagues (Ontario institute of cancer research) performed the statistical analysis described in chapters 3 and 5. Statistical help was also received from Dr. Danny Liew (Monash Health) for statistical analysis described in chapter 4.

The OncoScan assay was performed in part at the Ramaciotti centre for Genomics, University of New South Wales, under Dr. Helen Speirs and in part at the Ontario Institute for Cancer Research under Dr. Paul Boutros and team. The analysis of the data obtained was done by Dr. Boutros and Adriana Salcedo.

Dr. Carmel Murone and Marzena Walkiewicz assisted with initial training for construction of tissue microarrays and immunohistochemistry. I was responsible for the completion of TMA construction, immunohistochemical staining and subsequent analysis.

Acknowledgements

The list of people I need to express gratitude towards is long and it reflects the phenomenal amount of help and support I have received throughout my PhD candidature. First and foremost I would like to express my deepest gratitude towards my supervisors Dr. Thomas John and Professor. D Neil Watkins. Thank you for believing in me and providing this wonderful opportunity for me to work with you in this project which I know is very close to your hearts. I cannot thank Tom enough for investing so much of his time, energy and thoughts to guide, help and correct me. Thank you for making the whole process challenging yet stress free. Thank you for patiently listening through my many flights of ideas, correcting some and allowing me to trial and work on many. I will always endeavour to inculcate in myself your calm demeanour and thoughtful ways.

I am deeply indebted by Marzena for all she has so selflessly done to help and guide me throughout my PhD. Thank you for teaching me so unwearingly almost everything that I have learned to do in the lab in the past 3 years. A huge thankyou to Dr. Carmel Murone and team from the Austin chapter of the Victorian Cancer Bio-bank for assisting me in retrieval of the archival and fresh tissue samples and the construction of the tissue microarrays. My gratitude to Richard Young from the Peter Mac Cancer Centre for going out of the way to teach me FISH and allowing me to conduct all of my FISH experiments in his lab. I must also acknowledge the significant help I received from Peter Lock from the La Trobe University, my co-PhD students Miles Andrews, Prashanth Prithviraj, Simon Tsao and everyone in the Cancer Immunobiology lab.

It would have been very difficult to conceive of this large scale study in Mesothelioma had it not been for the meticulous data-keeping of Mr Simon Knight over the past three decades. Thank you Simon for providing the platform I could build on. I must also acknowledge the constant help and encouragement I received from him and Mr Stephen Barnett throughout my PhD. Dr. Prudence Russell from the Department of anatomical pathology, St. Vincent's hospital and Dr. Khashyar Asadi

from the Department of anatomical pathology, Austin hospital deserve special mention. I received a lot of support and guidance from them during my work involving immunohistochemistry and FISH.

This work and the resulting thesis would not have been possible without the continued help, support and encouragement of my family. For this I shall be forever be indebted towards my parents, my wife Hosim and daughter Imani. Thank you for all your assistance and understanding.

I cannot possibly finish without expressing my deepest gratitude towards the patients whose tissues and clinical data were used during this work.

Publications

- 1) **Thapa B**, Walkiewicz M, Murone C, Asadi K, Deb S, Barnett S, Knight S, Mitchell P, Liew D, Watkins DN, John T. Calretinin but not caveolin-1 correlates with tumour histology and survival in malignant mesothelioma. *Pathology*. 2016;48(7):660-665. doi:10.1016/j.pathol.2016.08.003.
- 2) **Thapa B**, Watkins DN, John T. Immunotherapy for malignant mesothelioma: reality check. *Expert Rev Anticancer Ther*. 2016;Oct:1-10,1167-76 doi: 10.1080/14737140.2016.1241149
- 3) **Thapa B**, Salcedo A, Lin X, Walkiewicz M, Murone C, Ameratunga M, Asadi K, Deb S, Barnett SA, Knight S, Mitchell P, Watkins DN, Boutros PC, John T. The Immune Microenvironment, Genome-wide Copy Number Aberrations, and Survival in Mesothelioma. *J Thorac Oncol*. 2017;28:pii: S1556-0864(17)30124-7. doi:10.1016/j.jtho.2017.02.013.
- 4) John T, Russell P A., **Thapa B**. Is Mesothelioma in China Rare or Misdiagnosed? *J Thorac Oncol*. 2017;12(4):607-609. doi:10.1016/j.jtho.2017.02.004.
- 5) Do H, Cameron D, Molania R, **Thapa B**, Rivalland G, Mitchell PL, Murone C, John T, Papenfuss A, Dobrovic A. Digital PCR of Genomic Rearrangements for Monitoring Circulating Tumour DNA. *Adv Exp Med Biol*. 2016;(924):139-146.

Conference proceedings:

- 1 “Correlation of PD-L1 expression with tumour infiltrating lymphocytes, genome wide copy number aberrations and survival in mesothelioma” at the meeting of American Society of Clinical Oncologists (June 2016). Poster discussion. **Awarded Merit award.**
- 2 “PD-L1 expression in Mesothelioma and its correlation with genome wide copy number aberrations and survival” in the Australian Lung Cancer Conference (Aug 2016). Oral presentation. **Awarded travel grant.**

- 3 “Genome-wide copy number aberrations in mesothelioma and its correlation with tumour microenvironment including PD-L1 expression.” Poster. Presented at the world lung cancer conference (Dec 2016).
- 4 “VATS Sub-lobar Anatomical Pulmonary Resections: Indications and Outcomes in Thoracic Oncological Practice.” Poster. Presented at the world lung cancer conference (Dec 2016).
- 5 “Association of ¹⁸Fluorodeoxyglucose (FDG) PET, Complete Pathological Response and Overall Survival in Patients with Pancoast Tumours Treated with Trimodality Therapy” Poster. Presented at world lung cancer conference (Dec 2016).
- 6 “Immune microenvironment in mesothelioma: looking beyond PD-L1.” Presented at the meeting of the American Society of Clinical Oncologists (June 2017). Poster discussion.
Awarded Merit award.

Contents

Abstract:	i
Declaration	ii
Preface	iii
Acknowledgements	iv
Publications	vi
Conference proceedings:	vi
List of figures	xvi
List of tables	xviii
Chapter 1: Introduction	1
1.1 History of asbestos use and discovery of asbestos related health problems	1
1.2 Mesothelioma epidemiology	3
1.3 Pathogenesis of mesothelioma	5
1.4 Genetic abnormalities in mesothelioma	7
1.4.1 Mutations in mesothelioma:	7
1.4.2 Structural variations in MPM genome	11
1.4.3 Pathways affected by genomic change in MPM	13
1.5 Clinico-pathological features of MPM	17
1.5.1 Clinical features and presentation of MPM	17
1.5.2 Diagnosis of MPM.....	17
1.5.2 Histological classification of MPM	21
1.6 Staging of MPM	22

1.7 Prognosis of MPM	24
1.8 Treatment of MPM	26
1.8.1. Surgery.....	26
1.8.2. Radiotherapy.....	28
1.8.3 Chemotherapy.....	29
1.8.4 Targeted therapy.....	29
1.8.5 Immunotherapy	36
1.9 Conclusion	45
Chapter 2: Materials and methods.....	47
2.1 Generation of the MPM cohort	47
2.2 Collection of clinical data: clinical annotation of the cohort.....	47
2.3 Collection of archival formalin fixed paraffin embedded (FFPE) MPM samples	48
2.4 Confirmation of diagnosis of MPM	48
2.5 Construction of the MPM tissue microarray (TMA)	49
2.6 Immunohistochemistry and pathological evaluation.....	51
2.6.1 Deparaffinization and rehydration	51
2.6.2 Antigen retrieval	51
2.6.3 Incubation.....	52
2.6.4 Visualization.....	52
2.7 MPM cell lines used in this study	53
2.8 Preparation of cell block from MPM cell lines	53
2.9 Extraction of genomic DNA from FFPE samples.....	53

2.10 Quantification and quality check of extracted DNA.....	54
2.11 Fluorescent in situ hybridization (FISH)	55
2.11.1 Preparation and depaffinization.....	55
2.11.2 Target retrieval	55
2.11.3 Probe hybridization	56
2.11.4 Stringent washes.....	56
2.11.5 Visualization	57
2.11.6 Assessment	57
2.12 Copy number analysis.....	57
2.12.1 OncoScan FFPE assay	57
2.12.2 Processing of copy number data.....	62
2.12.3 Test of correlation with clinical covariates	63
2.13 Statistical analysis.....	63
 Chapter 3: Clinical and pathological characteristics of MPM patients operated at the Austin Hospital.....	 64
3.1 Introduction	64
3.2 Aims	65
3.3 Methods	65
3.4 Results	65
3.4.1 Demographic characteristics of the MPM cohort	65
3.4.2 Diagnosis – modalities and histology.....	66
3.4.3 Surgical procedures performed on the cohort	67

3.5.4 Post-operative treatment received by the cohort	67
3.4.5 Changing pattern of MPM treatment at the Austin hospital	67
3.4.6 Treatment outcomes of patients with MPM treated in Austin hospital between 1988 and 2014	68
3.4.7 Relationship between clinicopathological covariates and patient survival.....	70
3.5 Summary and discussion.....	72
 Chapter 4: Caveolin-1: A novel immunohistochemical marker of mesothelioma and its correlation with clinicopathological parameters.....	 75
4.1 Introduction	75
4.1.1 Calretinin and its expression in MPM	76
4.1.2 Caveolin-1: a potential novel marker in mesothelioma.....	76
4.1.3 Expression of calretinin and caveolin-1 in MPM and association with tumour histology and differentiation.....	76
4.2 Aims	78
4.3 Specific methods	78
4.3.1 Immunohistochemistry for calretinin and caveolin-1 in MPM and lung adenocarcinoma	78
4.3.2 Statistical analysis	79
4.4 Results	79
4.4.1 Expression of calretinin and caveolin-1 and relationship with tumour histology.	79
4.4.2 Correlation between expression of calretinin and caveolin-1	81
4.4.3 Correlation of calretinin and caveolin-1 with clinicopathological parameters	81
4.4.4 Caveolin-1 expression in lung adenocarcinoma.....	81

4.4.5 Association of expression of calretinin and caveolin-1 with survival	81
4.5 Discussion.....	83
Chapter 5: Immune microenvironment in MPM – identifying the “inflamed phenotype”	
.....	87
5.1 Introduction	87
5.1.1 Inflammation in MPM – basis for suitability for immunotherapy.....	88
5.1.2 The search for predictive biomarkers – study of the tumour immune microenvironment.....	89
5.1.3 PD-L1 expression in MPM – prognostic implications and predictive ability	91
5.1.4 Assessment of Tumour infiltrating lymphocytes (TILs) in MPM	92
5.2 Aims	93
5.3 Specific methods	94
5.3.1 Immunohistochemistry	94
5.3.2 Statistical analysis	96
5.4 Results	96
5.4.1 PD-L1 expression	96
5.4.2 Infiltration with CD4+, CD8+ and FOXP3+ lymphocytes in MPM and their correlations	97
5.4.3 Temporal variations in PD-L1 expression and CD8+ infiltration.....	100
5.4.4 Prognostic implications of immune based markers	101
5.5 Discussion.....	102
Chapter 6: Looking beyond PD-L1 in MPM -defining the hot, the warm and the cold tumours.....	106

6.1 Introduction	106
6.1.1 Programmed cell death receptor ligand -2 (PD-L2)	107
6.1.2 T-cell immunoglobulin and mucin-domain containing-3 (TIM-3)	108
6.1.3 Lymphocyte activation gene -3 (LAG-3)	110
6.1.4 Toll-like receptor-3 (TLR-3)	111
6.1.5 Assessment of tumour infiltrating lymphocytes (TILs)	112
6.1.6 Tertiary lymphoid structures (TLS).....	112
6.2 Aims	114
6.3 Specific methods	114
6.3.1 Immunohistochemistry	115
6.3.2 Assessment of TILs and TLS in MPM.....	117
6.4 Results	117
6.4.1 PD-L2 expression	117
6.4.2 TIM3 expression in MPM.....	118
6.4.3 LAG3 expression in MPM.....	119
6.4.4 TILs and TLS	119
6.4.5 TLR3 expression	119
6.4.6 Survival analysis	121
6.4.7 Development of Immune checkpoint score (ICS)	122
6.4.8 Comparing the immunological milieu in MPM and NSCLC	125
6.5 Discussion.....	127

Chapter 7: Genome-wide copy number aberrations in MPM, correlation with tumour histology, immune characteristics and patient survival.	132
7.1 Introduction	132
7.2. Aims and objectives	134
7.3 Specific methods	134
7.4 Results	137
7.4.1 Percent genome alteration (PGA)	137
7.4.2 Relationship of age of the sample to copy number aberrations.....	140
7.4.3 PGA, tumour histology and clinical covariates	141
7.4.4 PGA and OS	142
7.4.5 PGA and immune characteristics of the tumour.....	144
7.4.6 Copy number profile and consensus clustering	145
7.4.7 Relationship of copy number profile with tumour histology.....	149
7.4.8 Relationship of copy number profile with survival	153
7.4.9 Correlation of individual CNAs with PD-L1 expression status.....	155
7.5 Discussion:	156
Chapter 8: Investigating common CNAs in MPM and validation of the ONCOSCAN data	168
8.1 Introduction	168
8.1 Commonly altered genes in MPM	169
8.1.1 Cyclin-dependent kinase inhibitor 2A (<i>CDKN2A</i>)/alternative reading frame (ARF) gene.....	169
8.1.2 Neurofibromatosis 2 (<i>NF2</i>)	170

8.1.3 <i>BRCA1</i> -associated protein 1 (BAP1)	170
8.2 Aims	171
8.3 Specific methods.....	171
8.3.1 IHC for BAP1, <i>CDKN2A</i> and NF2	171
8.3.2 FISH analysis for <i>CDKN2A</i> and <i>CDK6</i>	173
8.4 Results	174
8.4.1 BAP1 IHC.....	174
8.4.2 <i>CDKN2A</i> (p16) IHC.....	174
8.4.3 NF2 IHC.....	174
8.4.4 FISH assessment of <i>CDKN2A</i>	175
8.4.5 FISH assessment of <i>CDK6</i>	177
8.4.6 Relationship between status of <i>CDKN2A</i> and <i>CDK6</i>	178
8.4.7 Survival analysis	178
8.5 Discussion.....	181
Chapter 9: General discussion, limitations and future directions.....	187
9.1 Limitations	191
9.2 Future directions	192
References:	196

List of figures

Figure 1.1: Age standardised incidence of mesothelioma in the world.	3
Figure 1.2: Age standardised incidence rates of mesothelioma in Australia 1982-2015.	4
Figure 1.3: Age standardised mortality rate of mesothelioma in Australia 1997-2015.	5
Figure 1.4: Possible mechanisms of asbestos-induced carcinogenesis.	7
Figure 2.1: Flowchart of collection of mesothelioma cohort to TMA construction	50
2.6 Immunohistochemistry and pathological evaluation	51
Figure 2.2: The Molecular Inversion Probe: Target generation and hybridization procedures.....	61
Figure 3.1: Overall survival of the Austin MPM cohort.....	69
Figure 4.1: Representative pictures of the IHC: expression of calretinin and caveolin-1 in MPM.	81
Figure 4.2: Correlation between calretinin and caveolin-1 H scores and association with survival.	82
Figure 5.1: Representative pictures of the IHC for PD-L1 in MPM	97
Figure 5.2: IHC evaluation of CD4+, CD8+ and FOXP3+ lymphocytes in MPM.....	98
Figure 5.3: Temporal changes in PD-L1 and CD8+lymphocyte infiltration. Changes in PD-L1 status and CD8+ infiltration status between first and second biopsies.	100
Figure 6.1: Representative pictures of PD-L2 staining in MPM.....	118
Figure 6.2: TLR3 expression in different MPM histotypes.	120
Figure 6.3: Representative pictures of IHC for TIM3, LAG3 and TLR	121
Figure 6.4: Univariate survival analysis.	124
Figure 7.1: Comparison of the structural aberrations in the test and validation cohorts.....	137
Figure 7.2: Sample age and its effect on PGA and copy number changes	141
Figure 7.3: Correlation of PGA with different clinicopathological covariates.	142
Figure 7.4: Prognostic implication of PGA in MPM.....	143
Figure 7.5: Relationship between PGA and PD-L1 expression by tumour	144
Figure 7.6: Correlation of PGA with other immunological characteristics of the tumour	145
Figure 7.7: Consensus clustering based on copy number profile.	149
Figure 7.8: Copy Number profile of different histological subtypes of MPM.	150
Figure 7.9: Absolute CNA counts and its relation with tumour histology and survival	151
Figure 7.10: Differences in CNA frequency between different MPM histotypes.....	152

Figure 7.11: Effect of cluster membership and individual CNAs on survival	153
Figure 7.12: Analysis of effect of commonly described MPM related genes and top GISTIC related genes with survival.....	154
Figure 7.13: Individual CNAs and PD-L1 status of tumours.....	155
Figure 8.1: Representative pictures of the IHC assessment of BAP1, CDKN2A and NF2	175
Figure 8.2: Representative pictures of the FISH for CDKN2A.	176
Figure 8.3: Representative pictures from the FISH analysis for CDK6.	177
Figure 8.4: Prognostic significance of BAP1, CDKN2A and CDK6.....	179
Figure 8.5: Prognostic implications of CDK6 and CDKN2A CNAs.	180
Figure 8.6: Heavy infiltration of MPM and high cellularity a potential source of errors in FISH analysis.....	183
Figure 8.7: Extent and position of amplifications seen in 7q21.2 in our samples.....	184

List of tables

Table 1.1: Immunohistochemistry based markers useful in diagnosis of MPM	19
Table 1.2: TNM staging of Mesothelioma.	22
Table 3.1: Demographic and clinical parameters of the MPM cohort.....	66
Table 3.2: Treatment received by MPM patients at the Austin Hospital.	68
Table 3.3: Prognostic implications of demographic, clinical and pathological features in the MPM cohort (Univariate analysis).....	70
Table 3.4: Multivariate analysis of overall survival	71
Table 4.1: H scores of calretinin and caveolin-1 according to histology.....	80
Table 5.1: IHC methods for some immune markers in MPM	95
Table 5.2: PD-L1 expression in MPM and its clinicopathological correlation	99
Table 5.3: Multivariate analysis for overall survival.....	102
Table 6.1: Methodology of the IHC assays used in chapter 6.....	115
Table 6.2: Multivariate analysis for OS.....	122
Table 6.3: Immune checkpoint score composition.	123
Table 6.4: ICS and its relationship with other immune parameters, histology and survival.....	125
Table 6.5: Comparison of the expression of some checkpoint receptors and ligands in NSCLC and MPM	126
Table 7.1: QC results of individual samples.	134
Table 7.2: Genome wide copy number status of individual samples.	138
Table 7.3: Chromosomal regions with highest percentage of loss/gains	146
Table 7.4: Genes with greatest frequencies of CNAs in our cohort.....	146
Table 7.5: Top 20 genes with greatest frequency of deletions.	147
Table 7.6: Top 20 genes with greatest frequency of gains.	147
Table 7.7: Copy number status of some commonly described MPM associated genes.	148
Table 7.8: Genes with marginally significant differences in CNA frequency among tumour subtypes.	152
Table 7.9: Common copy number aberrations described in previous studies.....	159
Table 8.1: Brief description of the IHC used in this chapter	172
Table 8.2: Brief description of methodology of FISH for CDKN2A and CDK6.....	173
Table 8.3: Status of CDKN2A in our cohort as assessed by FISH	176

Table 8.4: Cross tabulation between the results of FISH and OncoScan on the status of CDKN2A.....	176
Figure 8.3: Representative pictures from the FISH analysis for CDK6.	177
Table 8.5: Status of the CDK6 gene in our cohort.....	177
Table 8.6: Concordance between the results of FISH and OncoScan on status of CDK6.....	178
Table 8.7: Cross-tabulation of the status of CDK6 and CDKN2A in our cohort.	178
Table 8.8: Multivariate analysis of survival.	180

Chapter 1: Introduction

Mesothelioma is a malignant neoplasm that develops from cells of the mesothelium. The mesothelium consists of a single layer of avascular flat nucleated cells that lines serosal cavities (e.g. abdominal and chest cavities) and the majority of internal organs, playing important roles in maintaining normal serosal integrity and function. The most common anatomical site for mesothelioma is the pleura (around 70%). However, it can also arise in the peritoneum (15-20%) the pericardium (1%) or the tunica vaginalis (very rare). The focus of this thesis is on malignant pleural mesothelioma (MPM). Mesothelioma is most commonly caused by exposure to asbestos¹ but nearly 20% of patients report no known exposure and this number may be as high as 60% in female patients.² Mesothelioma has also been associated with irradiation,³ intrapleural thorium dioxide and inhalation of other fibrous silicates, such as erionite.^{4,5} Some studies suggest that simian virus 40 (SV40) may act as a co-carcinogen in the development of mesothelioma,⁶ but recent epidemiological studies have been inconclusive.^{7,8} A long latency, insidious growth, delayed diagnosis often at advanced stage and refractoriness to even aggressive surgical and multimodal treatment has led to the probability of cure remaining elusive.⁹

1.1 History of asbestos use and discovery of asbestos related health problems

Asbestos use was popularised mainly because of its ability to be woven and its fire resistant properties. Its use in pottery in Finland dates back to 4500 years ago, in Norway to the 4th and 5th centuries AD. Marco Polo (1254-1354 AD) has described its mining and use in China.¹⁰ Applicability of asbestos as an insulating agent lead to industrial scale mining and use for insulation of water and combustion pipes, materials for house construction and ship building, car brakes, toys, jewellery etc.¹⁰

Health related problems in people working with asbestos were first noticed as early as 1st century AD. However, it was only in the early 1900s that researchers began to notice a large number of early deaths and lung problems in asbestos-mining towns. The first such study was conducted by Dr. H. Montague Murray at the Charring Cross Hospital in 1900. In a post-mortem investigation of a young man who had died from pulmonary fibrosis after having worked for 14 years in an asbestos textile factory, he discovered asbestos traces in the victim's lungs.¹¹ The first diagnosis of asbestosis was made in the UK in 1924 by a Dr. Cooke.¹¹ Joseph Lieutand had described the pleural tumour in 1797 and Klemperer and Rabin first characterised it in 1931.¹² The study that first linked asbestos to mesothelioma came from South Africa nearly 30 years after its characterisation.¹³ Studies from Europe, USA, Australia and Japan followed suit to conclusively establish the causal relationship.

Despite undeniable evidence of the causal relationship of asbestos with a number of pulmonary conditions including mesothelioma, the use of asbestos continued well into the 21st century and continues to be mined in large quantities in countries like Russia, China Brazil and Canada.¹⁴ Use of asbestos products has also continued in many developing and some developed countries like the US. A particularly disturbing fact is that developed and wealthy countries like Canada continued to mine and export white asbestos (chrysotile) to less wealthy developing nations like India. Canada was a proponent of the controlled use of white asbestos till 2013 at which time it was finally banned. The argument was that chrysotile is different than the amphibole type in being less crumbly and used for things like cement, a solid that is less likely to release the deadly fibres into the atmosphere.

In Australia, asbestos was widely used in construction and other industries between 1946 and 1980. From the 1970s there was increasing concern about the dangers of asbestos, and its use was phased out. The use of crocidolite (blue) asbestos was banned in 1967, while the use of amosite (brown) asbestos continued in the construction industry until the mid-1980s. It was finally banned from building products in 1989, although it remained in gaskets, and was banned entirely in December 2003. Use of white asbestos was also banned in 2003.

1.2 Mesothelioma epidemiology

Despite asbestos use now being banned in 60 countries, there is no indication of a slowing of the world wide mesothelioma epidemic. The highest rates of mesothelioma are reported from Europe, mainly the UK. In the UK, the annual number of deaths from mesothelioma progressively increased, being 153 in 1968 and 2,535 in 2012.¹⁵ Australia ranks second only after the UK. Other countries with high incidence are the Netherlands, New Zealand, Belgium and Republic of Malta (Figure 1.1).

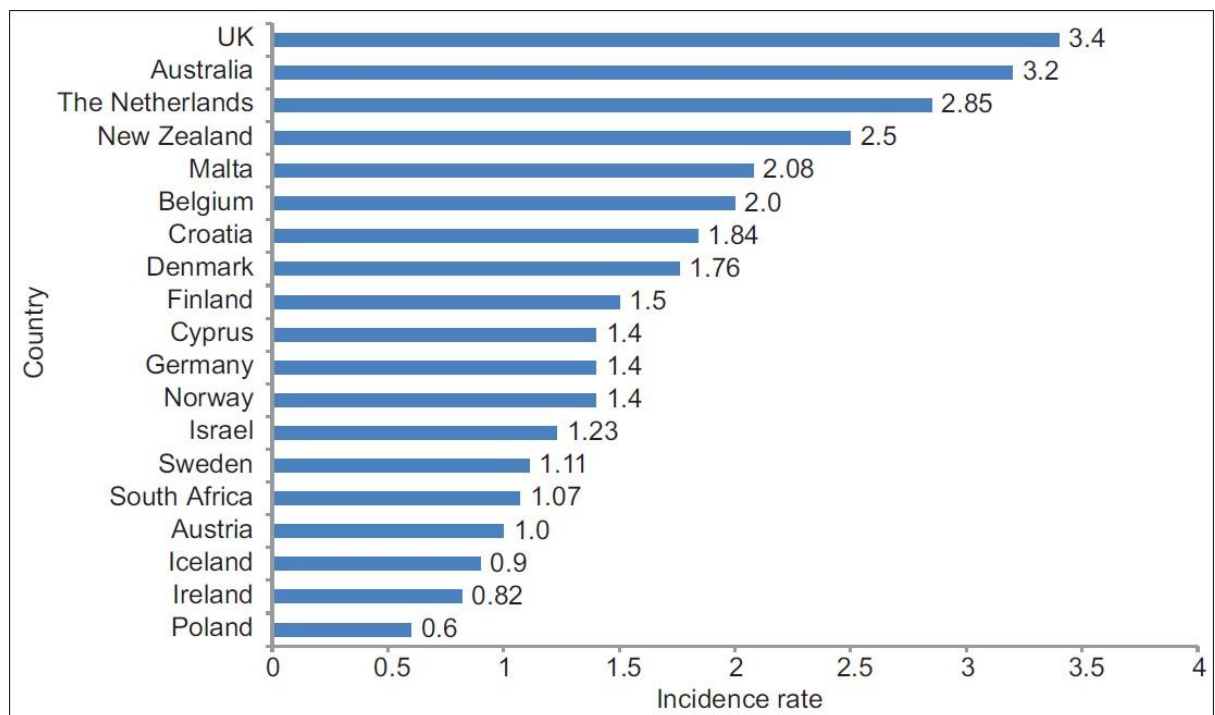


Figure 1.1: Age standardised incidence of mesothelioma in the world.

Adapted from Bianchi et al. (*Indian Journal of Occupational and Environmental Medicine* - 2014)¹⁶

The annual number of mesothelioma cases in Australia has progressively increased from 156 in 1982 to highest of 732 in 2014 (Figure 1.2). The age-standardised incidence rate of mesothelioma increased from 1.1 new cases per 100 000 population in 1983 to a peak of 3.2 in 2010. The rate per 100,000 persons in 2015 was 2.3.¹⁷ The rate for males (3.9/100,000) was higher than for females (1/100,000). The overall 2015 age-standardised mesothelioma incidence rate was slightly lower than those in previous years. The age-standardised mortality rate due to mesothelioma for 2015 was 2.2 per 100,000. Where cause of death was known, mesothelioma was reported as the primary cause in

90.8% of cases. The age standardised mortality rate of mesothelioma in Australia has shown little change between 1997 and 2015 (Figure 1.3).

Due to the prolonged history of active mining and use of asbestos and long latency of Mesothelioma, it was anticipated that Australia would reach the peak around 2015. However, there has been a shift in asbestos exposure from workers directly involved in the asbestos manufacturing industry, to renovators and bystanders inadvertently exposed by directly handling asbestos materials or indirectly being exposed to asbestos fibres.¹⁸ This would ensure that MPM will continue to be a significant problem in Australia for many years to come.

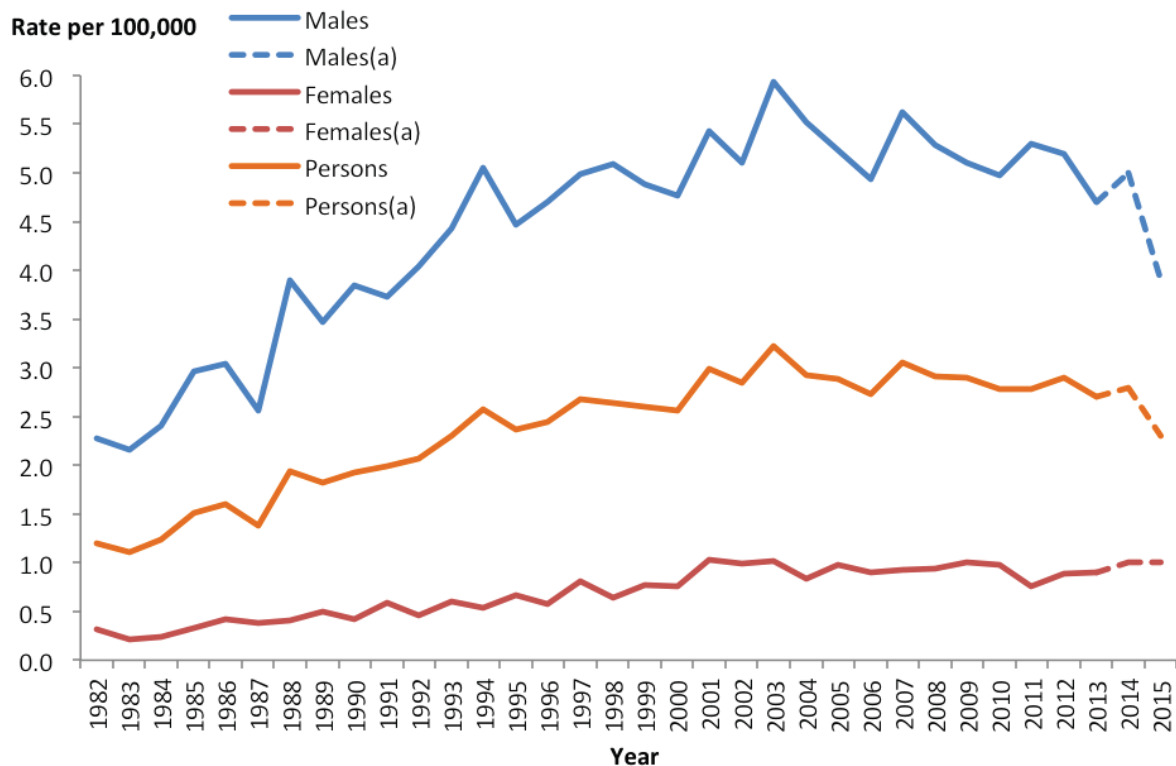


Figure 1.2: Age standardised incidence rates of mesothelioma in Australia 1982-2015. Dotted lines indicate data that are expected to change by three or more percent as data are updated. Adapted from the 5th annual report of the Australian mesothelioma registry (Mesothelioma in Australia 2015)

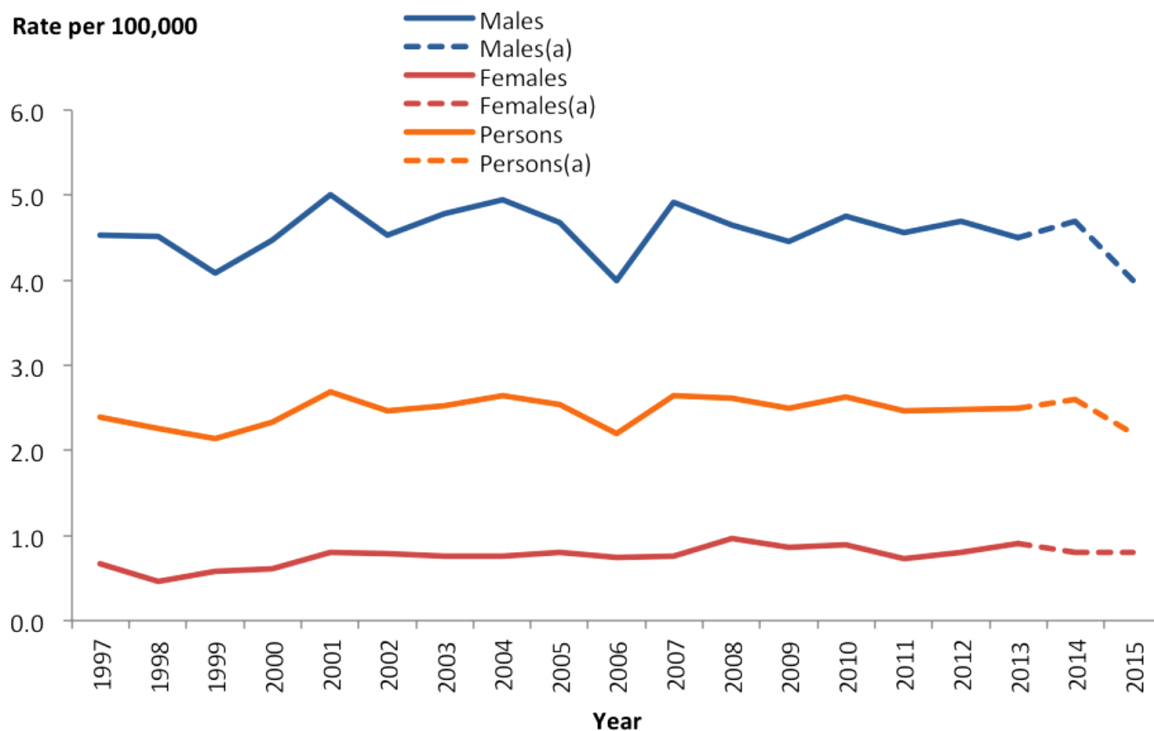


Figure 1.3: Age standardised mortality rate of mesothelioma in Australia 1997-2015. Dotted lines indicate data that are expected to change by three or more percent as data are updated. Adapted from the 5th annual report of the Australian mesothelioma registry (Mesothelioma in Australia 2015)

1.3 Pathogenesis of mesothelioma

The understanding of the molecular pathogenesis of mesothelioma has lagged behind those of more common malignancies. However, recent development of global genetic and epigenetic analysis has served to reveal its fundamental molecular abnormalities.⁹ There are several possible mechanisms involved in how asbestos fibres cause mesothelioma (Figure 1.4). Four representative models by which asbestos fibres are thought to induce genetic/cellular damages of the cells and chronic inflammation, which is linked to carcinogenesis, are as follows.⁹

- (i) Reactive oxygen species generated by asbestos fibres with their exposed surface lead to DNA damage and strand breaks of the cells. Macrophage, which phagocytises asbestos fibres but is unable to digest them, also produces abundant reactive oxygen species.¹⁹
- (ii) Asbestos fibres are also engulfed by mesothelial cells. Asbestos fibres taken up into the cells can physically interfere with the mitotic process of the cell cycle by disrupting

mitotic spindles. Tangling of asbestos fibres with chromosomes or mitotic spindles may result in chromosomal structural abnormalities and aneuploidy of mesothelial cells.^{20,21}

- (iii) Asbestos fibres absorb a variety of proteins and chemicals to the broad surface of asbestos, which may result in the accumulation of hazardous molecules including carcinogens. Asbestos fibres also bind important cellular proteins and the deficiency of such proteins may also be harmful for normal mesothelial cells.²²
- (iv) Asbestos-exposed mesothelial cells and macrophages release a variety of cytokines and growth factors, which induce inflammation and tumour promotion. Those include tumour necrosis factor- α (TNF- α), interleukin-1 β , transforming growth factor- β (TGF β) and platelet-derived growth factor. TNF- α has been shown to activate nuclear factor- κ B, which leads to mesothelial cell survival and inhibits asbestos-induced cytotoxicity.²³
- (v) Asbestos induces necrotic cell death of the mesothelial cells with resultant release of high mobility group box protein-1 (HMGB1) into extra-cellular space. HMGB1 is a prototypical damage-associated molecular pattern molecule (DAMP) that is normally present in the nucleus of the cells. HMGB1 is passively released by necrotic cells or actively secreted by immune and cancer cells, and is responsible for the initiation and perpetuation of the inflammatory response. This, together with the prolonged bio-persistence of asbestos fibres, initiates a vicious cycle of chronic cell death and inflammation that over a period of many years can lead to mesothelioma.²⁴ Thus, HMGB1 functions as a 'master switch' by which the chronic inflammation that drives mesothelioma growth is initiated and maintained.

Aberrantly activated signalling network among mesothelial cells, inflammatory cells, fibroblasts and other stromal cells may create a pool of mesothelial cells, which harbor aneuploidy and DNA damage, potentially developing into cancer cells and together forming a tumour microenvironment that supports and nourishes them.⁹

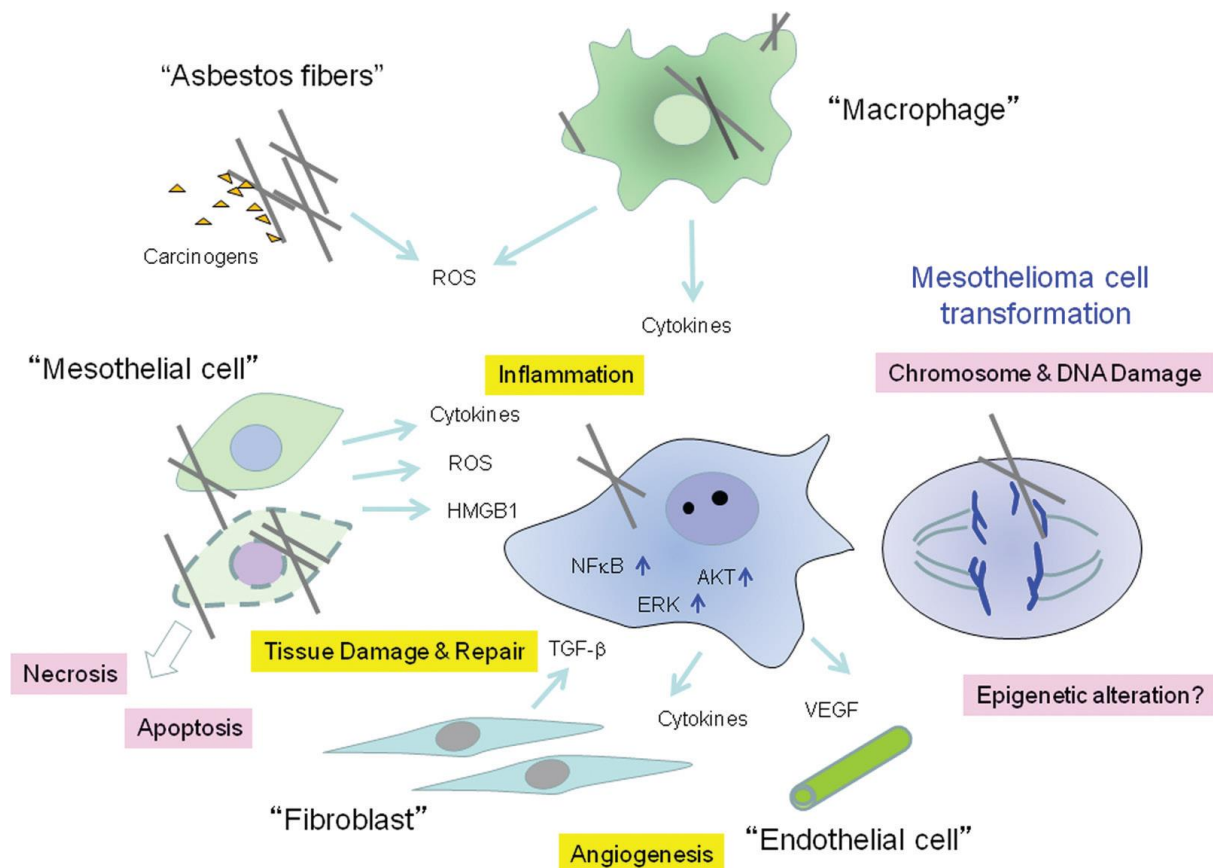


Figure 1.4: Possible mechanisms of asbestos-induced carcinogenesis.

HMGB1, high-mobility group box 1 protein; ROS, reactive oxygen species; TGF- β , transforming growth factor- β ; VEGF, vascular endothelial growth factor. Adapted from Sekido et al. – *Carcinogenesis* 2013⁹

1.4 Genetic abnormalities in mesothelioma

Malignant mesothelioma is thought to result from the accumulation of a number of acquired genetic events. The complexity of the genetic changes involved in this malignancy was first demonstrated by use of karyotyping techniques using chromosomal banding.²⁵

1.4.1 Mutations in mesothelioma:

Recurrent somatic mutations in a number of tumour suppressor genes namely cyclin-dependent kinase inhibitor 2A gene (*CDKN2A*), neurofibromatosis 2 (merlin) gene (*NF2*), and BRCA1 associated protein 1 gene (*BAP1*) were among the first genomic changes to be reported in MPM. However, more recent studies using newer technologies like next (or second) generation sequencing strategies

applied to whole genome sequencing, whole transcriptome sequencing, and targeted sequencing have been able to provide a more genome-wide view on the genetic landscape of MPM.²⁶

The most comprehensive genomic analysis in MPM was done by Bueno et al. in 2016 in 216 MPM tumours. To define the mutational landscape, they conducted whole exome analysis in 99 paired MPM samples in addition to 103 paired MPMs for mutations in 460 genes by targeted capture using single primer enrichment technology (SPET) and sequencing. They confirmed that none of the samples carried germ line variants in known cancer-associated genes. A total of 2,529 protein-altering somatic mutations were identified, including 2,069 missense, 190 nonsense, 3 stop-loss, 63 essential splice site and 204 frame shift mutations a vast majority of which (85%; 2,144/2,529) were novel, as they were not reported in COSMIC29 or OncoMD. At an average of 24 ± 11 (mean \pm s.d.) protein-coding alterations per sample, MPMs showed a low protein-altering mutation rate compared to other cancers; higher than only thyroid carcinoma and acute myeloid leukemia. Interestingly, they did not observe significant differences in mutation rate between histological subtypes ($P = 0.8$). Also, they did not observe a significant difference in the mutational signature in samples with or without known asbestos exposure. Clustering cancers by mutational signatures showed that the mutational processes in MPMs were closer to those observed in ovarian cancers. The protein-altering somatic variants identified in 2,028 genes were found in multiple gene families. These included recurrent mutations in 21 protein kinase–encoding genes, including *TTN*, *LATS2* and *ULK2*; 18 chromatin-modifying genes, including *SETD2*, *SETDB1*, *SETD5*, *ASH1L*, *CREBBP*, *PRDM2*, *KDM2B* and *KMT2D*; and *GRM3*, *GPR149* and *GPR98*, encoding G protein–coupled receptors. Fifty-two percent of non-synonymous mutations were predicted to have a functional impact. Ten significantly mutated MPM-associated genes (q -score ≥ 0.8 ; false discovery rate (FDR) $\leq 16\%$) included *BAP1*, *NF2*, *TP53*, *SETD2*, *DDX3X*, *ULK2*, *RYR2*, *CFAP45*, *SETDB1* and *DDX51*. Among the significantly mutated genes, only *BAP1*, *NF2* and *TP53* have been reported in MPM. *BAP1* and *NF2* were found to be mutated in 23% (46/202) and 19% (38/202) of the samples. Tumour suppressor *TP53* was mutated in 8% (17/202) of MPMs. Bueno et al. also conducted an expression analysis on

211 samples. To define molecular subgroups of MPMs, they performed unsupervised consensus clustering of RNA-seq-derived expression data and identified four major clusters: sarcomatoid, epithelioid, biphasic- epithelioid (biphasic-E) and biphasic-sarcomatoid (biphasic-S) with significant differences in survival and histotype. Forty-three gene fusions were identified in 22 samples; 13 fusions in *NF2*, 7 in *BAP1*, 8 in *SETD2*, 7 in *PBRM1*, 2 in *PTEN* and 6 in other genes. In 2010, Bueno et al²⁷ also reported on the only whole genome sequencing of a primary MPM along with matched normal lung sample. Using a combination of Illumina sequencing by synthesis and Roche/454 pyrosequencing, they identified homozygous mutations in NK6 homeobox 2 gene (*NKX6-2*), cadherin 8 gene (*CDH8*), and nuclear factor related to kappa B binding protein gene (*NFRKB*).

In 2015, Guo et al. were the first to sequence the exomes of 22 MPMs and paired blood samples using the Illumina HiSeq platform.²⁸ They reported 517 somatic mutations in 490 genes. However, only 13 were recurrent (in two or more samples) and three (*BAP1*, *NF2* and *CUL1*) were significantly more mutated than the background mutation rate. The highest prevalence was noted in *BAP1*, the second most frequently mutated gene was *NF2*. Somatic mutations in tumour protein p53 gene (*TP53*), cullin 1 gene (*CUL1*), phosphatidylinositol-4-phosphate 3-kinase catalytic subunit type 2 beta gene (*PIK3C2B*), TAO kinase1 gene (*TAOK1*), and radixin gene (*RDX*) were each found in two patients with MPM.

Mäki-Nevala et al. also used the Illumina HiSeq platform to sequence the exomes of 21 formalin-fixed, paraffin-embedded malignant mesothelioma samples.²⁹ Overall, the somatic status of three of the detected mutations could be confirmed. They found mutations in *BAP1*, mitochondrial ribosomal protein L1 gene (*MRPL1*), tubulin tyrosine ligase like 6 gene (*TTL6*), inositol polyphosphat-4-phosphatase type I A gene (*INPP4A*), semaphorin 5B gene (*SEMA5B*), serine/threonine kinase 11 gene (*STK11*), *EGFR*, *NF2*, coatomer protein complex subunit gamma 1 gene (*COPG1*), EPH receptor B1 gene (*EPHB1*), and EPH receptor B2 gene(*EPHB2*). Investigating the exome of a single MPM and matched normal pleura sample using SOLid 5500 technology (Applied Biosystems, Foster City, CA

Kang et al. found 11 non-synonymous variants and were able to further validate those in six namely SET domain bifurcated 1 gene (*SETDB1*), Rap guanine nucleotide exchange factor 6 gene (*RAPGEF6*), actin, beta gene (*ACTB*), glutamic-oxaloacetic transaminase 1 gene (*GOT1*), nucleotide-binding oligomerization domain containing 2 gene (*NOD2*), and tumour protein 53 (*TP53*). They further evaluated the entire coding region of *SETDB1* (identified as a potential oncogene in lung cancer³⁰ and a frameshift mutation in *SETDB1* previously described in a mesothelioma cell line), in tissue samples from 68 additional patients. Four point mutations and three deletions in *SETDB1* were detected in those samples whereas there were no *SETDB1* in 10 matched normal pleura samples.³¹

Sugarbaker et al. reported in 2008 on the results of transcriptome shotgun 454 pyrosequencing on frozen samples of four MPMs, one pulmonary adenocarcinoma, and one normal lung sample.³² They detected 619 previously unknown single-nucleotide variants (SNVs). Of these, the frequency of seven tumour-specific SNVs that were nonsynonymous and not present in dbSNP (i.e., a database for SNVs) was further examined in 49 MPMs. These SNVs occurred in genes x-ray repair complementing defective repair in Chinese gene (*XRCC6*), ARP1 actin-related protein 1 homolog A, contractin alpha gene (*ACTR1A*), ubiquinol-cytochrome c reductase core protein 1 gene (*UQCRC1*), proteasome 26S subunit, non-ATPase 13 gene (*PSMD13*), PDZK1 interaction protein 1 gene (*PDZK1IP1*), collagen, type V alpha 2 gene (*COL5A2*), and matrix remodelling associated 5 gene (*MXRA5*). In total, three of these SNVs (in *COL5A2*, *UQCRC1*, and *MXRA5*) were observed in at least one additional tumour.

Lo Iacono et al. used next generation sequencing on a large MPM sample cohort (123 formalin-fixed, paraffin-embedded MPM samples).³³ They sequenced amplicons of 52 genes on Ion Torrent Personal Genome Machine. They used a commercial library kit designed to amplify amplicons covering mutations from 50 cancer-associated and because this panel did not include *BAP1* and *NF2*, a library was designed to cover all exons of these two genes. Several genetic variations were detected in *BAP1* and *NF2*. In *BAP1*, these variations were mainly clustered in exons 13 and 17,

whereas those in *NF2* were more randomly distributed. In total, 20 of the other investigated genes showed variations in at least 20% of the patients. Considering only those variations that were previously correlated with cancer or affected protein stability for further evaluation, four of these variations (in *TP53*, *PIK3CA*, v-kit Hardy-Zuckerman 4 feline sarcoma viral oncogene homolog gene [*KIT*], and kinase insert domain receptor gene [*KDR*]) were non-synonymous. They were able to identify a higher number of genetic variations in the p53/DNA repair and the receptor tyrosine kinase–phosphatidylinositol 3-kinase (PI3K)–*AKT* pathways. A Harvey rat sarcoma viral oncogene homolog (*HRAS*) silent genetic variation previously reported in bladder cancer was identified in 72 of 123 (58.5%) patients. More relevantly, a mutation in the catalytic subunit of Phosphatidylinositol-4,5-bisphosphate 3-kinase (*PI3K*) was detected and associated to disease progression.³³

Melaiu et al. reviewed papers which studied the mesothelioma transcriptome and found 931 genes which were found to be deregulated in at least one study but only 119 that were found in two or more papers. They investigated these genes by reverse transcriptase - polymerised chain reaction (rt-PCR) and found 59 of them were significantly deregulated in their set of 15 patient samples when compared to 20 normal pleura and only 9 of them were further found to be deregulated in two mesothelioma cell lines they tested. They suggested roles for a number of possible candidate genes mainly *ACSL1*, *CCNO*, *CFB*, *PDGFRB*, *SULF1*, *THBS2*, *TIMP3*, *XPOT*, *TACC1* but concluded that mesothelioma is just too heterogeneous a disease.³⁴

1.4.2 Structural variations in MPM genome

Comparisons of human genomes show that more base pairs are altered as a result of structural variation including copy number variation (CNV) than as a result of point mutations.³⁵ However, the degree to which these genomic structural abnormalities correlate with disease phenotype is still being explored.³⁶ Starting from early studies using chromosomal banding technologies, studies have consistently shown multiple clonal chromosomal abnormalities in MPM. All chromosomes have been seen to contribute to numerical changes, with losses being more common than gains.²⁵ Deletions in

1p21-22, 3p21, 4, 6q14-25, 9p21, 13q, 14q, 15q15, 17p13, and 22 3 have been the most frequent events observed in mesothelioma and monosomy 22 the most frequent numerical change.³⁷ The preponderance of losses suggested a greater role for tumour suppressor genes (TSGs).

Many studies utilizing G-banding, conventional comparative genomic hybridization (cCGH), and array comparative genomic hybridization (aCGH) have suggested that areas in 9p21.3, 22q12.2, and 13q12.11, which contain the *CDKN2A/p16INK4A*, *CDKN2A/p14ARF*, *CDKN2B/p15*, *NF2*, and *LATS2* TSGs and possibly the *MTAP* gene, were deleted and perhaps causally involved in mesothelioma tumorigenesis. In A FISH based analysis, Takeda et al. found genomic losses and gains found to be commoner in non-epitheloid versus epitheloid mesothelioma.³⁸ The *CDKN2A/CDKN2B* genes (9p21.3) were found to be homozygously deleted in a high percentage of mesothelioma cell lines and tumours. Diagnostic value of 9p21.3 with detection of homozygous deletion being used to differentiate mesothelioma from reactive mesothelial proliferation has also been suggested.³⁸ The *NF2* gene (22q12.2) has been found to undergo frequent biallelic inactivation by homozygous deletions in tumours and cell lines.^{39,40} Homozygous and heterozygous deletions of 3p21.1 which includes the tumour suppressor gene *BAP1* has also been exhibited.⁴¹ Frequent mutation of *BAP1* has also been reported in patients with metastasizing uveal melanoma and other malignancies.⁴²

Klorin et al. using aCGH and spectral karyotyping (SKY) recently identified a total of 88 homozygous deletions in their set of 17 mesothelioma cell lines. These deletions ranged from one to nine per cell line. There were 52 recurrent homozygous deletions spanning 10 genomic regions i.e. 9p21.3, 9p21.2, 16p13.3, 22q11.23, 22q12.2, 3q26, 8p11.22, 3p21.2, 4q22.1, and 13q12.11.²⁵ In their copy number analysis they found several regions of gains covering 150 genes and losses covering 127 genes. From their whole exome sequencing of 22 MPM samples and matched blood, Guo et al. observed some CNVs. The most striking alteration noticed was a loss of 22p and 22q. Moreover, focal deletion of a region at 9p21 was noted in 10 of the MPMs, and microRNA31 gene (*MIR31*) in eight.

As a part of their genomic analysis of MPM, Bueno et al. assessed 95 MPMs for copy number alterations using 2.5M Illumina SNP array and/or whole-genome data. They found regions of recurrent copy loss that include genes such as *BAP1*, *NF2*, *CDKN2B*, *LATS2*, *LATS1* and *TP53*. Copy number loss correlated with loss of expression in these genes. Recurrent gains in genes such as *RPTOR* and *BRD4* were also observed and they showed elevated expression. Widespread loss of heterozygosity (LOH) was also seen in a few samples. Further, some of these samples showed copy-neutral LOH and heterozygous *NF2* mutations. Whole-genome sequencing uncovered additional structural variations that did not result in gene fusions but were associated with loss of function or copy number loss. Importantly, chromosomal rearrangements within *BAP1*, *NF2* or *CDKN2A* were discovered in 9 (45%) of the 20 samples with whole-genome sequencing data.

In 2014, de Assis et al. reviewed the available literature on the key genes and pathways studied in relation to mesothelioma pathogenesis. They have emphasized on the relative absence of mutations/alterations of important tumour suppressor genes like *TP53* and *Rb* which are found to be common in other malignancies. Loss of *PTEN* function, deletions and mutations in *LATS2* (a TSG), over expression of the receptor tyrosine kinase *EGFR*, alteration in methylation patterns of genes, reduced expression of miR-31 and miR-15/16, alterations in *BCL2* family of genes homozygous deletions in *SAV* (component of hippo cascade) and *CTNNB1* (positive growth stimulating factor in many cancers) amongst others have been presented as being important in mesothelioma pathogenesis.⁴³ Several molecular pathways like cell cycle regulation, apoptosis, growth factor pathways, and angiogenesis have been found to be involved.^{43,44}

1.4.3 Pathways affected by genomic change in MPM

The mutations and other genomic changes observed in MPM appear to cluster in four main pathways: the tumour protein p53 (*TP53*)/DNA-repair pathway, the cell cycle pathway, the mitogen-activated protein kinase (MAPK) pathway, and the phosphatidylinositol-3 kinase (PI3K)-AKT pathway.²⁶ The *TP53*/DNA repair pathway is the first affected pathway due to mutations and

deletions reported in *TP53*, *CDKN2A*, and *BAP1*. *TP53* is a gene that encodes the p53 transcription factor involved in the response of cells to different types of stress, including DNA damage and is well known to be mutated in several cancer types. Activated p53 can induce cell cycle arrest (through stimulation of p21) and apoptosis.⁴⁵ *CDKN2A* encodes p14ARF, a protein that interacts with a negative regulator of p53, *MDM2*. As a result, p53 stays active.⁴⁶ *BAP1* is a nuclear ubiquitin carboxyterminal hydrolase involved in repairing double-strand DNA breaks.⁴⁷ Because of its crucial role in cell survival and DNA repair, the TP53/DNA repair pathway is often inactivated in cancer processes. The Cell Cycle Pathway is the second pathway that seems to be altered in MPM. Mutations in *CDKN2A* and *CUL1* affect this pathway as *CDKN2A* also encodes p16ink4a, which is a cyclin-dependent kinase inhibitor negatively influencing cyclin-dependent kinase 4 (*CDK4*) and cyclin-dependent kinase 6 (*CDK6*). As a result, it blocks the phosphorylation of the retinoblastoma protein. Non-phosphorylated retinoblastoma protein (*Rb*) forms a complex with the E2F transcription factor, inhibiting it to activate its target genes involved in cell cycle progression.⁴⁸ *CUL1* encodes an essential component of the skp cullin F-box E3 ubiquitin ligase complex, mediating the ubiquitination of proteins involved in cell cycle progression.⁴⁹ The third affected pathway is the MAPK pathway. This pathway is activated in response to extracellular stimuli such as growth factors (MAPK/ERK pathway) and stress (p38/MAPK14 stress-activated *MAPK* cascade). Activation of this pathway results in activation of transcription factors, influencing cell proliferation and cell cycle progression.⁵⁰ Alterations in the cell surface receptors *KIT* and *KDR*, alterations in *TAOK1* and *MAP2K6* reported in MPM cause alteration of this pathway. The PI3K/AKT pathway is the last involved pathway. Activation of PI3K results in phosphorylation and activation of AKT, a protein kinase involved in several cellular processes. Among other things, AKT inhibits a conformational change in the pro-apoptotic Bax protein and its translocation to mitochondria, hence preventing the disruption of the mitochondrial membrane and promoting cell survival.⁵¹ Moreover, it also activates mechanistic target of Rapamycin (*mTOR*), a serine/threonine protein kinase regulating cell proliferation, cell motility, and cell survival. In MPM, mutations in phosphatidylinositol-4,5-

bisphosphate 3-kinase, catalytic subunit alpha (*PIK3CA*) and phosphatidylinositol-4-phosphate 3-kinase C2 domain-containing beta polypeptide (*PIK3C2B*) were noted. These paralogs both encode the catalytic subunit of PI3K and hence are crucial for its function. *NF2* encoding merlin, is involved in contact-dependent inhibition of cell proliferation, mainly by inhibiting mTOR signaling.⁵²

The understanding of MPM pathogenesis, the genetic alterations predisposing to its development and involved in its progression has come a long way since asbestos exposure was implicated more than 65 years ago but still lags behind that of other cancers. The fact that MPM is relatively rare, does not seem to have a well-defined premalignant stage and that most patients present in late stages has meant that discovery and widespread use of prognostic and predictive factors has been elusive.⁵³ Recently published work from Chernova et al may have shed some light into the the early molecular changes that possibly drive carcinogenesis during the long latency period of mesothelioma. They demonstrated that instillation of either long carbon nano tubules (CNTs) or long asbestos fibres into the pleural cavity of mice induces mesothelioma that exhibits common key pro-oncogenic molecular events throughout the latency period of disease progression. They were able to show that sustained activation of pro-oncogenic signalling pathways, increased proliferation, and oxidative DNA damage form a common molecular signature of long- CNT- and long-asbestos-fiber-induced pathology. Hypermethylation of p16/Ink4a and p19/Arf in the CNT- and asbestos-induced inflammatory lesions were shown to precede mesothelioma resulting in silencing of Cdkn2a (Ink4a/Arf) and loss of p16 and p19 protein. In end-stage mesothelioma, silencing of p16/Ink4a was sustained and deletion of p19/Arf was detected.⁵⁴

Available literature discussed in brief above do suggest the roles of multiple genes in the pathogenesis and progression of MPM and also identify some that might be important for prognostication and potential development of therapeutic strategies. However, consensus view seems to be that MPM is a disease with relatively few somatic mutations compared to other solid tumours.^{43,55,56} In a recent review M Carbone et al. said “Despite a large body of research, driver

mutations in mesothelioma have not been evident and that every tumour seems to have a separate set of genetic alterations making the development of targeted therapy elusive".⁵⁶

Also, although the above described genes are now known to have prominent roles in the pathogenesis, what role if any they play in determining prognosis is still a matter of study. A relatively small scale study using Representative Oligonucleotide Microarray Analysis (ROMA) on DNA isolated from tumours of 22 patients who recurred at variable interval with the disease after surgery found *CDKN2A / CDKN2B* loss to be specific for the early recurrence group.³⁷ In a mouse model, Altomare et al. demonstrated that *NF2* loss lead to markedly hastened mesothelioma development.⁵⁷ The evidence about the prognostic implication of *BAP1* loss/inactivation is inconclusive at best with an IHC based study showing worse survival for higher expressing (Wild type *BAP1*) patients.⁵⁸ Large scale studies using patient samples⁵⁸ which look into the genomic alterations in MPM and their clinical and prognostic implications have been sparse. This short review of available literature suggests a greater role of structural aberrations (deletions, gains etc.) than point mutations in MPM. It appears deletions of chromosomal regions harbouring important TSG and high gains in regions with known oncogenes are by far the commoner and more important genetic alterations seen in this incredibly complex disease.⁴³ Mesothelioma is driven by the copy number aberrations and chromothripsis and widespread chromosomal instability perfectly fits within a model of MPM pathogenesis, caused by the concurrent activities of asbestos-induced DNA damage, and inflammation, acting in concert with genetic susceptibility and instability and possibly other cofactors.⁵⁹

1.5 Clinico-pathological features of MPM

1.5.1 Clinical features and presentation of MPM

Patients with MPM more often than not present late in the course of the disease. The early signs and symptoms of the disease can be subtle and are often misinterpreted delaying diagnosis of MPM frequently by months. Patients frequently experience lower back pain or side chest pain. In addition, shortness of breath is frequently the presenting symptom if pleural fluid is present. A small number of patients may experience difficulty swallowing, persistent cough, fever, weight loss, or fatigue.

1.5.2 Diagnosis of MPM

Diagnosis of MPM can be suggested by the radiological findings of pleural effusion on chest X-rays and pleural effusion ± pleural thickening on CT scan in patients who have history of occupational or environmental exposure to asbestos. However, the presence of multiple other malignant (secondary tumours of the pleura) and non-malignant (chronic pleuritis, empyema) pleural afflictions which can present with similar clinical and radiological features often make diagnosis of MPM difficult.

Although histology is the mainstay of diagnosis in MPM, pleural fluid cytology can give an initial indication. While absence of malignant cells on cytology does not completely exclude MPM, it makes it much more unlikely, especially if an alternative diagnosis can be made (e.g. tuberculosis, heart failure). Pleural biopsies can be obtained via radiological guided tru-cut biopsy or surgical biopsies via thoracoscopy or thoracotomy. The accurate diagnosis of MPM depends on the presence of appropriate tumour morphology with concordant immunohistochemistry in patients with appropriate clinical, radiological and surgical findings.⁶⁰ Current recommendations are that in patients with concordant clinical and morphological features, at least two mesothelial IHC markers and two epithelial markers with either sensitivity or specificity greater than 80% should be used.⁶¹ As to which antibodies are used in any particular case depends on the histological pattern of MPM, the likely differential diagnosis being considered and also on the experience of the concerned

laboratory. Calretinin, Wilms tumour -1 (WT-1), cytokeratin 5/6 (CK5/6) and podoplanin (D2-40) are considered the most useful mesothelial markers.⁶¹ However, sarcomatoid MPMs and sarcomatoid components of biphasic MPMs may lose immunoreactivity for most markers. A brief overview of the different markers used for MPM diagnosis is presented in Table 1.1.⁶²

Table 1.1: Immunohistochemistry based markers useful in diagnosis of MPM

Marker	Uses in MPM diagnosis	Limitations
Mesothelial markers		
Calretinin	<ul style="list-style-type: none"> In differentiating MPM (nearly all epithelioid MPM are positive) from lung adenocarcinoma (LUAD) (5-10%), Renal cell carcinoma (RCC) (~10%), non-gynaecological adenocarcinomas in the peritoneum. 	<ul style="list-style-type: none"> Expression often lost sarcomatoid tumours or sarcomatoid components of biphasic tumours In differentiation of pleural MPM from squamous cell cancers (SQCC) (~40%) and peritoneal MPM (85-100%) from primary serous carcinomas (PSC) (up to 38%)
Cytokeratin 5/6	<ul style="list-style-type: none"> Differentiating MPM (75-100%) from LUAD (2-20%), RCC (negative) 	<ul style="list-style-type: none"> To differentiate from SQCC (almost all positive), PSC (22-35%) and pancreatic adenocarcinomas (38%)
WT-1	<ul style="list-style-type: none"> Differentiating MPM (75-95%) from LUAD (negative), SQCC (negative), RCC (2%), gastric adenocarcinomas (3%) and pancreatic adenocarcinomas 	<ul style="list-style-type: none"> To differentiate from PSC (up to 83%)
D2-40 (podoplanin)	<ul style="list-style-type: none"> Differentiating MPM (90-100%) from LUAD (15%), RCC (negative) 	<ul style="list-style-type: none"> To differentiate MPM from SQCC (50%)
Mesothelin	<ul style="list-style-type: none"> Differentiating MPM (100%) from RCC (negative) 	
Epithelial markers		
MOC-31	<ul style="list-style-type: none"> Differentiating MPM (2-10%) from LUAD (nearly 100%), lung SQCC (100%), PSC (98%) and non-gynaecological abdominal carcinomas (87%) 	<ul style="list-style-type: none"> To differentiate MPM from RCC (50%)
CEA	<ul style="list-style-type: none"> Differentiating MPM (<5%) from LUAD (80-100%), and non-gynaecological abdominal carcinomas (81%) 	<ul style="list-style-type: none"> To differentiate from SQCC, RCC, PSC

Ber-EP4	<ul style="list-style-type: none"> Differentiating MPM (up to 20%) from LUAD (95-100%), SQCC (85-100%), PSC (83-100%), gastric and pancreatic carcinomas (>98%) 	<ul style="list-style-type: none"> Not useful in RCC (40%)
TTF-1	<ul style="list-style-type: none"> Differentiating MPM (negative) from LUAD (75-85%) 	
Napsin A	<ul style="list-style-type: none"> Differentiating MPM (negative) from LUAD (80-90%) 	
BG8 (LewisY)	<ul style="list-style-type: none"> Differentiating MPM (93-75 positive) from LUAD (90%), SQCC (80%), PSC (73%) and non-gynaecological abdominal carcinomas (89%) 	<ul style="list-style-type: none"> In differentiating from RCC (4%)
B72.3	<ul style="list-style-type: none"> Differentiating MPM (very low positivity) from LUAD (75-85%), 	<ul style="list-style-type: none"> In differentiating from PSC (63%)
p63 or p40	<ul style="list-style-type: none"> Differentiating MPM (up to 7%) from SQCC (nearly 100%) 	
PAX8 or PAX2	<ul style="list-style-type: none"> Differentiating MPM (negative) from RCC (80-100%) and tumours of Müllerian origin 	
ER/PR	<ul style="list-style-type: none"> When positive very useful in differentiating MPM (negative) from breast carcinoma and PSC 	
CDX2	<ul style="list-style-type: none"> Useful in differentiation of MPM (negative) from colon (100%), intestinal (80%) and gastric cancers (70%) 	

Adapted from John T et al. – Journal of Thoracic Oncology⁶².

CEA, carcinoembryonic antigen; TTF-1, thyroid transcription factor 1; PAX8, paired box gene-8; PAX2, paired box gene 2; ER, estrogen receptor; PR, progesterone receptor; CDX2, caudal type homebox 2

1.5.2 Histological classification of MPM

MPM is pathologically divided the following subtypes:

- 1) Epithelioid mesothelioma accounts for approximately 70% of all diagnosed cases. These tumours contain polygonal, oval or cuboidal cells that often mimic reactive mesothelial cells that occur in response to various types of injury.
- 2) Sarcomatoid mesothelioma is a less common subtype of MPM, accounting for approximately 15% to 20% of mesothelioma. Under a microscope, sarcomatoid mesothelioma consists of spindle cells that may mimic malignant mesenchymal tumours such as malignant fibrous histiocytoma, leiomyosarcoma or synovial sarcoma.
- 3) Biphasic mesotheliomas are a mix of epithelial and sarcomatoid cell types. To be classified as a biphasic tumour, it should contain at least 10% of epithelioid and sarcomatoid components. They account for the remaining percentage of mesothelioma cases.

It is currently unclear whether the different histological subtypes of mesothelioma evolve from a common ancestor or through polyclonal development. It is now known that MPM, like some colonic and breast cancers are polyclonal in origin.⁶³ This is probably to be expected given that many mesothelial cells are subjected to the asbestos fibres and also asbestos induced inflammation simultaneously. Mesothelial cells express characteristics of mesodermal, epithelial and mesenchymal phenotypes and have been proven to exhibit plasticity by transforming into different tissues under specific growth conditions therefore pointing towards origin from a progenitor cell population with multipotential differentiation.⁶⁴ It is therefore possible the histological subtype of the individual MPM tumour is a function of the pluripotent mesothelial differentiation. Polyclonality in association with the multipotent differentiation may explain the origin of biphasic tumours. However, this remains an important unanswered question.

1.6 Staging of MPM

A number of MPM staging systems have been developed and used, the most recent and widely used TNM system was proposed by the International Mesothelioma Interest Group (IMIG) in 1994.⁶⁵

This TNM classification is as detailed in the Table 1.2 below.

Table 1.2: TNM staging of Mesothelioma.

Primary tumour (T)	
TX	Primary tumour cannot be assessed
T0	No evidence of primary tumour
T1	Tumour limited to the ipsilateral parietal pleura with or without mediastinal pleura and with or without diaphragmatic pleural involvement
T1a	No involvement of the visceral pleura
T1b	Tumour also involving the visceral pleura
T2	Tumour involving each of the ipsilateral pleural surfaces (parietal, mediastinal, diaphragmatic, and visceral pleura) with at least 1 of the following: <ul style="list-style-type: none"> • Involvement of the diaphragmatic muscle • Extension of tumour from the visceral pleura into the underlying pulmonary parenchyma
T3	Locally advanced but potentially resectable tumour; tumour involving all of the ipsilateral pleural surfaces (parietal, mediastinal, diaphragmatic, and visceral pleura) with at least 1 of the following: <ul style="list-style-type: none"> • Involvement of the endothoracic fascia • Extension into the mediastinal fat • Solitary, completely resectable focus of tumour extending into the soft tissue of the chest wall • Nontransmural involvement of the pericardium
T4	Locally advanced, technically unresectable tumour; tumour involving all of the ipsilateral pleural surfaces (parietal, mediastinal, diaphragmatic, and visceral pleura) with at least 1 of the following: <ul style="list-style-type: none"> • Diffuse extension or multifocal masses of tumour in the chest wall, with or without associated rib destruction • Direct diaphragmatic extension of the tumour to the peritoneum • Direct extension of the tumour to the contralateral pleura • Direct extension of the tumour to a mediastinal organ • Direct extension of the tumour into the spine • Tumour extending through to the internal surface of the pericardium with or without a pericardial effusion or tumour involving the

	myocardium
Regional lymph nodes (N)	
NX	Regional lymph node(s) cannot be assessed
N0	No regional lymph node metastases
N1	Metastases in the ipsilateral bronchopulmonary or hilar lymph node
N2	Metastases in the subcarinal or in the ipsilateral mediastinal lymph node, including the ipsilateral internal mammary and peridiaphragmatic nodes
N3	Metastases in the contralateral mediastinal, contralateral internal mammary, ipsilateral or contralateral supraclavicular lymph nodes
Distant metastases (M)	
M0	No distant metastasis
M1	Distant metastasis

Stage	T	N	M
I	T1	N0	M0
IA	T1a	N0	M0
IB	T1b	N0	M0
II	T2	N0	M0
III	T1, T2	N1	M0
	T1, T2	N2	M0
	T3	N0-2	M0
IV	T4	Any N	M0
Any T	N3	M0	
Any T	Any N	M1	

The International Association for the study of Lung Cancer (IASLC) and IMIG have developed an international database of MPM patients that was geographically representative and included patients with MPM irrespective of treatment, pathological subtype, and stage to develop a data driven revision of the current staging system for the eighth edition of the Union for International Cancer Control (UICC) and the American Joint Committee on Cancer (AJCC) manuals. It has therefore been recently proposed that the key elements of the T component remain unchanged except for collapsing the stages T1a and T1b into a single T1 because it was found that this distinction was not only difficult to make clinically but also prognostically insignificant.⁶⁶ Also, it was found that the

current system in 'N' staging in which ipsilateral intra-thoracic nodes based on the anatomy (hilar - N1; mediastinal -N2) are not associated with different survivals. The survival was found to be influenced by the extent of nodal involvement rather than by the location of the involved node. Consequently, for the 8th edition of UICC and AJCC staging manual, it has been proposed to redefine N1 as any involved ipsilateral, intra-thoracic nodes and N2 as involved ipsilateral supraclavicular or contralateral nodes.⁶⁷

1.7 Prognosis of MPM

The prognosis of MPM remains dismal with a median survival of 9-12 months after the first signs of illness.⁶⁸ There is however, variability ranging from a few weeks to over 10 years. Prognostication is especially important in MPM as a means of selecting patients in whom the expected survival is long enough to justify potentially hazardous treatment modalities. Previous analyses of pooled clinical trial data, have demonstrated the prognostic impact of certain demographic variables (age and gender), clinical and pathological data (haemoglobin levels, leukocyte and platelet counts, and performance status), and tumour characteristics (histological subtype) leading to the development of two scoring systems, one developed by the European Organisation for Research and Treatment of Cancer (EORTC) and the other by the Cancer and Leukaemia Group B (CALGB).⁶⁸ The EORTC prognostic model used poor performance status, high white blood cell (WBC) count, probable/possible histologic diagnosis of mesothelioma, male gender, and sarcomatoid histologic subtype to MPM patients into good prognosis (40% one year survival) and bad prognosis (12% one year).⁶⁹ The CALGB index used regression trees to examine prognostic variables in 337 patients treated in seven phase II clinical trials. Six prognostic groups were identified based on age, performance status, haemoglobin (Hb) level, WCC and the presence or absence of chest pain and weight loss. Both these prognostic scoring systems have been validated in subsequent studies.⁷⁰⁻⁷² However, these systems do not include more recently identified prognostic factors, such as clinical stage at diagnosis, hypo-albuminaemia⁷³ and the neutrophil-lymphocyte ratio (NLR).^{74,75} NLR is a

marker of systemic inflammation. It has been proposed as a prognostic factor from an analysis of a group of 173 patients undergoing systemic therapy.⁷⁵ A baseline NLR of <5 was an independent predictor of better survival. Although the prognostic value of NLR has been subsequently validated in independent studies,⁷⁶⁻⁷⁹ the cut-offs for NLR used has not been uniform in these studies. Furthermore, a retrospective study of 274 consecutive eligible, newly presenting patients from Western Australia failed to confirm the prognostic value of NLR.⁸⁰ In a recent metaanalysis (including 11 studies with 1533 MPM patients), an elevated NLR was significantly associated with a poor OS (HR=1.48, 95%CI=1.16- 1.89, P=0.001). NLR was found to be associated with histology (odds ratio (OR)=0.59, 95%CI=0.40-0.86, P=0.005), (patients with non-epithelioid histological subtype are more likely in an elevated NLR) but no other clinical factors.⁸¹

Other features like radiologic parameters at presentation as determined by scrutiny of computerized tomograms (CT) or positron emission tomography (PET), molecular and pathologic approaches, using state of the art platforms such as genomics, microRNA, epigenetics, or proteomics have been used in order to define single or combinations of candidate prognostic biomarkers from tissue or blood. However, many of these have remained un-validated in separate datasets.⁸²

Validated gene sets for prognostication of MPM have been hard to develop despite there being a multitude of studies investigating single or multiple genes in tissue for predicting MPM survival. Gordon et al.⁸³ first used the 12,000 U95 Affymetrix gene chip to develop a four-gene expression ratio test which was able to predict treatment-related patient outcome in mesothelioma, independent of the histologic subtype of the tumour. In a follow-up publication, these MPM prognostic genes and gene ratio-based prognostic tests were able to predict clinical outcome in a separate cohort of 39 independent MPM tumour specimens.⁸⁴ Pass et al.⁸⁵ also used the U133A microarray on 21 MPM samples to develop a 27-gene expression array for mesothelioma prognostication. There has, however, been variability in the gene sets and results of these prognostic tests when used in other MPM cohorts. Affymetrix U133A microarray analysis on 99 pleural

mesotheliomas from the Memorial Sloan-Kettering Cancer Centre revealed that advanced-stage, sarcomatoid histology and *P16/CDKN2A* homozygous deletion to be significant, independent, adverse prognostic factors.⁸⁶ *BAP1* and *CDKN2A* have been most extensively studied in relation to MPM prognostication. Loss of *BAP1* expression has been associated with better overall survival (OS).⁸⁷⁻⁸⁹ However, the association of *BAP1* with survival in MPM patients have not been consistent across studies. Zauderer et al.⁹⁰ studying 121 cases found no difference in survival between MPM patients who did and did not harbour *BAP1* mutations. Poor prognostic implications of both loss of p16 expression on IHC and loss of *CDKN2A* on FISH analysis have been reported.^{91,92}

1.8 Treatment of MPM

The National Comprehensive Cancer Network (NCCN) guidelines recommend that all patients affected by MPM must be managed by a multidisciplinary team with experience in thoracic neoplasms. Surgery, radiotherapy, chemotherapy and more recently immunotherapy are all used in treatment of MPM patients depending on the disease stage, performance status, age, comorbidities, and histological subtype. Selected patients could be candidates for multimodality approach and may attain acceptable long-term survival rate and acceptable perioperative risks when treated in specialized centers.⁹³ However, the proportion of such patients is very small given the delayed presentation of MPM.

1.8.1. Surgery

The role for surgery in management of MPM remains multifaceted ranging from diagnosis, radical treatment with curative intent to effective palliation. The superiority of a large surgical biopsy as compared to tru-cut biopsy or aspiration cytology for accurate diagnosis is irrefutable. The need to perform a large panel of IHC studies to confirm diagnosis requires ample tissue. Palliation in the form of video-assisted thoracoscopic surgery (VATS) pleurodesis has an established role. In a recent trial, palliative VATS partial pleurectomy was compared to talc pleurodesis alone in 196 patients. The authors found significant benefits in terms of quality of life and control of pleural

effusion, with the partial pleurectomy but at the cost of increased post-op complications, [24/78 (31%) vs 10/73 (14%); $p = 0.01$], prolonged hospital stay (median 7 vs 3 days; $p = 0.0001$) and no survival benefit.⁹⁴

Two types of operations have been developed with the aim to attain macroscopic resection of the tumour. Pleurectomy/decortication (PD) is a total pleurectomy, a lung-sparing surgery with complete removal of the involved pleura and all gross tumours. In cases that include resection of the diaphragm and pericardium, in addition to total pleurectomy, the technique is called extended PD. As an alternative, the extra-pleural pneumonectomy (EPP) is an en-bloc resection of the involved pleura, ipsilateral lung, diaphragm, and pericardium. In PD and EPP, mediastinal nodal dissection is always recommended. Comparisons between results of PD and EPP have been all retrospective but have consistently shown lower perioperative mortality, less severe morbidity profile and equivalent survival outcomes of PD to EPP.⁹⁵⁻⁹⁷ Which of these two procedures if any offers the best results in patients amenable to surgery is still debated. Although a number of retrospective studies have shown a small benefit in survival with EPP, there is agreement that even in subgroups with the best prognostic indicators (epithelial histology and NO/N1 disease), EPP still results in high complication rates with minimal symptomatic improvement.⁹⁸ The MARS trial, demonstrated the detrimental effects of conducting radical EPP surgery compared to conservative management.^{99,100} The MARS trial has been criticised as being only a small scale pilot study not adequately powered (50 patients included- representing fewer than 10% of required sample size for arm comparisons) to analyse endpoints such as survival. There have also been criticisms with regards to poor protocol compliance (6/26 in NO EPP group received surgery off protocol and only 16/24 patients in the EPP group were actually operated upon), higher than expected morbidity and mortality in the EPP group and uncontrolled chemotherapy regimens.¹⁰¹ One other criticism was that operations had been performed in relatively small volume centres with cumulative experience of the chief operating surgeons of less than 100 EPPs.¹⁰² Despite these criticisms, the MARS trial did hint to not only absence of benefit from radical surgery but also potential greater harm and thus would justify the

move away from EPP in MPM treatment. The MARS-2 trial (Clinicaltrials.gov identifier: NCT02040272) is a multicentre randomised clinical trial that seeks to evaluate the impact of extended PD on OS. Having successfully demonstrated feasibility by recruiting 50 MPM patients by December 2015, this trial is now progressing with an aim to recruit and randomize 326 patients. The results of this trial would be paramount in deciding if resectional surgery has any role at all in MPM.

1.8.2. Radiotherapy

In treatment of MPM, radiotherapy has a role as a part of a multimodality regimen but is not recommended as the sole form of treatment. The SMART protocol incorporates 25 gray (Gy) of neoadjuvant intensity modulated radiation therapy (IMRT) given in five daily fractions during one week to the entire ipsilateral hemithorax with concomitant 5 Gy boost to tumour areas. This was followed by EPP within one week of completing neoadjuvant IMRT. Adjuvant chemotherapy was offered to pN2 patients on final pathologic findings. This protocol, when applied to 25 cT1-3N0M0 operable MPM patients achieved cumulative 3-year survival of 84% in epithelial subtypes and 13% in biphasic subtypes.¹⁰³

Radiation is also useful in palliation of chest pain, bronchial or oesophageal obstruction and treatment of other symptomatic sites like brain or bone metastasis. It has been used in a preventative role to try and prevent tumour seeding in surgical port sites and scars.¹⁰⁴ The dose of radiation depends on the purpose of treatment and the timing is best discussed in a multidisciplinary setting. CT simulation- guided planning using either IMRT or conventional photo/electron radiotherapy is desirable. Post-operative radiation may reduce recurrence after EPP when given to patients with good lung and kidney function¹⁰⁵ but radiation therapy in a chest with intact lung is not seen to improve survival while increasing toxicity.¹⁰⁶ A dose of 60 Gy or more is recommended for macroscopic residual tumours covering not only the surgical bed but also the surgical scars and the biopsy tracks.¹⁰⁷ The optimum dose for palliative purposes is still remains unclear but for those with chest pain due to chest wall infiltration a 20-40 Gy dose usually provides relief.¹⁰⁴

1.8.3 Chemotherapy

Chemotherapy is recommended alone in patients with medically inoperable stage I-IV disease, those who refuse surgery or those with high grade sarcomatoid disease.^{108,109} It is also an integral part of multimodality treatment in medically operable MPM and in operable stage I-III disease; it can be given before or after surgery.

A combination of pemetrexed/cisplatin is considered the gold standard and currently the only regimen that has been approved by the FDA.¹¹⁰⁻¹¹² As such this is the only treatment demonstrated to improve survival in patients who are not operable.¹¹¹ A recent French multicentre phase III randomised control trial (MAPS study) compared adding bevacizumab to cisplatin/pemetrexed (with maintenance bevacizumab) versus cisplatin /pemetrexed alone in patients with unresectable MPM and performance score 0-2 who did not have bleeding/thrombosis.¹¹³ They demonstrated an increase in overall survival (OS) of 2.7 months in the bevacizumab + chemotherapy group compared to chemotherapy alone (18.8 vs 16.1 months; HR = 0.77; p = 0.0167) at the cost of increased hypertension and grade 3 proteinuria. Other acceptable first-line combination chemotherapy regimens include pemetrexed/carboplatin,¹¹⁴ gemcitabine/cisplatin.¹¹⁵ Carboplatin/pemetrexed combination has been found to have similar results to pemetrexed/cisplatin and is thought to be better in patients with poorer performance status.¹¹⁶ Second-line options include pemetrexed (when not used in first line), vinorelbine or gemcitabine.

1.8.4 Targeted therapy

To date, no oncogene driver mutation that may be responsive to targeted therapies in MPM has been discovered and therefore the promise of targeted therapy is yet to be realised. In MPM inactivation of TSGs by genetic or epigenetic events rather than driver mutations in oncogenes are considered to be major causative factors and this has strongly hindered the development of new therapies. Despite multiple molecular alterations as well as deregulation of signalling pathways having been evinced in MPM, a relevant target has not emerged. The presence of complex

interconnection among different signalling pathways, may explain the limited efficacy of therapeutic approaches with single specific targeted agents. Pre-clinical studies indicate that concurrent targeting of multiple components of key signalling pathways might be a valuable therapeutic option for MPM management. This approach might also allow lower doses of individual drugs, with the advantage of reducing toxicity to the patients. In addition, both pre-clinical and clinical evidence suggest that the efficacy of targeted agents can be significantly enhanced by combination with chemotherapy.¹¹⁷ A variety of biological agents have however been tested in recent times both at pre-clinical and clinical level against over-expressed targets or deregulated signalling pathways.

Bap1 loss in mice has been shown to result in increased trimethylated histone H3 lysine 27 (H3K27me3), elevated enhancer of zeste 2 polycomb repressive complex 2 subunit (*EZH2*) expression, and enhanced repression of polycomb repressive complex 2 (PRC2) targets.¹¹⁸ In a pre-clinical study, *EZH2* was found to be overexpressed in approximately 85% of MPMs compared with normal pleura, correlating with diminished patient survival. Overexpression of *EZH2* coincided with decreased levels of miR-101 and miR-26a. Knockdown of *EZH2* was found to significantly inhibited proliferation, migration, clonogenicity, and tumorigenicity of MPM cells.¹¹⁹ Mesothelioma cells that lack *BAP1* were found to be sensitive to *EZH2* pharmacologic inhibition, suggesting a novel therapeutic approach for *BAP1*-mutant malignancies.¹¹⁸ Arising from these findings, a phase II, multicenter, open-label, 2-part, single-arm, 2-stage study is being conducted to evaluate the efficacy of tazemetostat (*EZH2* inhibitor) in patients with relapsed or refractory MPM with *BAP1* loss (ClinicalTrials.gov identifier NCT02860286).

Focal adhesion kinase (FAK) is a non-receptor tyrosine kinase that mediates signalling through several downstream pathways, leading to cell migration, growth factor signalling, cell cycle progression, and cell survival.¹²⁰ Although FAK itself has not been demonstrated to be an oncogene, FAK overexpression has been reported in tumours of various tissue origins, especially in invasive and metastatic tumours.¹²¹ There is increasing evidence to indicate that FAK has an important role in

regulating cell cycle progression through cyclin D1 transcription, p27 expression, and MAPK activation.¹²² Recently, studies have indicated that FAK can suppress p53-mediated apoptosis and inhibit the transcriptional activity of p53.¹²³ FIP200, a FAK inhibitor, has been shown to induce cell cycle arrest by increasing the expression and phosphorylation of p53 in human breast cancer cells.¹²⁴ The *NF2* inactivation is known to up regulate FAK activity.¹²⁵ In a pre-clinical study, constitutive activation of FAK was found in each of 10 mesothelioma cell lines and each of the nine mesothelioma surgical specimens studied. FAK knockdown/inhibition and MDM2 inhibition caused p53 expression, apoptosis, anti-proliferative effects, and cell-cycle arrest.¹²⁶ A recent study showed that mesothelioma cells that lack *NF2* expression are more sensitive to FAK inhibition (Shapiro et al, 2014).¹²⁷

Based on these encouraging pre-clinical data, the FAK inhibitor defactinib (VS-6063) has been trialled in mesothelioma. An open label window of opportunity phase II study of Defactinib given in a neo-adjuvant setting to patients with surgically resectable MPM has been completed (ClinicalTrials.gov identifier NCT02004028). Another study (ClinicalTrials.gov identifier: NCT01938443) assessing the safety of combination treatment of GSK2256098 (FAK inhibitor) and trametinib (MEK inhibitor) in mesothelioma has also been completed. Combination of FAK inhibitor with PD-1 inhibition is also being trialled (ClinicalTrials.gov identifier: NCT02758587) and is discussed in section 1.8.6. The COMMAND trial (ClinicalTrials.gov identifier NCT01870609).was a phase II, randomized, double-blind, placebo-controlled, multicentre study of defactinib in subjects with MPM who have not progressed (confirmed partial response or stable disease) following ≥ 4 cycles of treatment with pemetrexed/cisplatin or pemetrexed/carboplatin. After establishing Merlin expression status using immunohistochemistry, subjects were randomized in a 1:1 ratio to receive oral defactinib 400 mg twice per day, or matched placebo. Randomization was stratified by tumor Merlin status (high versus low). This trial was terminated early after interim analysis failed to demonstrate any clinical efficacy of defactinib versus placebo.

Merlin also regulates mitogenic signalling by suppressing mammalian target of rapamycin complex 1 (mTORC1) in mesothelial cells and it is thought that mTORC1 signalling broadly sustains the expansion of merlin deficient cancer cells.¹²⁸ Recently, it was also discovered that the dephosphorylated conformer of merlin accumulates in the nucleus and suppresses tumorigenesis by inhibiting the cullin E3 ubiquitin ligase CRL4^{DCAF1}.¹²⁹ Cullin E3 ligases, including CRL4^{DCAF1}, are the best-characterized substrates of the ubiquitin-like modifier protein neural precursor cell expressed, developmentally down-regulated 8 (NEDD8). MLN4924 (pevonedistat) is an inhibitor of the NEDD8-activating enzyme (NAE), blocking activation of NEDD8 and thereby depleting the pool of active NEDD8.¹³⁰ In a pre-clinical study it was shown that inhibition of CRL4^{DCAF1} using MLN4924 sensitizes cells to traditional chemotherapy but displays limited preclinical activity even in combination with chemotherapy. However, combined inhibition of CRL4^{DCAF1} and mTOR/PI3K almost completely suppresses the growth of NF2 loss-driven tumors.¹³¹ Importantly, a recent phase I study of MLN4924 in patients with advanced solid tumors established efficient ontarget inhibition of NAE, acceptable dose-limiting toxicities, and antitumorigenic activity in some patients.¹³² A single institution phase I/II study looking at the efficacy and adverse effect profile of pevonedistat when given either alone or in combination with standard (cisplatin/pemetrexed) in patients with *NF2* mutant mesothelioma is now underway at the Memorial Sloan Kettering Cancer Centre (ClinicalTrials.gov identifier: NCT03319537).

A phase II study of mTOR inhibitor everolimus (RAD001) (SWOG S0722) in inoperable MPM patients who had received one to two prior line of platinum based chemotherapy yielded very poor results. When treated with 10 mg of everolimus daily, overall response rate was 2%. The 4-month progression free survival (PFS) rate was 29% (95% CI: 17–41%), and the median OS was 6.3 months: leading the investigators to conclude that additional studies of single-agent everolimus in advanced MPM are not warranted.¹³³

Studies have indicated that asbestos fibres can physically interact with epidermal growth factor receptor (EGFR), causing its auto phosphorylation and activation with downstream induction of MAPK and/or protein kinase B (AKT) downstream signalling cascades.¹³⁴ It can also up-regulate EGFR mRNA and protein expression. Based on this, anti- EGFR tyrosine kinase inhibitors (TKIs) have been trialled in MPM. A phase II studies in advanced or recurrent MPM patients reported that erlotinib and gefitinib (ATP-competitive, small-molecule EGFR tyrosine kinase inhibitors, TKIs) were not effective as single-agents^{135,136} despite overexpression of EGFR being detected in 50–95% of cases. The low prevalence of EGFR activating mutations may explain the lack of clinical efficacy. Studies on the combination with cytotoxic therapies, such as the study evaluating the combination of gefitinib with gemcitabine and cisplatin, did not show any synergistic or additive effects in vitro.¹³⁷ A study of cetuximab combined with cisplatin or carboplatin/pemetrexed as first line treatment in patients with MPM with EGFR protein over-expression is ongoing (MesoMab; ClinicalTrials.gov identifier NCT00996567).

Insulin growth factor receptors (IGF-1R and IGF-2R) together with insulin growth factor (IGF) are expressed in MPM cells. It has been reported that signalling mediated by insulin receptor substrate (IRS)-1 is associated with increased cellular growth, whereas signalling through IRS-2 is associated with increased cellular motility. The efficacy of cixutumumab, a fully human monoclonal antibody to IGF-1R, has been investigated in relation with IGF-1R expression in a panel of established cell lines and in early passage tumour cells obtained from MPM patients.¹³⁸ A strong correlation was found between the IGF-1R expression level and cixutumumab anti-tumour activity. There is an ongoing phase II study (ClinicalTrials.gov identifier NCT01160458) testing cixutumumab as single agent in pre-treated MPM patients.

MET is expressed in the majority of MPMs, and its activation by the related ligand (hepatocyte growth factor/scattering factor, HGF/SF) contributes to disease pathogenesis by promoting cell growth and survival, motility and invasion. Tivantinib, a selective non-ATP competitive oral inhibitor

of MET, has been tested in MPM cell and mouse xenograft models in combination with GDC-0980 and NVP-BEZ235, dual inhibitors of class I isoforms of PI3K and mTOR. This combination was strongly synergic in suppressing MPM cell proliferation and tumour growth.¹³⁹ A Phase I/II study to evaluate the safety and tolerability of tivantinib in combination with carboplatin and pemetrexed as first-line treatment in patients with advanced non-squamous non-small cell lung cancer (NSCLC) or MPM is currently recruiting patients (ClinicalTrials.gov identifier NCT0204906)

Bevacizumab is a humanized monoclonal antibody neutralizing all of the isoforms of human vascular endothelial growth factor (VEGF). Its addition to pemetrexed/cisplatin chemotherapy was shown to improve survival in the MAPS study.¹¹³ Nintedanib is a small molecule tyrosine-kinase inhibitor, targeting vascular endothelial growth factor receptor (VEGFR), fibroblast growth factor receptor (FGFR) and platelet derived growth factor receptor (PDGFR). In the recently reported phase II results of the LUME-Meso trial, 87 chemotherapy-naïve patients with unresectable non-sarcomatoid MPM were randomly assigned in a 1:1 ratio to up to six cycles of pemetrexed and cisplatin plus nintedanib (200 mg twice daily) or placebo followed by nintedanib plus placebo monotherapy until progression. PFS was significantly better with nintedanib (HR, 0.54; 95% CI, 0.33 to 0.87; P = .010) and there was a trend toward improved OS favouring nintedanib (HR, 0.77; 95% CI, 0.46 to 1.29; P = .319). Benefit was evident in epithelioid histology, with a median OS gain of 5.4 months and median PFS gain of 4.0 months. Neutropenia was the most frequent grade3 adverse event (AE; nintedanib 43.2% v placebo 12.2%); rates of febrile neutropenia were low (4.5% in nintedanib group v 0% in placebo group). A global, prospectively randomized, phase III trial is recruiting patients with epithelioid MPM to confirm the activity of nintedanib in this patient population (ClinicalTrials.gov Identifier: NCT01907100). In addition, there are two other trials; a phase II trial investigating nintedanib in recurrent MPM (ClinicalTrials.gov Identifier NCT02568449) and a further phase II trial investigating nintedanib as switch maintenance treatment in MPM (NEMO) (ClinicalTrials.gov Identifier: NCT02863055). An additional trial is also investigating

combinations of pemetrexed and cisplatin with cediranib (an oral inhibitor of PDGFR and VEGF-1, -2, and -3 receptor family) (phase I/II ClinicalTrials.gov identifier NCT01064648).

Mesothelin is a glycoprotein physiologically expressed on the surface of mesothelial cells and highly expressed in many cancers including MPM. For this reason it is considered a tumour antigen and an appropriate target for immunotherapy.¹⁴⁰ Pre-clinical studies indicate that mesothelin expression promotes cell invasion and matrix metalloproteinase secretion both in vitro and in an orthotopic MPM model.¹⁴¹ Amatuximab which is a chimeric monoclonal antibody directed against mesothelin and was tested combined with pemetrexed and cisplatin in a single-arm phase II study in 89 patients with unresectable MPM. Although there was no improvement in PFS (6.1 months), the median OS was superior (14.8 months) to historical controls (13.3 months).¹⁴² A phase II double-blind, randomized multicentre study (ClinicalTrials.gov identifier NCT02357147) of amatuximab 5 mg/kg, administered weekly, in combination with pemetrexed and cisplatin as first line treatment in subjects with unresectable MPM is currently recruiting patients. Anetumab ravtansine (BAY94-9343) is a fully human anti-mesothelin antibody conjugated to the maytansinoid tubulin inhibitor DM4 with efficacy in pre-clinical studies.¹⁴³ In a phase I study (ClinicalTrials.gov identifier NCT01439152); anetumab ravtansine at the maximum tolerated dose (6.5 mg/kg) was well tolerated and showed encouraging durable tumour responses in patients with metastatic mesothelioma. A phase Ib study of anetumab ravtansine in combination with pemetrexed and cisplatin in mesothelin- expressing solid tumours (ClinicalTrials.gov identifier NCT02639091) and a randomized phase II study of anetumab ravtansine or vinorelbine in patients with MPM overexpressing mesothelin in the second-line setting (ClinicalTrials.gov identifier NCT02610140) are recruiting patients. SS1P is a recombinant anti-mesothelin immunotoxin that consists of a murine antimesothelin variable antibody fragment linked to PE38, a portion of *Pseudomonas* exotoxin A. SS1P was tested in a phase I trial (ClinicalTrials.gov identifier NCT01445392) in combination with pemetrexed and cisplatin in chemotherapy-naive patients. The combination of SS1P with cisplatin and pemetrexed resulted in response rates of 60% in 20 evaluable patients and 77% in 13 patients who received the MTD (45

mcg/kg).¹⁴⁴ SS1P combined with pentostatin and cyclophosphamide, with the aim to minimize neutralizing antibody formation, is under evaluation in a phase I/II trial (ClinicalTrials.gov identifier NCT01362790).

1.8.5 Epigenetic targeted therapy

Knowledge regarding the mechanisms and clinical relevance of epigenetic derangements in MPM is only just evolving.^{145,146} Although initially thought not to contribute to the pathogenesis of mesotheliomas, it has become clear that epigenetic alterations are common events in this disease. MPM exhibit silencing of tumor suppressor genes via site specific DNA hypermethylation and/or polycomb repressive complexes in the context of genome wide hypomethylation that facilitates loss of imprinting (LOI) and de-repression of cancer-germline (CG) genes.¹⁴⁷ DNA methyltransferases (DNMTs) were perceived to be attractive targets for MPM therapy because of their direct roles in silencing tumor suppressor genes and maintaining pluripotency.¹⁴⁸ However, in what was a disappointing result, Yogelzang et al. reported only a 17% objective response rate in 41 MPM patients receiving continuous 120 hours dihydro-5-azacytidine (a DNA methyltransferase inhibitor) infusions.¹⁴⁹ Similarly, trial of continuous 72 h decitabine (5-aza-2'-deoxycytidine, an nucleic acid synthesis inhibitor) infusions yielded only transient stabilization of disease in 2 of 6 MPM patients treated.¹⁵⁰ Efforts to target histone deacetylases (HDACs) in MPM have been discouraging as well. When 661 MPM patients were randomized to receive the vorinostat (HDAC inhibitor), or placebo as 2nd or 3rd line therapy, median OS for vorinostat treated patients was 30.7 weeks (95% CI: 26.7–36.1) compared to 27.1 weeks (95% CI: 23.1–31.9) for patients receiving placebo.¹⁵¹ Interestingly, preclinical studies have demonstrated that DNA demethylating agents and HDAC inhibitors mediate potentially significant immunomodulatory effects.¹⁵² This has therefore generated interest in utilizing chromatin remodeling agents in conjunction with either adoptive cell transfer or immune checkpoint inhibitors for cancer therapy. Recently, Corve *et al.*¹⁵³ evaluated the potential efficacy of combining a gene induction regimen with anti-CTLA 4 therapy in MPM. The murine anti-CTLA4 Mab 9H10 did not significantly inhibit growth of MPM xenografts. 5-azacytidine (5-AZA) induced a slight

but insignificant reduction in growth of MPM xenografts. In contrast, combined 5-AZA/9H10 treatment mediated an 81% inhibition of MPM xenograft growth ($P < 0.05$). These along with observations that combined decitabine/GSK126 (EZH2 inhibitor) or 5-AZA/entinostat (HDAC inhibitor) treatment markedly augment efficacy of adoptively transferred cytotoxic T lymphocytes or anti-PD-L1 via up-regulation of Th1 signalling and inhibition of immunosuppressive myeloid derived suppressor cells within the tumor microenvironment in murine cancer models^{154,155} could encourage evaluation of such combinatorial regimens in clinical settings.

Argininosuccinate synthetase1 (ASS1) is a urea cycle and arginine biosynthetic enzyme. Arginine is essential for biosynthesis of proteins, nitric oxide, and polyamines and contributes to proline and glutamate production.¹⁵⁶ ASS1 is a tumor suppressor gene and its loss is known to occur due to epigenetic mechanisms. Tumors deficient in ASS1 display increased tumorigenesis due to diversion of the precursor aspartate for enhanced pyrimidine synthesis.^{157,158} Exogenous arginine is dispensable for normal cells due to ASS1 expression, whereas its supply is essential for ASS1-negative cancers. Various ASS1-negative tumors have been shown to be sensitive to the arginine depleters, mycoplasma-derived pegylated arginine deiminase (ADI-PEG20) and recombinant human arginases, in preclinical studies.^{159,160} This led to several arginine deprivation studies in patients with hepatocellular carcinoma and melanoma with single-agent ADI-PEG20, showing low toxicity and evidence of efficacy.^{161,162} Loss of the ASS1 was observed in 63% of archival mesotheliomas by immunohistochemical analysis in mesothelioma cell lines.¹⁶³ A multicentre phase II randomized clinical trial, the Arginine Deiminase and Mesothelioma (ADAM) study, assessed the clinical impact of arginine depletion in patients with ASS1-deficient MPM. Immunohistochemical screening of 201 patients identified 68 with advanced ASS1-deficient MPM. They were randomized 2:1 to arginine deprivation (ADI-PEG20, 36.8mg/m², weekly intramuscular) plus best supportive care (BSC) or BSC alone. At median follow-up of 38 (2.5-39) months, the PFS hazard ratio was 0.56 (95%CI, 0.33-0.96), with a median of 3.2 months in the ADI-PEG20 group vs 2.0 months in the BSC group ($p = .03$). The OS curves crossed, and life expectancy was 15.7 months in the ADI-PEG20 group vs 12.1 months in the

BSC group (difference of 3.6 [95%CI, -1.0 to 8.1] months; $P = .13$). The incidence of symptomatic adverse events of grade at least 3 was 11 of 44 (25%) in the ADI-PEG20 group vs 4 of 24 (17%) in the BSC group ($P = .43$), the most common being immune related, non-febrile neutropenia, gastrointestinal events, and fatigue. Differential *ASS1* gene-body methylation correlated with *ASS1* immunohistochemistry, and longer arginine deprivation correlated with improved PFS.¹⁶⁴

The TRAP (ClinicalTrials.gov identifier NCT02029690) trial was a phase I trial that sought to estimate the efficacy of ADI-PEG20 when used in combination with first line pemetrexed and cisplatin in several cancers including MPM. It revealed a 94% disease control rate in non-epithelioid (biphasic and sarcomatoid) MPM subtypes.¹⁶⁵ ATOMIC-Meso (ClinicalTrials.gov identifier NCT02709512) is an ongoing large randomized, double-blind, phase II/III study in MPM patients with low *ASS1* expression to assess ADI-PEG 20 with pemetrexed and cisplatin. Up to 386 good performance (ECOG 0-1) patients with non-epithelioid MPM are expected to be enrolled. Patients will be randomized to receive weekly ADI-PEG20 (36 mg/m² IM) or placebo with standard doses of pemetrexed and cisplatin for a maximum of 18 weeks (6 cycles) of treatment.

Given the frequency and negative prognostic impact of EZH2 over-expression in MPM (90, 92), PRC-2 has emerged as a major therapeutic target in these neoplasms- particularly those with BAP1 mutations. Whereas DZNep is not available for clinical trials, several potent and specific inhibitors of EZH2 activity are in early clinical development. A multicenter phase II trial (NCT02860286) is underway to examine response rates in patients with inoperable, BAP1 mutant MPM treated with oral tazemetostat (800 mg BID). A two arm phase II trial will commence in the near future at the NCI to examine response rates in patients with wild type vs mutant BAP1 MPM receiving GSK126 as induction therapy prior to pleurectomy/decortication; a variety of translational endpoints will be assessed in this trial. Additionally, mithramycin, which depletes EZH2 as well as several other PRC-2 associated proteins (102), is being evaluated in patients with inoperable thoracic malignancies (including MPM) at the NCI (NCT01624090, NCT02859415). It may be possible to further exploit

BAP1 mutations for MPM therapy. BAP1 functions to stabilize BRCA-1 and promote poly (ADP-ribose)-dependent recruitment of polycomb deubiquitylase complex PR-DUB to DNA damage sites (126,127). This activity is dependent on deubiquitinase activity as well as phosphorylation of BAP1 (128). BAP1 mutations, which always appear to be manifested as loss of function, decrease BRCA-1 levels (129), and inhibit double strand DNA repair (126-128). Parotta et al (130) observed that a BAP1 isoform lacking part of the catalytic domain sensitized MPM cells to the PARP1 inhibitor, olaparid; and this sensitivity could be augmented by concomitant treatment with the dual PI3K-mTOR inhibitor, GDC0980, which down regulates BRCA-1. Such strategies might enhance responses to cisplatin/pemetrexed in patients with BAP1 mutant MPM, and should be evaluated in future clinical trials.

1.8.6 Immunotherapy

Immune based therapy, especially checkpoint inhibition has shifted treatment paradigms in many cancers types and initial data showed promise for improving MPM treatment. Several different approaches to immunotherapy including cytokines (IL-2), therapeutic vaccines and adoptive transfer of lymphocytes have been applied to MPM treatment with variable results.¹⁶⁶ However, it has been the studies incorporating immune checkpoint inhibitors into MPM treatment which have shown unprecedented activity^{167,168} and as such have infused considerable enthusiasm and optimism.

Initial enthusiasm for checkpoint inhibition in MPM was created by studies investigating tremelimumab [anti- cytotoxic T-lymphocyte associated protein 4 (CTLA-4) antibody]. In an open-label, single-arm, phase 2 study, among 29 patients treated with at least one dose of tremelimumab (15mg/kg every 90 days) after a first line platinum-based chemotherapy, the authors noted disease control in nine (31%) patients; a median PFS of 6.2 months (95% CI 1.3-11.1) and a median OS of 10.7 months (0.0-21.9).¹⁶⁷ The same authors investigated an intensified dosage regimen (10mg/kg every 4 weeks; 1-6 doses) in 29 advanced mesothelioma patients. They achieved a partial response

in one patient (3%) and disease control in 11 (38%) patients. Grade 1-2 treatment-related adverse events (TRAE) occurred in 26 (90%) patients and grade 3-4 adverse events in two (7%) patients.¹⁶⁸ A much larger multi-institutional, multi-national study (DETERMINE) however demonstrated no statistically significant difference in OS for tremelimumab vs placebo (median 7.7 vs 7.3 months; HR = 0.92, 95% CI 0.76–1.12, P = 0.408). In this phase 2b, randomized, double-blind study of unresectable pleural or peritoneal MPM, eligible patients who progressed after 1–2 lines of prior therapy were randomized 2:1 to receive tremelimumab (10 mg/kg q4w for 7 doses, then q12w) or placebo. Five hundred and seventy-one patients were randomized (382 to tremelimumab, 189 to placebo).¹⁶⁹

The keynote-028 study evaluated the response to whether {anti-programmed cell death protein 1(PD-1) antibody} in (programmed cell death ligand 1 (PD-L1) positive advanced solid tumours. In this phase Ib trial 25 patients with PD-L1 positive pleural MPM were treated with pembrolizumab 10 mg/kg given every 2 weeks for up to 2 years or until confirmed progression or unacceptable toxicity. Preliminary overall response rate (confirmed and unconfirmed) was 24% (n = 6); 13 patients (52%) had stable disease, resulting in a disease control rate of 76%. Four patients (16%) had progressive disease, and 2 patients had no assessment at the time of analysis. Fifteen patients (60%) experienced a drug-related adverse event of which only 3 (12%) were grade ≥ 3 .¹⁷⁰ Another phase II trial is currently underway to determine the objective response rate of patients with MPM treated with pembrolizumab in an unselected patient population, as well as in a PD-L1 positive population (ClinicalTrials identifier no NCT02399371). This trial also seeks to determine the optimal threshold for PD-L1 expression using the 22C3 antibody based immunohistochemistry (IHC) assay in correlation to tumour response. Another phase II study being conducted in the Netherlands (ClinicalTrials identifier no NCT02497508) aims to evaluate the response of previously treated MPM to nivolumab (IgG4 anti-PD-1 monoclonal antibody) given at 3 mg/kg every 3 weeks. Initial reports from this study of PD-L1 unselected patients demonstrated a disease control rate of 39% in the 18

patients who were evaluated at 18 weeks. Five patients had partial response and two had stable disease. Nine patients had progressive disease.¹⁷¹

Avelumab is a fully human anti-PD-L1 IgG1 antibody under clinical investigation in multiple cancers. A phase I, open label study (The JAVELIN trial) (ClinicalTrials identifier no NCT01772004) studied the safety, tolerability, pharmacokinetics biological and clinical efficacy in patients with metastatic or locally advanced solid tumour.¹⁷² The results were presented at ASCO 2016. In this trial, 53 patients with unresectable pleural or peritoneal (mostly pleural) mesothelioma who had progressed after a platinum-pemetrexed-containing regimen and were unselected for PD-L1 expression, were treated with Avelumab 10 mg/kg IV every two weeks until progression, unacceptable toxicity, or withdrawal. Most patients had received more than two lines of therapy indicating that it was a highly selected subgroup. Disease control rate observed was 56.6% with unconfirmed objective response rate (ORR) of 9.4% (5 PRs; 95% CI: 3.1, 20.7). Stable disease was observed in 25 patients (47.2%). Median PFS was 17.1 weeks (95% CI: 6.1, 30.1). Interestingly, objective responses were seen in both PD-L1+ (14.3%; 2/14) and PD-L1—patients (8%; 2/25) with median PFS of 17.1 weeks and 7.4 weeks respectively. TRAEs occurred in 41 patients (77.4%); most common were infusion-related reactions (20 [37.7%]), fatigue (8 [15.1%]), chills (8 [15.1%]), and pyrexia (6 [11.3%]). All were grade 1 or 2. Grade ≥ 3 TRAEs occurred in 4 patients and included colitis, decreased lymphocytes and altered liver functions.

PROMISE-meso (ClinicalTrials.gov Identifier: NCT02991482) is a multicentre randomised phase III trial seeking to compare pembrolizumab versus standard chemotherapy with vinorelbine or gemcitabine and for advanced MPM that has progressed on platinum based therapy. It is expected to enrol 142 patients and results expected after 2020. CONFIRM (ClinicalTrials.gov Identifier: NCT03063450) is a randomized, double blind placebo controlled trial of patients with mesothelioma who are third relapse following a platinum based chemotherapy treatment. 336 patients recruited from 25 UK centres over a four-year period are expected to be randomized in a 2:1 ratio (nivolumab:

placebo). All patients will be on treatment for 12 months unless they progress or withdrawal prior to this.

Results of immune checkpoint inhibitor trials in multiple cancers to date have been encouraging but can hardly be called satisfactory. Less than 20% of unselected patients across different cancers mount a response to single-agent immune checkpoint inhibition.¹⁷³ Attempts to optimize the anti-tumour immune response are now being made by combining two different immune checkpoint inhibitors or an immune checkpoint inhibitor and a therapeutic cancer vaccine. Anti-CTLA-4 antibody treatment has the potential to drive T-lymphocytes into the tumour. This can cause up regulation of PD-L1 expression in the tumour micro environment thus potentially increasing response to anti-PD-1/PD-L1 therapy. This combination has induced immune synergy in patients with various tumour types. CheckMate 067 (a phase III study in previously untreated advanced melanoma) randomized 945 patients to receive ipilimumab, nivolumab, or the combination. The progression-free survival (PFS) was 11.5 months (95% CI, 8.9–16.7) for the combination compared to 2.9 months (95% CI, 2.8–3.4; $P < 0.001$) for ipilimumab alone and 6.9 months (95% CI, 4.3–9.5; $P < 0.001$) for nivolumab alone. More interestingly, the PFS was same for the combination group and the nivolumab group (14 months) among patients with PD-L1-positive tumours but PFS was longer with the combination therapy than with nivolumab alone (11.2 vs. 5.3 months) among PD-L1 negative tumours¹⁷⁴. Preliminary results in RCC¹⁷⁵ and NSCLC¹⁷⁶ also appear to demonstrate better results with nivolumab and ipilimumab as compared to nivolumab alone.

In MPM, the NIBIT-MESO-1 trial (ClinicalTrials.gov identifier no NCT02588131) is a phase II, open-label, study evaluating the efficacy and safety of combination of tremelumimab and anti-PD-L1 MEDI4736 (Darvalumab). The safety analysis from the fully-enrolled NIBIT-MESO-1 study was presented in ASCO 2017. Forty mesothelioma patients (38 pleural and 2 peritoneal),

median age 64 years (range 41-80), ECOG performance status 0 (n = 19) or 1 (n = 21) were enrolled in the study. At the time of data collection (January 2017), the patients (12 1st line; 28nd line) had received a median of 5.5 doses of therapy (range = 1-13). Twenty-four patients (60%) had experienced any grade immune related adverse effects (irAEs) : 5 patients (12.5%) had grade 3-4 adverse effects, the most frequent being hepatotoxicity (7.5%). Three patients (7.5%) were discontinued due to treatment-related AEs (1 thrombocytopenia, 1 limbic encephalitis, 1 liver toxicity).¹⁷⁷ Another phase II study (ClinicalTrials.gov identifier no NCT0 271672; MAPS-2) is comparing nivolumab + ipilimumab versus nivolumab alone in unresectable advanced MPM. This is a multicentre randomized non comparative phase II trial in which histologically proven MPM relapsing after 1 or 2 prior lines including pemetrexed/platinum doublet with measurable disease and PS<1 were randomized 1:1 to receive nivolumab 3 mg/kg q2w, or nivolumab 3 mg/kg q2w + ipilimumab 1 mg/kg q6w, until progression or unacceptable toxicity. The results were presented in ASCO 2017 and the twelve weeks-disease control rate in the first 108 eligible patients was found to be 42.6% [IC95%: 29.4-55.8%] with nivolumab (n=23/54), and 51.9% [38.5-65.2%] with nivolumab + ipilimumab (n=28/54). ORR was 16.7% [6.7%-26.6%] with nivolumab (n=9/54), and 25.9% [14.2-37.6%] with nivolumab + ipilimumab (n=14/54). All grade/grade 3-4 toxicities were slightly increased in the combination arm (86.9%/16.4%) vs nivolumab alone (77.8%/9.5%); 3 treatment-related deaths were observed in the combo arm (1 metabolic encephalopathy, 1 fulminant hepatitis, 1 acute renal failure).¹⁷⁸

Some other combinations are also being actively explored. Preclinical studies that focal adhesion kinase (FAK) inhibition can re-model multiple aspects of the tumour immune microenvironment, shifting the balance from inhibitory Tregs, & MDSCs, to one which supports an active CD8+ T cell adaptive immune response, suitable for synergistic anti-PD-1 therapy.^{179,180} Based on this, a phase I/IIa clinical study of defactinib (FAK inhibitor) in combination with pembrolizumab (anti-PD-1) therapy is ongoing in several solid tumours including mesothelioma (ClinicalTrials.gov identifier:

NCT02758587). Combinations of VEGF inhibitor (axatinib) and PD-L1 inhibitor (avelumab) is being studied (ClinicalTrials.gov identifier: NCT02493751) in advanced renal cell carcinoma and initial results presented in ESMO 2016 (OCT 2016), clinical benefit was seen in all six patients treated with 5 patients showing partial response. Another trial is investigating combination of axatinib with pembrolizumab (ClinicalTrials.gov identifier: NCT02133742) again in advanced renal cell carcinoma. Given the recent results of MAPS study and the encouraging results of checkpoint inhibition in MPM, this combination could be an avenue to explore. However, there are no trials investigating this combination in MPM to the best of my knowledge.

Response to immune checkpoint inhibition in MPM like in most other malignancies has not been uniform and predicting which patients with MPM are most likely to benefit with anti-PD-1/PD-L1 therapy has been difficult. A multitude of biomarkers predominantly involving indices from the patient's tumour (cancer cells or cells of the tumour microenvironment) or blood (circulating cells or serum) have been studied in many cancers. In MPM, the MESOT-TREM-2008 study explored different immune markers potentially predictive of response to treatment and/or of survival. Circulating levels of CD4⁺-inducible costimulator (ICOS)⁺ T-cell subpopulation were found to be increased in the course of therapy with tremelimumab, and they significantly associated with a better survival in the early phases of treatment.¹⁶⁷

As results of trials looking at checkpoint inhibition therapy in various malignancies become available, it is becoming clear that there are three broad populations of patients i.e. responders: those that respond initially and continue to respond; those that fail to ever respond (innate resistance), and those that initially respond but eventually develop disease progression (acquired resistance).¹⁸¹ Mechanisms of innate and acquired resistance to checkpoint inhibition therapy are incompletely understood but are understandably very important in order to individualize and guide optimal combination/sequencing immunotherapy. Insufficient generation of anti-tumour T cells is one modality of resistance to checkpoint inhibition therapy. Genetic and epigenetic alterations

which influence neoantigen formation, presentation, and/or processing, as well as alterations in cellular signalling pathways that disrupt the action of cytotoxic T cells can lead to insufficient anti-tumour T cells.¹⁸² Inadequate function of the tumour-specific T cells is thought to be another cause of ineffectiveness of checkpoint inhibition therapy. This is because the expanded repertoire of anti-tumour T cells faces an inhospitable tumour micro environment that may preclude proper T-cell function. Mutations in key effector pathways, high levels of PD-L1 on tumour cells, high levels of alternate immune checkpoints or co-inhibitory receptors on T cells (e.g., PD-1, CTLA-4, TIM3, LAG3 etc.), high levels of immune suppressive cytokines or metabolites, and associated recruitment of immune suppressive cells are some of the causes of inadequate function.^{183,184} How these mechanisms of checkpoint inhibition failure relate to MPM remains to be studied.

1.9 Conclusion

MPM is a deadly malignancy mainly arising as a result of occupational exposure to asbestos. Long latency and delayed presentation lead to most patients presenting late in the stage of the disease. Treatment options are limited and as of now, the survival remains dismal. Multimodality treatment incorporating aggressive resectional surgery, pre or post-operative chemotherapy and hemi thoracic irradiation have been seen to marginally improve survival but the proportion of patients suitable for such approach is low.

The promise of targeted therapy has not been realized in MPM and majority of clinical trials of molecular agents targeting the classical hallmarks of cancers have yielded disappointing results. In fact, a clear targetable driver event has not been identified. It has now becoming clearer that a more comprehensive knowledge of the multiple molecular alterations, deregulation of the different signalling pathways as well as their interaction in MPM is required. This will be essential to better identify target/s which are able to address the complex interconnection among different signalling pathways, which limits the efficacy of these therapeutic approaches.

Immunotherapy has shown promise in improving outcome in MPM patients and recently reported trials using checkpoint inhibitors have been encouraging. However, not all patients have derived benefit and credible and reproducible biomarkers have yet to be identified. It has become obvious that we would need to improve our ability to predict which patients will benefit. Also, given the multitude of immunomodulatory factors known to be present in the tumour microenvironment, a better understanding of these factors will be needed to be able to tailor immunotherapy either alone or in combination to individual cases based on the profile of their immune microenvironment.

An impediment to the study of MPM is its relative rarity and also the lack of large well annotated cohorts to study these parameters. In the research described in the thesis, we have used a large well annotated cohort of confirmed MPM patients and their archival formalin fixed paraffin embedded (FFPE) tissue to study the genomic changes and the tumour immune microenvironment, two areas which have shown potential in development of novel therapeutic approaches in multiple other cancers.

Chapter 2: Materials and methods

All general materials and methods used in this research are described in this chapter. Additional methods and details of the statistical analysis relevant to a specific chapter are described accordingly.

2.1 Generation of the MPM cohort

Ethics approval was obtained from the human research ethics committee of the Austin hospital, Melbourne, Australia (Local Reference Number: H2006/02394). In collaboration with our co-researchers in the Department of Thoracic Surgery, Austin Hospital, Heidelberg, Melbourne, we conducted a retrospective search of the prospectively maintained thoracic surgery database. We searched for all patients who were operated with a diagnosis of pleural mesothelioma between 1988 and 2014. This included patients undergoing diagnostic surgery (pleural biopsies via thoracotomy or thoracoscopy), resectional surgery (pleurectomy and decortication or extra pleural pneumonectomy) or palliative procedures (pleurodesis).

2.2 Collection of clinical data: clinical annotation of the cohort

A thorough search of the medical records of each individual patient identified from the database was conducted. Paper records were retrieved from the medical records department of the Austin Hospital. For patients who were operated after 2009, electronic medical records were available and were accessed in lieu of paper records. Data pertaining to the demographics, mode of presentation and symptoms, investigations and their results, clinical staging information based on pre-operative investigations, operations performed, operative findings, post-operative treatment (chemotherapy, radiotherapy) and dates of death (where death was known to have occurred)/last follow up were captured. For patients in whom the survival status was not clearly documented in the records, the information was sourced from the Victorian Cancer Registry of the Cancer Council Victoria.

2.3 Collection of archival formalin fixed paraffin embedded (FFPE) MPM samples

A search was conducted of the Kestral record software of the Department of Anatomical Pathology, Austin Hospital for the report of the original histopathological examination. They were reviewed to record their unique identifying biopsy numbers, to corroborate the diagnosis of MPM and to record data regarding the histological subtype classification and results of any IHC that had been done. Also, when indicated by the pathologist, the block with the best and most representative tumour was recorded. The FFPE blocks corresponding to the biopsy numbers were then retrieved from the archives of the department. While a single most representative block with ample tumour tissue was chosen for most patients, when the tumour was thought to be scant in one block, two or more blocks were retrieved. When patients had undergone more than one operation (for example, biopsy followed by resectional surgery), the blocks of FFPE tissue available from both instances were retrieved but kept separately.

2.4 Confirmation of diagnosis of MPM

Regardless of the initial assessment at the time of the diagnosis, all FFPE tumour samples were subjected to diagnostic reassessment based on the morphology and also the IHC profile. Four μm sections of all blocks were cut and stained with Hematoxylin and Eosin (H&E) and these were assessed for tumour content and morphology by a pathologist (Dr. Khashyar Asadi, Department of Anatomical Pathology, Austin Hospital).

The IHC based markers used in the initial diagnosis was not uniform across samples. As the samples were derived from a very long time period, many of the markers used presently would not have been available in the time of diagnosis of older samples. Based on the IHC profile information available from original histopathology report, samples were divided into:

Group A: Adequate IHC done at time of diagnosis. Confirmed MPM diagnosis based on tumour morphology and IHC profile.

Group B: Some IHC was done at time of diagnosis but the IHC profile was not adequate to confidently call a diagnosis of MPM

Group C: No IHC done at the time of diagnosis. Confirmation of MPM could not be made.

In consultation with the pathologist (KA) and in keeping with the current panel of IHC markers used to diagnose MPM and rule out metastatic pleural disease, a panel of markers were chosen. They were as follows: [mesothelial markers: Calretinin (clone- DAK- Calret1 Dako, Glostrup, Denmark), WT-1(clone- 6F-H2 Dako, Glostrup, Denmark) and CK5/6 (clone- D5/16 B4 Dako, Glostrup, Denmark), epithelial markers: BER-EP4(clone- Ber-EP4 Dako, Glostrup, Denmark) , CEA(clone - IL7 Dako, Glostrup, Denmark) and MOC31(clone – MOC-31 Dako, Glostrup, Denmark)]. Samples in group C were stained with all these markers while those in group B were stained with the markers that had not been done at the time of their diagnosis. Histological diagnosis of MPM was only confirmed after review of the tumour morphology (H&E) and IHC profile. Samples not satisfying either/any of these criteria were excluded from further study.

2.5 Construction of the MPM tissue microarray (TMA)

H&E stained sections of samples for which a diagnosis of MPM could be confidently established were reviewed by the pathologist (KA) for tumour content. Areas of tumour were marked on the slides. Samples with inadequate tumour (in which the amount of archival tissue available was deemed not enough to make 3x1 mm cores) were excluded at this stage.

TMA's were created using a tissue arrayer (Tissue Arrayer I, Beecher Instruments Inc, Sun Prairie, Wis, USA). One millimetre cores were taken from areas in the block which corresponded to tumour marked on the H&E slides. The cores were transplanted to empty pre-made paraffin recipient blocks. The cores were arranged in nine columns and seven rows with columns named numerically and rows named alphabetically. Additional orientation cores were placed in front of rows A and D. Three cores were taken from different areas of the tumour and placed sequentially in the rows. Sixty –three

cores from 23 samples were therefore placed in each TMA. Sixteen TMAs with MPM tissue samples were therefore created. When there were more than one tissue samples from any particular patient (arising from operations performed at different time points), we ensured that all cores included in the TMA came from the same biopsy. Duplication of representation in the TMA due to multiple tissue samples was avoided.

After the creation of the TMA, the recipient block was kept at 37°C for one hour, followed by room temperature for one hour. This was repeated three times and at the end of the procedure, the block was left at 37°C overnight. The blocks were then stored in room temperature. For assessment of the cores, four µm cuts of the TMAs were stained with H&E and reviewed by the pathologist (KA) for tumour content and for presence of excessive necrotic or crushed tissue. Cores with insufficient tumour content (<20%) were marked on the TMA grid constructed so as to exclude them from assessment and analysis in further studies. A flow chart of collection of patients, their archival samples, their assessment and final TMA construction is depicted below (Figure 2.1).

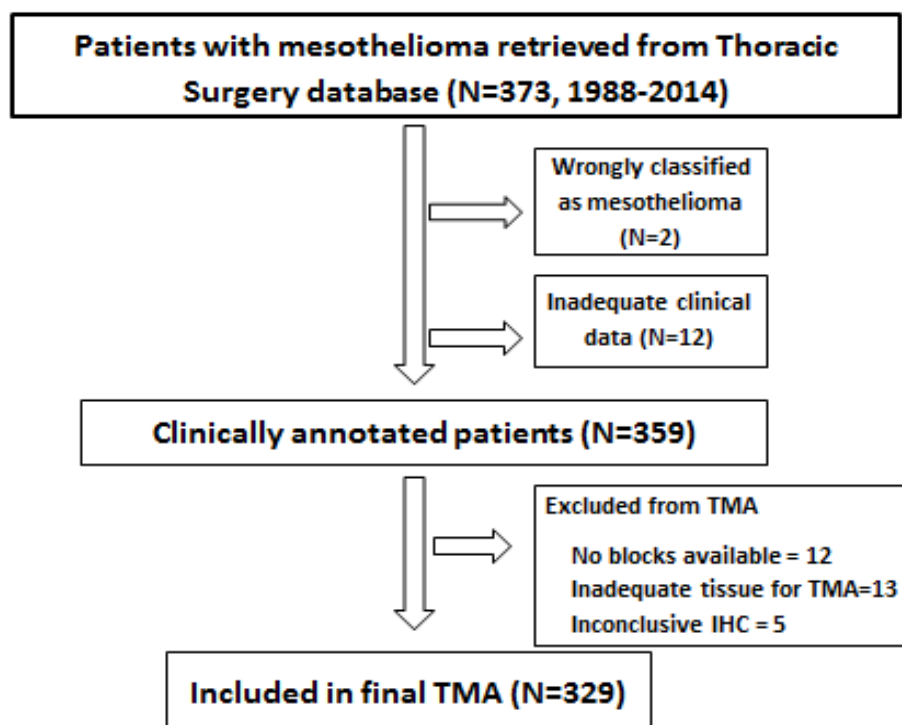


Figure 2.1: Flowchart of collection of mesothelioma cohort to TMA construction

2.6 Immunohistochemistry and pathological evaluation

IHC combines anatomical, immunological and biochemical techniques to identify discrete tissue components by the interaction of target antigens with specific antibodies tagged with a visible label. IHC makes it possible to visualise the distribution and localisation of specific cellular components within cells and in the proper tissue context. IHC was performed on 4 µm paraffin sections of TMAs and full sections of tissue blocks (when necessary) that were mounted on charged slides. Although a more detailed description of the IHC protocol for each antigen is included in the relevant chapters, a brief overview is presented here.

2.6.1 Deparaffinization and rehydration

The paraffin-embedded tissue slides were deparaffinised by incubating sections at 60°C for one hour, followed by incubation in xylene for 10 minutes. The slides were then rehydrated progressively with two 5-minute washes in ethanol 100%, then 70%. Endogenous peroxidase activity was blocked by incubating the slides with 3% hydrogen peroxide for 10 minutes. Sections were kept hydrated in Tris-buffered saline with 0.5% Tween 20 (TBST) in between all subsequent steps.

2.6.2 Antigen retrieval

We used heat induced epitope retrieval (HIER) methods for all our IHC assays. HIER is believed to reverse some cross-links and allows for restoration of secondary or tertiary structure of the epitope. As is usually necessary, the specific protocol was optimized for each antigen to be studied. HIER was performed using microwave ovens, or water baths. For microwave, the slides were immersed in the respective buffer in coplin jars and heated at 100% power till the buffer boiled. Subsequently, microwave was turned to 20% power and the buffer was left to boil for 15 minutes. For water bath, a coplin jar with the buffer was placed in a water bath and heated. The slides were immersed in the buffer when the temperature in the coplin jar had reached 95°C. The slides were then left in the water bath for 45 minutes. Following HIER, the slides were cooled for 30 minutes at room temperature prior to subsequent incubations. The buffer used also varied with the antigen to be

studied and was in accordance to the directions of the manufacturers of the individual antibodies used.

2.6.3 Incubation

Primary antibody was then applied at a concentration suggested by the manufacturer or that derived by a series of IHC optimization experiments done prior. Incubation with primary antibody was carried out at 4°C overnight. When using polyclonal antibodies, this step was preceded by incubation with background sniper blocking reagent SKU:BS966M500 ml from MetaGene Pty Ltd for 30 minutes at room temperature to prevent non-specific binding. Suitable positive control slides (based on antigen being studied and derived from literature) and negative controls (isotype control/tissue used for positive control without primary) were included in each IHC run.

2.6.4 Visualization

After overnight incubation with primary antibody, the slides were washed with TBST (3 washes, 5 minutes each). They were then subjected to 60 minute incubation with secondary antibody using the horse radish peroxidase system specific to the species of origin of the primary antibody. This was again followed by TBST wash (3X5minutes) prior to two minute exposure to chromogen (DAB from SignalStain, DAB Substrate Kit #8059, Cell signalling technologies, Massachusetts, USA). The slides were rinsed in TBST, stained with Mayer's haematoxylin (Sigma-Aldrich, St. Louis, Missouri, USA) for 60 seconds, and then rinsed until clean with tap water. This was followed by 60 minutes incubation in Scott's water and then rinsed with tap water. The slides were then dehydrated by incubating in 70 % Ethanol x 1 minute, 90 % Ethanol x 1 minute, 100 % Ethanol x 1 minute x 2 and Xylene x 1 minute x 2. The slides were then covered with permanent mountant and stored in room temperature.

IHC slides were scanned using a ScanScope XT system (Aperio Technologies, Vista, CA, USA) with the images exported from ImageScope v10 software. The scoring system employed was dependent on the antigen being studied and details have been included in relevant sections. The assessment of

immunological reactivity was done by several investigators independently. Interobserver variability was assessed by deriving kappa scores and disagreements were settled by combined review.

2.7 MPM cell lines used in this study

The cell lines utilized in the study were NCI- H28 [28] (ATCC®CRL5420) and NCI-H2452 [H2452] (ATCC® CRL5946™). NCI-H 28 has been derived from the pleural effusion of a young male patient with metastatic sarcomatoid MPM. NCI-H2452 is derived from a patient with epithelioid MPM.

The standard growth medium used for these cell lines was RF10, which consists of basal RPMI-1640 (Invitrogen, Carlsbad, CA, USA) supplemented with 2 mM Glutamax (Invitrogen), 100 U/mL penicillin (Invitrogen), 100 µg/mL streptomycin (Invitrogen), and 10% foetal calf serum (CSL, Melbourne, Vic Australia). RF10-cultured cells were grown as adherent cultures in tissue culture-treated Falcon flasks (Becton Dickinson, Franklin Lakes, NJ, USA).

2.8 Preparation of cell block from MPM cell lines

Cultured cells were washed in PBS and pelleted by centrifugation. Approximately 150 µl of human plasma was added to the cell pellet, and a wooden dowel rod was used to mix the plasma and cells. Approximately 150 µl of thrombin were added and further mixed, giving a clot of cells adhered to the wooden rod. The clot was then encased in filter paper and fixed in formalin.

2.9 Extraction of genomic DNA from FFPE samples

One millimetre diameter cores (1-2 cores, depending on the depth of the block) were extracted from the area of tumour previously marked by the pathologist. For extraction of the genomic DNA (gDNA), we used the DNeasy Blood and Tissue kit, Qiagen cat # 69504 (Qiagen, Hilden, Germany). The paraffin block was placed in an eppendorf tube and 180 of ATL buffer (supplied with the kit) was added to it. The tube was then placed in a heater at 98 °C for 15 minutes. This was then allowed to cool down and stay at room temperature for 5 minutes. Subsequently, 20 µl of Proteinase K was added to the tube and it was left overnight at 56 °C. The next morning, the process was restarted by

briefly vortexing and then spinning the tube. 200 µl of AL buffer (supplied in the kit) was added and the tube vortexed to mix. To this 200 µl 100 % ethanol was added and it was mixed again. The mixture was then pipetted into a spin column and spun in a centrifuge at 8000 rotations per minute (RPM) for one minute. The supernatant was discarded.

Again, 500 µl of AW1 buffer (supplied in the kit) was added and it was spun for one minute at 8,000 RPM. The supernatant was again discarded. AW2 buffer (500 µl) was now added and the column was spun at 14,000 RPM for 3 minutes. The collection tube was discarded and the column was placed in a new collection tube. Hundred µl of AE buffer was now added to the column and it was incubated at room temperature for 5 minutes. The column was then centrifuged again at 8000 RPM for one minute. The DNA was now precipitated.

For precipitation, 1/10 volume of 3 M NaOAc and 3 volumes of 100 % Ethanol were added and the mixture was left at -80 °C freezer overnight. The next morning, it was spun at 14,000 RPM for 15 minutes and then washed twice with 70% ethanol spinning each time for 5 minutes. The DNA was then air dried and finally resuspended in 50 µl water.

2.10 Quantification and quality check of extracted DNA

To check quantity and quality of genomic DNA extracted from patient tissues, cell lines and xenografts derived from MPM patients, we used the Qubit dsDNA BR Assay Kits Catalog number: Q32850 (Thermo Fisher Scientific, Waltham, Massachusetts, USA). First, required number of 0.5 ml polymerised chain reaction (PCR) tubes ($N = \text{no of DNA samples to be tested} + 2$ for standards) were prepared and appropriately labelled. Next, the Qubit® working solution was prepared by diluting the Qubit® dsDNA BR reagent 1:200 in Qubit® dsDNA BR buffer. Enough working solution was prepared for 198 µl per sample to be tested plus 190 µl per standard. For the standards, 190 µl of the solution was mixed in the PCR tube with 10 µl of the Qubit standard and vortexed for 2-3 seconds being careful to avoid creation of bubbles. For each sample, 198 µl of the

working solution was mixed with 2 μl of the genomic DNA to have a final volume of 200 μl and vortexed. Allow all tubes to incubate at room temperature for 2 minutes.

The reading was done using the Qubit[®] 3.0 Fluorometer (Thermo Fisher Scientific, Waltham, Massachusetts, USA). For this the dsDNA Broad Range was selected as the assay type. Before proceeding to read the samples, the instrument was calibrated using the standards prepared earlier. Once satisfactorily calibrated, each individual sample was read separately to give the concentration of the genomic dsDNA in $\text{ng}/\mu\text{l}$. The ratio of absorbance at 260 nm and 280 nm was used to assess the purity of DNA. A ratio of around 1.8 was taken as “pure” DNA. The ratio was attained and recorded for each sample.

2.11 Fluorescent in situ hybridization (FISH)

2.11.1 Preparation and depaffinization

The charged slides containing the tissue and TMAs were incubated at 60°C for 30 minutes followed by incubation in xylene for 10 minutes. The slides were then rehydrated progressively with two 5-minute washes in ethanol 100%, then 70%.

2.11.2 Target retrieval

HIER was used for target retrieval. The slides were placed in 200ml Heat Pretreatment Solution (Zymed #00-8401) from Thermo Fisher (Thermo Fisher Scientific, Waltham, Massachusetts, USA) in rack in white tissue tek container. A programmable pressure cooker (Pascal, Dako, Glostrup, Denmark) was set up to reach 125°C and maintain for 2'30 seconds. This was followed by cooling to 90°C for 10 seconds before the pressure cooker was opened and the container with the slides taken out. The slides were then transferred to a tub of water and subjected to three washes of two minutes each. The tissue on the slides were then covered with few drops (just enough to cover the tissue) of Enzyme Pre-treatment Reagent (Zymed #00-8401, from Thermo Fisher) for 15 minutes at 37°C. The slides were then washed in a tub of tap water three times, 2 minutes each time.

2.11.3 Probe hybridization

The slides were then dehydrated by immersing them in graded alcohol. They were placed in a Hellendahl jar and immersed in 70%, 80%, 90% and 100% ethanol each for 2 minutes. Thereafter, they were left to air dry for 15 minutes. To minimize the amount of probe mix use, the tissue on the slide was marked on the back of the slide with black texta so as to identify the exact area that needed to be covered. The probe mixes to be used were prepared according to the manufacturer's directions and the composition of the individual probe mixes are discussed in the relevant sections.

The probe mix was then carefully spread to cover the tissue previously marked. Two μl of the probe mix was used for small tissue (for controls), 8 μl was used to cover the TMAs. The TMAs were covered with 22x25 mm coverslips and any bubbles formed were gently removed from over the tissue using forceps. The coverslips were then sealed on all sides using rubber cement (Fixogum- SKU 11FIXO0125, MP biomedicals, Santa Ana, California, USA) to prevent evaporation during incubation. Hybridization was carried out in a programmable hybridizer (Thermobrite, Abbott Biologicals, Des Plaines, Illinois, USA). Using a pre-set programme, the slides were first denatured at 80°C for 5 minutes and then left to hybridize at 37°C for 17 hours (overnight). Wet paper towels were placed in the hybridizing chamber to increase humidity.

2.11.4 Stringent washes

In the following morning, 2x 50ml aliquots of stringent wash were prepared by adding 1.25ml of SSC buffer concentrate (20X) from Thermo Fisher, cat # 008400 to 48.75ml of distilled water (dH_2O). One aliquot (in a Hellendahl jar) was placed in the water bath and allowed to heat up to 75°C and the other was placed in room temperature. The slides were taken out of the hybridizer and the coverslips were gently removed and immersed in the stringent wash at room temperature for two minutes to wash off the excess probes. Thereafter, the slides were transferred to the stringent wash at 75 °C in the water bath. At the end of five minutes of the slides being in the water bath, they were washed again with water, three times, two minutes each time.

2.11.5 Visualization

The slides were dried around the tissue using tissue paper. Eight μl of Vectashield Antifade mounting medium with DAPI (cat # H-1200, Vector laboratories, Burlingame, CA, USA) was applied on the tissue and covered with a coverslip (22x50mm). The sides of the coverslip were sealed by smearing them with nail polish. The slides were then stored in a slide box at 4°C before and after assessment.

2.11.6 Assessment

Assessment was carried out on a fluorescent microscope, Nikon Eclipse PS4-214 (Nikon Instruments Inc, Tokyo, Japan). Controls used (obtained with thanks from Richard Young, TRL, Peter MaCCullum Cancer Centre) were SKOV3 (6439/09) xenograft for positive (loss) and; PC3 xenograft tumour (2846/04) for negative (disomy) for *CDKN2A* and NCI H2452 for negative (disomy) for *CDK6* amplification. For every sample, cancer cells were counted for green fluorescent signals [centromere probe labelled with Fluorescein Isothiocyanate (FITC)] and bright orange fluorescent signals [locus specific probe labelled with Tetramethyl Rhodamine Isothiocyanate (TRITC)]. The FITC signals were visualised at 495nm and the TRITC at 532nm. The green and bright orange signals were counted individually in 50 cancer cells taking care to count signals only in cells where both signals could be clearly counted. For both signals a mean of the numbers from all 50 cells was obtained and a ratio of the number of TRITC signals/number of FITC signals was obtained.

2.12 Copy number analysis

2.12.1 OncoScan FFPE assay

We determined copy number profiles for 113 patient tumours chosen randomly but to represent the histological subtype mix of the cohort (described in section 3.4.2), two MPM cell lines (NCI-H28 and NCI-H2452) and two patient derived xenografts (PDXs) using Affymetrix OncoScan™ FFPE assay (Affymetrix, Santa Clara, California, United States) . The assay was performed partly at the

Ramaciotti Centre for genomics, University of New South Wales, Sydney and partly at Ontario Institute of Cancer Research, Toronto, Canada.

Steps of the MIP assay performed for OncoScan are presented below.

- 1) Annealing: Probe and gDNA hybridization
- 2) Gap filling with A/T or G/C nucleotides
- 3) Exonuclease selection for gap filled probes
- 4) Cleavage at site 1 for probe opening and inversion
- 5) Probe amplification and biotinylation
- 6) Cleavage at site 2 to release the tag sequence
- 7) Array hybridization followed by staining with phycoerythrin through the biotin-streptavidin interaction
- 8) Array scanning

A brief description of the assay and methodology is presented below and a pictorial depiction is presented in figure 2.2.

OncoScan is a single nucleotide polymorphism (SNP) based DNA array which works with molecular inversion probe (MIP) technology. MIP belongs to the class of molecular techniques included in Capture by Circularization techniques used for performing genomic partitioning, a process for capturing and enriching specific regions of the genome.¹⁸⁵ In this technique, the probes used are single stranded DNA molecules and contain sequences that are complementary to the target in the genome; these probes hybridize to and capture the genomic target. MIP stands unique from other genomic partitioning strategies in that MIP probes share the common design of two genomic target complementary segments separated by a linker region. Directions of the homology regions in the probe are designed to generate an incomplete circular form between the gDNA target and the probe. When gDNA is hybridized for 16–18 h with the probe mixes, the probe hybridizes to the target and undergoes an inversion in configuration (as suggested by the name of the technique)

and circularizes. Specifically, the two target complementary regions at the 5' and 3' ends of the probe become adjacent to one another while the internal linker region forms a free hanging loop. Following the overnight hybridization, the incomplete circular probe and gDNA mixes are equally divided into two tubes.¹⁸⁶ To each tube, a mix of A and T nucleotides or a mix of G and C nucleotides is added to fill the gap. Depending on the nucleotide in the gap, a group of probes will be present in the completed circular form, while other probes will remain as incomplete circular forms. Exonucleases, which are specific for linear DNA, digest excess probes as well as incomplete circular forms of probes, and gDNA. Following the digestion step, there are two tubes per sample and each of the tubes harbors circular forms of probes, which have been gap-filled either with A/T or G/C. Within the probe, there are two cleavage sites, and a set of PCR primer sites.¹⁸⁷ A mix of cleavage enzymes recognizes one of the cleavage sites to generate a linear form of the probe from the circular form. A significant difference between the unprocessed and processed (gap-filled) probes is the direction of PCR priming sites. In the unprocessed probes, PCR priming sites face outward and away from each other; therefore, no PCR products are amplified. In contrast, PCR products are amplified from gap-filled and cleaved probes because these processes make the PCR priming sites face each other. An additional critical part of the MIP technology is a tag sequence that plays the role of a barcode for a specific gDNA target region. The homology region sequences hybridize to a specific gDNA target region so that they should be complementary to each other. The tag sequence is an artificial DNA fragment and assigned to a specific gDNA target according to a specific homology region in a probe. Thus, the tag sequences are unique to the assigned genomic DNA region. The tag sequences are the only part involved in the hybridization to targets on microarrays. PCR products are digested with another restriction enzyme to separate the tag sequence (with a forward priming site) from the remaining sequence including homology regions. Each tag sequence region is designed for optimal hybridization with minimal cross-hybridization in the array procedure to increase the efficiency of the assay. During PCR, biotin-labelled nucleotides are incorporated into the product. Following hybridization, the biotin is bound by phycoerythrin through serial staining of a

streptavidin-phycoerythrin conjugate and an ant streptavidin biotinylated antibody. Phycoerythrin fluorescence signal is recorded by the Affymetrix GeneChip® Scanner.¹⁸⁸

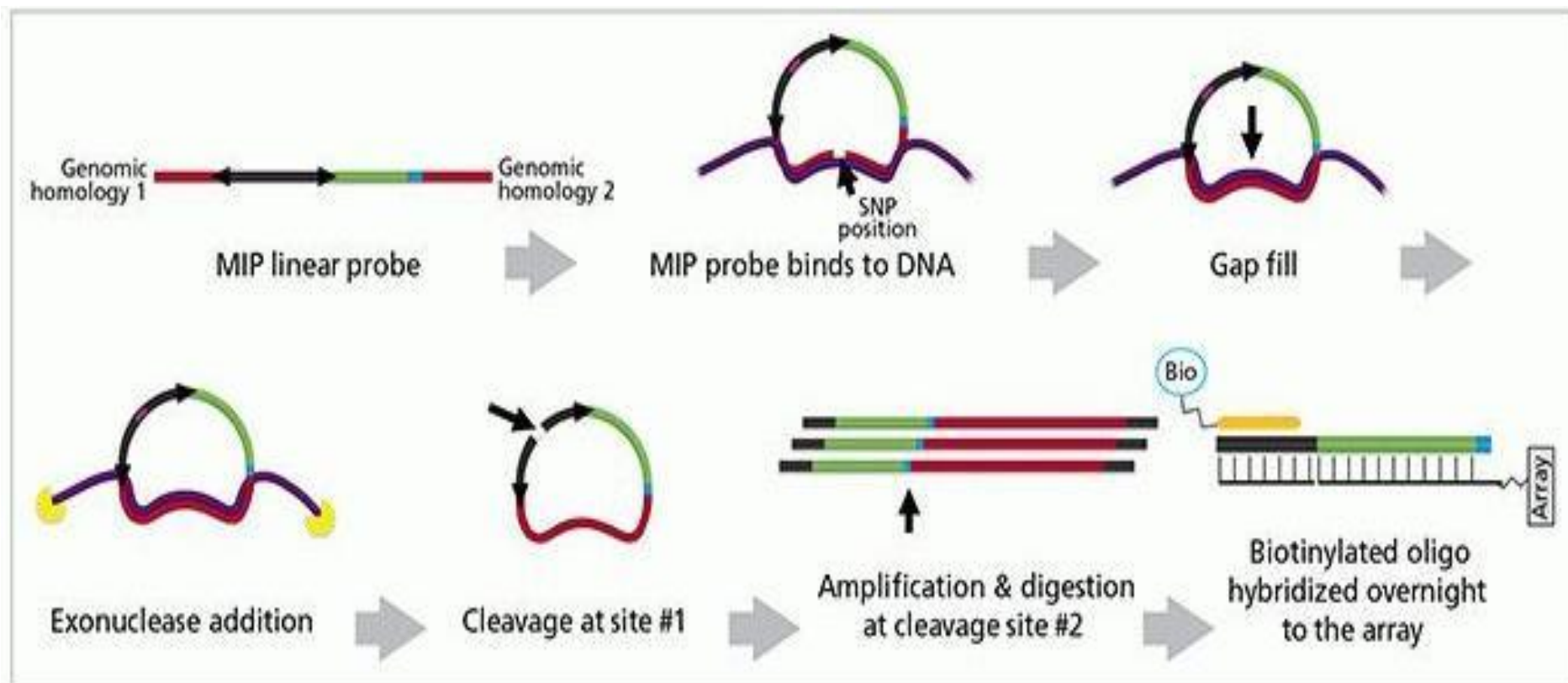


Figure 2.2: The Molecular Inversion Probe: Target generation and hybridization procedures. Pictorial representation of the steps of OncoScan assay starting from Annealing to array scanning in a sequential manner. (Adapted from user guide for User Guide for OncoScan FFPE assay- accessed 6/5/2017)

The technology has been used extensively for large-scale SNP genotyping¹⁸⁷ as well as for studying gene copy alterations¹⁸⁹. This assay has been shown over time to perform well with highly degraded DNA, such as that derived from FFPE- preserved tumour samples of various ages and with <100 ng DNA. The assay has been purported to have 50–100 kilo base(kb) copy number resolution in around 900 cancer genes 300 kb genome-wide copy number resolution outside of the cancer genes.

2.12.2 Processing of copy number data

This analysis was done in conjunction with Dr. Paul Boutros and team from Ontario Institute of Cancer Research, Toronto, Canada. The copy number profile data obtained were processed using the Nexus Express (Biodiscovery, El Segundo, California, USA). The Nexus Express Software for OncoScan® FFPE Assay Kit is specifically designed software which supports the OncoScan® FFPE Assay Kit.

Based on quality metrics [median of the absolute values of all pairwise differences (MAPD) scores above 0.3; SNP quality control of normal diploid markers (ndSNPQC) score < 30] and visual inspection, we removed low quality samples that displayed high level of noise. We then estimated tumour ploidy and purity using the allele-specific copy number analysis of tumours (ASCAT),¹⁹⁰ and Qpure¹⁹¹ algorithms, respectively. Finally, we defined aberrated genes based on the hg19 reference genome and the GENCODE reference gene annotation.¹⁹² We then investigated patterns in copy number alteration (CNA) occurrence among patients. We identified significantly recurrent CNAs using GISTIC 2.0¹⁹³ with the default settings. The percent genome aberration (PGA) was computed as a proxy for genomic instability and was defined as the total number of base pairs within altered regions, divided by the total number of base pairs in each region included in the array. To reduce multiple testing for all gene level analyses, we collapsed CNAs at contiguous genes with identical signatures in all patients, resulting in a reduced set of 11416 loci. We used consensus clustering with 1000 repetitions to group patients based on CNA profiles.

2.12.3 Test of correlation with clinical covariates

We tested for associations between CNA profiles and clinical covariates. We tested whether PGA was significantly associated with sex, tumour subtype, PD-L1 status, or consensus cluster membership using Mann Whitney U-tests. We also examined for independence between consensus cluster membership and clinico-pathological covariates using Fishers exact test. Similarly, we used Fishers exact tests to examine independence between the number of patients with a CNA present or absent and PD-L1 status or tumour subtype at each aberrated locus followed by a false discovery rate (FDR) correction for multiple testing. We also repeated this analysis using only the top 20 most significant GISTIC genes. To more explicitly test the effects of CNAs on PD-L1 levels, we also compared the number of patients with a CNA present or absent between all pairwise combinations of PD-L1 levels for each locus using U-tests and an FDR correction. Finally, we used univariate Cox-PH regressions and Log-rank tests to test associations in CNA status and survival both in all loci in the collapsed dataset and in the top 20 GISTIC genes. We also tested the effect of PGA and consensus cluster membership on survival with Cox PH regressions and estimated Kaplan Meier curves for each covariate, including age at diagnosis as a covariate to control for its significant effect on survival. For estimating Kaplan Meier curves we dichotomized PGA between the low, and two upper tertiles.

2.13 Statistical analysis

Statistical analysis was performed using the R statistical package (in part) and also the Statistical package for the social sciences (SPSS) version 22. Details of the statistical tests employed have been detailed in individual chapters. In brief, Clinico-pathological data were described using summary statistics. Categorical variables were compared using the Chi-square test or Fisher exact test (as appropriate) and continuous variables using one way ANOVA test. Correlation among continuous variables was estimated using Spearman's test. Survival curves were estimated by means of the Kaplan-Meier method and Cox proportional hazards regression was used to derive hazard ratios (HRs).

Chapter 3: Clinical and pathological characteristics of MPM patients operated at the Austin Hospital.

3.1 Introduction

MPM remains a global problem and Australia ranks second only to the UK in terms of incidence. The annual number of mesothelioma cases in Australia has progressively increased from 156 in 1982 to highest of 732 in 2014. In 2015, 650 cases were reported giving a rate of 2.3 cases per 100,000 persons.¹⁷ It continues to be a disease with limited effective therapeutic options and a generally poor outlook. There is limited ability to apply aggressive multimodality therapies in most patients on account of their advanced age and poor physiological status. Even choosing which patients are likely to do well with aggressive therapy has been difficult. This has made the identification of accurate and reproducible predictive biomarkers and also reliable prognostic biomarkers imperative.⁸²

The search for prognostic indicators in MPM has led to the study of multiple clinical, lab based markers, radiological assessments and more recently molecular markers. In the past, these variables have usually been studied one at a time, in many centres and with limited numbers of patients. Although univariate and multivariate analyses have been performed in these studies, there are few markers that have been validated in different MPM cohorts.

We were able to assemble a large cohort of MPM patients with the latest available IHC markers for confirmation of diagnosis. Using this cohort we tried to validate the prognostic effect of some previously described clinical and pathological variables and explore new parameters in MPM.

3.2 Aims

The aims of the research described in this chapter were

- 1) To define the clinical and pathological characteristics of MPM patients operated at the Thoracic Surgery department of Austin hospital
- 2) To explore the correlation of these clinical and pathological parameters with survival in this MPM cohort.

3.3 Methods

We conducted a retrospective search of a prospectively maintained database of the department of Thoracic Surgery at the Austin Hospital, Melbourne. All patients who were operated (diagnostic/therapeutic/palliative) with a diagnosis of MPM were included. Medical records (both paper and electronic) were reviewed to capture data regarding the demographics, clinical presentation, baseline investigations including blood test, radiology and nuclear medicine results, treatments (surgical and non-surgical) received and outcomes. Data regarding survival status and date of death when it had occurred were obtained from the medical records. When these data were not available, it was requested from the Victorian Cancer Registry of the Cancer Council Victoria.

3.4 Results

3.4.1 Demographic characteristics of the MPM cohort

Of the 373 patients recorded in the Thoracic Surgery database between 1988 and 2014, we excluded two patients who were wrongly diagnosed with MPM and 12 for whom adequate clinical data was not available. A further 30 patients were excluded either because no tissue sample (FFPE sample) corresponding to the patient could be found or because a diagnosis of MPM could not be confidently established. Amongst the remaining 329 patients, we found males outnumbered females by more than 5:1. The age at presentation ranged from 26-89 years (median = 67 years). Twenty six per cent of patients had no definite history suggestive of asbestos exposure. Chest pain (50%) and worsening dyspnoea (34%) were the commonest presenting features. All but nine patients were

residents of Victoria at the time of diagnosis (New South Wales = 5, Tasmania = 2, Queensland = 1, New Zealand = 1). One hundred and thirteen (31.4%) patients had one or more co-morbidities of which cardio-vascular and respiratory diseases were the commonest. Forty (11.1%) patients had a prior history of cancer at another site. There were 163 (45.4%) never smokers and the median pack years of smoking amongst smokers was 20. The demographic and clinical characteristics of our cohort were as presented in Table 3.1.

Table 3.1: Demographic and clinical parameters of the MPM cohort.

Parameter	Category	Number	Percentage
Age	≤ 50 years	22	6.7
	51-60	65	19.9
	61-70	120	36.1
	>70	122	37.1
Sex	Male	274	83.2
	Female	55	16.7
Definite history of asbestos exposure	Yes	239	72.6
	No	90	27.3
Significant weight loss	Yes	154	47
	No	175	53
ECOG	≥2	129	39.3
	<2	200	60.7
Laterality	Right	191	58
	Left	138	42

3.4.2 Diagnosis – modalities and histology

The diagnosis of MPM was made on thoracoscopic pleural biopsies in 216 (66.2%) patients, by open pleural biopsies in 78 (23.9%), closed pleural biopsies in 21 (6.4%), biopsies of chest wall nodules in 7 and aspiration cytology in seven. Epitheloid histological subtype was the commonest, as expected ($n=203$, 61.7%). The other histological subtypes were: biphasic ($n = 72$, 21.8%), sarcomatoid ($n = 42$, 12.7%) and desmoplastic ($n = 2$, 0.06%). Ten patients could not be confidently classified.

3.4.3 Surgical procedures performed on the cohort

Twenty-two (6.6%) patients underwent only diagnostic procedures. One hundred and forty (42.5%) patients had pleurodesis at the time of the diagnostic surgery and had no further surgery. One hundred thirty-five (41.0%) patients had photodynamic therapy (PDT) coupled with various extents of PD. PDT is a form of phototherapy involving light and a photosensitizing chemical substance, used in conjunction with molecular oxygen to elicit cell death. The photosensitiser given 24 hours prior to the operation accumulates in the tumour. When it is activated by light of a specific wavelength during operation, after resection, creates reactive singlet oxygen species which mediates cellular toxicity and cell death in cancer cells where the photosensitiser has accumulated.¹⁹⁴ Twenty-nine (10%) patients underwent PD only. Only one patient underwent EPP and five patients had palliative procedures only. Therefore 162 (49.2%) of patients had no cytoreductive surgery.

3.4.4 Post-operative treatment received by the cohort

One hundred and twenty-two (37%) patients received no further treatment. Fifty-nine (18%) patients had post-operative palliative chemotherapy; 26 (8%) had post-operative chemoradiotherapy; 41 (12.5%) had post-operative radiotherapy only. Nine (2.5%) patients had chemoradiotherapy in the neo-adjuvant setting as part of a tri-modality treatment plan (one in conjunction with EPP and 8 in conjunctions with PD). In 70 patients, information regarding any further adjuvant treatment was not available.

3.4.5 Changing pattern of MPM treatment at the Austin hospital

In order to demonstrate the changing treatment paradigms over the study period, we divided the period of study into five year blocks. We listed the treatment received by MPM patients diagnosed in these time periods (Table 3.2). We found a shift from mainly diagnostic procedures (open/thoracoscopic pleural biopsies) in the late 80's & early 90's to more aggressive procedures in the form of PD + PDT in till mid 2000's. This change was seen to reverse more recently with the focus

of the surgical management being shifted to adequate biopsy and pleurodesis. This later change in surgical approach coincided with the wider use of chemotherapy following the report from Vogelzang et al. that found the combination of cisplatin and pemetrexed offered better survival than cisplatin alone.¹¹¹

Table 3.2: Treatment received by MPM patients at the Austin Hospital.

Period	No. of Patients	Surgical Procedures			Post-surgical treatment			
		Diagnostic/palliative	PD+PDT	PD/EPP	NONE	Chemo+Radio	Radio only	Neo-adj chemo
'88-'93	56	28	21	2	28	1	4	0
'94-'98	96	39	45	9	48	15	15	0
'99-'03	91	34	49	5	32	20	17	0
'04-'08	75	42	20	7	17	32	7	5
'09-'14	41	34	0	7	9	19	3	4

PD: Pleurectomy and decortication, EPP: Extrapleural pneumonectomy

3.4.6 Treatment outcomes of patients with MPM treated in Austin hospital between 1988 and 2014

Overall survival (OS) was calculated from the time of initial diagnosis to date of death or of last follow up. Patients who were lost to follow up or were alive were censored. The median follow up was just over 10 months (1-157). The OS of the whole cohort was 12.05 months (Figure 3.1). Due to the retrospective nature of the study, the data regarding progression and PFS after surgery or chemotherapy was not universally available especially in patients who received their chemotherapy and/or radiotherapy in another centre.

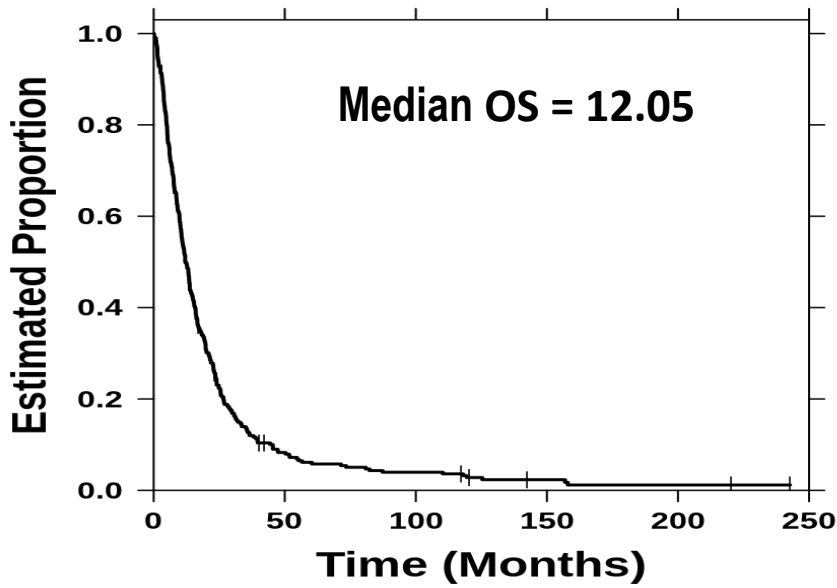


Figure 3.1: Overall survival of the Austin MPM cohort

We looked at the OS of MPM patients in the different five year periods. We found a modest increase in OS in 2004-2008 with no further increase in median OS thereafter. Patients who were treated in or before 2004 had a significantly worse OS when compared to those treated in 2004 and thereafter (Median survival 10.66 Vs 16.06 months; HR: 1.26; CI 1.012, 1.66; p = 0.03) (Figure 3.2)

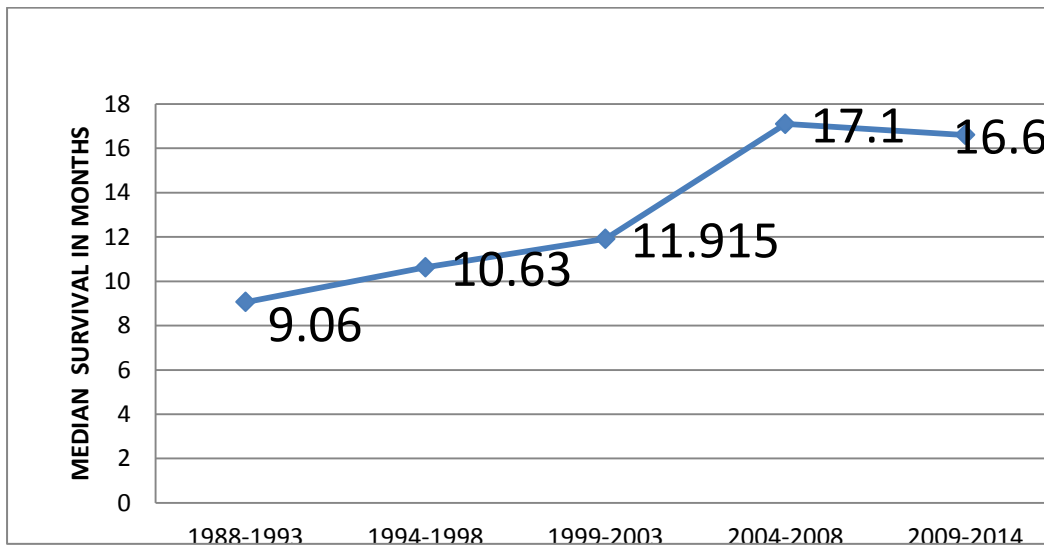


Figure 3.2: Overall survival trends at Austin Hospital over a period of 26 years

3.4.7 Relationship between clinicopathological covariates and patient survival.

We examined the prognostic implications of several demographic (age at diagnosis, sex), clinical (stage at presentation, physiological status, history of weight loss or exposure to asbestos) and histopathological (histotype) and treatment related covariates on OS. On univariate analysis, advanced age at diagnosis (taken as a continuous variable), advanced stage (III&IV Vs I &II), non-epithelioid histology, history of significant weight loss and poor physiological status (ECOG \geq 2) were found to be associated with poorer survival (Table 3.3). Also, patients who had received some form of resectional surgery (P/D or P/D with PDT) achieved better OS compared to those who did not (HR = 0.83; 95% CI: 0.66, 1.04; Wilcoxon P value = 0.014) as did patients who received chemotherapy (HR = 0.53; 95% CI: 0.41, 0.71; Wilcoxon p <0.0001).

Table 3.3: Prognostic implications of demographic, clinical and pathological features in the MPM cohort (Univariate analysis)

	Hazard Ratio	Lower 95% CI	Upper 95% CI	Wald-type p Value	Schoenfeld p Value (PH)	Wilcoxon p Value
Age (per year)	1.01	1.00	1.02	0.032	0.59	NA
Sex (Female vs Male)	0.79	0.58	1.07	0.12	0.21	0.45
Stage (I & II vs III & IV)	1.59	1.27	2.00	5.2e-05	0.0053	<0.0001
Histology (Epithelioid vs Non-epithelioid)	0.60	0.48	0.76	<0.0001	0.37	<0.0001
Asbestos exposure (Yes vs No)	1.29	1.00	1.67	0.05	0.56	0.049
Significant weight loss (Yes vs No)	1.48	1.18	1.85	0.0007	0.0052	<0.0001
ECOG (\geq 2 vs \leq 1)	1.61	1.27	2.02	<0.0001	0.21	<0.0001
Smoking (Yes vs No)	1.11	0.89	1.39	0.36	0.13	0.13
Surgery (cytoreductive vs palliative+diagnostic)	0.83	0.66	1.04	0.1	0.034	0.014

Chemotherapy (Yes vs No)	0.53	0.41	0.70	<0.0001	<0.0001	<0.0001
---------------------------------	------	------	------	---------	---------	---------

On multivariate analysis, non-epithelioid histological subtype and poor functional status (ECOG \geq 2) were found to remain significantly associated with worse outcome (Table 3.4). A Schoenfeld residual test validating the proportional hazard (PH) assumptions failed for chemotherapy, history of weight loss and stage indicating that their effects (hazard ratios) change with time. Schoenfeld residuals are plotted and we found that time around 10 months is a turning point, and thus chosen as a threshold. A multivariate Cox model with time-variant hazard ratios for these variables were then fitted and PH assumptions are validated. We found that the effect of these variables were significant in the early part of the follow up (\leq 10 months) but faded thereafter (Table 3.4).

Table 3.4: Multivariate analysis of overall survival

	Time period (month)	HR	Lower 95%	Upper 95%	p Value
Histology (Epithelioid vs Non-epithelioid)		0.75	0.59	0.96	0.021
ECOG (\geq2 vs <2)		1.34	1.02	1.76	0.036
History of significant weight loss (Yes vs No)	\leq 10	2.11	1.44	3.07	0.00011
	> 10	1.04	0.74	1.46	0.83
Stage (III & IV vs I & II)	\leq 10	2.50	1.73	3.62	<0.0001
	> 10	1.18	0.87	1.62	0.28
Chemotherapy received (Yes vs No)	\leq 10	0.29	0.16	0.50	<0.0001
	> 10	0.88	0.63	1.22	0.44

Wald type P values from Cox regression model

We sought to explore if the effect of the different variables on OS is different in the epithelioid and non-epithelioid histology sub cohorts. To test this, we conducted multivariate analyses

separately using the methods previously described. We found that in the non-epithelioid cohort only advanced stage (III & IV) remained significantly associated with survival. In the epithelioid cohort, female sex (HR = 0.60; 95%CI: 0.39, 0.94; p = 0.03) was associated with improved OS but poor physiological status (HR = 2.11; 95%CI: 1.44, 3.2; p < 0.0001), advanced stage (HR = 1.74; 95%CI: 1.23, 2.5; p < 0.0001) and history of weight loss (HR = 1.48; 95%CI: 0.99, 2.2; p = 0.05) were indicative of poorer OS. The effect of receiving chemotherapy was again found to be time dependent and effected survival significantly only in the first 10 months in both histotypes.

3.5 Summary and discussion

In this retrospective review of a large cohort of confirmed MPM patients treated in a quaternary referral centre, we found a plurality of older male patients with history of asbestos exposure. Over the long span (1988 to 2014; 26 years), we were able to trace the evolving pattern of MPM treatment at the centre but found only modest change in the OS. In keeping with previous reports⁸² we found tumour histological subtype and performance status at diagnosis to be significantly associated with prognosis. Advanced stage of disease and history of weight loss were associated with poorer OS and patients who received chemotherapy had better survival but their effect on prognosis was found to be time dependent. Additionally, female sex was found to a favourable prognostic indicator in epithelioid MPMs.

Most patients with MPM are not candidates for surgical resection by virtue of having clinically advanced disease at presentation, advanced age, or comorbidity. Management options for such patients are palliative in nature, with median survival of approximately 7 to 12 months.¹⁹⁵ Optimum surgery for MPMs thought to be eminently resectable at diagnosis is a subject of ongoing debate. Proponents of radical surgery in the form of EPP continue to report reasonably good results in selected patients treated at high volume centres.¹⁹⁶ However, results of the MARS feasibility trial¹⁰⁰ cast great doubts not only regarding the efficacy of EPP in improving patient survival but also their overall safety. As such the present consensus is generally against radical surgery.⁹⁸ PD has been

touted as a less radical and better tolerated operation which achieves similar survival to EPP.¹⁹⁷ However, PD is not without significant perioperative morbidity and mortality and as such although some retrospective studies showed small benefits in survival for patients who underwent PD, PD is now only recommended in the setting of trimodality therapy in patients enrolled in prospective trials.¹⁹⁸ The surgical treatments received by patients in our cohort shadows the prevailing concepts at the time regarding the role of surgery in MPM. The initial pessimism of the decades of 1980's and 90's was replaced by the aggressive approach of the 2000's with a large proportion of patients in that time period receiving pleurectomy decortication with or without PDT. More recently, surgery has most widely been used only for diagnosis via a thoracoscopic biopsy and for palliation using pleurodesis. In our cohort, although patients who underwent some surgical debulking (PD and EPP) had better survival in univariate analysis, it did not remain significant on multivariate analysis probably pointing to the limited effect this treatment modality had in the OS in the cohort.

The results of intrapleural PDT as a post resectional adjunctive therapy in the last two decades have at best been inconclusive.¹⁹⁹ Initial reports of PDT in MPM did not show survival benefit.^{200,201} Some studies like those of Takita et al.,²⁰² Moskal et al.²⁰³ and Friedberg et al.^{204,205} have shown benefit mainly amongst early stage and epithelioid tumours. However, these were all retrospective studies with small cohorts and non- standardized adjuvant treatment. Due to paucity of data on the conduct of the PDT, we were unable to assess accurately any survival benefit PDT may have had in the patients who received it.

The addition of pemetrexed to cisplatin based chemotherapy is the only change in practice that has been demonstrated to significantly improve survival in MPM.¹¹¹ A detailed analysis of the effect of the different chemotherapy regimens and dosages on patient survival was not possible on our series due to the retrospective nature of the study and lack of specific information in a large proportion of patients. However, we do notice a rise in OS in patients treated after 2004 when the pemetrexed-cisplatin combination therapy was adopted in the institution.

The relative rarity of MPM combined with the lack of large complete datasets on MPM patients has made the simple goal of identifying reliable and reproducible biomarkers elusive. Our study independently verified the prognostic implication of non-epithelioid histological subtype and poor physiological status. The time variation of the hazard posed by variables like the negative impact on OS of advanced stage and history of weight loss is a frequently occurring but sparsely reported effect of long follow up periods in oncological trials.²⁰⁶ A significant limitation of the survival analysis in our study is the temporal spread of the cases over which time there were changes in treatment paradigms. As such, this could have effected survival and made validation of the clinical prognostic factors problematic. However, this is to be expected in a study spanning 26 years.

In this descriptive segment of our research we annotated and characterized a large cohort of MPM patients. We have used the cohort to then independently validate the association of some demographical, clinical and treatment related variables to patient survival. Our cohort matches previous literature on demographics; is typical in terms of the mix of MPM histological subtypes and is accompanied by adequate matching tissue. This makes the cohort very well suited to be used in our subsequent study of the genome and immune landscape of this rare but deadly disease.

Chapter 4: Caveolin-1: A novel immunohistochemical marker of mesothelioma and its correlation with clinicopathological parameters

4.1 Introduction

The diagnosis of MPM remains a challenge and use of a panel of immunohistochemistry (IHC) markers is now routine. The current recommendation is that when all clinical, radiological and histological features are concordant, at least two mesothelial markers and two carcinoma markers with greater than 80 % sensitivity and specificity must be used.⁶¹ Calretinin, Wilm's tumour-1 (WT-1), cytokeratin 5/6 (CK5/6) and podoplanin (D2-40) are considered the most useful mesothelial markers. The most useful carcinoma markers are MOC31, BG8, carcinoembryonic antigen and BerEp4. However, discordance between the clinical, radiological and histological features often pose diagnostic dilemma. Also, sarcomatoid MPMs (pure sarcomatoid and sarcomatoid component of biphasic tumours) commonly lose immunoreactivity to most markers in a majority of cells.⁶¹ These situations require additional IHC markers.

In the previous chapter, we described a cohort of MPM patients whose clinical characteristics closely resemble previously defined cohorts in terms of their demographics, presentation, diagnosis and outcomes.^{74,75} Here, we seek to further characterise our cohort using IHC seen as it is now an integral part of MPM diagnosis and potentially its subclassification and prognostication. Also, our tissue samples constituted of FFPE samples from a very long period of time. Whether the age of the samples and variations in methods of tissue fixation during that period could impact our IHC procedures and results needs to be ascertained. For this, we studied in our cohort the expression of calretinin, which is the most widely used MPM IHC marker. However, because calretinin expression is known to be low amongst sarcomatoid MPM, we also employed a recently described IHC marker caveolin-1, which is thought to be widely expressed in this histological subtype of MPM.^{207,208}

4.1.1 Calretinin and its expression in MPM

Calretinin, which is a calcium binding protein has been established as a useful marker in distinguishing MPM from adenocarcinomas with pleural metastases.²⁰⁹ In an evaluation of the sensitivity and specificity of 12 different antibodies to differentiate between epithelioid MPMs and adenocarcinoma, calretinin had the highest sensitivity (95%). Its specificity (87%) though was behind thrombomodulin (92%) and cytokeratin 5 (89%).²¹⁰ Calretinin expression is also observed in 15% of adenocarcinomas of breast origin²¹¹ and 4-18% of pulmonary adenocarcinomas.^{212,213} Another limitation of calretinin IHC is the loss of expression in a proportion sarcomatoid MPMs which are often the most difficult to differentiate from other sarcomatoid tumours involving the pleural lining.²¹⁴

4.1.2 Caveolin-1: a potential novel marker in mesothelioma

Caveolin-1, one of a three member caveolin protein family is a membrane-associated protein possibly involved in integrin signalling and in cell migration. It is expressed in endothelial and mesothelial cells as well as in alveolar type I pneumocytes.²¹⁵ Caveolin-1 has been purported to play a dual and opposite role in tumorigenesis, as it has been implicated in both tumour suppression and oncogenesis. In human cancers, caveolin-1 is a marker of extracellular matrix remodelling²¹⁶ and epithelial to mesenchymal transition.²¹⁷ It has been associated with aggressive biology and resistance to apoptotic signals in several malignancies.²¹⁸⁻²²⁰ Caveolin-1 has also been described as a marker of dedifferentiation in soft tissue and bone sarcomas.^{221,222} It has also recently been projected as a novel marker for MPM. In a study comparing its expression in 80 epithelioid MPM and 80 lung adenocarcinoma, a 100% sensitivity and 93% specificity for caveolin-1 in epithelioid MPMs was reported.²¹⁵

4.1.3 Expression of calretinin and caveolin-1 in MPM and association with tumour histology and differentiation

Besides their importance in MPM diagnosis, both these IHC markers have also been studied for their association with tumour differentiation, histology and prognosis. Takeshima et al. found that higher calretinin scores were seen in more well differentiated tumours, which in turn have more favourable prognosis.²²³ The prognostic role of calretinin expression has also been explored by Kao et al., who demonstrated low expression of calretinin to be poorly prognostic in two different patient cohorts.^{68,74,75} They also reported calretinin expression in 828/910 (91%) of all MPMs; with 530/545 (97%) of epithelioid and 113/119 (94%) of biphasic but only 92/153 (60%) of sarcomatoid MPM.⁶⁸ In a series of 131 MPM patients Righi et al. found higher rates of caveolin-1 expression amongst nonepithelioid MPM (40/40; 100%) as compared to epithelioid MPM (70/91; 77%) and suggested that its expression increases with dedifferentiation from low grade epithelioid to high grade sarcomatoid histology.²⁰⁸ The same authors also described a poorer outcome for epithelioid MPM in whom caveolin-1 expression was detected in stromal cells.

Emerging literature suggests caveolin-1 is a sensitive IHC based diagnostic marker for MPM especially the sarcomatoid subtype which typically has lower rates of calretinin. Added to established IHC markers like calretinin, it may be of significant clinical use in the differential diagnosis of metastatic malignancy in the pleura. However, its specificity is still questionable given its expression in other mesenchymal cells such as endothelial and smooth muscle cells. Also, the purported relationship of these two IHC markers to tumour histology and differentiation and consequently patient prognosis is interesting and warrants further exploration.

We hypothesized that Caveolin-1 is a sensitive IHC marker for MPM and contrary to calretinin, caveolin-1 expression increases with tumour dedifferentiation (sarcomatoid MPM > biphasic MPM > epithelioid MPM) , and is therefore associated with poorer survival.

The research described in this section has been published in the article titled "Calretinin but not caveolin-1 correlates with tumour histology and survival in malignant mesothelioma."²²⁴

4.2 Aims

The aims of the research described in this section were

- 1) To study and compare the extent and pattern of calretinin and caveolin-1 expression in MPM
- 2) To explore the relationship of calretinin and caveolin-1 expression with tumour histology and other clinical covariates including patient survival

4.3 Specific methods

4.3.1 Immunohistochemistry for calretinin and caveolin-1 in MPM and lung adenocarcinoma

Four μm sections of our MPM TMAs (described in chapter 2) were cut and collected onto charged slides, deparaffinised and rehydrated. Endogenous peroxidase activity was blocked using 3% hydrogen peroxide for 10 minutes. Antigen retrieval for calretinin was performed in 24 min at 95 °C in cell conditioning buffer. Monoclonal mouse anti human calretinin antibody (clone- DAK- Calret1 Dako, Glostrup, Denmark) in 1:50 dilution for 32 minutes was incubated using the automated Ventana system (Ventana medical systems, Tuscon, Arizona, USA). Opt iView DAB detection kit (Ventana medical systems, Tuscon, Arizona, USA) was used for visualization. For caveolin-1, antigen retrieval was performed by boiling in a microwave for 20 minutes in target retrieval solution buffer. Polyclonal rabbit anti human caveolin-1 antibody (cat#3238 Cell Signalling Technology, Danvers, Massachusetts, USA) was incubated in 1:250 dilutions. Staining was performed manually with slides incubated overnight at 4°C. DAB was used as the chromogen.

The slides were digitally scanned using Aperio Scan- Scope CS (Aperio Technologies, Vista, CA, USA), and the scanned images were analysed using Image Scope (Aperio Technologies). Scoring for calretinin and caveolin-1 was performed taking into account both the percentage of neoplastic cells stained and also the intensity of the staining (marked as 1+/2+/3+). An 'H score' was calculated for each core separately and an average was taken as the final score based on intensity and percentage

of cells stained as follows: (% tumour cells staining 1+ x 1) + (% of tumour cells staining 2+ x 2) + (% tumour cells staining 3+ x 3). Cores with poor tumour content (<20%) (136/987 cores= 13.9%) were excluded from the analysis. Scoring was performed by BT and pathologist KA independently. Inter-observer reliability was good (Kappa for calretinin = 0.77 and for caveolin-1 = 0.74). Disagreements were settled by a combined review. Median H scores were used to stratify patients into high and low expressing groups.

Additionally, we also stained an available TMA of lung adenocarcinomas with 58 cases (sequential 1 mm cores in triplets) with caveolin-1 as described above. We then compared the expression of caveolin-1 in the lung adenocarcinomas with that in MPM.

4.3.2 Statistical analysis

Statistical analyses were performed using SPSS version software (v22). OS was calculated from the time of initial diagnosis to death or last follow up. Patients who were lost to follow up or were alive were censored. Clinico-pathological data were described using summary statistics. Categorical variables were compared using the Chi-square test or Fisher exact test (as appropriate) and continuous variables using one way ANOVA test. Correlation among continuous variables was estimated using Spearman's test. Survival curves were estimated by means of the Kaplan-Meier method and Cox proportional hazards regression was used to derive HRs.

4.4 Results

4.4.1 Expression of calretinin and caveolin-1 and relationship with tumour histology

Calretinin expression was detected in 246 of the 324(76%) evaluable patients with median H score of 98 (Table 1). Of 198 epithelioid MPM, calretinin expression was positive in 173 (87.3%), compared to 54/69 (78%) biphasic and 6/42 (14.2%) sarcomatoid. The median H scores were 125, 63 and 0 for the epithelioid, biphasic and sarcomatoid MPM, respectively. Caveolin-1 expression was

detected in 298 (94%) of 317 evaluable patients with median H score of 135. One hundred seventy-seven of 193 epithelioid (91%), 66/68 (97%) biphasic and 41/42 (97.6%) sarcomatoid MPM were found to express caveolin-1. The median H scores were 132, 132 and 157.5 for the epithelioid, biphasic and sarcomatoid MPM respectively. When the whole cohort was dichotomised by the median value, higher H score for calretinin expression was significantly associated with epithelioid histology. There was, however, no association between histology and caveolin-1 expression (Table 4.1). Representative pictures of the staining are demonstrated in figure 4.1.

Table 4.1: H scores of calretinin and caveolin-1 according to histology.

		Epithelioid	Biphasic	Sarcomatoid	P Value*
Calretinin H score	>98	125	29	2	<0.0001
	≤98	75	40	40	
Caveolin-1 H score	>135	93	30	24	0.409
	≤ 135	100	38	18	

*P values from Chi-square tests

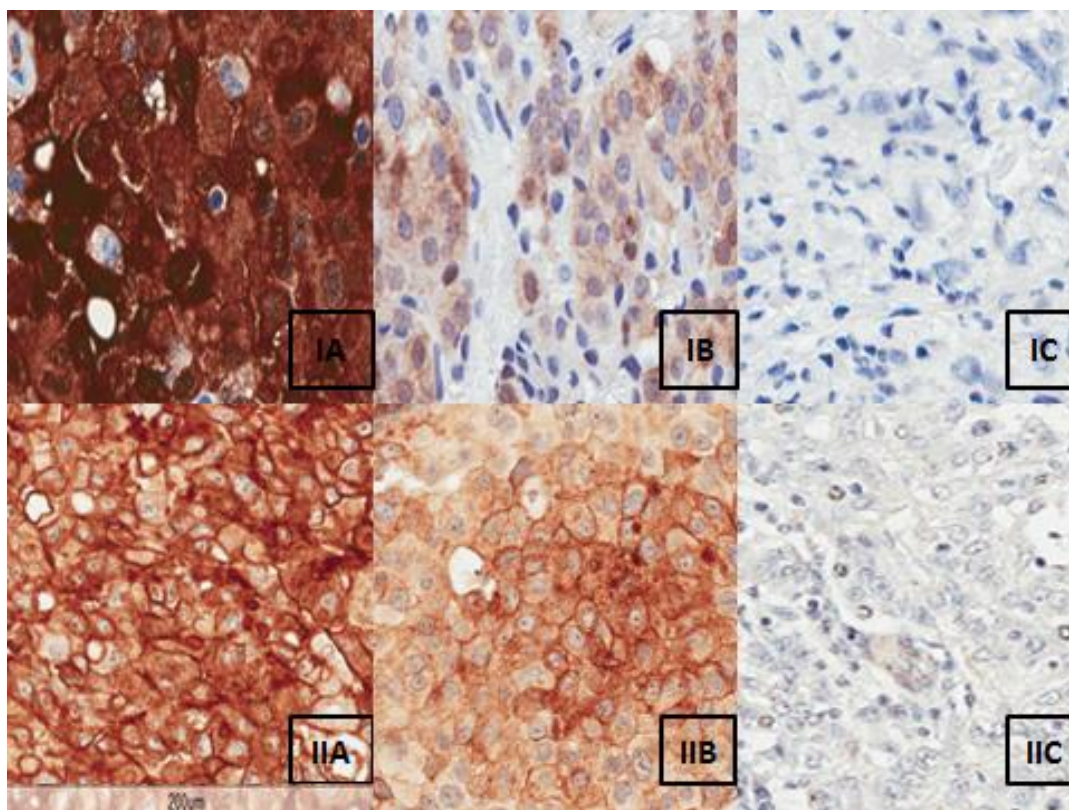


Figure 4.1: Representative pictures of the IHC: expression of calretinin and caveolin-1 in MPM.

IA: Strong expression of Calretinin IB: Weak expression of Calretinin IC: Negative for Calretinin
IIA: Strong expression of caveolin-1 IIB: Moderate to expression of Caveolin-1
IIC: Negative for Caveolin-1

4.4.2 Correlation between expression of calretinin and caveolin-1

There was a negative correlation between calretinin and caveolin-1 expression when the whole cohort was considered, but this was weak (Pearson $r = -0.14$; $p=0.01$) (Figure4.2). The associations were similarly weak when the epithelioid (Pearson $r = -0.12$; $p = 0.08$) and non-epithelioid (Pearson $r = -0.09$; $p = 0.45$) sub-cohorts were considered separately.

4.4.3 Correlation of calretinin and caveolin-1 with clinicopathological parameters

No significant relation was found between calretinin scores and age at diagnosis, sex, smoking history, asbestos exposure, weight loss, ECOG status, stage and neutrophil-lymphocyte ratio (NLR). Increased caveolin-1 expression was associated with advanced age at diagnosis (ANOVA test $p = 0.04$) and history of asbestos exposure (Pearson's chi square $p = 0.02$) but not with sex, smoking history, weight loss, ECOG status, stage and NLR.

4.4.4 Caveolin-1 expression in lung adenocarcinoma

Caveolin-1 expression was detected in only eight of 58 (13.7%) lung adenocarcinomas as compared to 94% of MPM.

4.4.5 Association of expression of calretinin and caveolin-1 with survival

On univariate analysis, high calretinin expression was associated with better OS when taken as a continuous variable (HR = 0.997; 95 % CI: 0.996, 0.999; $p < 0.001$) and also when the cohort was dichotomized using the median H score for Calretinin expression (HR = 0.749; 95% CI: 0.595, 0.941; $p = 0.012$). High caveolin-1 expression however, was not found to be prognostic when taken as a continuous variable (HR = 1.001; 95% CI: 0.999, 1.002; $p = 0.26$) and when the cohort was

dichotomized by the median H score for caveolin-1 expression (HR = 1.24; 95% CI; 0.985, 1.562; p = 0.06) (Figure 4.2). A direct ratio of calretinin/caveolin-1 also showed no association with OS (HR = 0.996; 95% CI 0.983, 1.009; p = 0.507). In multivariate analyses, calretinin expression considered as a continuous variable but not when dichotomised by median was significantly associated with improved OS (HR=0.997; 95% CI: 0.997-1.00; P=0.009). Other predictors of improved OS in this analysis were absence of significant weight loss (HR=0.64; 95% CI: 0.47-0.87; P=0.005), early stage (I&II vs III&IV) at diagnosis (HR=0.28; 95%CI: 0.15-0.55; P=0.002), and epithelioid (compared to non-epithelioid) histology (HR=0.37; 95%CI: 0.23-0.58; P=0.0001). High NLR (taken as a continuous variable) (HR=1.03; 95%CI: 1.007-1.058; P=0.04) was associated with poorer prognosis.

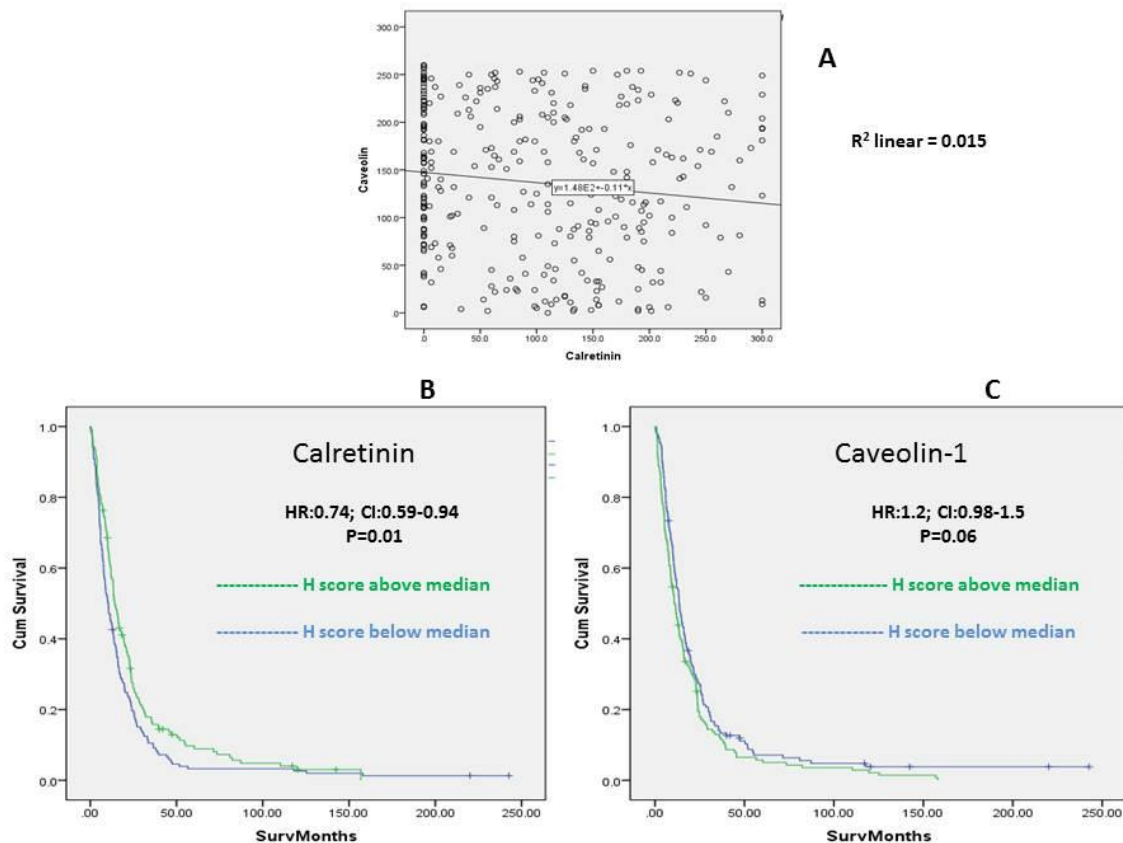


Figure 4.2: Correlation between calretinin and caveolin-1 H scores and association with survival.

A: Correlation between calretinin and caveolin-1 H scores **B+C:** Association of calretinin (B) and caveolin-1 (C) H scores (dichotomised by median) with survival (univariate analysis)

4.5 Discussion

In this large cohort of patients with MPM, we investigated two markers which are purported to be closely associated with tumour differentiation. We investigated their expression and association with clinicopathological parameters including tumour histological subtype and OS. Positivity with caveolin-1 was found to be higher than Calretinin in the entire cohort. Previous findings of a statistically significant association of calretinin expression with epithelioid histology and also survival were reconfirmed. Calretinin expression was found to be a predictor of survival independent of histology. Caveolin-1 expression did not correlate with histology and had no association with survival. High caveolin-1 expression was, however, associated with advanced age and history of asbestos exposure. Moreover caveolin-1 positivity was found to be much higher in MPM than in lung adenocarcinoma.

Calretinin expression as an independent prognostic factor in MPM was first described by Kao et al.⁷⁴ However, this series comprised only 85 patients who had undergone extrapleural pneumonectomy and lacked patients with sarcomatoid histology. In a much larger series⁶⁸ with 910 patients, the same authors again demonstrated the prognostic value of calretinin. Our results are in accord with these prior observations and also demonstrate the association of calretinin expression with epithelioid histology.

Caveolin-1 expression is thought to correlate with poor tumour differentiation and has been associated with worse prognosis in a multitude of malignancies including sarcomas, renal cell carcinoma, lung cancer, brain cancer and gastric cancer.^{219,221,222} In a study of NSCLC, caveolin-1 expression was found in none of the pure bronchoalveolar carcinomas (0/12) as opposed to 42.8% (3/7) of large cell carcinomas (neuroendocrine subtype excluded). Adenocarcinomas (8.5%; 6/70) and squamous cell carcinomas (29%; 8/27) displayed an intermediate percentage of positivity, thus suggesting that caveolin -1 expression followed a gradient according to tumour histotype-related aggressiveness. Also, the authors found that caveolin-1 positivity was double among metastatic

tumours (8.1%; 3/37) as compared to non-metastatic ones (17.8%; 15/84) irrespective of histology.²¹⁸ In contrast, loss of caveolin-1 expression in tumour stroma has been associated with unfavourable outcome in breast cancer. Decreased stromal caveolin-1 expression correlated with lower disease-free survival, advanced tumour stage, higher recurrence rate, and shorter progression free breast cancer survival.^{225,226}

Data regarding caveolin-1 expression and its clinical relevance in MPM has been sparse. Amatya et al.²¹⁵ first studied caveolin-1 as an IHC based marker to differentiate epithelioid MPM from lung adenocarcinoma. They found that of their 80 epithelioid MPM, 42 cases (52.5%) showed caveolin-1 expression in >50% of tumour cells, 34 cases (42.5%) in 6–50% of tumour cells, and four cases (5.0%) in <5% of tumour cells. In contrast, only six cases (7.5%) of lung adenocarcinoma stained focally for caveolin-1. This is in line with our own findings and could suggest a useful role for caveolin-1 in differentiating MPM from lung adenocarcinomas metastasizing to the pleura although its specificity appears lower compared to other epithelial markers such as Ber-Ep4.²¹⁰

In the only other series addressing the issue of differential expression of caveolin-1 in different histological subtypes of MPM, Righi et al.²⁰⁸ studied 131 cases and found caveolin-1 expression in all 23 sarcomatoid and 17 biphasic, but only 70% of their 91 epithelioid MPMs, leading them to conclude that caveolin-1 was differentially expressed in MPM according to low to high grade histology. In our much larger series, we did find that almost all patients (98%) with sarcomatoid histology expressed caveolin-1. However, expression rates were similarly high among biphasic (97%) and epithelioid MPMs (91%), and as such (unlike with calretinin expression), we found no association with histology. This difference could have stemmed from the use of different antibodies and their lower antibody concentration (Righi et al. used 1:800; rabbit polyclonal, Santa CruzBiotechnology, Santa Cruz, CA, USA). Our results in this regard are supported by those of Amatya et al. who found staining in all of their 80 epithelioid MPM samples. Seventy-six (95%) showed moderate to marked staining in more than 5% cells.

Contrary to the prognostic value assigned to caveolin-1 expression in several other malignancies, Righi et al. found no such association in MPM.²⁰⁸ Our findings also do not support any such role for caveolin-1 either used alone or as a direct ratio of calretinin/caveolin H scores. Righi et al. have described a poorer prognosis for epithelioid MPM whose stromal cells expressed caveolin-1, an analysis that is difficult to accurately replicate using a TMA. We found caveolin-1 expression to be high among people with advanced age and also those with a definite history of asbestos exposure. While they are both interesting findings, their clinical relevance is not immediately clear and as such, they warrant further validation.

Using a TMA in lieu of full sections is subject to sampling error and this could be considered a limitation of this study. However, TMAs allow efficient assessment of large cohorts and high concordance between TMA and whole sections in the evaluation of IHC in MPM has been previously demonstrated.⁷⁶ Another factor that could at least in theory have effected the staining of our samples is their age and also the potential variability in the tissue fixation methods over the long period of time (26 years) to which our samples belong. Unfortunately, it was not possible to account for the effect of the differing fixation methods and any bearing that it may have had in the staining. We did however review whether staining was different based on the age of the sample and did not find a consistent difference according to the year of the sample.

In conclusion, we found higher rates of expression of caveolin-1 as compared to calretinin in MPM. While we established the relation of calretinin expression in MPM to histology and survival, no such association was demonstrable with caveolin-1. Contrary to expectation, there was no inverse relation between the expression of calretinin and caveolin-1. Near uniform expression of caveolin-1 across MPM histological subtypes makes it an attractive potential new marker for MPM diagnosis especially in troublesome cases of sarcomatoid differentiation. Remarkably lower expression of caveolin-1 in adenocarcinomas of lung origin is an important finding. If confirmed in

independent large series, caveolin-1 could potentially be established as a differentiating marker between MPM and lung adenocarcinoma metastasizing to the pleura.

Chapter 5: Immune microenvironment in MPM – identifying the “inflamed phenotype”

5.1 Introduction

Despite several trials investigating novel therapies in MPM, there have been no practice changing therapies since pemetrexed and cisplatin were found in a phase III trial to improve survival over cisplatin alone.^{53,111} Harnessing the immune system to eradicate malignant cells is becoming a most powerful new approach to cancer therapy. FDA approval of the immunotherapy-based drugs, sipuleucel-T (Provenge), ipilimumab [Yervoy, anti-cytotoxic T-lymphocyte-associated protein 4 (CTLA-4) antibody], and more recently, the programmed cell death (PD)-1 antibody (pembrolizumab, Keytruda), for the treatment of multiple types of cancer have greatly advanced research and clinical studies in the field of cancer immunotherapy. In the context of this unmet need for effective therapeutic options for MPM, these exciting new developments in cancer therapy have helped shift the focus of research in MPM therapeutics away from cytotoxic approaches towards immunotherapies. Immune checkpoint inhibition therapy has shifted treatment paradigms in many cancers types and some recent data show promise for improving MPM treatment.^{167,168,170,172}

Despite these advances, the results of immunotherapy across cancer types have not been consistent. Even in cancers like melanoma and lung cancer which are thought to be most amenable to immunotherapy, large proportions of patients continue to not benefit from these therapies. Moreover, several cancers have proven largely refractory.²²⁷ Considering the significant costs and the potential for serious immune related side effects of these therapies, it has become imperative to identify biomarkers that can predict efficacy and identify tumours and patients who are most likely to respond to such therapies. Also, it could be hoped that a detailed understanding of the factors that render individuals responsive or refractory to immunomodulatory agents in general and checkpoint inhibitors in particular could in time lead to development of strategies or agents that could help convert refractory to responsive.

5.1.1 Inflammation in MPM – basis for suitability for immunotherapy

Asbestos induced chronic inflammation is said to play a major role in the pathogenesis of MPM.²²⁸ Asbestos-exposed mesothelial cells and macrophages are thought to release a variety of cytokines and growth factors, which induce inflammation and facilitate malignant transformation of mesothelial cells that have accumulated DNA damage.²²⁹ Also, there is some evidence to suggest that MPM has immunogenic capabilities^{230,231} and some cases of spontaneous temporary regression have been attributed to anti-tumour immune response.^{232,233} In light of this, MPM was considered to be suited to immune based treatment modalities. However, recent studies have tempered initial enthusiasm for immune checkpoint inhibition.²³⁴ The large Phase IIb DETERMINE study demonstrated no OS benefit for the anti-CTLA-4 antibody tremelimumab relative to placebo.¹⁶⁹ Recent data confirm that mutational load in MPM is low,⁵⁵ which may in part explain why the DETERMINE study was negative: in both melanoma and non-small cell lung cancer (NSCLC), mutational load is a predictor of benefit from CTLA-4 or PD-1 inhibition.^{235,236} However, results of trials of anti-PD-1 and anti-PD-L1 therapy in MPM have not been completely negative^{167,168,170,172} and as with other tumour histologies, predicting which patients will respond has been difficult.

Data regarding putative predictive biomarkers for immunotherapy in MPM is very sparse. The MESOT-TREM-2008 study explored different immune markers potentially predictive of response to treatment and/or of survival. Circulating levels of CD4+ inducible costimulator (ICOS)+ T-cell subpopulation were found to be increased in the course of therapy with tremelimumab, and they were found to be significantly associated with a better survival in the early phases of treatment.¹⁶⁷ However, this study only included a very small number of patients (n= 29). While blood was collected, these assays have not been reported for the much larger (n = 571) DETERMINE study to date.¹⁶⁹ In this light, identifying features in tumour histology, immunological milieu and genetic makeup that are reasonably able to point towards MPM cases likely to benefit from immunotherapeutic agents has come to be of prime priority.

5.1.2 The search for predictive biomarkers – study of the tumour immune microenvironment

A multitude of biomarkers have been studied as putative predictive markers in many cancers. Leading tumour biomarker strategies under development for checkpoint immunotherapy have been related to indices involving the patient's tumour like characteristics of cancer cells or cells of the tumour microenvironment.²³⁷ IHC-based assessment of the proportion of PD-L1-positive tumour cells, immune cells, or both; IHC-based assessment of T cells at invasive tumour margin or tumour parenchyma and study of T cell receptor clonality have been widely studied.²³⁸ The tumour mutation burden, burden of neo-antigens and immune signatures has similarly been studied as putative biomarkers. Biomarker strategies pursued thus far have therefore focused on identifying aspects of the T-cell inflamed phenotype and tumour-foreignness caused by the mutational and neoantigen load.²³⁸ This is appropriate considering that growing evidence suggests that the major barrier to more successful cancer immunotherapy is the tumour microenvironment, where chronic inflammation plays a predominant role in tumour survival and proliferation, angiogenesis, and immunosuppression.

To date, PD-L1 expression in both tumour and immune cells is the most readily assayable marker. Although there are many caveats to its expression and predictive power, it remains in wide-use for its ability to enrich patients likely to respond, and for the ease of application as an IHC assay. While numerous reports in melanoma,^{239,240} NSCLC,^{241,242} gastric cancer,²⁴³ renal cell cancer^{239,240} and bladder cancer²⁴⁴ have reported positive correlation between tumour PD-L1 expression and response to anti-PD-1/PD-L1 therapy, some others have clearly demonstrated that a significant proportion of PD-L1 negative patients do show response.^{245–247} Some reports in squamous cell cancer of lung²⁴² and melanoma²⁴⁸ have found tumour expression of PD-L1 to be non-predictive and there have been reports attributing predictive function to expression of PD-L1 on tumour infiltrating immune cells(TILs) rather than on tumour cells.²⁴⁹

The diversity and composition of TILs have been reported to significantly affect clinical outcomes in cancer patients.²⁵⁰ Tumours with an active immune microenvironment with increased infiltration of activated effector T cells are thought to be better primed to respond to immunotherapy and as such the positive prognostic influence of high T-cell (CD8+/CD4+) infiltration has been demonstrated in several malignancies^{234,251–253} including MPM.^{230,254} The immune recognition of these tumours is thought to result in a host-immune response or T-cell inflamed tumour phenotype, which improves disease control through immune mechanisms.

The presence of an inflamed tumour microenvironment has also been associated with clinical benefit from immunotherapies such as the MAGE-A3 vaccine and high-dose interleukin 2.²⁵⁵ Therefore, it is thought that baseline tumour infiltrating lymphocytes (TILs) status could also serve as a predictive biomarker for checkpoint inhibitor immunotherapy. Tumeh et al. analysed the relationship between TILs and response to pembrolizumab in patients with melanoma enrolled on the KEYNOTE-001 study. TILs density was quantified both in the tumour parenchyma and at the invasive tumour margin. Pre-treatment tumour samples showed higher CD8+ (but not CD4+) T-cell densities at the invasive margin and within the tumour parenchyma in responding patients than in patients with disease progression. An increase in CD8+ T-cell density was seen in serial biopsy samples of tumours during anti-PD-1 treatment in the responding group, but not in the disease progression group.²⁵⁶ Another study of patients with melanoma given anti-PD-1 therapy showed a modest association between CD8+, CD3+, and CD45RO+ T-cell densities in pre-treatment samples of responders versus non-responders.²⁵⁷ Conversely, in a phase 2 study of ipilimumab in patients with metastatic melanoma, baseline tumour-infiltrating lymphocyte status was not associated with clinical activity. However, increases in TILs density in tumour biopsy samples collected after the second dose of ipilimumab were associated with significantly greater clinical activity with ipilimumab than samples without increases in lymphocyte density.²⁵⁸

PD-L1 positivity has also been correlated with an increased tumour infiltration of CD4+ and CD8+ cells.²⁵⁹ It is also known to impact the proliferation and activity of regulatory T cells (Tregs).^{260–262}

5.1.3 PD-L1 expression in MPM – prognostic implications and predictive ability

Studies reporting on PD-L1 expression in MPM have typically included small numbers of patients with positivity ranging from 20-50%.^{263–265} Mansfield et al. used the 5H1-A3 clone to investigate PD-L1 expression status in 106 MPM patients with immunohistochemistry. Using a cut off of positive expression $\geq 5\%$ cells, they reported a 40% positivity rate.²⁶⁴ In 77 MPM patients, using the E1L3N clone and with a cut off of 1% staining on tumour cells and TILs, Cedrés et al. reported 20% positivity.²⁶³ In their series of 58 patients, Combaz-Lair et al. showed variability in PD-L1 expression status when using different commercially available PD-L1 antibodies. Taking 1% staining on tumour cells and TILs as positive, they found 50% (29/58) positivity with the E1L3N clone and 29% (17/58) with SP142 clone.²⁶⁵ Despite differing in the histological mix of the cohort, the antibody used and the criteria of positivity, all reported studies demonstrated association between PD-L1 positivity, sarcomatoid (non-epithelioid histology) and poorer patient survival.

Whether PD-L1 expression status in MPM allows for selection of patients for anti-PD-1/PD-L1 treatment is still unknown. Four studies have been reported to date, with the JAVELIN study being the largest with 53 patients treated with Avelumab, a PD-L1 inhibitor. The objective response rate (ORR) in a heavily pre-treated patient group was 9.4% (5/56) although clinical benefit was seen in a larger group of 30/56 (53%). ORR was 14.3% in PD-L1+ (2/14) vs 8.0% in PD-L1– patients (2/25). The median PFS was 17.1 weeks in PD-L1+ vs. 7.4 weeks in PD-L1– patients. In the smaller, but PD-L1-selected, Keynote-028 study, 25 patients with MPM were treated with pembrolizumab (anti-PD-1 antibody). Preliminary overall response rate (confirmed and unconfirmed) was 24% (n = 6); 13 patients (52%) had stable disease, for a disease control rate of 76%.²⁶⁶ Updated reports from another phase II study which treated 34 MPM patients unselected for PD-L1 with nivolumab (anti-

PD-1 antibody) demonstrated a disease control rate of 50%.²⁰⁵ Disease control was observed 11/20 in patients who were PD-L1-, 2/4 in patients with PD-L1 expression in 1-5% of cells, 2/4 in patients with 25% positivity and 2/3 in patients with $\geq 50\%$ positivity. In another study of 35 patients treated with pembrolizumab, low PD-L1 positivity (1-49% cells) was seen in 19% and high PD-L1 positivity ($\geq 50\%$) in 26%. There were 7 (21%) partial responses and 19(56%) stable disease with a disease control rate of 80% but PD-L1 expression did not correlate with response (ROC area 0.62; 95% CI:0.32,0.94).²⁶⁸

Available literature in MPM therefore points towards PD-L1 expression being associated with sarcomatoid histology and poorer survival. However, as in other tumour histologies, its predictive value remains doubtful. Some reasons presented for the poor reliability of PD-L1 in this regard are that PD-L1 expression is inducible by a variety of factors, it can be temporal and transient, there can be significant intra-patient and intra-tumour heterogeneity and most importantly, the assays used to define positivity are not yet standardised.²³⁸ These fallacies apply to the assessment of PD-L1 in MPM too. While the subject of differences in positivity when using different PD-L1 antibodies has been aptly demonstrated by Combaz-Lair et al.²⁶⁵, temporal differences in PD-L1 expression in the same patient have not been studied.

5.1.4 Assessment of Tumour infiltrating lymphocytes (TILs) in MPM

Akin to PD-L1 status, studies investigating the TILs in MPM and their prognostic/predictive value have been sparse and have typically included small numbers of patients undergoing extrapleural pneumonectomy. Anraku et al. performed an immunohistochemical analysis of 32 extrapleural pneumonectomy specimens to assess the distribution of T-cell subtypes (CD31, CD41, and CD81), regulatory subtypes (CD251 and FOXP31), and memory subtype (CD45RO1) within the tumour. Patients with high levels of CD8+ tumour-infiltrating lymphocytes demonstrated better survival than those with low levels (3-year survival: 83% vs 28%; $p = .06$). Moreover, high levels of CD8+ TILs were associated with a lower incidence of mediastinal node disease ($p = .004$) and longer progression-free

survival ($p = .05$). Patients presenting high levels of CD4+ or CD25+ TILs or low levels of CD45RO+ also demonstrated a trend toward shorter survival. However, the presence of FOXP3+ TILs did not affect survival. After multivariate adjustment, high levels of CD8+ TILs remained an independent prognostic factor associated with delayed recurrence (hazard ratio = 0.38; confidence interval = 0.09–0.87; $p = .02$) and better survival (hazard ratio = 0.39; confidence interval = 0.09–0.89; $p = .02$). Yamada et al. evaluated TILs (CD4+, CD8+, and NK cells) using IHC in a series of 44 MPM cases. The density of CD4+ and CD8+ TILs were strongly correlated ($R = 0.76$, $P = 0.001$). A high density of CD8+ TILs was a significantly better prognostic factor for the survival of patients with extrapleural pneumonectomy ($p = 0.05$). Multivariate analysis revealed that a high density of CD8+ TILs is an independent prognostic factor for patients who underwent extrapleural pneumonectomy. Both these studies concluded that increased CD8+ T cells in tumour could be beneficial in MPM immunotherapy. However, they were very small scale studies and did not take into account features of the tumour microenvironment like PD-L1 expression and presence of Tregs that modulate and dampen T cell activity.

In this section of the research we sought to use our large cohort of confirmed MPM cases to characterise the tumour and immune cell interface for PD-L1 expression and infiltration by TILs (CD4+, CD8+ and FOXP3+). Using a subset of our patients for whom FFPE samples from two different operations (initial biopsy and subsequent resection samples) were available, we also tried to study any temporal differences in PD-L1 expression in MPM. The research described in this section has been published in the Journal of Thoracic Oncology in the article titled “The Immune Microenvironment, Genome-wide Copy Number Aberrations, and Survival in Mesothelioma.”²⁶⁹

5.2 Aims

The aims of the research described in this chapter were:

- 1) To define the immune microenvironment (expression of PD-L1; infiltration by CD4+, CD8+ and Tregs) in MPM.

- 2) To explore the correlations of immune microenvironment in individual tumours to clinicopathological cofactors including tumour histotype and survival.
- 3) To explore the occurrence and degree of temporal variations in PD-L1 expression in our MPM cohort.

We hypothesized that the tumour microenvironment characteristics in MPM correlates with tumour histology and also has prognostic implications.

5.3 Specific methods

5.3.1 Immunohistochemistry

A general description of methods used for IHC is given in chapter 2 section 2.6. A brief description of the protocol used for the conduct and subsequent assessment of IHC staining is presented in Table 5.1

Table 5.1: IHC methods for some immune markers in MPM

Antibody	Manufacturer	Catalogue number	Concentration used	Antigen Retrieval buffer/time/temp	Incubation time/temp	Controls	Assessment
PD-L1 (E1L3N) Rabbit IgG	Cell Signalling Technology	136845	7.0 µg/ml	15 minutes in microwave TRS buffer Ph 9	4°C overnight	placenta	≥ 5% membranous staining on tumour cells = positive(PD-L1 +) ≥ 50% moderate or intense staining on tumour cells = high positive (PD-L1 + ^{hi})
CD4 Rabbit IgG, SP35 clone	Cell Marque	104R-15	1.0 µg/ml	52 minutes at 95 °C in CC1 buffer	32 minutes at 36 °C	tonsils	Counted using the Aperio automated counting system The counts were expressed as no. of cells staining with CD4 per 1000 nucleated cells in the core
FoxP3 mouse IgG1	Abcam	22510	17 µg/ml	15 minutes in microwave TRS buffer Ph 9	4°C overnight	tonsils	Counted using the Aperio automated counting system The counts were expressed as no. of cells staining with FOXP3 per 1000 nucleated cells in the core
CD8 mouse IgG1 C8/144B clone	Dako	M 7103/	1.0 µg/ml	52 minutes at 95 °C in CC1 buffer	32 minutes at 36 °C	tonsils	Counted using the Aperio automated counting system The counts were expressed as no. of cells staining with CD8 per 1000 nucleated cells in the core

For assessment of PD-L1, membranous staining on ≥5% tumour cells was taken as PD-L1+ as per previous reports.^{259,270} PD-L1+^{HI} was defined as moderate to intense staining ≥50% tumour cells.²⁴¹ Cytosolic expression of PD-L1 and expression solely only on TILs was disregarded. See methods section for description.

In addition to conducting an assessment of the immunological markers on our TMAs, we also retrieved full sections of FFPE blocks of 42 patients for whom samples from 2 separate operations were available. These sections were stained by methods described above for PD-L1 and CD8+ lymphocytes. The assessment was done in a similar manner as described above.

5.3.2 Statistical analysis

OS was calculated from the time of initial diagnosis to death or last follow up; patients who were lost to follow up or were alive were censored. Descriptive statistics were used for clinico-pathological data. Comparisons of different parameters between the groups with respect to PD-L1 expression were performed using an ANOVA test for continuous variables and Fisher's exact test for categorical variables. Values NLR, CD4⁺, CD8⁺, FOXP3⁺ counts and ratios of CD4⁺/CD8⁺, FOXP3⁺/CD4⁺ and FOXP3⁺/CD8⁺ were dichotomised using the median. For survival analysis, a Wald-type test from Cox's PH model was performed on R statistical environment.

5.4 Results

5.4.1 PD-L1 expression

Of the 329 patients on the TMA, cores of 311 were evaluable for PD-L1 staining. One hundred and thirty (41.47%) were found to be PD-L1 positive using a 5% membranous staining in malignant cells as the cut off. Using $\geq 50\%$ moderate or intense membranous staining to define a high positive group, we found 30(9.64%) patients to be highly positive. There was a strong correlation between PD-L1 expression and non-epithelioid histology (Fisher's exact test $p < 0.0001$). When samples were dichotomised based on the levels of infiltration with CD4⁺, CD8⁺ and FOXP3⁺ cells using the median, a higher level of infiltration was seen in patients who were PD-L1+hi (Table 5.2). PD-L1+ tumours however showed significantly increased CD4⁺ and CD8⁺ infiltration but not FOXP3⁺.

PD-L1 status showed no correlation with the age, sex and performance status of the patient, stage of disease at diagnosis, history of asbestos exposure or of smoking and NLR. Representative pictures of IHC for PD-L1, CD4, CD8 and FOXP3 are presented in figures 5.1 and 5.2

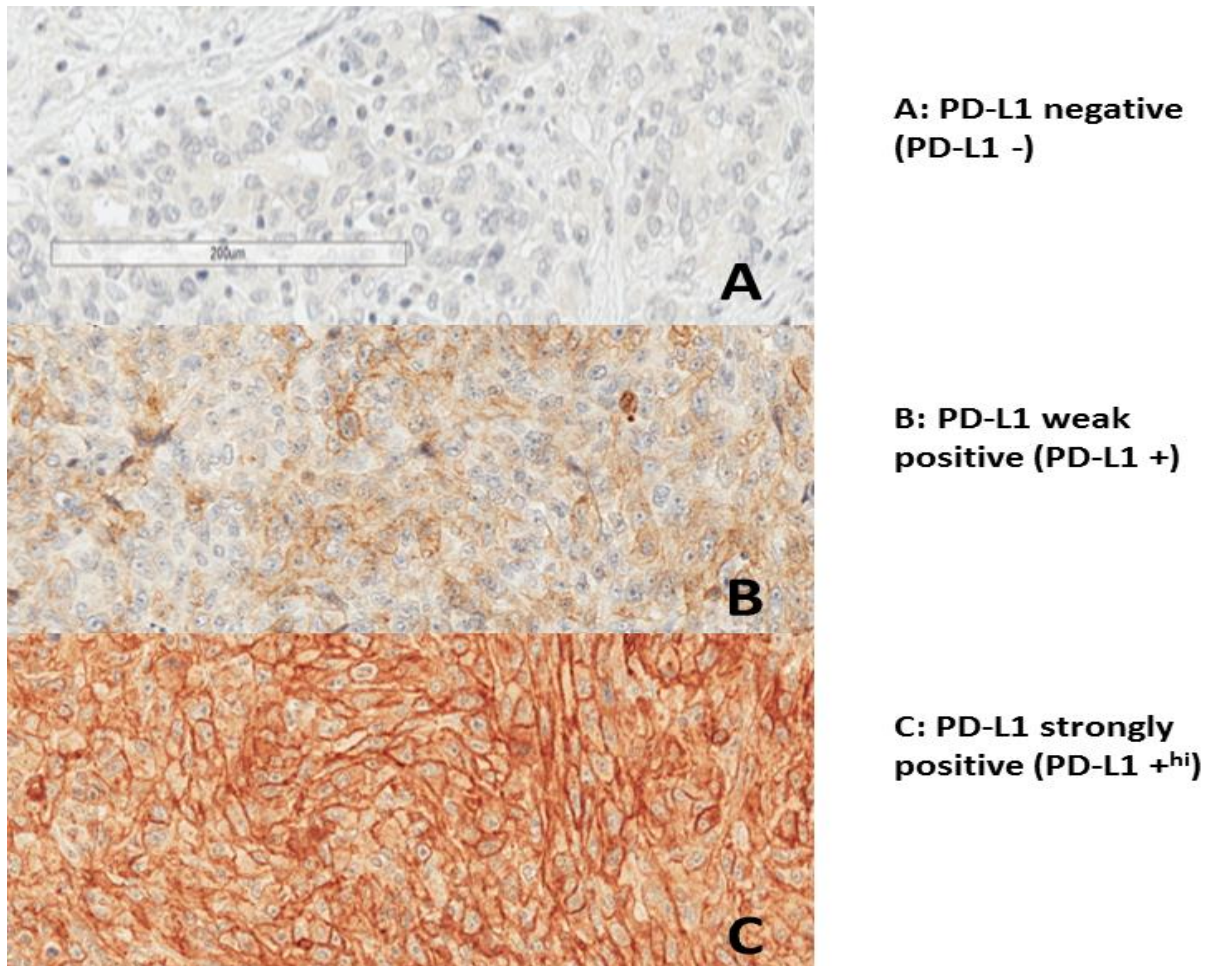


Figure 5.1: Representative pictures of the IHC for PD-L1 in MPM

5.4.2 Infiltration with CD4+, CD8+ and FOXP3+ lymphocytes in MPM and their correlations

The TILs were quantified using the Leica Aperio positive pixel count algorithm version 9.1, as previously described,²⁷¹ and expressed as number of cells per 1000 nucleated cells in the core. Dichotomised using the median we found that level of infiltrations with CD8+, CD4+ and FOXP3+ cells did not correlate with the age sex and performance status of the patient, stage of disease at diagnosis, history of asbestos exposure or of smoking, NLR, and tumour histological type. However,

they were strongly related to PD-L1 status (Table 5.2). Additionally, we found a positive correlation between CD4 and CD8 infiltration (Pearson $r = 0.59$; $p < 0.0001$), between FOXP3 and CD4 (Pearson $r = 0.14$; $p < 0.0001$) and also between FOXP3 and CD8 (Pearson $r = 0.25$; $p < 0.0001$).

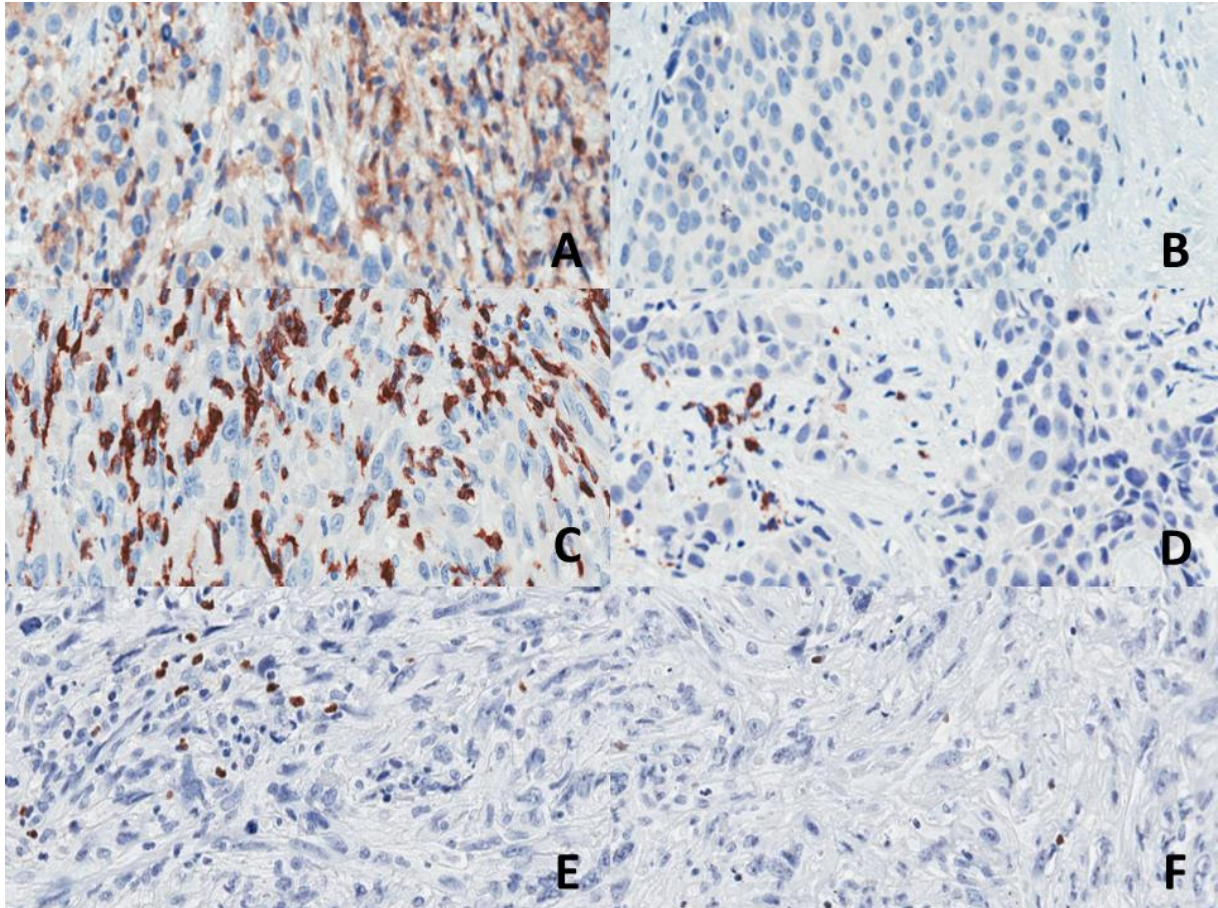


Figure 5.2: IHC evaluation of CD4+, CD8+ and FOXP3+ lymphocytes in MPM

A: High infiltration with CD4+ lymphocytes B: Low infiltration with CD4+ lymphocytes C: High infiltration with CD8+ lymphocytes D: Low infiltration with CD8+ lymphocytes E: High infiltration with FOXP3+ lymphocytes F: Low infiltration with FOXP3 + lymphocytes

Table 5.2: PD-L1 expression in MPM and its clinicopathological correlation

		PD-L1 -	PD-L1 +	PD-L1 + ^{HI}	p Value
Number (%)		181(58.2)	100(32.2)	30(9.6)	
Age (Mean)		65.3	66.7	68.4	0.27 [*]
Sex N(%)	Male	152(50.17)	77(25.41)	24(7.92)	0.27 [*]
	Female	26(8.58)	21(6.93)	3(0.99)	
Stage N(%)	I & II	94(31.02)	45(14.85)	8(2.64)	0.068 [¥]
	III & IV	84(27.72)	53(17.49)	19(6.27)	
NLR (Mean)		5	5.7	4.9	0.42 [*]
Histology N(%)	Non-epitheloid	85(27.33)	49(15.76)	23(7.40)	0.0091 [¥]
	Epitheloid	96(30.87)	51(16.40)	7(2.25)	
CD4 N(%)	<= 120	96(35.16)	38(13.92)	4(1.47)	<0.0001 [¥]
	> 120	65(23.81)	47(17.22)	23(8.42)	
CD8 N(%)	<= 125	101(35.44)	39(13.68)	3(1.05)	<0.0001 [¥]
	> 125	65(22.81)	51(17.89)	26(9.12)	
FOXP3 N(%)	<= 1.26	87(33.59)	41(15.83)	2(0.77)	<0.0001 [¥]
	> 1.26	64(24.71)	45(17.37)	20(7.72)	
Asbestos N(%)	No	45(14.85)	26(8.58)	5(1.65)	0.73 [¥]
	Yes	133(43.89)	72(23.76)	22(7.26)	
ECOG N(%)	<= 1	111(36.63)	59(19.47)	15(4.95)	0.75 [¥]
	>=2	67(22.11)	39(12.87)	12(3.96)	
Smoking N(%)	No	76(25.08)	50(16.50)	11(3.63)	0.37 [¥]
	Yes	102(33.66)	48(15.84)	16(5.28)	

CD4, CD8 and FOXP3 are dichotomized by their medians. * P values from ANOVA test; ¥P values from Fisher's exact test

5.4.3 Temporal variations in PD-L1 expression and CD8+ infiltration

Of 42 patients who had two operations at the Austin hospital for MPM, adequate FFPE tissue samples were available from both operations in 36. The median separation between the biopsies was 26 days (2-298). There were 23 epithelioid, 8 biphasic and 5 sarcomatoid tumours. There was a change in PD-L1 status in 7 (19%) patients (Figure 5.3). Five patients in whom the first biopsy was PD-L1- were found to be PD-L1+ in the second biopsy and two that were PD-L1+ in first biopsy were found to be PD-L1- in second sample. However, the proportion of PD-L1 positivity between cohorts of first biopsy and second biopsy specimens was not statistically significantly different. Although the numbers were very small, we did not find any difference in rates of change of PD-L1 status between epithelioid and non-epithelioid histology (Fisher's exact test $P = 0.22$). Similarly when we assessed the differences in levels of CD8+ infiltrations in these two sets of samples, there was no significant difference. Also when we looked at the difference in CD8+ levels in the two samples in individual cases and compared these among patients who did and did not have change in PD-L1 status, there was no difference (Figure 5.3).

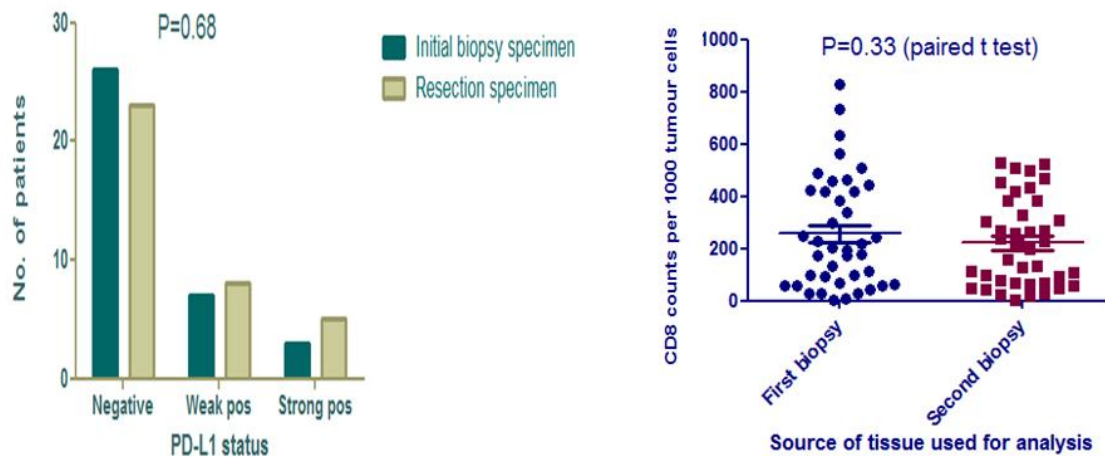


Figure 5.3: Temporal changes in PD-L1 and CD8+lymphocyte infiltration. Changes in PD-L1 status and CD8+ infiltration status between first and second biopsies.

5.4.4 Prognostic implications of immune based markers

Patients with PD-L1+ve tumours had a non-significant trend towards poorer OS, 9.8 vs. 13.5 months (HR= 1.19; 95% CI = 0.91-1.53; Wald-type p = 0.15). However, when restricting the analysis to those who were strongly positive, PD-L1+^{hi} expression was associated with a significantly worse OS (HR = 2.37; CI = 1.57-3.56; Wald-type p <0.001). The poorer prognosis associated with PD-L1+^{hi} status was maintained even when the epithelioid (Log rank p = 0.01) and non epithelioid (Log rank p = 0.03) subtypes were analysed separately.

Dichotomised by the median, levels of CD4+, CD8+ and FOXP3+ infiltration demonstrated no association with survival, although patients with high CD4+/CD8+ ratios achieved better survival (HR = 0.71; CI = 0.55-0.90; Wald-type p = 0.005).

On multivariate analysis, epithelioid histology and high CD4+/CD8+ ratio were found to independently associated with better survival while high NLR (values dichotomised by median) and advanced age at diagnosis (stages III and IV) were independently associated with poorer OS. However, PD-L1+^{hi} status failed the Schoenfeld residual test to validate the proportional hazard assumptions, suggesting that its effect change with time. Schoenfeld residuals were plotted and 10 months period was again found to represent a turning point, and was therefore chosen as a threshold. When a multivariate Cox model with time-variate hazard ratios was performed, we found that while these parameters had a significant effect in the earlier period (within 10 months), their effect faded thereafter. When we stratified by histology, we found that the effect of PD-L1+^{hi} status was time dependent in non-epithelioid histology but stayed constant with a hazard ratio of >6 in the epithelioid cohort (Table 5.3).

Table 5.3: Multivariate analysis for overall survival

Variable		Time period (month)	Hazard ratio	Lower 95%	Upper 95%	P value	
Histology	Epithelioid vs. Non-epithelioid		0.58	0.41	0.80	<0.001	
Stage	III&IV vs I&II		1.73	1.37	2.20	<0.001	
NLR	>3.94 vs ≤3.94		1.38	1.10	1.74	0.005	
CD4+/CD8+	>0.93 vs ≤ 0.93		0.67	0.53	0.86	0.001	
PD-L1 high positivity	Yes vs No	Non - epithelioid	≤ 10	2.98	1.69	5.26	<0.001
		Non - epithelioid	>10	0.61	.22	1.73	0.36
		Epithelioid	≤ 10	6.03	2.56	14.19	<0.001
		Epithelioid	>10	7.81	1.04	58.35	0.045

Wald-type P value from Cox model with time variate hazard ratios for PD-L1^{hi}

5.5 Discussion

Using a clinically well-annotated TMA, we demonstrate that PD-L1 is strongly expressed in a subset of MPMs, but the majority are weakly positive or negative. These strongly positive samples were associated with high immune infiltration of CD4+, CD8+ and FOXP3+ lymphocytes, as well as poorer survival, in a time dependent fashion.

With a predefined stringent scoring criteria in accordance with previous reports,^{241,259} we observed a PD-L1 positivity rate of 41.4%. Mansfield et al.²⁶⁴ reported 40% positivity in 106 patients when they regarded both cytoplasmic and membranous staining taking 5% as a cut off. They found a lower (24%) rate of exclusive membranous staining. Cedrés et al.²⁶³ found 20% positivity in their 77 evaluable patients despite considering cytoplasmic, membranous staining and staining of infiltrating lymphocytes. Given that non-epithelioid MPM are more likely to be PD-L1 +ve, the comparatively lower positivity rates noted by Cedrés et al. may be explained by a larger proportion of epithelioid MPM in their series. Mansfield et al.²⁶⁴ used a different antibody (clone 5H1-A3). The effect of different antibodies on PD-L1 positivity rates was recently demonstrated by Combaz-Lair et al.²⁶⁵ Lack of uniformity in staining procedures, use of different antibodies, differing cut-offs (1% vs 5%; membranous only vs membranous and cytoplasmic; tumour only vs expression on TILs) and also the fact that PD-L1 expression is dynamic and heterogeneous within the tumour makes comparison

between different series difficult.²⁷² Setting a higher benchmark by defining a group with very high expression ($\geq 50\%$ staining in our case) may therefore help identify the truly positive cases. Also, the location of PD-L1 on tumour cells is thought to be germane to its prognostic role. It is presumed that membranous expression is the most relevant form of PD-L1 because PD-1 mediates downstream signalling cascades only when it has been ligated.²⁷³ Cytosolic PD-L1 has not been reported to correlate with patient response to immunotherapy and as such its importance is unclear.^{245,274} As this is a large cohort and we have only considered membranous staining, we believe our results are more representative of PD-L1 expression in MPM.

Infiltration of tumour nests by CD8⁺ lymphocytes has been shown to correlate with a favourable prognosis in several cancers, particularly colorectal cancer.²⁵⁰ Data regarding the prognostic implications of TILs including that of Tregs in MPM are sparse. Yamada et al. and Anraku et al. found a higher infiltration with CD8⁺ T cells heralded a better prognosis in MPM.^{230,254} However, both studies had limited numbers (44 and 32 respectively). We found no association between infiltration with CD4⁺, CD8⁺, or FOXP3⁺ T-Cells and survival. A direct correlation of the absolute ratios of higher CD4⁺/CD8⁺ with better survival has been described in hepatoma²⁷⁵ and cervical cancers.²⁵³ Our findings suggest that this parameter could potentially be used as a prognostic marker in MPM too but further validation in independent datasets would be required.

A significant finding of our study was the correlation of PD-L1 expression with TILs. Increased CD8⁺ T-Cells in PD-L1^{hi} is in keeping with the current understanding that the PD-1/PD-L1 interaction results in clonal proliferation of CD8⁺ lymphocytes that are functionally impaired.²⁷⁶ A similar correlation was observed by Cedrés et al.²⁶³ such that patient tumours with increased CD8⁺ TILs were seen in 68% and CD4⁺ in 59% of PD-L1⁺ patients. The antibody used for our IHC (E1L3N) has been known to stain immune cells and could potentially confound these results; however we have tried to avoid this by exclusively scoring PD-L1 expression on malignant cells and discounting the immune infiltrates.

This study confirmed the findings of the two smaller studies^{263,264} showing that PD-L1 positivity was related to worse outcome. However, the association with survival was lost in multivariate analysis when histology was included in the model, suggesting that the poor outcome seen in PD-L1+ patients was more a function of poorer histology rather than PD-L1 expression alone. Analyses of survival restricted to PD-L1+^{hi} showed the hazard associated to be significant but time dependent. Time variance of risks is thought to be common in oncology related studies with long follow up although it is only looked for and reported in a very small proportion of studies.²⁰⁶ Our finding of a constant HR of more than 6 amongst epithelioid MPMs could suggest that patients with PD-L1+^{hi} status would stand to benefit more from anti- PD-1/PD-L1 therapy. However, the proportion of these patients in our cohort of epithelioid patients (7/154; 4%) was small and therefore this finding needs to be validated in another cohort.

The association between PD-L1 positivity and histology is an important finding because it has been consistent in all reported series. Given that PD-L1 expression on tumour cells has to date been the most promising predictive biomarker,^{249,277} our data suggest that non-epithelioid MPM: a disease with few treatment options and universally poor outcomes may be best suited to these therapies. Interestingly, given their overall poorer prognosis, such patients are rarely eligible for clinical trials and so there are limited data currently available for these subtypes.

By comparing PD-L1 expression in tumour samples obtained from the same patient at two different time points, we tried to assess if there is significant temporal changes in PD-L1 expression. Elements of the surgical intervention such as pleural washing and iodine pleurodesis are known to induce pleural inflammation. We also sought to find if there are significant changes in the level of infiltration evidenced by the CD8+lymphocyte count before and after a surgical intervention. While the numbers were small for a comprehensive study of this aspect, we did find changes in PD-L1 status in 7 (19%) of patients evaluated. However, given our knowledge of the possible intra-tumour heterogeneity and the possibility that the samples may have been taken from very different areas of

the tumour, it is difficult to attribute the changes in PD-L1 expression status solely to temporal variation.

Using a TMA in lieu of full sections for assessment of PD-L1 expression and infiltration of CD4+ and CD8+ lymphocytes is subject to sampling error and this could be considered a limitation of this study. To reduce this, we sampled three cores from separate areas of the tumour. TMAs allow efficient assessment of large cohorts and as such has been used to assess PD-L1 and immune infiltrates for a multitude of malignancies.^{278,279} Also, high concordance between TMA and whole sections in the evaluation of IHC in mesothelioma has been previously demonstrated, although our study focuses not just on tumour expression but also immune cell infiltrates which may not be as concordant across a sample.⁷⁶

Our characterisation of the immunological infiltrates and PD-L1 in MPM provides important data from a large patient cohort. Our data suggest that the immune axis is a valid target in MPM, however single agent immune checkpoint inhibitors are unlikely to be effective in the majority of MPM patients, given the low rates of strong PD-L1 expression and previous data confirming low mutational burden. As combination immune checkpoint inhibition threatens to shift treatment paradigms in melanoma and NSCLC, these data provide further rationale towards study of other checkpoints and their ligands in MPM and perhaps the implementation of such combinations in this rare but deadly disease.

Chapter 6: Looking beyond PD-L1 in MPM -defining the hot, the warm and the cold tumours

6.1 Introduction

The successful use of immune checkpoint inhibitors has been a big advance in the development of cancer immunotherapy and as such, cancer immunotherapy was elected as the breakthrough of 2013 in 'Science'.²⁸⁰ Several studies with ipilimumab (IgG1 antibody against CTLA-4) showed impressive clinical responses in patients with advanced melanoma.^{281,282} The blockade of PD-1/PD-L1 interactions has been shown to improve clinical outcome in a variety of tumour types. The PD-1 inhibitors nivolumab and pembrolizumab have demonstrated response rates superior to ipilimumab in initial clinical trials in advanced melanoma patients.^{249,277,283} Importantly, several phase I/II trials have demonstrated durable clinical activity of anti-PD-1 immunotherapy even after treatment cessation with possible correlation with histological PD-L1 expression on primary tumours.^{277,284,285} In a phase I trial, anti-PD-L1 immunotherapy (ClinicalTrials.gov number, NCT00729664) also showed clinical activity across a wide array of advanced cancers including non-small cell lung cancer, melanoma and renal cell carcinoma.²⁸⁶ In MPM, although the DETERMINE trial¹⁶⁹ with tremelimumab(anti-CTLA-4 antibody) was negative, results with nivolumab,²⁶⁷ pembrolizumab (anti-PD-1 antibodies)^{170,268} and Avelumab (anti-PD-L1 antibody) have shown disease control rates of 50-80%.¹⁷² However, as results of these numerous trials come in, what is becoming clear is that a significant majority of cancers do not respond to these therapies. Available predictive markers including PD-L1 expression have not been able to reliably identify tumours and patients likely to respond.²³⁸

Results of reported series in MPM have made it clear that while checkpoint inhibition does have some activity in this malignancy with very limited therapeutic options, we don't yet know which patients are most likely to benefit. The quest to understand additional factors that dictate response to checkpoint inhibition have led to enthusiasm for research into the roles of other immune

suppression mechanisms like other ligands of PD-1 namely PD-L2 and checkpoints other than CTLA-4 and PD-1. Some of these checkpoints that have generated considerable interest are T-cell immunoglobulin mucin-3 (TIM-3) and lymphocyte activation gene-3 (LAG-3), OX-40 ligand and many others are upcoming.^{287,288} In addition, this could probably help understand some innate and acquired mechanisms to resistance to checkpoint inhibition therapy

6.1.1 Programmed cell death receptor ligand -2 (PD-L2)

PD-L2 (B7-DC) is the second ligand to PD-1. However, its expression is thought to be more restricted than that of PD-L1. PD-L2 expression by different cell types is regulated by signal transducer and activator of transcription (STAT) 6 and NF- κ B, and its most potent inducers appear to be Th2 cytokines, particularly IL-4. The main physiological function of PD-L2 could lie in the dampening and regulation of Th2- driven T-cell immune responses both during the induction and the effector phase. In recent years evidence has accumulated showing that tumour microenvironments are often deviated towards an ineffective Th2 type of immune milieu, resulting in cancer cell escape from immune surveillance. Hence, there is a clear rationale to further investigate the relevance of PD-L2 in cancer.²²⁷

The prognostic implications of PD-L2 positivity has been investigated in several tumour types. Ohigashi et al.²⁸⁹ found that similar to patients who stained positively for PD-L1, those who were PD-L2 positive also had significantly poorer survival. Similarly, in an analysis of 85 patients with hepatocellular carcinoma Jung et al.²⁹⁰ found that expression of PD-L1 and PD-L2 were associated with poorer survival on univariate analysis but only PD-L1 expression remained an independent prognostic factor on multivariate analysis. In a cohort of 70 patients with ovarian cancer, the majority of the tumours were negative or weakly positive and although PD-L2 expression was correlated with an impaired survival, this did not reach statistical significance.²⁹¹ Another study involving 125 patients with hepatocellular carcinoma found that a minority had high PD-L2 expression, and again, although PD-L2 expression was correlated with an impaired disease free

survival, this difference was not statistically significant.²⁹² Other studies investigating PD-L2 expression in squamous cell carcinoma lung²⁹³ and sarcomatous lung cancer²⁹⁴ have found no prognostic implications attached to PD-L2 expression. To the best of our knowledge, no studies evaluating the expression of PD-L2 in MPM patient samples have been reported yet.

6.1.2 T-cell immunoglobulin and mucin-domain containing-3 (TIM-3)

TIM-3 is a T-cell inhibitory receptor which was first identified 12 years ago as a molecule selectively expressed on IFN- γ -producing CD4+ T helper 1 (Th1) and CD8+ T cytotoxic 1 (Tc1) T cells.²⁹⁵ These studies showed that anti-TIM-3 antibody exacerbated experimental autoimmune encephalomyelitis, a T-cell-mediated autoimmune disease of the central nervous system providing the first indication that TIM-3 may function as a Tcell inhibitory receptor. Galectin-9 has been recognised to be the TIM-3 ligand and TIM-3-galectin-9 interaction has been shown to induce cell death in TIM-3 + Th1 cells.²⁹⁶ TIM-3 is now considered a key immune checkpoint in tumour-induced immunosuppression. Studies have demonstrated that Tim3+ T cells mark the most suppressed or dysfunctional population of CD8+ T cells in preclinical models.^{297,298} Unlike senescent T cells, it was found that the CD8+TIM-3+ T cells in cancer are not irreversibly cell-cycle arrested and that their proliferation can be restored by blockade of TIM-3 together with PD-1.²⁹⁹

In addition to its key role in regulating CD8+ T-cell effector function in cancer, recent studies further implicate TIM-3 in the biology of intratumoral FoxP3+ Tregs. In a cohort of NSCLC patients, approximately 60% of CD4+FoxP3+ TILs were found to express TIM-3. Interestingly, these TIM-3+ Tregs were infrequent in the peripheral blood of patients, and the presence of TIM-3+ Tregs correlated with the presence of nodal metastases and advanced cancer stage.³⁰⁰ TIM-3+ Tregs have been reported in hepatocellular, ovarian, colon, and cervical carcinomas.³⁰¹

Beside its role in T cells, TIM-3 has been noted to have effects in the myeloid compartment too. T-cell expression of TIM-3 has been shown to promote myeloid-derived suppressor cells (MDSC) in a

galectin-9– dependent manner.³⁰² TIM-3 is specifically up regulated on tumour-associated dendritic cells (TADC), in which it interferes with the sensing of DNA released by cells undergoing necrotic cell death. TIM-3 binds to high mobility group protein 1(HMGB1), thereby preventing HMGB1 from binding to DNA from dying cells. Thus, TIM-3 binding to HMGB1 interfering with the alarmin function of HMGB1 and dampening activation of the innate immune response in tumour tissue.³⁰³

Targeting the TIM-3 pathway in preclinical cancer models has shown very promising results. In the Wilms tumour-3 (WT3) sarcoma and the transgenic adenocarcinoma of the mouse prostate C-1 (TRAMP-C1) cancer models, TIM-3 blockade alone was found to be effective in a dose-dependent manner. In preclinical models of colon carcinoma (CT26 and MC38), TIM-3 blockade alone exhibited similar efficacy to PD-1 pathway blockade.³⁰⁴ More interestingly, the combination of TIM-3 blockade with PD-1 pathway blockade was remarkably more effective in these models, such that tumour regression is more complete and observed with higher frequency than with blockade of either the TIM-3 or PD-1 pathway alone.^{300,304} Although the molecular mechanisms by which TIM-3/PD-1 pathway co-blockade achieves these effects have not yet been elucidated, TIM-3 pathway blockade alone is thought to restore IFN-g and TNF-a production as well as the frequency and proliferation of NY-ESO-1–specific CD8+ T cells in response to tumour antigen stimulation. Co-blockade of TIM-3 and PD-1 further restores IL-2 production in NY-ESO-1–specific CD8+ T cells.³⁰⁰

A unique feature of TIM-3 is its expression only on selective T cells that have differentiated toward an IFN-g–producing phenotype²⁹⁵, and in patients with cancer, TIM-3 seems to be expressed primarily in intratumoral T cells.³⁰⁰ This is in contrast to CTLA-4 and PD-1. CTLA-4 is known to be up regulated on all effector T cells and is also expressed on all Tregs. PD-1 is similarly up regulated on all effector T cells. This is of importance because blockade of checkpoint receptors that are widely expressed could promote autoimmune-like side effects. Thus, TIM-3 blockade is less likely to interfere with the regulation of T-cell responses outside of tumour tissue than blockade of either CTLA-4 or PD-1.³⁰⁵ TIM-3 blockade is therefore less likely to be associated with adverse autoimmune-

like toxicities. This notion is supported by studies which have demonstrated that TIM-3-deficient mice do not exhibit autoimmunity,³⁰⁶ unlike both CTLA-4-deficient³⁰⁷ and PD-1 deficient mice.³⁰⁸ Also, tumour-bearing mice treated with anti-TIM-3 antibody do not exhibit autoimmunity.³⁰⁴

Given its selective expression on tumour tissue and its role in multiple immunosuppressive mechanisms, TIM-3 is now emerging as an interesting target for checkpoint inhibition therapy. In MPM, studies investigating TIM-3 expression have been sparse and typically small scale. Studying 43 resected cases of MPM Awad et al. found greater expression of TIM-3 in T cells of PD-L1+ cases than in PD-L1-. They also found a greater population of PD-1+TIM-3+ T cells in PD-L1+ cases.³⁰⁹ Another study incorporating 54 patients (40 untreated and 14 chemotherapy pre-treated) studied the expression of the checkpoints PD-1, LAG3 and TIM-3. The authors found that TIM-3 was expressed less often in pre-treated samples compared to untreated samples. After multivariate analysis, expression of CD4 and TIM-3 in lymphoid aggregates were good prognostic factors ($p=0.008$; $p=0.001$).³¹⁰

6.1.3 Lymphocyte activation gene -3 (LAG-3)

LAG-3 was cloned in 1990 as a membrane protein with diverse effects on T cell function. It is a checkpoint receptor that is not expressed by resting T cells but is up regulated several days after T cell activation.³¹¹ LAG-3 plays a role in the negative regulation of T cell function³¹² and is up regulated on exhausted T cells compared with effector or memory T cells.³¹³ As such blockade of LAG3 *in vitro* augments T cell proliferation and cytokine production.³¹⁴ In the context of cancer, LAG3 is up-regulated on TILs^{315,316} and blockade of LAG3 can enhance anti-tumour T cell responses.³¹⁷ Dual blockade of the PD1 pathway and LAG3 has been shown in mice and humans to be more effective for anti-tumour immunity than blocking either molecule alone.^{315,318,319} LAG3 has a role not only in effector T cells but also in Tregs. LAG3 is expressed on activated TReg cells at higher levels than on effector T cells. LAG3 blockade has been shown to inhibit the suppressive activity of Tregs *in vitro* and *in vivo* in a model of autoimmune pulmonary vasculitis.³²⁰ Also, LAG-3 interaction with MHC

class II molecules expressed by melanoma cells has been shown to protect the tumour cells from apoptosis.³²¹ Therefore, LAG-3-specific monoclonal antibodies could interfere with this protection from apoptosis, thus leading to enhanced tumour cell death.

Although clinical efficacy of LAG-3-specific monoclonal antibodies remains to be seen, some studies investigating antibody mediated LAG-3 blockade in haematological malignancies (ClinicalTrials.gov, number: NCT02061761) and LAG3 blockade in combination with PD1 blockade for solid tumours (ClinicalTrials.gov, number: NCT01968109, ClinicalTrials.gov, number: NCT03005782, ClinicalTrials.gov, number: NCT02658981) are currently underway. Investigation into LAG-3 expression in MPM and the potential anti-LAG-3 treatment has been sparse. A small scale study reported no detection of LAG-3 expression in TILs in 54 MPM samples³¹⁰ but comprehensive study in this field remains to be done.

6.1.4 Toll-like receptor-3 (TLR-3)

Toll like receptors are a class of membrane-spanning, non-catalytic receptors that play a key role in the innate immune system. They are usually expressed in sentinel cells such as dendritic cells and macrophages that recognize viral dsDNA. TLR-3 is one of 10 such receptors found in humans.³²² TLR-3 is also a death factor, triggering the release of apoptotic bodies inducing cancer cell apoptosis.^{322,323} TLRs also regulate cancer immunity and tolerance through innate immune responses mediated by Tregs, dendritic and other immune cells.^{324,325} TLR-3 can stimulate cancer cells to secrete pro-inflammatory cytokines and chemokines involved in anticancer immune responses.³²² Beside normal immune, epithelial and endothelial cells, TLR-3 is also known to be expressed by several malignancies including breast,³²⁶ prostate,³²⁷ and head and neck carcinomas.³²⁸ Interestingly, TLR-3 triggering was found to induce a strong up-regulation of both MHC class I and PD-L1 on neuroblastoma cells.³²⁹ This has created interest in combining TLR-3 ligand to anti-PD-1/PD-L1 treatment. Although comprehensive data on TLR-3 expression in MPM is still lacking a recent study reported positivity for TLR-3 on IHC in 96% of 58 MPM cases with weaker expression amongst

sarcomatoid MPMs.²⁶⁵ Considering that PD-L1 positivity has been consistently reported to be lower in epithelioid MPMs than in non-epithelioid MPMs,^{237,263,265} the high expression of TLR-3 in epithelioid MPMs could be exploited as an opportunity to convert PD-L1- to PD-L1+ cases potentially rendering them responsive to anti-PD-1/PD-L1 therapy.

6.1.5 Assessment of tumour infiltrating lymphocytes (TILs)

TILs are mononuclear immune cells that infiltrate tumour tissue, and have been described in most types of solid tumours. They have been studied in a variety of cancers for prognostication and its perceived predictive value. Increased TILs have been associated with better prognosis in many cancers including breast,^{330,331} colorectal,^{252,332} cervical³³³ and lung³³⁴ cancers. Most studies evaluating these roles have been based on evaluation of individual types of T lymphocytes namely cytotoxic T cells (CD8+), T helper cells (CD4+), regulatory T cells (Tregs) etc. It is known that the composition of the TILs is known to vary between tumour types and the prognostic and predictive prowess of these different components of the innate and adaptive immune system is not uniform across different tumours. More recently, a morphological assessment of the TILs based on a simple hematoxylin & eosin (H&E) slide examination has been shown to be an independent positive prognostic factor in HER2 positive early stage breast cancer.³³⁵ Similar assessment of TILs in lung cancer showed that patients with intense infiltration had better overall and disease free survival in two separate large cohorts.³³⁴ Although MPM pathogenesis is known to involve significant inflammation, the assessment of TILs in MPM has been very limited and has included very small number of patients. Higher infiltration with CD8+ lymphocytes has been associated with better survival in 32 patients who underwent EPP,²³⁰ but comprehensive assessment of clinicopathological associations of TILs in MPM is still lacking.

6.1.6 Tertiary lymphoid structures (TLS)

TLS are ectopic organized lymph node-like structures that typically form at sites of chronic inflammation and are involved in adaptive immune responses.³³⁶ Their occurrence in cancer is

sporadically documented and its role and clinical relevance is largely unknown. In solid tumours, a role for TLS in the organization of the local immune response and in lymphocyte recruitment has been suggested.³³⁷ TLS have been observed in almost all solid cancers including the most frequent tumours (i.e. NSCLC, CRC, breast, pancreatic, and gastric carcinoma, melanoma, ccRCC) and rare tumours (i.e. Merkel cell carcinoma, oral squamous cell carcinoma, Warthin tumour, liposarcoma) as well.³³⁶ In general, regardless of the approach used for assessment, and the stage of the disease, the presence of tumour-associated TLS has always correlated with a favourable clinical outcome in cancer patients.³³⁶ It is thought therefore that these ectopic lymphoid structures are critical for the development of a long-term protective adaptive immunity even in unfavourable tumour microenvironment.

In addition to a powerful prognostic biomarker, TLS has also been purported to be a predictive marker of efficient immunotherapies in cancer. In cases of pancreatic cancer treated with GVAX vaccination, a huge TLS density was observed in responders compared with non-responders or untreated patients.³³⁸ Therapeutic vaccination against HPV16 in patients with high-grade cervical intraepithelial neoplasia was also found to generate organization of immune infiltrates into TLS in comparison to untreated patients.³³⁹ An assessment of whether TLS are present in MPM and whether they have any prognostic role or predictive value for MPM immunotherapy remains unexplored.

Emerging literature suggests that a better and more comprehensive understanding of the immunological milieu of MPM is needed in order to better choose patients for checkpoint inhibition. Given our recent understanding of the roles of different checkpoint molecules and their interaction in tumour immunosuppression, awareness of their expression in MPM will likely also be important in development of personalized or tailored immunotherapy and in choosing combinations of different checkpoint inhibitors where indicated. Also, some characteristics of tumour immune microenvironment like TILs and TLS which remain yet unexplored could provide much needed

prognostic and predictive biomarkers in MPM. In this section of the research, we investigate expression of PD-L2, TIM-3, LAG-3 and TLR in our cohort. Combining this information with an objective assessment of the level of TILs, TLS and assessment of PD-L1 expression (from previous chapter) we derive a score to classify MPM samples based on their immunological characters and correlate this with clinicopathological features and survival.

6.2 Aims

The aims for this section of the research were

- 1) To define the expression of PD-L2, TIM-3, LAG-3 and TLR-3 in MPM
- 2) To study the level of TILs and presence of TLS in the MPM tumour microenvironment
- 3) To study the relationship of the above factors with clinicopathological parameters

6.3 Specific methods

A general description of methods used for IHC is given in chapter 2, section 2.6. A brief description of the protocol used for the conduct and subsequent assessment of IHC staining is presented in table 6.1

6.3.1 Immunohistochemistry

Table 6.1: Methodology of the IHC assays used in chapter 6

Antibody	Manufacturer	Catalogue number	Antigen Retrieval	Incubation time/temp	Controls	Assessment
PD-L2	Cell Signalling Technology	82723S	15 minutes in microwave TRS buffer Ph 9	4°C overnight	Tonsils	<p>PD-L2+ = \geq 10% membranous or cytoplasmic staining on tumour cells</p> <p>PD-L2+^{Hl} = \geq50% moderate to intense staining on tumour cells</p>
TIM3	Cell Signalling Technology	45208S	15 minutes in microwave EDTA buffer Ph 8	4°C overnight	Tonsils	<p>Counted using the Aperio automated counting system</p> <p>The counts were expressed as no. of cells staining with TIM3 per 1000 nucleated cells in the core</p>

LAG3	Cell Signalling Technology	15372S	15 minutes in microwave Citrate buffer Ph 6	4°C overnight	Tonsils	Counted using the Aperio automated counting system The counts were expressed as no. of cells staining with TIM3 per 1000 nucleated cells in the core
TLR3	Abcam	Ab6256 6	15 minutes in microwave TRS buffer Ph 9	4°C overnight	Testis	'H' Score

For assessment of PD-L2 IHC, in contrast to PD-L1, membranous and or cytoplasmic staining on $\geq 10\%$ tumour cells was considered as positive based on prior reports.^{289,290,294,340} To identify the subset with very high expression of PD-L2, as previously described for PD-L1, we defined PD-L2^{HI} as patients showing moderate to intense staining in $\geq 50\%$ tumour cells.²⁴¹ For calculation of 'H' score, the % of cells thought to be positive and the intensity of staining was taken into consideration. An 'H' score was calculated as follows: (% tumour cells staining weakly x 1) + (% of tumour cells moderately x 2) + (% tumour cells staining intensely x 3). This was calculated separately for each core and an average of evaluable cores was taken as final score. Cores with < 20% tumour were discarded.

6.3.2 Assessment of TILs and TLS in MPM

The assessment of TILs and TLS was performed on the H&E slides. The slides were first scanned on low power (2x, 4x) to look for the presence of TLS (lymphoid follicles or lymphoid aggregates) around the edge of the tumour and then in the surrounding normal tissue. The samples were marked as positive or negative for the presence of TLS. An approximate preliminary assessment of the amount of stroma present was also done on low power. The slide was then looked at in high power (20x, 40x) to evaluate the mix of the inflammatory cells in the stroma. Cases in which there were excessive neutrophils or eosinophils or these cells admixed with necrotic tumour were not evaluated further and were excluded from analysis. The whole stroma in the section was assessed to determine the approximate % of the stroma that is covered by mononuclear inflammatory cells (lymphocytes, plasma cells, dendritic cells and histiocytes). This was taken as the TILs score.

6.4 Results

6.4.1 PD-L2 expression

Cores of 306 patients were evaluable for PD-L2 staining. Seventy-five (24.5%) were found to be PD-L2 positive using a 10% membranous or cytoplasmic staining in tumour cells as the cut off. Using $\geq 50\%$ moderate or intense membranous staining to define a high positive group, we found 15(4.9%) patients to be highly positive. For 294 patients, results of both PD-L1 and PD-L2 results were available. Amongst 173 PD-L1- patients in this group, 28 (16.1%) were positive for PD-L2 (27 were PD-L2 + and one was PD-L2+^{hi}). Conversely, amongst 219 patients who were PD-L2 negative, 74 (33.7%) were positive for PD-L1 (67 were PD-L1+ and 7 PD-L1+^{hi}). Although there was a strong association between PD-L1 and PD-L2 expression (Fisher exact test $p < 0.0001$), in a significant proportion of our MPM cohort (102/294 = 34.6%), the expression of these two ligands of PD-1 were independent of each other. Like PD-L1 positivity, PD-L2 positivity (PD-L2 + and PD-L2 +^{hi}) was also associated with non-epithelioid histology (Fisher's exact test $p < 0.0001$) and also with increased

infiltration with CD4+ (Fisher exact test $p = 0.0009$), CD8+ (Fisher's exact test $p = 0.0002$) and FOXP3 (Fisher's exact test $p < 0.0001$). PD-L2 expression did not show any relationship with history of asbestos exposure (Fisher's exact test $p = 0.31$) stage of the disease (Fisher's exact test $p = 0.21$) or physiological status (Fisher's exact test $p = 0.18$) at diagnosis. Representative IHC pictures of PD-L2 in MPM are presented in figure 6.1.

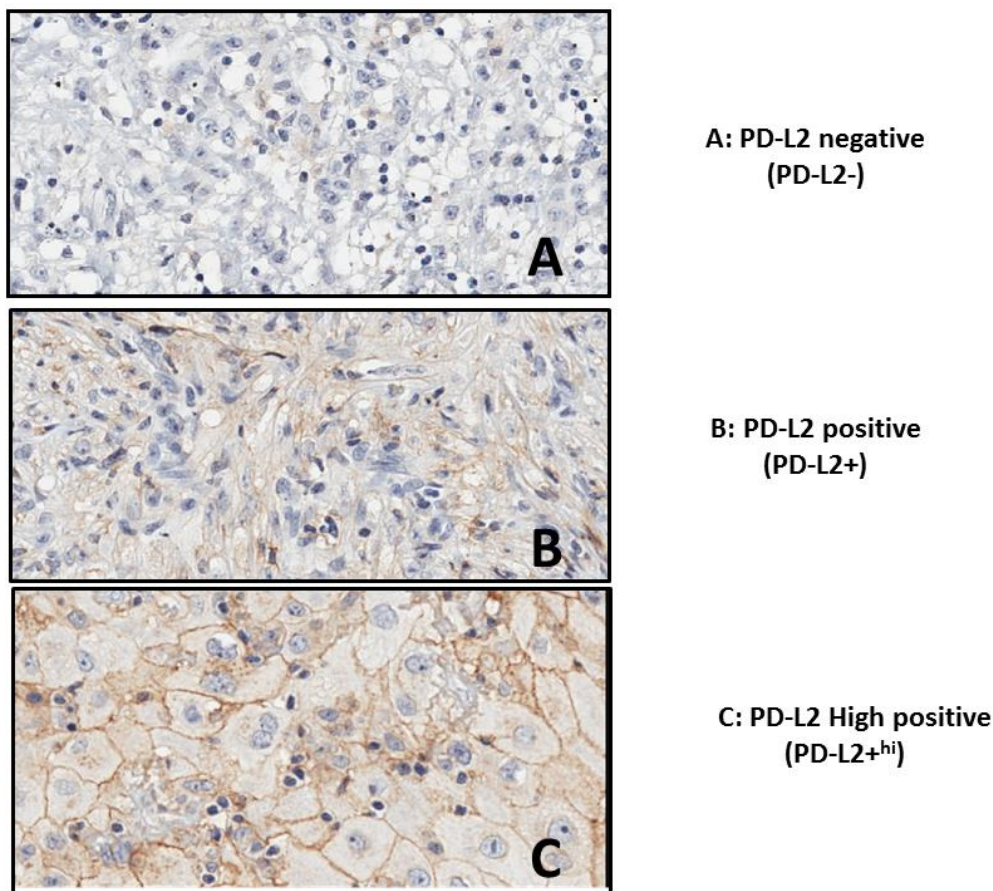


Figure 6.1: Representative pictures of PD-L2 staining in MPM.

6.4.2 TIM3 expression in MPM

We found expression of TIM3 in 279 of 297 (99.4%) evaluable patients. When divided by the tertiles, high TIM3 expression (highest tertile) was associated with PD-L1 (Chi square test $p = 0.028$) and PD-L2 (Chi square test $p < 0.0001$) expression. Non epithelioid MPM were more likely to have a high infiltration with TIM3+ lymphocytes (Chi square test $p = 0.012$) and patients with high TILs also

had high TIM3 (Pearson R = 0.53; $p < 0.0001$) possibly signalling that most of the infiltrating lymphocytes represented an exhausted phenotype. Presence of TLS was not different between patients who did and did not have high TIM3+ lymphocytes (Fisher's exact test $p = 0.31$).

6.4.3 LAG3 expression in MPM

We found LAG3 positive lymphocytes in only 7/297 (0.2%) evaluable patients. On account of the near universal lack of expression of LAG3 in lymphocytes infiltrating MPM, we did not further evaluate its relationships with other clinicopathological covariates.

6.4.4 TILs and TLS

Three hundred and eight samples were deemed evaluable for morphological assessment of TILs. Expressed as the percentage of the stroma covered by infiltrating mononuclear inflammatory cells (lymphocytes, plasma cells, macrophages and histiocytes), the scores ranged from 0-90 (median 30). Stratified using tertiles, high TILs were seen in patients who were PD-L1 (Chi square test $p = 0.002$) and PD-L2 positive (Chi square test $p < 0.0001$) and of non-epithelioid histological subtype (Fischer's exact test $p = 0.01$).

Two hundred and seventy nine samples were assessable for the presence of TLS of which the majority (220/279; 78.8%) were positive. Presence of TLS however did not correlate with PD-L1 (Chi square test $p = 0.47$) or PD-L2 (Chi square test $p = 0.43$) positivity or high TIM3 expression (Chi square test $p = 0.38$). The levels of TILs were not different between patients who did and did not have TLS (Unpaired T test $p = 0.14$). Their presence was also independent of histology (Chi square test $p = 0.91$).

6.4.5 TLR3 expression

Three hundred and twenty four patients were evaluable for TLR3. The "H" score for TLR3 expression on tumour cells in our MPM cohort ranged from 0 to 300 (median = 100). We found a significantly higher TLR expression in epithelioid MPMs than biphasic and sarcomatoid MPMs (Figure

6.2). Also, TLR expression was significantly higher amongst PD-L1- ('H' score 115 ± 5 vs 92.98 ± 7.1 ; unpaired T test $p = 0.01$) and PD-L2- (116.2 ± 5.5 vs 74.4 ± 8.2 ; unpaired T test $p = 0.002$). Representative pictures of IHC for TIM3, LAG3 and TLR3 have been presented in Figure 6.3

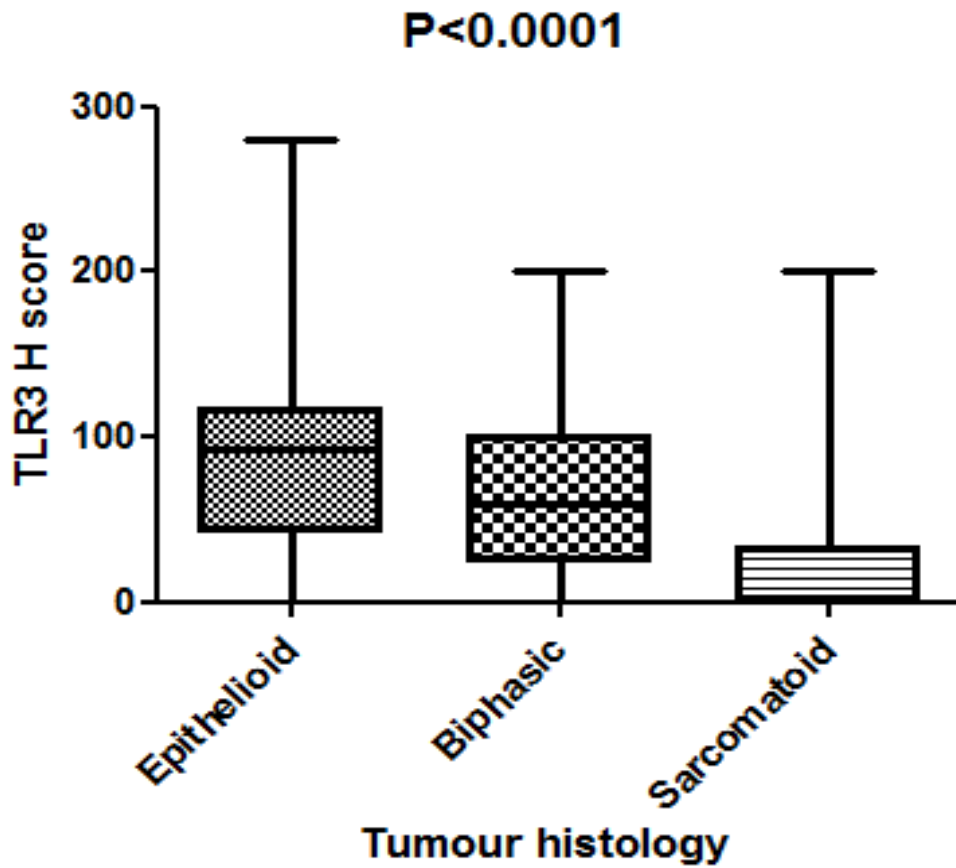


Figure 6.2: TLR3 expression in different MPM histotypes.

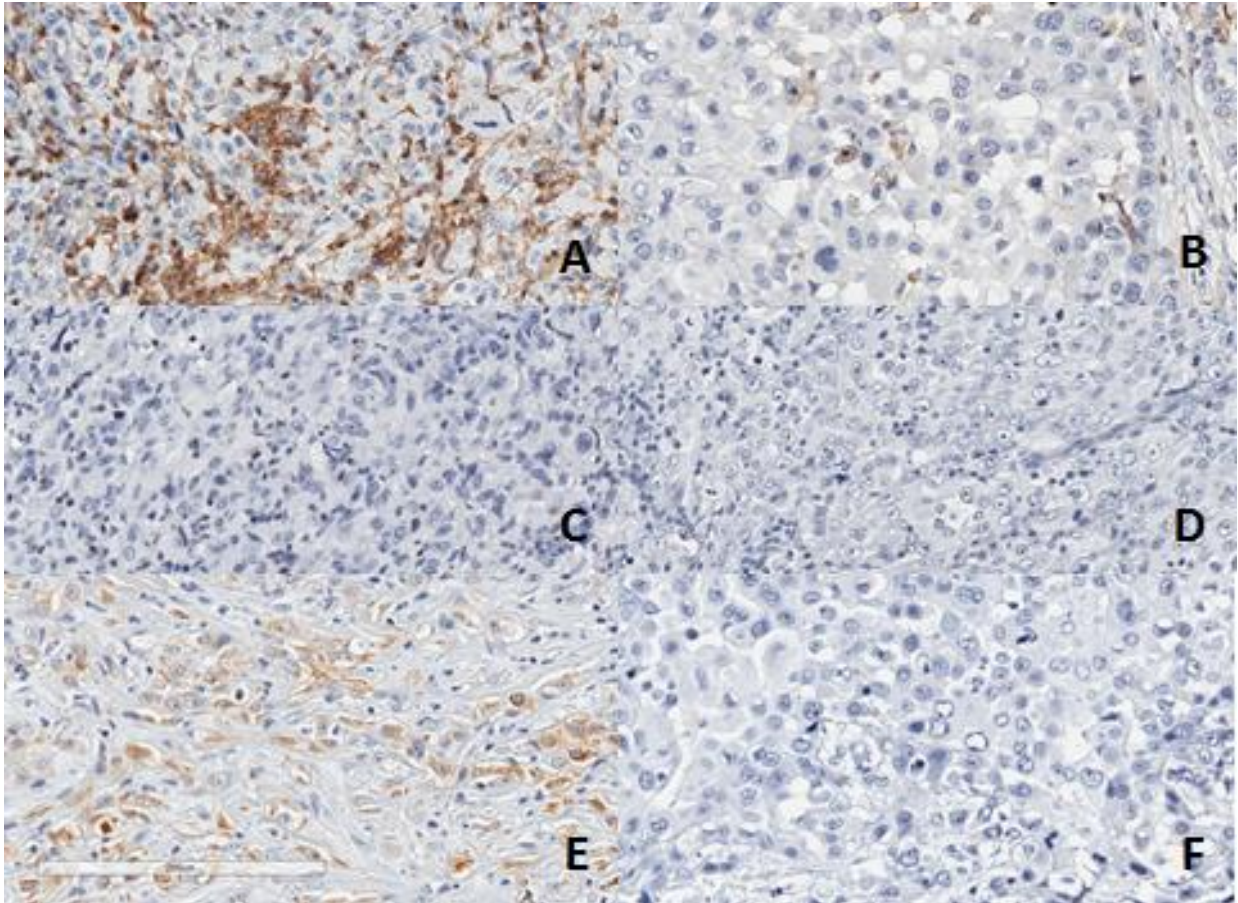


Figure 6.3: Representative pictures of IHC for TIM3, LAG3 and TLR

A: High infiltration with TIM3+ lymphocytes B: Low infiltration with TIM3+ lymphocytes C: Positive for LAG3+ lymphocytes D: Negative for LAG3+ Lymphocytes E: Positive staining for TLR3 in tumour cells F: Negative for TLR3 in tumour cells

6.4.6 Survival analysis

On univariate analysis, PD-L2 positivity (HR = 3.2; CI = 2.2-4.6; Log rank P < 0.0001), high TILs (HR = 2.03; CI = 1.5-2.6; Log rank P < 0.0001), and high TIM3+ lymphocytes (HR = 1.3; CI = 1.0-1.7; Log rank P < 0.04) were found to be related to poorer OS. Patients with TLS were seen to do better (OS = 13.7 vs 9.2 months) but this was not statistically significant (Log rank p = 0.11) (Figure 6.3). On multivariate analysis, TILs and TLS were found to remain significantly associated with survival along with histology and physiological status (Table 6.2).

Table 6.2: Multivariate analysis for OS

Variables in the Equation				
	P Value	Hazard Ratio	95.0% Confidence interval	
			Lower	Upper
Lymphoid aggregate	.002	0.61	.45	0.83
TILS scoring (High vs Low)	.000	2.12	1.4	2.6
Histology (non-epithelioid vs epithelioid)	.000	2.8	1.8	4.2
ECOG (≤ 1 vs ≥ 2)	.000	3.6	2.04	6.4

6.4.7 Development of Immune checkpoint score (ICS)

Our assessment of the immunological milieu in MPM suggests that this tumour expresses various checkpoint receptors and ligands in varying extents. Broadly, MPM tumours can be classified as immunologically “hot”, “warm” or “cold” based on the presence/absence of an active immune microenvironment. To enable us to clearly define these groups, we combined our assessment of the expression of PD-L1, PD-L2 and TIM3 to derive the “Immune checkpoint score (ICS)”. Assessment of LAG3 was not included because of the very low expression rates seen in our cohort. The score was derived as depicted in Table 6.3. We then studied the clinicopathological correlates of ICS. Our expectation was that high ICS would be most likely related closely with non-epithelioid histological subtype, heavy TILs and possibly poorer survival.

Table 6.3: Immune checkpoint score composition.

Marker	Assessment	Score
PD-L1	PD-L1 -	0
	PD-L1 +	1
	PD-L1 + ^{hi}	2
PD-L2	PD-L2 -	0
	PD-L2 +	1
	PD-L2 + ^{hi}	2
TIM3	Lower tertile	0
	Middle tertile	1
	Upper tertile	2

Total score 0-6

We found 284 patients in which valid assessments of all the three markers were available. When divided into three groups – scores ≤ 2 , scores 3&4 and >4 , we found that patients with high scores were more likely to be of non-epithelioid histology and had greater TILs. The presence of TLS however did not appear to be different between patients with low or high ICS (Table 6.4). Patients with high ICS had a poorer OS on univariate analysis (Figure 6.4) but not on multivariate analysis.

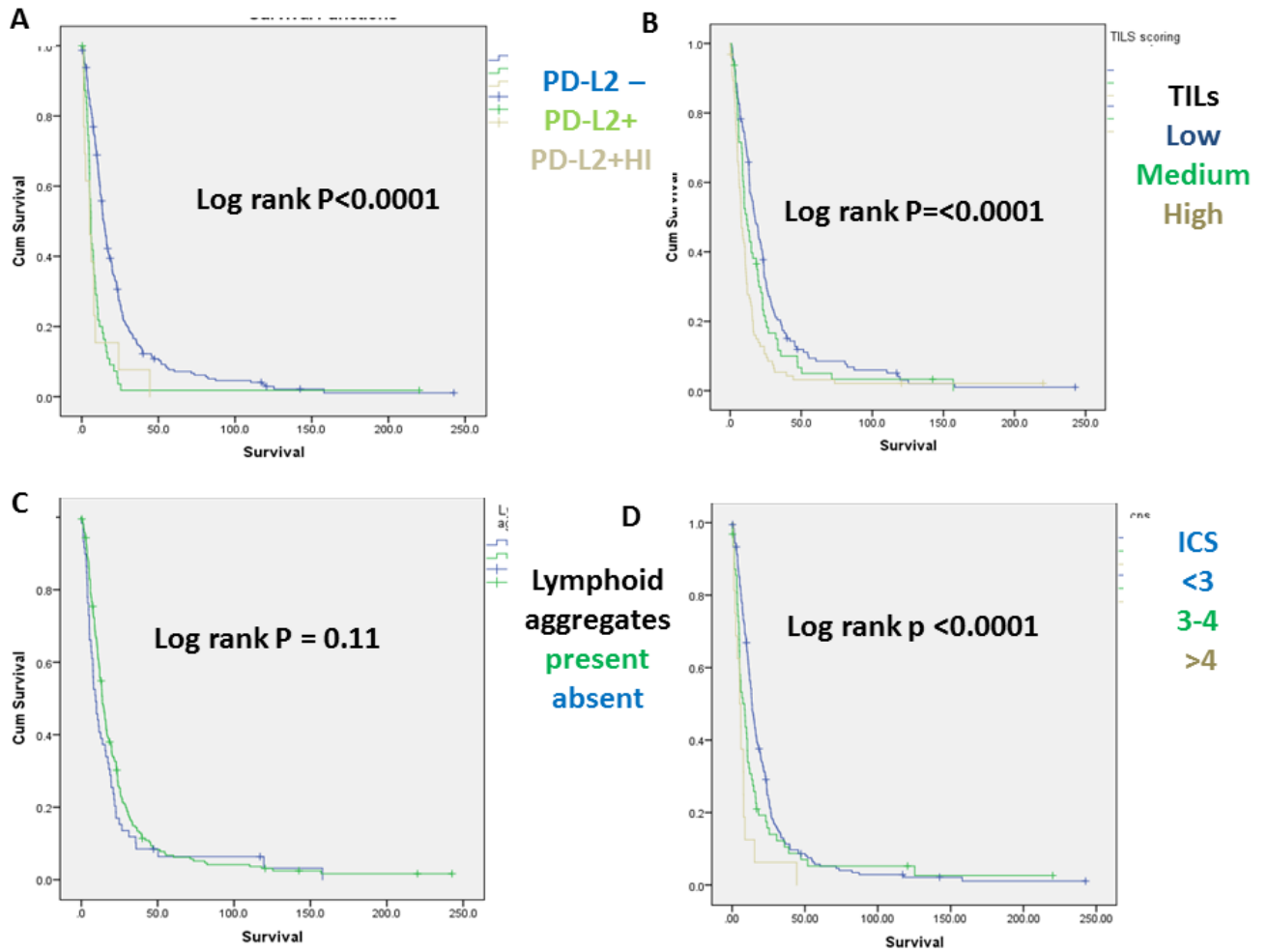


Figure 6.4: Univariate survival analysis.

A: KM curve comparing OS between PD-L2 groups. **B:** KM curve comparing OS between patients with high, medium and low TILs. **C:** KM curve comparing OS between patients who did and did not have TILs in tumour margin. **D:** KM curve comparing OS between patients with high, medium and low ICS.

Table 6.4: ICS and its relationship with other immune parameters, histology and survival.

	Total number evaluated	0-2	3+4	>4	P value
Total numbers	284	197	67	18	
TILs low	259	94	12	0	<0.0001°
TILs medium		49	10	2	
TILs high		42	36	14	
Lymphoid aggregates +	233	37	7	3	0.509°
Lymphoid aggregates -		134	42	10	
CD4 low	253	74	10	1	<0.0001°
CD4 medium		62	21	3	
CD4 high		44	27	11	
CD8 low	260	77	10	1	<0.0001°
CD8 medium		66	21	2	
CD8 high		43	31	15	
Epithelioid	270	132	29	2	<0.0001°
Biphasic		45	17	3	
Sarcomatoid		15	16	11	
Overall Survival (months)	282	13.7	8.6	5.2	<0.0001*

° P value from Chi square test. *P value from log rank

6.4.8 Comparing the immunological milieu in MPM and NSCLC

We used a large cohort of resected NSCLC to compare and contrast the expression of these markers in the two malignancies. A set of TMAs consisting of 1mm cores of FFPE tissue from 522 resected NSCLC patients previously constructed by our group and whose characteristics have been reported before²⁷⁰ was used. In brief, the cohort was composed of 265 adenocarcinomas, 182 squamous cell carcinomas and 75 lung cancers of other histologies. The data regarding PD-L1

expression status was derived from the prior study. However, studies into expression of PD-L2, TIM3+ and LAG3+ lymphocyte counts in these NSCLC samples were performed on the TMA described using IHC techniques described in table 6.1. Taking a 5% cut off, there was no difference in the rates of PD-L1 positivity rates between the two malignancies (Fisher's exact test $p = 0.65$) but when we considered the PD-L1+^{hi} group separately, a significantly higher proportion of NSCLC patients were found to be PD-L1+^{hi} than MPM patients. For PD-L2, we found a significant higher rate of positivity (negative vs positive; $p < 0.0001$) amongst MPM patients as compared to NSCLC. We found 4.5% of MPM patients to be PD-L2+^{hi} but none on the NSCLC cohort. Comparison of the presence of TIM3 positivity and LAG3 positivity between the two malignancies also showed significant differences (Table 6.5).

Table 6.5: Comparison of the expression of some checkpoint receptors and ligands in NSCLC and MPM

Marker		Number evaluated	NSCLC N (%)	Number evaluated	MPM N (%)	P value
PD-L1	PD-L1-	420	237 (56)	309	181 (58.2)	<0.0001 [¥]
	PD-L1+		83 (20)		100 (32.2)	
	PD-L1+ ^{hi}		100 (24)		30 (9.6)	
PD-L2	PD-L2-	461	411 (89)	306	231 (69)	<0.0001 [¥]
	PD-L2+		50 (11)		60 (17.9)	
	PD-L2+ ^{hi}		0 (0)		15 (4.5)	
TIM3	*TIM3-	438	175 (39.9)	297	80 (27)	0.0003 ^α
	TIM3+		263 (60.1)		217 (73)	
LAG3	*LAG3-	330	274 (83)	297	290 (99.7)	<0.0001 ^α
	LAG3+		56 (17)		7 (0.02)	

*TIM3/LAG3 positive lymphocytes $\geq 5\%$ of cells in the core. ¥ p value from chi square test, α p value from Fisher's exact test.

6.5 Discussion

Here, we broaden the search for biomarkers within the MPM immune microenvironment. Over and above our assessment of PD-L1 expression and its correlations with CD4+ and CD8+ lymphocytes described in chapter 5, we also examined the expression of PD-L2, the other known ligand of the checkpoint receptor PD-1. Additionally, we explore the expression of other checkpoint molecules TIM3 and LAG3 which are gaining prominence as immunosuppressive agents. We found that a large proportion of MPM express PD-L2, nearly all show TIM3 expression in the infiltrating lymphocytes but LAG3 expression is very minimal. PD-L1+/^{hi} patients were more likely to be PD-L2+ and more likely have high expression of TIM3 but, more interestingly, we found that their expression could be mutually exclusive. For the first time, we demonstrated that the morphological assessment of TILs on H&E slides can act as an independent poor prognostic factor in MPM. Combining our assessments of the different immunological markers in MPM, we demonstrated that MPM samples were divisible into “hot” tumours (characterised by high infiltration by lymphocytes but also high expression of PD-L1, PD-L2 and TIM3), “cold” tumours (low TILs and low/no expression of PD-L1, PD-L2 and TIM3). We found non-epithelioid MPMs more likely to be “hot” than epithelioid MPMs.

Drugs designed to disrupt the PD-1/PD-L1 axis and therefore prevent PD-1– mediated T-cell inhibition are monoclonal antibodies directed against PD-1 or PD-L1. Anti-PD- 1 antibodies (nivolumab, pembrolizumab) should block PD-1 binding to both of its ligands, PD-L1 and PD-L2, whereas anti- PD-L1 antibodies (atezolizumab, avelumab) should be selective in preventing PD-1 binding to PD-L1, maintaining the ability for PD-1 to interact and bind to PD-L2. Agents from both these classes are being used in checkpoint inhibition therapy in multiple malignancies including MPM.^{172,268} Although preclinical studies in mice have shown that in vivo administration of either anti-PD–1 or anti-PD-L1 antibodies inhibited the growth of myeloma cells and solid tumours, and prevented the metastatic spread of melanoma and colon cancer cells,³⁴¹ reported studies of the use of these two subclasses in lung cancer seem to suggest a difference in their activity in favour of PD-1 inhibitors.³⁴² In mesothelioma, the disease control rates (DCR) of pembrolizumab (76-80%)^{266,343} have

been reported as compared to DCR of 56%¹⁷² with avelumab. Although these results are very preliminary, they certainly necessitate a closer look at the expression of PD-L2 and its interaction with other components of the immune microenvironment. Our results suggest that a significant proportion of MPM express PD-L2. PD-L1 inhibitors leaving the PD-L2 free to interact with PD-1 and therefore allowing the PD-1 axis to continue its immunosuppressive action could at least in part explain the failure of anti – PD-L1 therapy even in PD-L1+ patients. Additionally, the presence of PD-L2 positivity could also be one of the factors responsible for activity of anti- PD-1 treatment seen in PD-L1- patients.

PD-L2 expression as a prognostic marker has been studied in several malignancies as discussed previously. We found that while PD-L2+/^{hi} patients had worse OS on univariate analysis; this variable did not remain significantly associated with OS on multivariate analysis. Significant association of PD-L2 expression status (like PD-L1) with tumour histology (PD-L2+/^{hi} with non-epithelioid MPM) suggests that effect of PD-L2 on survival is probably a function of this association rather than a real influence on OS. Further studies into this on independent patient cohorts may shed more light on this.

TIM3 is emerging as an important checkpoint with preclinical data suggesting that TIM3 blockade may be efficacious alone³⁰⁴ and also in combination with PD-1 blockade.^{300,304} Our finding of expression of TIM3 in a vast majority of MPM patients suggests this pathway may be an important immune evasion mechanism in MPM. This is important as it presents TIM3 blockade as a viable new strategy for checkpoint inhibition therapy in MPM. This widespread expression of TIM3 could probably also be the reason why only a small proportion of MPM patients mount an effective immune response to PD-1 blockade alone. Our finding that PD-L1 and PD-L2 positive patients are more likely to have high TIM3 expression suggests a role for combined PD-1/PD-L1 and TIM3 blockade. Like Marcq et al.³¹⁰ before us, we found very little expression of LAG3 in MPM. This

probably suggests this pathway is not utilised for immune evasion in MPM and so LAG3 blockade may not be a viable option in this malignancy.

Our findings demonstrate that MPM tumours have differing immunological milieu with samples broadly definable into “hot”, “warm” and “cold”. The immunological characteristics of the tumour are most closely related to histotype. Sarcomatoid MPMs are more likely to be “hot” and epithelioid MPMs are more likely to be cold. This would suggest that sarcomatoid MPMs are the best targets for immunotherapy. Also, importantly we found that although expression of PD-L1, PD-L2 and TIM3 track each other, in a significant proportion of patients, their expression are mutually exclusive. This would imply that a comprehensive assessment of expression of the different checkpoint receptors and their ligands would be necessary to tailor the checkpoint inhibition therapy for individual patients. This could also help guide combination checkpoint therapy in the future. The composite assessment may also be a better predictor than PD-L1 alone and as such this needs to be evaluated in MPM patients treated with anti- PD-1/anti- PD-L1 therapy.

The negative prognostic implication of TILs seen in our cohort is in stark contrast to previous studies in breast^{330,331} and lung cancers.³³⁴ One disadvantage of assessment of TILs on routine H&E sections is that although a good assessment of the degree of infiltration can be made, it does not delineate different lymphocyte subsets that might differ greatly in their roles in anti-tumour immunity. Also it offers no information on their functional status. Our research described in this chapter and in the previous one show MPM tumours have high infiltration with CD8+ and CD4+ T lymphocytes. However, the near universal expression of TIM3 suggests TILs in MPM might in fact represent accumulation of exhausted lymphocytes unable to mount an effective immune response to the cancer. Although, validation in independent cohorts would be necessary, TILs assessment may provide an important prognostic marker in MPM.

Presence of TLS in our cohort unlike other immunological markers was not associated with MPM histotype and was independent of expression of PD-L1, PD-L2 and TIM3. Presence of TLS was

independently associated with better survival. The prognostic role of TLS has been described in other solid malignancies and so it is not surprising that it is associated with favourable prognosis in MPM.³³⁶ Whether it has a role as a predictor for checkpoint inhibition therapy in MPM could be an interesting question for a future study.

With the expansion of our knowledge of immunosuppressive mechanisms utilized by cancer, it has become clear that multiple checkpoint receptors and their ligands are likely in play in the tumour microenvironment.³⁴⁴ Available literature suggests response to checkpoint inhibition therapy is not uniform across tumour types. While lung cancer along with melanoma has shown significant response, the success in mesothelioma has been modest at best.¹⁶⁶ The mutational burden and therefore the availability of cancer neoantigens has been suggested as a possible reason for the differences in response.²³⁵ Whether differences in the checkpoint expression landscape amongst cancers could also influence susceptibility to individual inhibitors would be an interesting and important question to answer. Our results show differences in expression patterns for PD-L1, PD-L2, TIM3 and LAG3 between lung cancer and MPM. This could suggest these tumours may use different pathways for immune evasion and therefore could benefit from different approaches in terms of choice of the checkpoint inhibitor.

Our findings on the expression on TLR3 expression in MPM validated results of a smaller prior study.²⁶⁵ Given the noted ability of TLR3 agonists to induce PD-L1 positivity,³²⁹ and our finding that its expression is higher amongst epithelioid MPMs, it may represent an opportunity to induce PD-L1 expression in PD-L1- tumours and possibly enhance their susceptibility to anti- PD-1/anti- PD-L1 treatment. Future lab based studies would be required to explore this avenue further.

Macrophages are known to be particularly abundant in the tumour microenvironment and present at all stages of tumour progression. Existing literature suggests that these macrophages generally play a pro-tumoural role and can stimulate angiogenesis and enhance tumour cell invasion, motility and intravasation.³⁴⁵ Therapeutic success in targeting these pro-tumoural roles in pre-clinical

models and in early clinical trials suggests that macrophages are attractive targets as part of combination therapy in cancer. Investigating the abundance and types (M1 vs M2) of macrophages in the MPM microenvironment would be an interesting extension to our present study. Similarly, it would also be prudent to study MDSCs and their role. We have uncovered interesting and potentially important biomarkers in TILs and TLS. Further investigations in independent cohorts need to be done to validate our findings and also to explore any predictive role for TILs and/or TLS in patients with MPM receiving checkpoint inhibition.

As the use of checkpoint inhibition therapy in treatment of MPM grows, the ability to profile the tumor immune infiltrate before, during, and after treatment with these immunomodulatory agents is likely going to be very important. They will be needed to improve patient care; to select appropriate immunotherapies for a given patient, and to advance our understanding of the complex cellular interactions occurring in the tumor microenvironment in response to these therapies. Recently described methods to quantitatively assess the immune cell composition and phenotype of the bulk tumor microenvironment using flow cytometry on FNA biopsies³⁴⁶ and digital enumeration of inflammatory leukocyte infiltrates using single cell RNA-seq data^{347,348} are important advances in this direction.

Our extended exploration of the tumour immune microenvironment in MPM described in this chapter outlines the pattern of expression of PD-L2, TIM3, LAG3 and TLR3 in a large cohort of MPM. Significant expression of PD-L2 and TIM3 in MPM suggests that checkpoint inhibition therapy in MPM possibly needs to be tailored according to the expression profile of these markers along with that of PD-L1. These data also strengthen the argument for combination checkpoint inhibition rather than single blockade of PD-1/PD-L1 axis in MPM.

Chapter 7: Genome-wide copy number aberrations in MPM, correlation with tumour histology, immune characteristics and patient survival.

7.1 Introduction

Identification of driver mutations and development of targeted therapies against them have led to the improvement in the outlook for several cancers including lung cancer and melanoma. Recent reports also suggest that mutational load and load of neo-antigens of tumours determine response to checkpoint inhibition therapy.^{235,236} In a cancer like MPM with limited effective therapeutic options,³⁴⁹ a comprehensive understanding of the genetic alterations that drive it would be very important for the development and successful application of personalised therapeutics.

Genomic studies have been conducted in MPM before.^{27,28,55,350,351} Loss-of-function mutations in *CDKN2A*, *NF2* and *BAP1* have been reported.^{28,351,352} Also, previous studies have reported copy gains and copy losses involving multiple regions of the genome.^{28,351–353} Germline mutations in *BAP1* have been found to predispose carriers to MPM.³⁵⁴ However, other than the study by Bueno et al.⁵⁵ which analysed transcriptomes ($n = 211$), whole exomes ($n = 99$) and targeted exomes ($n = 103$) from 216 MPMs, all previous studies have typically been small scale. These prior studies provide considerable insight into the genomic aberrations that are common in MPM and transcriptome analysis conducted by Bueno et al. defined distinct molecular subtypes with prognostic implications. However, to date genomic alterations that could be considered driver events have not been identified.⁵⁶ No attempt has yet been made to correlate the genomic aberrations in MPM with the immunological milieu which could in turn help predict response of these tumours to immune based therapies.

As discussed in chapter one, section 1.4, MPM results from the accumulation of a number of acquired genetic events. The complexity of the genetic changes involved in this malignancy was first

demonstrated by use of karyotyping techniques.²⁵ Relative to the other solid malignancies, we now know that the mutational load of MPM is low.⁵⁵ One amongst a myriad of possible mechanisms of asbestos carcinogenesis in the pleura is the ability of the fibres to cause genomic disruption. Asbestos fibres that are taken up into the mesothelial cells can physically interfere with the mitotic process of the cell cycle by disrupting mitotic spindles. Tangling of asbestos fibres with chromosomes or mitotic spindles may result in chromosomal structural abnormalities and aneuploidy of mesothelial cells.⁹ It is therefore not surprising that starting from early studies using chromosomal banding technologies, multiple clonal chromosomal abnormalities have consistently been shown in mesothelioma.^{25,355-357} All chromosomes have been seen to contribute to numerical changes, and losses were more common than gains²⁵. The most frequent events observed in MPM are deletions in 1p21-22, 3p21, 4, 6q14-25, 9p21, 13q, 14q, 15q15, 17p13, and 22q3. Monosomy 22 is the most frequent numerical change^{37,355,356}. However, even as our knowledge of the extent of these recurrent copy number events in MPM has grown, comprehensive understanding of their clinical and prognostic implications is still lacking. The relative rarity of the disease and lack of large scale studies into genome wide copy number aberrations in well characterised datasets have limited our knowledge.

Parts of the research described in this section has been published in the Journal of Thoracic Oncology in the article titled "The Immune Microenvironment, Genome-wide Copy Number Aberrations, and Survival in Mesothelioma."²⁶⁹

7.2. Aims and objectives

The aims of the research described in this section were:

- 1) To conduct an exploratory study of the genome wide CNA in MPM genome using OncoScan
- 2) To correlate extent and pattern of CNA in MPM genome with clinical and pathological covariates
- 3) To study differences in extent and pattern of CNAs between different histotypes of MPM
- 4) To correlate the extent and pattern of CNAs with the immunological milieu of the tumour especially PD-L1 expression and level of infiltration with CD4+ and CD8+ lymphocytes

7.3 Specific methods

Copy number analysis was performed on the FFPE derived DNA of 113 patients out of which 100 samples passed strict quality control measures described in the methods section 2.12.2. This analysis was performed in two cohorts named the test (n = 68; QC passed = 63) and validation (n = 45; QC passed = 37) cohorts. A list of samples and their QC status is given in table 7.1.

Table 7.1: QC results of individual samples.

Sample Name	Cohort	MAPD	ndSNPQC	Unmet Threshold	Accepted/Rejected
1B	Test	0.20	45.95		Accepted
2B	Test	0.31	15.80	MAPD & ndSNPQC	Accepted
3B	Test	0.53	5.99	MAPD & ndSNPQC	Rejected
4B	Test	0.19	47.42	ndSNPQC	Accepted
5B	Test	0.29	16.80	ndSNPQC	Accepted
6B	Test	0.19	50.34		Accepted
7B	Test	0.45	7.88	MAPD & ndSNPQC	Rejected
8B	Test	0.24	26.53		Accepted
9B	Test	0.19	42.55		Accepted
10B	Test	0.24	21.34	ndSNPQC	Accepted
11B	Test	0.24	47.94		Accepted
12B	Test	0.34	13.06	MAPD & ndSNPQC	Accepted
13B	Test	0.28	19.58	ndSNPQC	Accepted
14B	Test	0.29	13.70	ndSNPQC	Accepted
15B	Test	0.22	36.83		Accepted

16B	Test	0.19	51.36		Accepted
17B	Test	0.27	9.52	ndSNPQC	Accepted
18B	Test	0.24	28.49		Accepted
19B	Test	0.20	37.78		Accepted
20B	Test	0.20	38.86		Accepted
THA703A1	Test	0.20	39.46		Accepted
THA703A2	Test	0.30	22.90	ndSNPQC	Accepted
THA703A3	Test	0.22	41.20		Accepted
THA703A4	Test	0.25	41.20		Accepted
THA703A5	Test	0.21	43.84		Accepted
THA703A6	Test	0.24	31.10		Accepted
THA703A7	Test	0.21	45.35		Accepted
THA703A8	Test	0.21	43.72		Accepted
THA703A9	Test	0.27	28.82		Accepted
THA703A10	Test	0.22	41.57		Accepted
THA703A11	Test	0.23	36.89		Accepted
THA703A12	Test	0.24	42.80		Accepted
THA703A13	Test	0.26	21.93	ndSNPQC	Accepted
THA703A14	Test	0.29	28.31		Accepted
THA703A15	Test	0.24	26.73		Accepted
THA703A16	Test	0.21	40.76		Accepted
THA703A17	Test	0.27	25.69	ndSNPQC	Accepted
THA703A18	Test	0.23	42.04		Accepted
THA703A19	Test	0.24	31.38		Accepted
THA703A20	Test	0.21	36.00		Accepted
THA703A21	Test	0.30	13.08	ndSNPQC	Accepted
THA703A22	Test	0.21	32.01		Accepted
THA703A23	Test	0.26	26.98		Accepted
THA703A24	Test	0.30	6.31	MAPD & ndSNPQC	Rejected
THA703A25	Test	0.29	24.65		Accepted
THA703A26	Test	0.49	8.11	MAPD & ndSNPQC	Rejected
THA703A27	Test	0.32	20.64	ndSNPQC	Accepted
THA703A28	Test	0.32	16.43	MAPD & ndSNPQC	Accepted
THA703A29	Test	0.28	23.76	ndSNPQC	Accepted
THA703A30	Test	0.33	17.67	MAPD & ndSNPQC	Accepted
THA703A31	Test	0.28	22.76	ndSNPQC	Accepted
THA703A32	Test	0.30	25.23	ndSNPQC	Accepted
THA703A33	Test	0.28	27.08		Accepted
THA703A34	Test	0.41	13.43	MAPD & ndSNPQC	Rejected
THA703A35	Test	0.33	23.60	MAPD & ndSNPQC	Accepted
THA703A36	Test	0.33	24.53	MAPD & ndSNPQC	Accepted
THA703A37	Test	0.29	25.19	ndSNPQC	Accepted
THA703A38	Test	0.30	19.86	MAPD & ndSNPQC	Accepted
THA703A39	Test	0.31	20.03	MAPD & ndSNPQC	Accepted
THA703A40	Test	0.34	14.62	MAPD & ndSNPQC	Accepted

THA703A41	Test	0.29	24.21	ndSNPQC	Accepted
THA703A42	Test	0.37	12.99	MAPD & ndSNPQC	Accepted
THA703A43	Test	0.38	12.07	MAPD & ndSNPQC	Accepted
THA703A44	Test	0.31	15.64	MAPD & ndSNPQC	Accepted
THA703A45	Test	0.29	24.85	ndSNPQC	Accepted
THA703A46	Test	0.32	18.87	MAPD & ndSNPQC	Accepted
THA703A47	Test	0.44	7.12	MAPD & ndSNPQC	Rejected
THA703A48	Test	0.30	5.03	MAPD & ndSNPQC	Accepted
77	Validation	0.25	34.84		Accepted
80	Validation	0.27	20.87	ndSNPQC	Accepted
81	Validation	0.28	19.55	ndSNPQC	Accepted
82	Validation	0.29	19.11	ndSNPQC	Accepted
83	Validation	0.25	13.78	ndSNPQC	Accepted
84	Validation	0.26	30.08		Accepted
86	Validation	0.27	30.43		Accepted
87	Validation	0.30	18.93	ndSNPQC	Accepted
88	Validation	0.26	28.76		Accepted
89	Validation	0.30	15.16	MAPD & ndSNPQC	Accepted
90	Validation	0.29	22.14	ndSNPQC	Accepted
92	Validation	0.25	21.75	ndSNPQC	Accepted
93	Validation	0.28	18.25	ndSNPQC	Accepted
94	Validation	0.27	24.77	ndSNPQC	Accepted
95	Validation	0.25	22.49	ndSNPQC	Accepted
96	Validation	0.27	22.02	ndSNPQC	Accepted
97	Validation	0.25	22.78	ndSNPQC	Accepted
100	Validation	0.29	24.66	ndSNPQC	Rejected
101	Validation	0.27	27.43		Accepted
103	Validation	0.30	15.97	ndSNPQC	Accepted
104	Validation	0.31	20.15	MAPD & ndSNPQC	Accepted
105	Validation	0.33	14.81	MAPD & ndSNPQC	Accepted
106	Validation	0.24	30.92		Accepted
107	Validation	0.27	19.83	ndSNPQC	Accepted
110	Validation	0.50	5.23	MAPD & ndSNPQC	Rejected
111	Validation	0.25	29.52		Accepted
112	Validation	0.31	20.48	MAPD & ndSNPQC	Rejected
115	Validation	0.29	24.28	ndSNPQC	Accepted
116	Validation	0.29	20.08	ndSNPQC	Rejected
117	Validation	0.24	28.87		Accepted
120	Validation	0.27	18.18	ndSNPQC	Accepted
121	Validation	0.22	30.81		Accepted
122	Validation	0.25	3.45	ndSNPQC	Accepted
123	Validation	0.25	27.05		Accepted
124	Validation	0.25	26.21		Accepted
128	Validation	0.23	27.00		Accepted
129	Validation	0.25	23.47	ndSNPQC	Accepted

130	Validation	0.46	8.91	MAPD & ndSNPQC	Rejected
131	Validation	0.23	33.68		Accepted
132	Validation	0.31	16.73	MAPD & ndSNPQC	Rejected
134	Validation	0.25	39.13		Accepted
135	Validation	0.24	36.01		Accepted
136	Validation	0.26	23.05	ndSNPQC	Accepted
137	Validation	0.30	22.24	ndSNPQC	Accepted
138	Validation	0.31	20.48	MAPD & ndSNPQC	Rejected

Abbreviations: MAPD, median of the absolute values of all pairwise differences; ndSNPQC, SNP quality control of normal diploid markers

We found the copy number profile of both these cohorts to be similar with no significant difference in the PGA (Figure 7.1). They were therefore combined and all further analyses were done with the two cohorts coalesced.

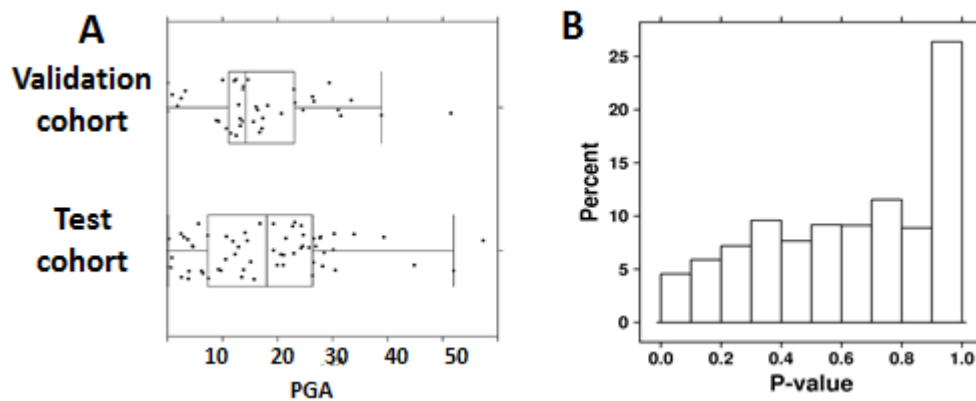


Figure 7.1: Comparison of the structural aberrations in the test and validation cohorts

A: Boxplot comparing PGA in the test and validation cohorts. **B:** Histogram showing p-values from Fisher's exact test comparing CNA proportions in the two sample cohorts for each CNA segment, none are significant after correction for multiple testing

7.4 Results

7.4.1 Percent genome alteration (PGA)

PGA taken as a proxy for genomic instability was calculated for each sample the total count of base pairs involved in copy number gains or losses divided by the total length of the genome in base pairs³⁵⁸ PGA in individual samples ranged from 0.1% to 55.5% (median = 15.2). Percent genome lost (PGloss) ranged from 0.10 to 52.60 (median = 11.55) and percent genome gained (PGgain) ranged

from 0 to 42.2 (median 2.44). Quantitative information on the PGA seen in individual samples is presented in Table 7.2.

Table 7.2: Genome wide copy number status of individual samples.

Sample ID	Gains	Losses	Number of CNAs	PGA	PGgain	PGloss
1B	12	38	50	1.184567	0.092850853	1.09171573
2B	17	56	73	27.97605	2.937121788	25.0389293
4B	89	39	128	21.1564	15.82596568	5.330438378
5B	28	88	116	25.95723	1.614056522	24.34317125
6B	7	77	84	2.218389	0.135255336	2.083133747
8B	17	73	90	21.36984	2.092355364	19.27748289
9B	2	16	18	0.618046	0.026516807	0.59152917
10B	147	224	371	20.29841	5.239180621	15.05923216
11B	10	53	63	3.971501	0.435540058	3.535961357
12B	4	16	20	14.83787	2.375671371	12.46220095
13B	105	23	128	2.234304	1.719971224	0.514333107
14B	178	377	555	43.83755	7.430509635	36.40704312
15B	85	60	145	3.261164	1.268293264	1.99287119
16B	29	46	75	6.411825	0.773133319	5.63869212
17B	103	148	251	55.50028	2.894208565	52.60606813
18B	181	280	461	21.74848	4.548390631	17.20009099
19B	1	52	53	6.032807	0.001714129	6.031092924
20B	4	62	66	2.330295	0.060129902	2.270164649
THA703A1	3	21	24	6.767875	0.853798474	5.914076115
THA703A2	177	171	348	25.25468	8.520101312	16.73457393
THA703A3	84	235	319	9.379761	1.974911673	7.404849399
THA703A4	138	106	244	20.34287	7.245338472	13.09753046
THA703A5	17	75	92	22.26908	0.828960191	21.44012326
THA703A6	68	106	174	13.41938	1.182845218	12.23653219
THA703A7	40	78	118	28.93678	3.670594729	25.26618536
THA703A8	40	144	184	22.37841	0.786034026	21.59237543
THA703A9	102	432	534	29.9217	1.477398549	28.4442967
THA703A10	92	86	178	20.02464	5.627904852	14.3967359
THA703A11	207	233	440	13.0521	3.157880634	9.894222033
THA703A12	106	114	220	4.864879	1.389158425	3.475720495
THA703A13	104	184	288	23.26275	6.648532908	16.6142213
THA703A14	10	84	94	47.75738	6.701006716	41.05637095
THA703A15	131	392	523	24.18361	2.678357564	21.50525524
THA703A16	36	64	100	17.44502	2.139170236	15.30584757
THA703A17	350	516	866	27.04196	8.664442058	18.37751762
THA703A18	11	52	63	20.70058	0.222412602	20.47817077
THA703A19	1	24	25	19.05166	0.051706108	18.99995409
THA703A20	186	126	312	9.932943	4.524095705	5.408847098

THA703A21	112	37	149	6.013619	5.009127927	1.004490632
THA703A22	0	92	92	13.74313	0	13.7431258
THA703A23	220	141	361	24.86617	7.985638924	16.8805326
THA703A25	76	92	168	19.26211	1.513342733	17.74876288
THA703A27	186	63	249	21.00345	14.42725611	6.576192731
THA703A28	178	52	230	9.824377	5.434839227	4.389538261
THA703A29	88	34	122	2.62195	1.775660296	0.846289456
THA703A30	171	130	301	11.94648	5.157051531	6.789427864
THA703A31	5	28	33	11.76981	0.390214719	11.37959062
THA703A32	38	74	112	3.63179	0.814072336	2.81771747
THA703A33	30	113	143	9.483131	1.122494224	8.360636637
THA703A35	0	3	3	0.11911	0	0.119109624
THA703A36	5	14	19	0.407782	0.060517163	0.347264424
THA703A37	14	168	182	20.23088	0.444039526	19.78684093
THA703A38	4	21	25	6.443587	0.202965084	6.240621744
THA703A39	159	108	267	26.20674	7.227354507	18.97938231
THA703A40	128	67	195	21.59429	3.312275693	18.28201666
THA703A41	5	69	74	4.839531	0.22459942	4.614931647
THA703A42	0	3	3	0.109082	0	0.109082183
THA703A43	58	249	307	39.54254	3.678216269	35.86432285
THA703A44	112	87	199	27.91431	21.85592124	6.058393529
THA703A45	50	203	253	24.44119	0.862619697	23.57856743
THA703A46	14	52	66	14.76856	3.249423776	11.51913165
THA703A48	6	6	12	10.66825	10.54438466	0.123866919
77	45	57	102	11.50931	0.464396178	11.04490888
80	116	188	304	29.50119	17.80840205	11.69279263
81	9	35	44	12.94209	0.164450041	12.77764116
82	220	171	391	13.73795	8.96313327	4.774815937
83	55	138	193	30.99963	6.533011017	24.46662324
84	108	351	459	31.49184	5.379403218	26.11243896
86	0	35	35	18.19138	0	18.19137985
87	0	17	17	2.489206	0	2.48920621
88	259	439	698	24.63907	5.863161773	18.7759038
89	338	100	438	51.49524	42.26516909	9.230068385
90	0	93	93	23.16325	0	23.16324887
92	3	25	28	12.15402	0.603116398	11.55090509
93	152	48	200	13.63272	9.409008086	4.223712422
94	72	88	160	26.59455	7.117487028	19.47706125
95	66	80	146	26.35131	7.188020762	19.16328452
96	179	152	331	8.879157	3.537616101	5.341541314
97	95	62	157	9.312365	6.786798863	2.525566151
101	57	94	151	33.38652	2.443444393	30.94307478
103	52	52	104	3.231343	1.731855758	1.499487723
104	2	20	22	0.858551	0.018103915	0.840447232
105	288	283	571	22.96565	8.091060537	14.87458721

106	47	46	93	1.806498	0.735982408	1.070515099
107	189	278	467	16.72772	3.856239409	12.87148336
111	5	41	46	12.49197	0.17253391	12.31943364
115	226	132	358	12.43656	3.307431568	9.129126745
117	242	250	492	16.36176	7.019776877	9.341979272
120	136	27	163	38.86617	34.99372779	3.872445239
121	37	42	79	14.60825	2.924648728	11.68360321
122	170	107	277	13.201	7.968532248	5.232470829
123	98	182	280	13.24443	5.707978103	7.536447798
124	356	114	470	10.72242	7.803797076	2.918619551
128	64	33	97	17.14934	7.616514578	9.532829869
129	41	129	170	16.09739	1.444956959	14.65243529
131	11	31	42	20.69314	3.124049411	17.56909351
132	233	140	373	15.61395	6.206094766	9.407859882
134	1	31	32	10.0341	0.001714129	10.03238474
135	8	122	130	13.79799	0.157778309	13.64021279
136	8	32	40	14.39146	0.184583339	14.20687362
137	11	34	45	15.72904	0.276144363	15.4528957

Abbreviations: PGloss, percent genome lost; PGgain, percent genome gained

7.4.2 Relationship of age of the sample to copy number aberrations

Our samples came from a very wide time span (1988-2014). Fixation methods for FFPE samples and people actually doing the fixation would have changed over time. A major concern was if the age of the sample and fixation methods used would have an effect on our assessment of the structural aberrations in the MPM genome. When samples were divided into three groups based on the date of their collection (before 2000, from 2001-2009 and 2010 and after), we found no statistically significant difference between these temporal groups in the PGA (ANOVA test $p = 0.08$) and also the absolute number of CNAs (ANOVA $p = 0.8$) (Figure 7.2). The samples that failed quality check too were almost uniformly distributed between these groups.

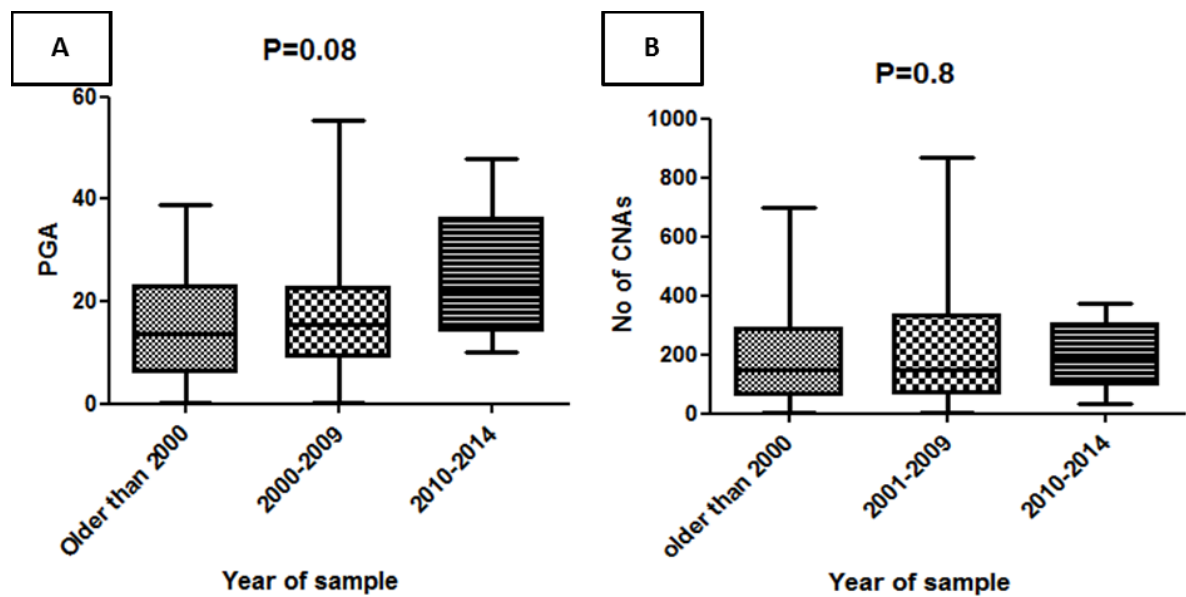


Figure 7.2: Sample age and its effect on PGA and copy number changes

A: Boxplot comparing PGA of samples belonging to different time periods

B: Boxplot comparing no of CNAs detected in sample belonging to different time periods

7.4.3 PGA, tumour histology and clinical covariates

Despite epithelioid MPMs being associated with better OS, we found that in our cohort epithelioid MPMs had a higher PGA than non-epithelioid MPMs (Figure 7.3). However, we found no correlation of PGA with history of asbestos exposure, age of the patient and stage of the disease at diagnosis. We explored if there was a difference between histotypes with regards to PGloss and PGgain. While we found that non-epithelioid MPM had significantly lower PGloss than epithelioid MPM (9.239 ± 1.147 vs 14.31 ± 1.380 ; $p = 0.01$), there was no difference between histotypes with respect to PGgain (4.831 ± 1.120 vs 4.222 ± 0.7906 ; $p = 0.44$).

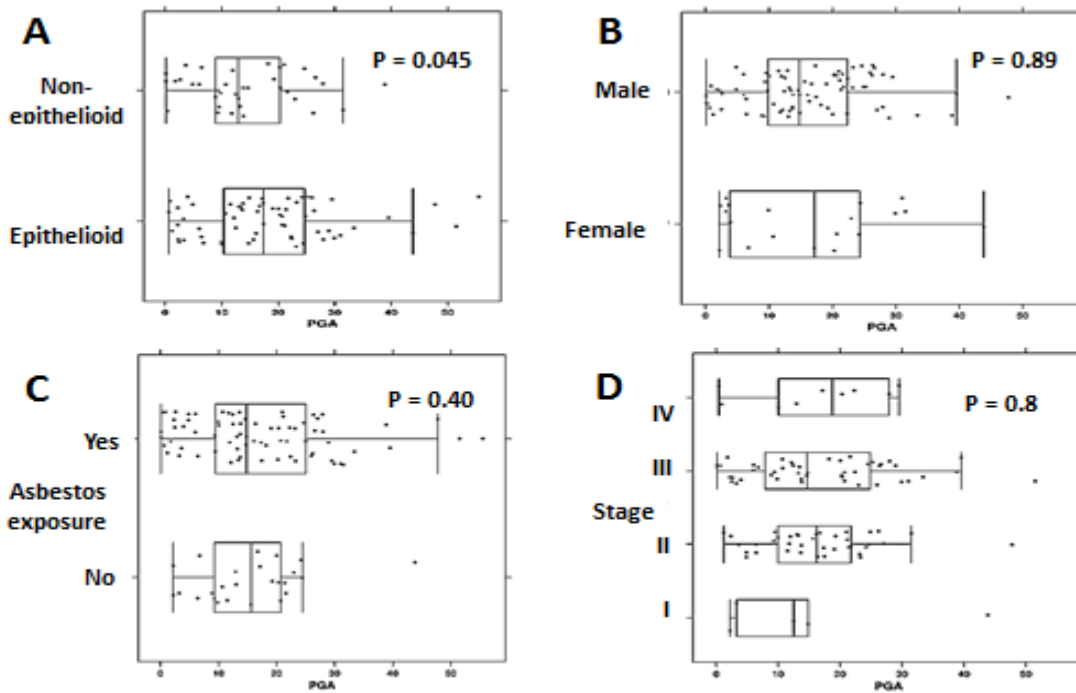


Figure 7.3: Correlation of PGA with different clinicopathological covariates.

A: Boxplot comparing PGA between epithelioid and non-epithelioid MPMs

B: Boxplot comparing PGA between the sexes

C: Boxplot comparing PGA between patients who did and did not have a clear history of asbestos exposure

D: Boxplot comparing the PGA between different clinical stages of MPM in our cohort

7.4.4 PGA and OS

Patients were dichomatised based on their PGA. They were divided between the lower third and upper two thirds. When controlled for age and stage at diagnosis, patients with higher PGA had significantly worse OS. Since we know that histology strongly effects survival and is also related to PGA from our results described in the preceding paragraph, we repeated the same survival analysis amongst only the epithelioid MPMs and found that in this cohort too, patients with greater PGA had worse outcome (Figure 7.4). We further sought to explore the effect of PGloss and PGgain taken separately on OS. When divided by tertiles (lower third and upper two third), higher PGloss was associated with significantly worse outcome amongst epithelioid MPMs and tended towards worse OS in the whole cohort. PGgain was not found to be associated with OS (Figure 7.4)

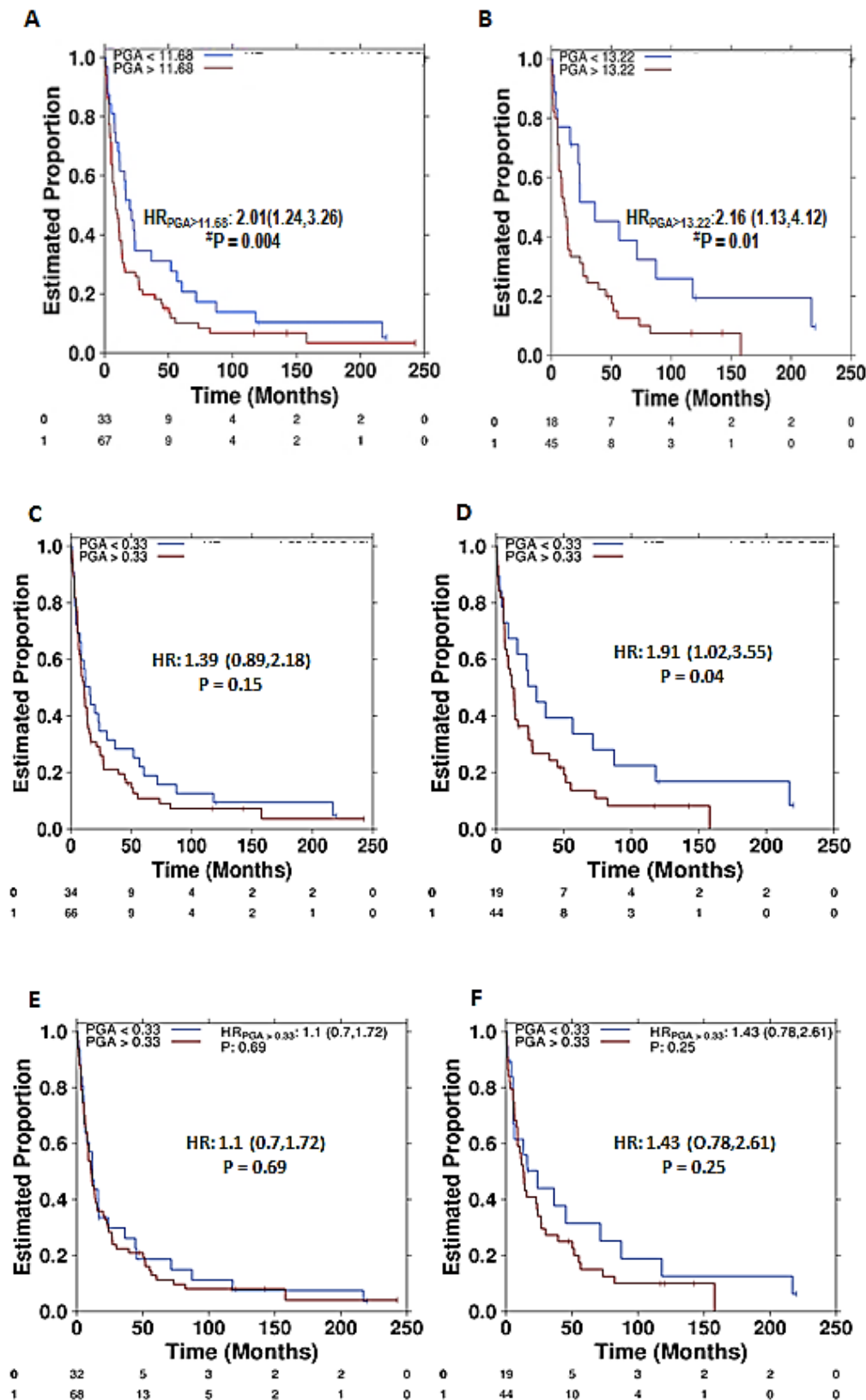


Figure 7.4: Prognostic implication of PGA in MPM.

A: KM curves comparing survival in PGA groups in whole cohort and the #Cox-PH P-value controlling for age and stratified by histology. PGA is divided between the lower and two upper tertiles. B: KM curves comparing survival in PGA groups in epithelioid MPM. C: KM curves

comparing survival in PGloss in whole cohort controlling for age. D: KM curves comparing survival in PGloss groups in epithelioid MPM. E: KM curves comparing survival in PGgain in whole cohort controlling for age. F: KM curves comparing survival in PGgain groups in epithelioid MPM.

7.4.5 PGA and immune characteristics of the tumour

We found no difference in the PGA of PD-L1⁻ and PD-L1⁺ patients (Figure 7.5). However, patients who were PD-L2 ^{+/+}^{hi} had a significantly lower PGA. Also, we found that lower PGA correlated significantly with higher infiltration with CD4⁺, CD8⁺, FOXP3⁺ and TIM3⁺ lymphocytes (Figure 7.6). We repeated these analyses with only epithelioid MPM and found that although in this cohort too, the correlation between lower PGA and higher infiltration with TILs was maintained, it was not statistically significant. This could be due to the lower number of patients analysed.

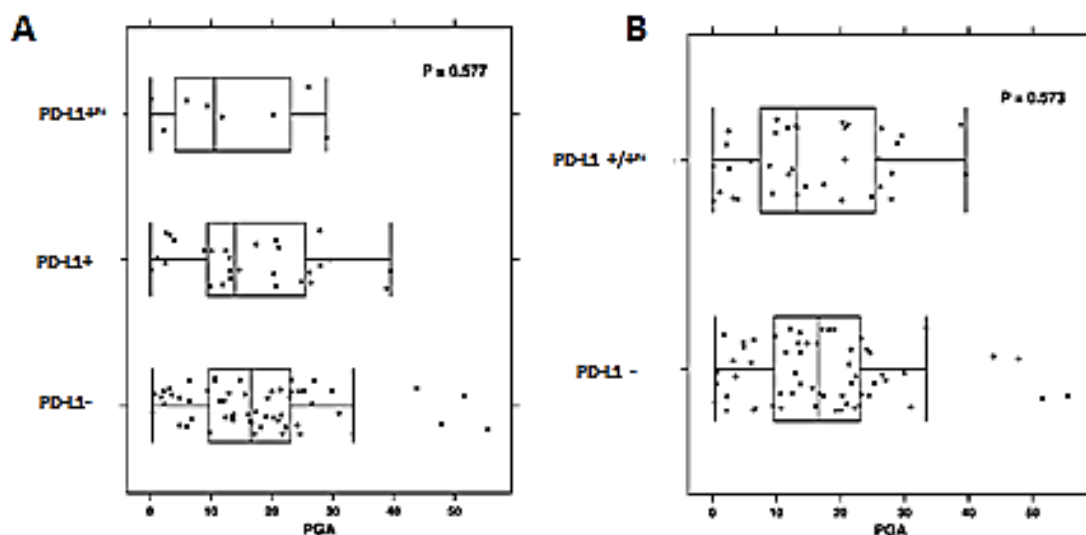


Figure 7.5: Relationship between PGA and PD-L1 expression by tumour

Boxplots comparing the PGA amongst patients with differing expression of PD-L1 on IHC.

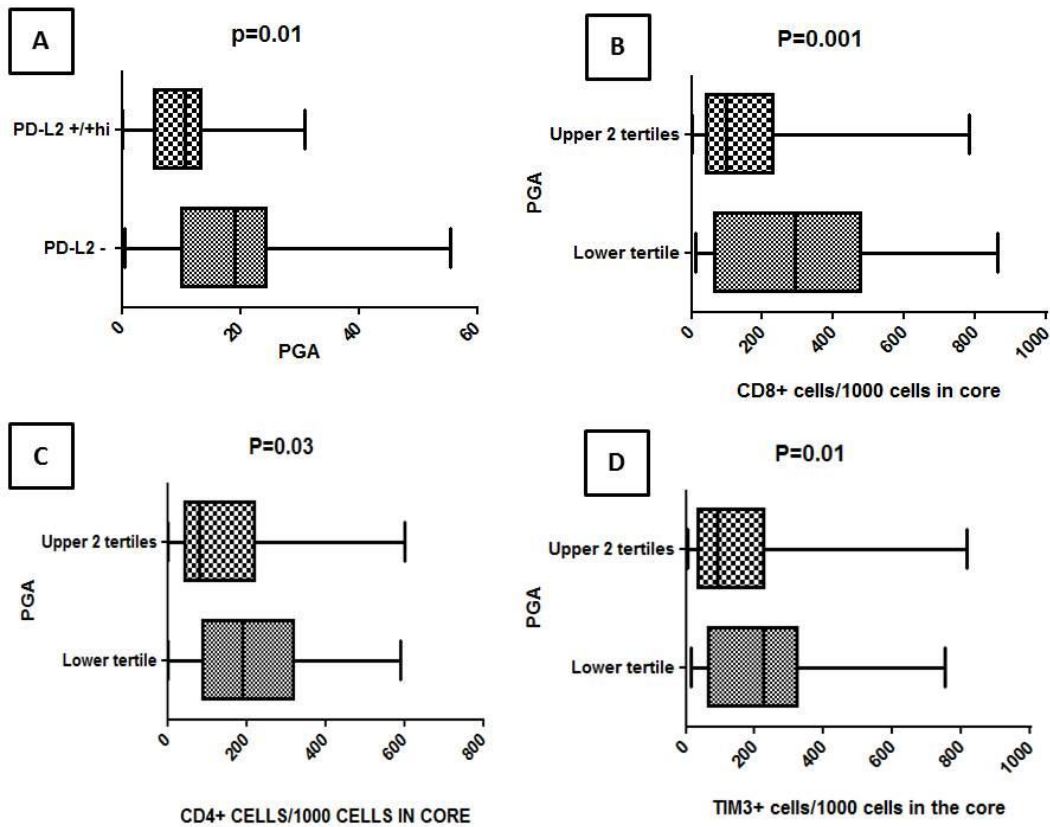


Figure 7.6: Correlation of PGA with other immunological characteristics of the tumour

A: Boxplot comparing PGA between patients who are PD-L2 negative and PD-L2 positive (+/+^{hi}) and P values from t test. **B:** Boxplot comparing CD8+ cells in tumours with low (lower tertile) and high (upper two tertiles) PGA and P values from t test. **C:** Boxplot comparing CD4+ cells in tumours with low and high PGA and P value from t test. **D:** Boxplot comparing TIM3+ cells in tumours with low and high PGA and P value from t test

7.4.6 Copy number profile and consensus clustering

After collapsing copy number aberrations at contiguous genes in order to avoid multiple testing for all gene level analysis, we found a total of 11416 loci of CNAs in our 100 evaluable samples. Our analysis revealed a median of 147 (3-866) CNA per sample. Losses (median = 79; 3-516) were more common than gains (median = 57; 0-516). The chromosomal regions with the highest number of losses and gains in our cohort were as depicted in Table 7.3. Table 7.4 lists the twenty genes with the highest number of CNAs in our cohort.

Table 7.3: Chromosomal regions with highest percentage of loss/gains

Losses (deletions)				Gains (amplifications)			
Serial number	Chromosome	Region	Percentage	SN	Chromosome	Region	Percentage
1	22	q12.3	72.89	1	8	q24.3	71
2	9	p21.3	67.8	2	7	p11.2	67
3	3	p21.2	61	3	17	q25.3	64.4
4	13	q12.11	57	4	1	q21	57.9
5	7	q11.22	49	5	12	q21	57.9
6	16	p13.3	49	6	15	q21	53
7	19	p13.2	49	7	3	q12	51
8	15	q11.22	41	8	21	q22	51

Table 7.4: Genes with greatest frequencies of CNAs in our cohort.

Symbol	Chromosome	CNVs	Gains	Deletions
CDKN2B-AS1	9	81	15	66
CDKN2A	9	78	15	63
LL22NC03-86D4.1	22	77	0	77
LL22NC03-13G6.2	22	77	0	77
C9orf53	9	76	13	63
CDKN2B	9	76	14	62
LARGE	22	76	0	76
MYO18B	22	73	1	72
CTA-125H2.2	22	72	1	71
CTA-125H2.1	22	72	1	71
7SK	22	72	1	71
RP1-288L1.5	22	72	1	71
RP1-288L1.4	22	72	1	71
SEZ6L	22	71	3	68
CTA-282F2.3	22	71	0	71
RP1-272J12.1	22	71	1	70
MTAP	9	70	5	65
CTA-796E4.3	22	70	1	69
CTA-796E4.4	22	70	1	69
CTA-342B11.2	22	70	0	70

All of the top 20 losses were localised to chromosome 22 (Table. 7.5) while the most frequent gains were localised in chromosomes 1, 3, 7 and 8 (Table 7.6).

Table 7.5: Top 20 genes with greatest frequency of deletions.

Symbol	Chromosome	Deletions	Gains	CNVs
LL22NC03-86D4.1	22	77	0	77
LL22NC03-13G6.2	22	77	0	77
LARGE	22	76	0	76
MYO18B	22	72	1	73
CTA-125H2.2	22	71	1	72
CTA-125H2.1	22	71	1	72
7SK	22	71	1	72
RP1-288L1.5	22	71	1	72
RP1-288L1.4	22	71	1	72
CTA-282F2.3	22	71	0	71
RP1-272J12.1	22	70	1	71
CTA-342B11.2	22	70	0	70
CTA-796E4.3	22	69	1	70
CTA-796E4.4	22	69	1	70
SLC5A1	22	69	0	69
AP1B1P1	22	69	0	69
RP1-127L4.7	22	69	0	69
C22orf42	22	69	0	69
RP1-90G24.8	22	69	0	69
RFPL2	22	69	0	69

Table 7.6: Top 20 genes with greatest frequency of gains.

Symbol	Chromosome	Gains	Deletions	CNVs
EGFR	7	54	4	58
TG	8	53	1	54
SLA	8	53	1	54
WISP1	8	53	1	54
NDRG1	8	51	1	52
ST3GAL1	8	50	1	51
NEK7	1	49	1	50
ATP6V1G3	1	49	1	50
CD200	3	49	0	49
RP11-231E6.1	3	49	0	49
BTLA	3	49	0	49
ATG3	3	49	0	49
SLC35A5	3	49	0	49
CCDC80	3	49	0	49
RP11-572C15.5	3	49	0	49
CD200R1L	3	48	1	49
RP11-629O1.2	8	48	1	49
RP11-180K7.1	3	48	0	48
PTK2	8	47	1	48

<i>RP11-128L5.1</i>	8	47	1	48
---------------------	---	----	---	----

We subsequently looked at the copy number status of some genes that have frequently been reported to be altered in MPM. The frequency and nature of copy number alterations seen in these genes in our cohort was as presented in Table 7.7.

Table 7.7: Copy number status of some commonly described MPM associated genes.

Symbol	Chromosome	Gains	Deletions	CNVs
<i>NF2</i>	22	1	49	50
<i>BAP1</i>	3	2	37	39
<i>CDKN2A</i>	9	15	63	78
<i>RBFOX1</i>	16	7	57	64
<i>XRCC6</i>	22	1	50	51
<i>LATS2</i>	13	1	36	37
<i>MTAP</i>	9	5	65	70
<i>DUSP7</i>	3	2	34	36
<i>MYC</i>	8	27	1	28
<i>ARHGDI1</i>	17	37	2	39
<i>TP53</i>	17	2	26	28

When we used consensus clustering with 1000 repetitions to group patients based on their CNA profiles, two primary clusters were identifiable (Figure 7.7). Cluster 1 had a significantly greater PGA than cluster 2 (Wilcoxon test $p = 9.5 \times 10^{-10}$). When broken down into PGloss and PGgain, we found that while cluster 1 had significantly greater PGloss than cluster 2 (Wilcoxon test $p = 2.4 \times 10^{-12}$), cluster 2 actually had greater PGgain than cluster 1 although the difference was not statistically significant (Wilcoxon test $p = 0.08$). We also found a higher proportion of non-epithelioid MPMs in cluster 2 (Fisher's exact test $p = 0.03$). The cluster classification however did not correlate with PD-L1 expression status (Fisher's exact test $p = 0.76$). Figure 7.7 demonstrates the copy number profile of individual samples and consensus clustering.

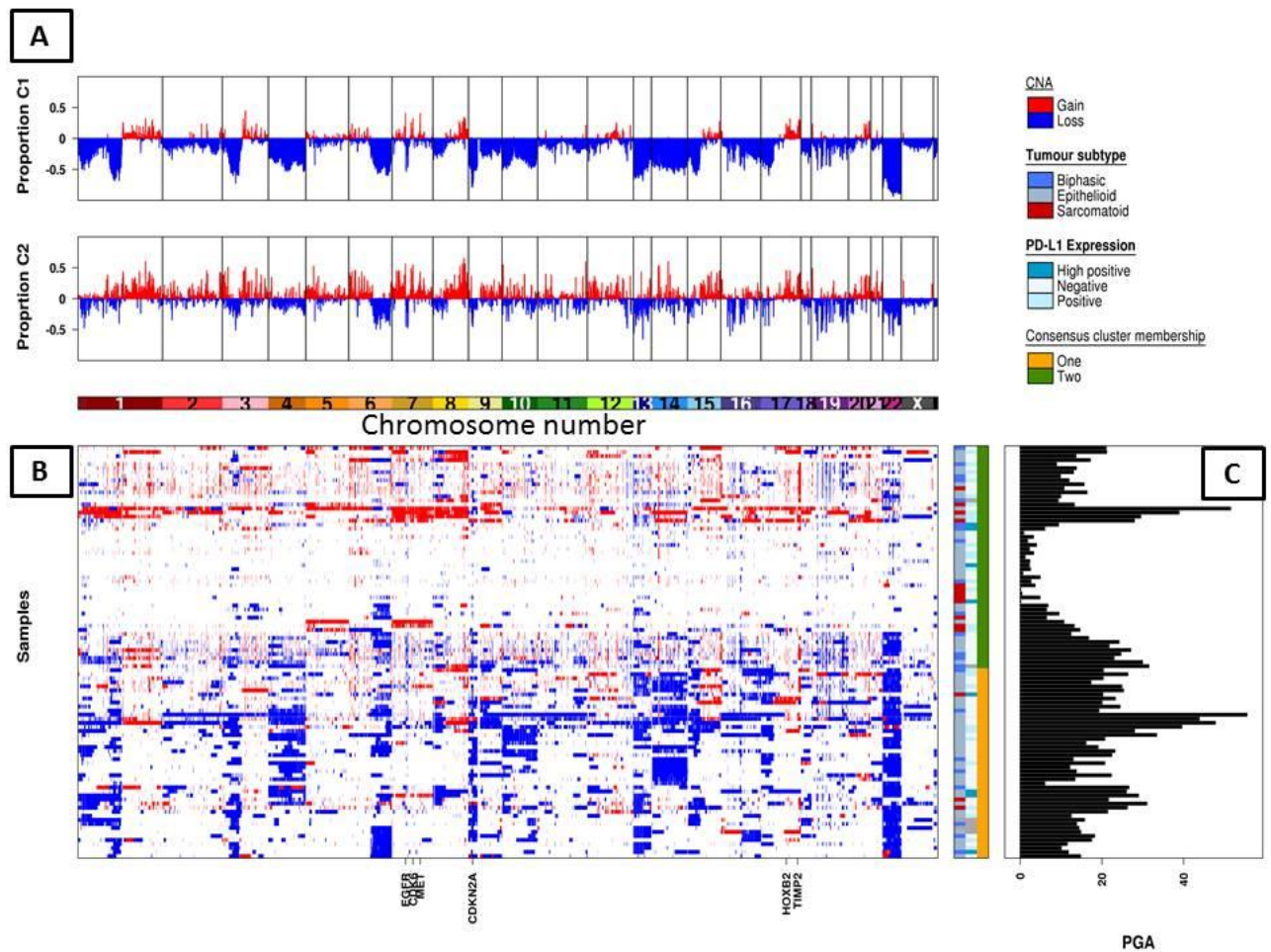


Figure 7.7: Consensus clustering based on copy number profile.

A: Diagram showing the proportion of samples in each of the two clusters with copy number events (red = gain; blue = loss) in each chromosome.

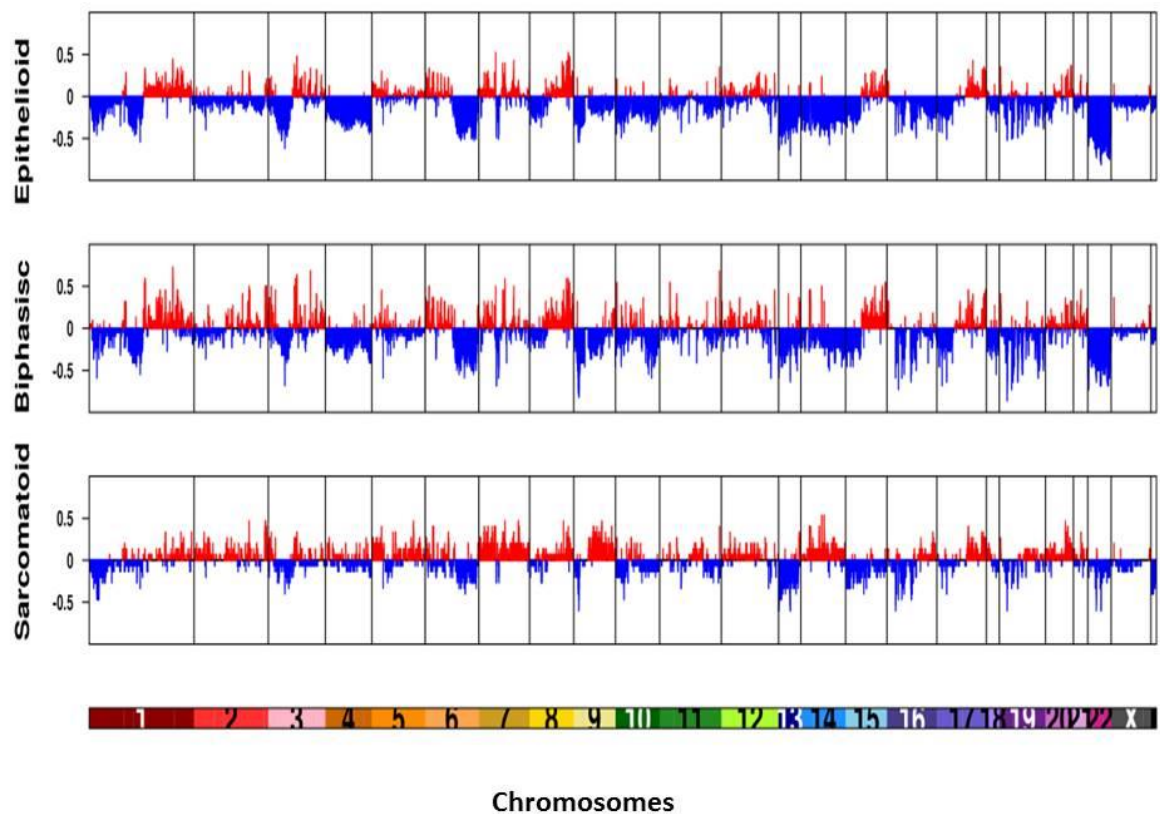
B: Heat map showing copy number status in individual samples. Each row represents a tumour sample and genomic regions are represented in columns (red = gain; blue = loss; white = no CNA).

C: The bar graph displays the PGA in individual tumour samples.

Abbreviations: CNA, copy number aberration; C1, cluster 1; C2, cluster 2; PGA, per cent genome aberration

7.4.7 Relationship of copy number profile with tumour histology.

We found that non-epithelioid MPM had lower PGA than epithelioid MPM. The copy number profile of the different histotypes taken individually was as represented in Figure 7.8.



CNA
■ Gain
■ Loss

Figure 7.8: Copy Number profile of different histological subtypes of MPM.

Diagram showing the proportion of patients in each of the histological subtypes showing copy number changes in each of the chromosomes

However, the absolute number of CNAs was not different between epithelioid and non-epithelioid MPMs. Also there were no differences with regards to the numbers of copy number gains and losses (Figure 7.9).

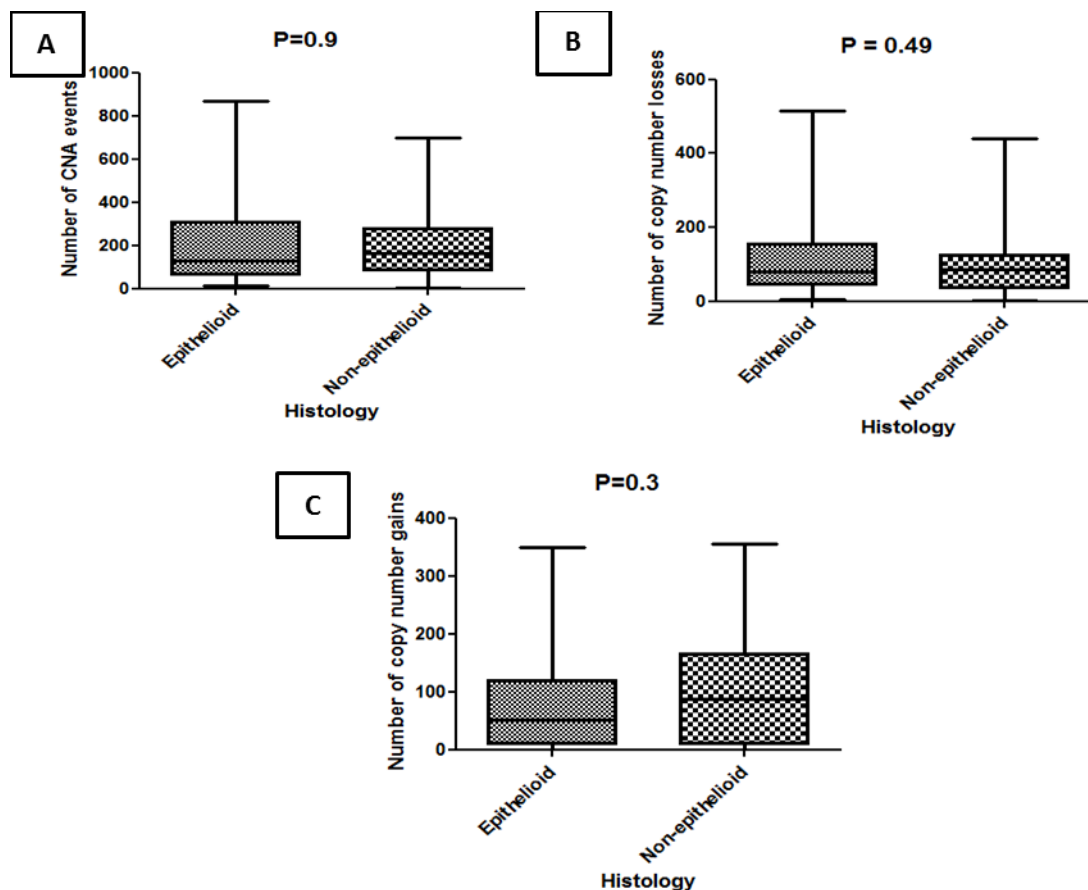


Figure 7.9: Absolute CNA counts and its relation with tumour histology and survival

A: Boxplot comparing number of CNAs in epithelioid and non-epithelioid MPMs **B:** Boxplot comparing number of copy number loss events in epithelioid and non-epithelioid MPMs **C:** Boxplot comparing number of copy number gain events in epithelioid and non-epithelioid MPMs. P values are from unpaired T tests.

We then looked at the difference of incidence of individual CNAs between different histotypes. Although the frequency of many individual CNA events were found to be different among histologies, none were significant after correction for multiple testing. However, it was also noted that power of our analysis to reliably detect significantly different CNA frequencies amongst different MPM histotypes was low (Figure 7.10). A list of the top 20 genes in which the difference in frequencies of CNAs between histotypes that approached significance is presented in Table 7.8

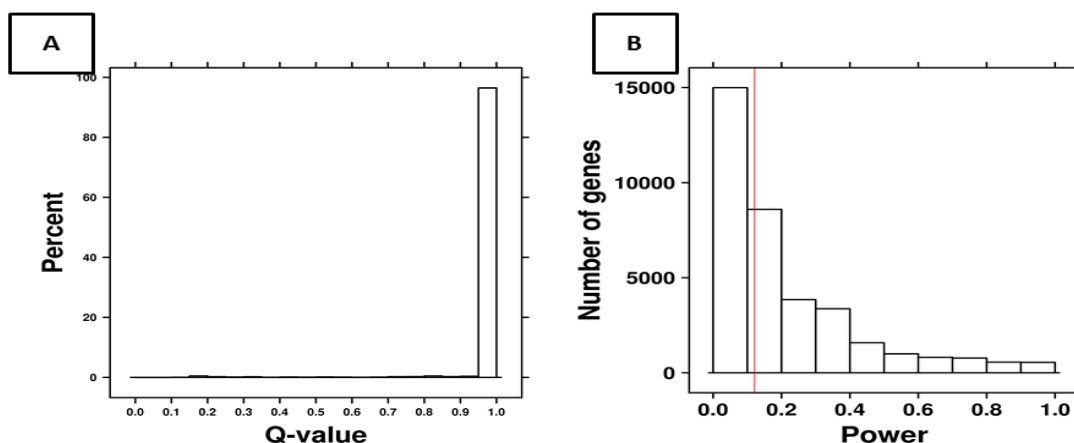


Figure 7.10: Differences in CNA frequency between different MPM histotypes

A: Histogram showing the distribution of Q-values from Fisher's exact test comparing CNA counts among tumour subtypes, none are significant after correcting for multiple testing. [A Q-value is a that has been adjusted for the false discovery rate (FDR). The False Discovery Rate is the proportion of false positives one can expect to get from a test. This is of special importance while running thousands of tests from small samples (which are common in fields like genomics). While a p-value of 5% means that 5% of all tests will result in false positives, a q-value of 5% means that 5% of significant results will result in false positives.] **B:** Histogram showing the distribution of the power to detect differing CNA proportions between epithelioid and non-epithelioid tumours, the median is marked with a red line.

Table 7.8: Genes with marginally significant differences in CNA frequency among tumour subtypes.

Symbol	Chromosome	Q- value	Epithelioid	Biphasic	Sarcomatoid
MCAT	22	0.12	0.7	0.59	0.07
TSPO	22	0.12	0.68	0.55	0.07
TLL12	22	0.12	0.7	0.55	0.07
SCUBE1	22	0.12	0.68	0.55	0.07
Z82214.3	22	0.12	0.68	0.55	0.07
Z82214.2	22	0.12	0.68	0.55	0.07
RP6-109B7.3	22	0.12	0.73	0.59	0.13
RP6-109B7.2	22	0.12	0.73	0.59	0.13
RP6-109B7.4	22	0.12	0.73	0.59	0.13
RP3-439F8.1	22	0.12	0.67	0.55	0.07
CERK	22	0.12	0.67	0.55	0.07
GRAMD4	22	0.12	0.67	0.55	0.07
CTA-29F11.1	22	0.12	0.67	0.5	0.07
TBC1D22A	22	0.15	0.65	0.45	0.07
HFE2	1	0.17	0.25	0.55	0
RP11-458D21.1	1	0.17	0.25	0.55	0
U1	1	0.17	0.25	0.55	0

7.4.8 Relationship of copy number profile with survival

Despite there being a significantly greater proportion of non-epithelioid MPMs in cluster 2, the cluster classification was not found to be prognostic with no statistically significant difference in OS between the clusters. We looked at the effect of each CNA on patient survival. After correction for multiple testing none of the individual CNAs were found to be significantly associated with survival (Figure 7.11). The P values derived from individual CNAs when arranged in ascending order ranged from 0.05-1 (Figure 7.11B). However, when their corresponding Q values were drawn, there were none that were <0.05 (Figure 7.11C). The power of our analysis to detect such an association was however found to be low with a median power of 0.7 (Figure 7.11D).

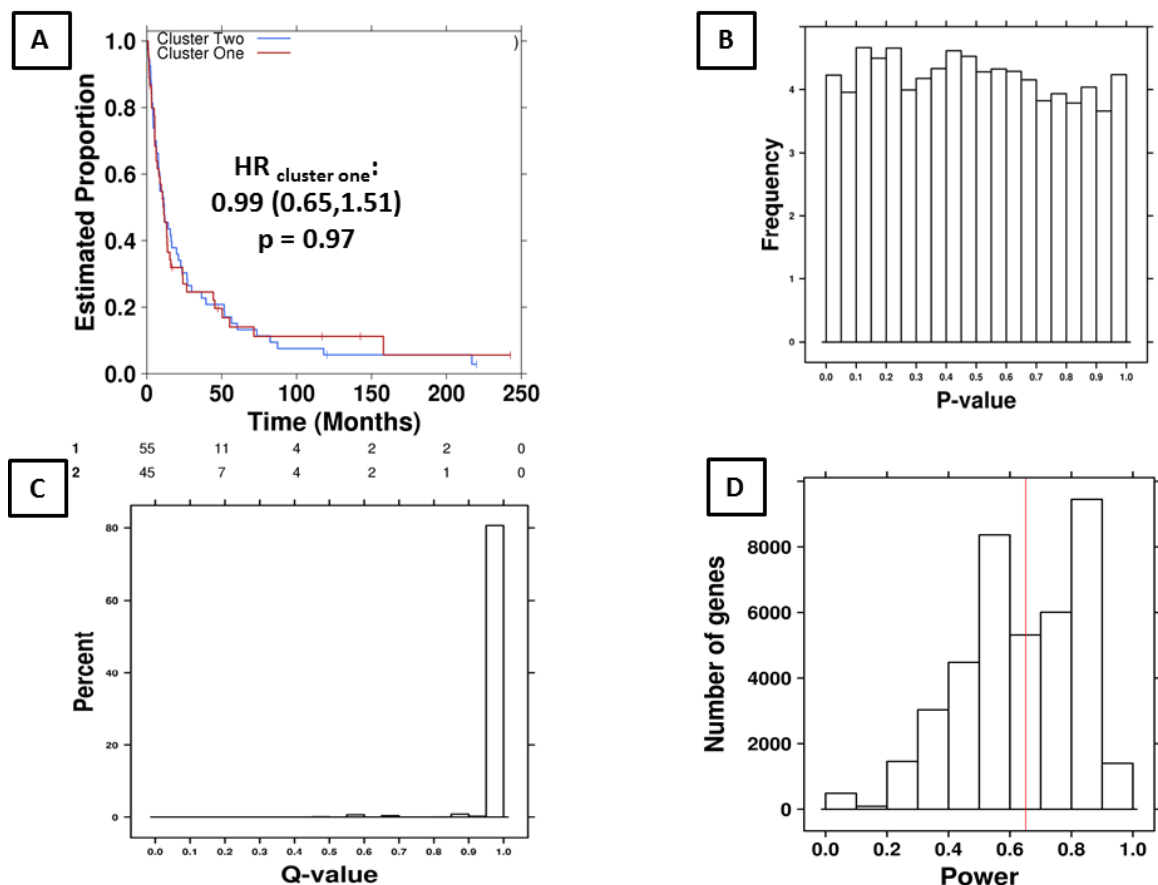


Figure 7.11: Effect of cluster membership and individual CNAs on survival

A: KM curves comparing survival between consensus cluster groups and the Cox-PH P-value controlling for age. **B:** Histogram showing the distribution of LogRank P-values for survival for each CNA segment. **C:** Histogram showing the distribution of LogRank Q-values for survival for each CNA

segment. D: Histogram showing the distribution of the power to detect a significant effect of a given CNA on survival through a Cox-PH regression. The red line indicates the median.

A more focused survival analysis of the genes commonly associated with MPM and a group of top 20 GISTIC genes from our cohort revealed that loss of *BAP1* was associated with better OS (HR = 0.67; 95%CI: 0.41, 1.0; p = 0.05). Loss of *MTAP* (HR = 1.67; 95%CI: 1.08, 2.59; p = 0.02) and *DMRTA1* (HR = 1.92; 95%CI: 1.25, 2.97; p = 0.001) along with gain in *CDK6* (HR = 2.01; 95%CI: 1.28, 3.15; p = <0.001) were found to be associated with poor prognosis on univariate analysis (Figure 7.12). However, we did find that the power of our analysis to detect a significant effect of a given CNA on survival through a Cox-PH regression was lower than ideal (Figure 7.11).

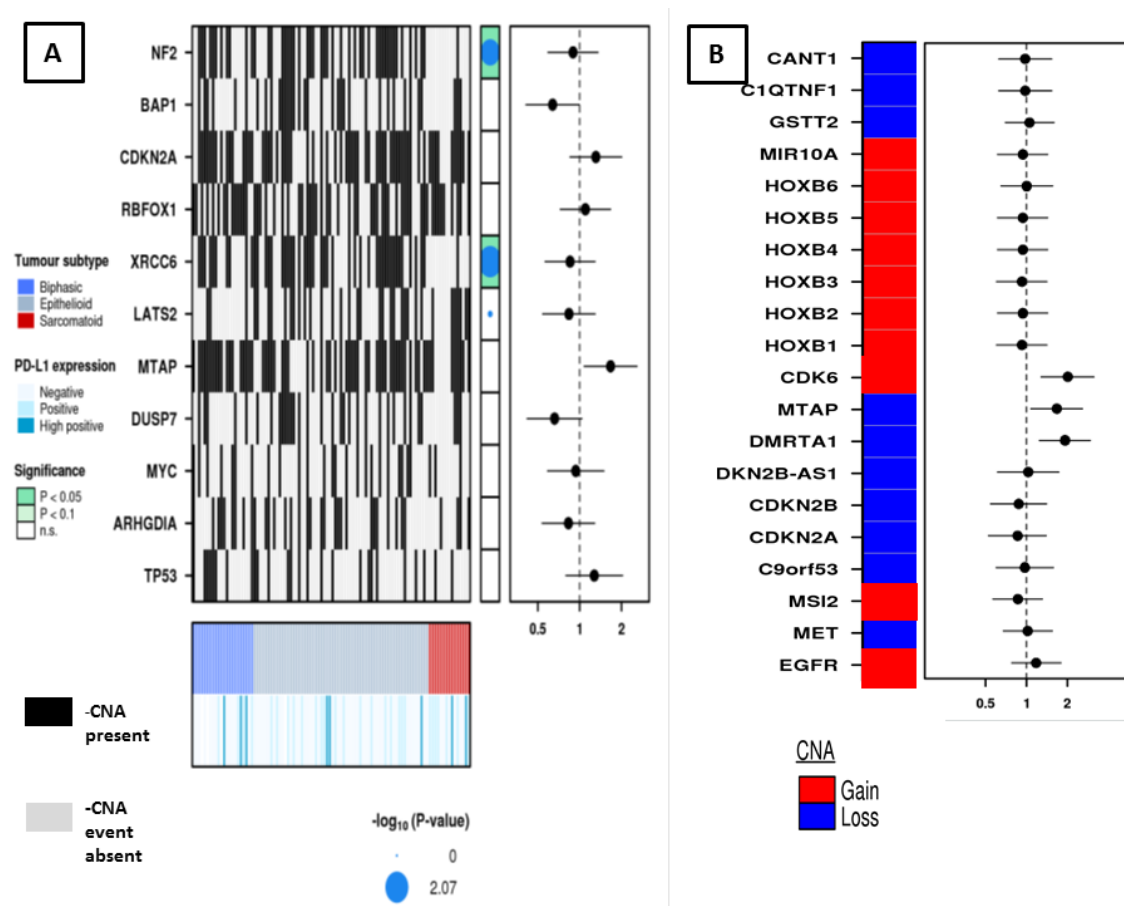


Figure 7.12: Analysis of effect of commonly described MPM related genes and top GISTIC related genes with survival.

A: Heat map showing the presence or absence of the expected CNA in select genes across patients with the corresponding Fisher's exact test P-value comparing the number of CNAs among tumour subtypes and corresponding hazard ratios and 95% confidence intervals. **B:** Forest plot showing hazard ratios of the top GISTIC genes in our cohort.

7.4.9 Correlation of individual CNAs with PD-L1 expression status

We studied the frequency of individual CNAs for their correlation with PD-L1 status. After correction for multiple testing frequencies of none of the CNAs were found to significantly correlate with PD-L1 expression status. However, like with previous analyses, the power for detection of differences in frequencies of individual CNAs between PD-L1+/^{HI} and PD-L1- patients was low.

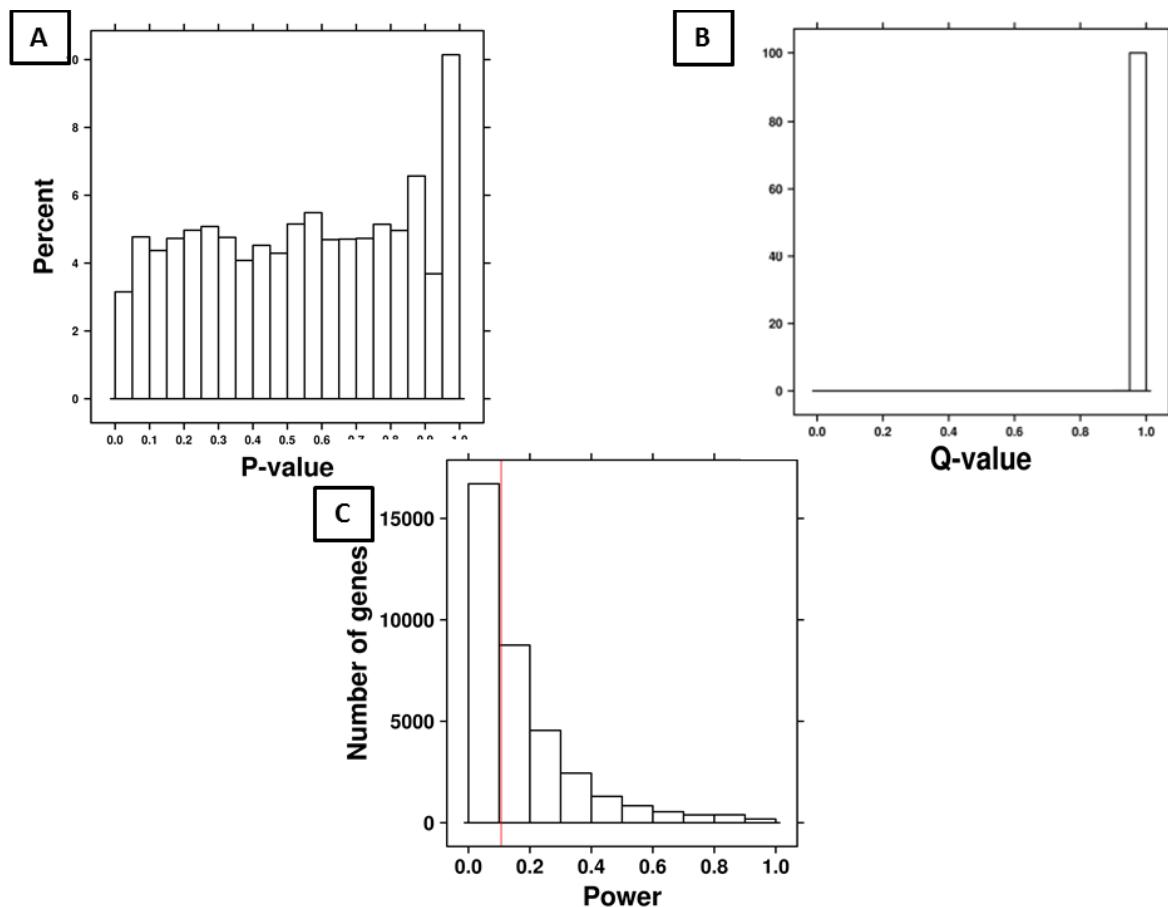


Figure 7.13: Individual CNAs and PD-L1 status of tumours.

A: Histogram of P-values from Fisher's exact tests comparing the number of patients with a CNA in each PD-L1 category for each locus. **B:** Q-values from Fisher's exact tests comparing the number of patients with a CNA in each PD-L1 category for each locus. **C:** Histogram showing the distribution of the power to detect differing CNA proportions between PD-L1 positive and negative tumours, the median is marked with a red line.

7.5 Discussion:

Using genomic DNA extracted from FFPE samples of confirmed cases of MPM, we studied genome wide copy number aberrations in a substantially large cohort. This cohort was clinically well annotated and representative in terms of the proportion of histological subtypes. We found a large number of CNAs with significant variation between cases in terms of both the numbers and the extent (represented by the PGA) of these structural abnormalities. Contrary to expectation, epithelioid MPMs showed greater PGA than non-epithelioid MPMs and yet greater PGA was associated with worse OS. PGA was not found to correlate with age of the sample, sex of the patient, stage at diagnosis, history of asbestos exposure and PD-L1 status. Neither absolute number of CNAs nor any individual CNA correlated with tumour histology, PD-L1 status and OS. Loss of *BAP1*, *MTAP*, *DMRTA1* and gain in *CDK6* genes did show prognostic value on univariate analysis but none remained significant after correction for multiple testing.

Array comparative genomic hybridization (aCGH), single nucleotide polymorphism (SNP) based arrays and second generation sequencing technologies are the three main technologies presently being used for accurate and high-resolution genome-wide copy number variations mapping.³⁵ Past studies into CNAs in MPM have used FISH,³⁸ conventional CGH,^{359–366} aCGH,^{25,355,356} and next generation sequencing technologies like sequencing by synthesis²⁷ and whole genome sequencing.⁵⁵ Sequencing based technologies are theoretically able to provide base pair resolution of CNA events. However, there remain several obstacles to using only sequencing based methods for CNA mapping. At present, it is still relatively expensive to sequence a genome to the required depth of coverage for reliable detection of CNAs greater than 1 kb.³⁶⁷ Moreover, it is still difficult to execute large-scale genome-wide association type studies due to the limited sample throughput of current 2nd generation DNA sequencing formats. Furthermore, the requisite computational analysis pipelines for identifying CNAs from whole genome sequence data have immense hardware and software requirements. Although CGH has proven to be a useful and reliable research technique, the applications involve only gross abnormalities. The resolution of conventional CGH is a major practical

problem that limits its clinical applications. Because of the limited resolution of metaphase chromosomes, aberrations smaller than 5–10 Mb cannot be detected using conventional CGH.³⁶⁸ Array CGH is a high resolution technique which overcomes many of these limitations. The standard resolution varies between 1 and 5 Mb, but can be increased up to approximately 40 kb. The greatest impediment to clinical application of aCGH has been the technical challenges encountered during the processing and analysis of FFPE samples. The aCGH data obtained from FFPE samples have previously found to be inconsistent and this has been attributed mainly to reduced integrity of DNA obtained therefrom.³⁶⁹ Early results of aCGH analysis of FFPE samples showed suboptimal sensitivity and specificity. Improvements in DNA extraction protocols, labelling techniques, and aCGH platforms have subsequently facilitated the analysis of FFPE samples in the research setting. However, reports in the literature indicate that one-third of FFPE specimens generate suboptimal aCGH results using standard methods.³⁷⁰ This is particularly relevant for older specimens such as those used in retrospective analysis.³⁶⁹ Our entire sample cohort consists of FFPE blocks coming from a long span of time (1988-2014). The degradation of DNA caused by formalin fixation is well described.^{371,372} FFPE blocks are known to produce poor-quality results with many of the currently available SNP genotyping assays or NGS technologies.³⁷³

Molecular Inversion Probe (MIP) belongs to the class of Capture by Circularization molecular techniques for performing genomic partitioning, a process through which one captures and enriches specific regions of the genome. The technology has been used extensively for large-scale SNP genotyping¹⁸⁷ as well as for studying gene copy alterations³⁷⁴ and characteristics of specific genomic loci. Key strengths of the MIP technology include its high specificity to the target and its scalability for high-throughput, whereby analyses where tens of thousands of genomic loci can be assayed simultaneously. Since the MIP probes can be applied directly to genomic DNA instead of shotgun libraries, low amount of sample DNA is required.¹⁸⁷ Also, MIP requires only 40 base-pairs of intact DNA giving it a distinct advantage when working with potentially degraded DNA from FFPE

samples.¹⁸⁶ A recent study has demonstrated the success of MIP for copy number variation in formalin-fixed paraffin embedded samples.¹⁸⁹ Using this technology, the authors found the performance of FFPE DNA was comparable to that obtained from matched fresh frozen tumour with only a modest loss of performance in FFPE.¹⁸⁹ Therefore, in order to derive quality data regarding genome wide structural variations in our large cohort of MPM for whom archival FFPE samples were available, we chose to do the Oncoscan FFPE array which is a SNP array based on MIP technology from Affymetrix (Santa Clara, USA).

Past investigations into CNAs in MPM have consistently demonstrated a sizeable number of structural aberrations of various lengths. Differences in the assay used to interrogate the CNAs, the types (patient tumour Vs cell lines) and numbers of samples have meant that the commonest chromosomal regions with CNAs have not always been consistent across studies. However, losses in 9p, 22q, 3p, 1p, 6q, 13q, 14q and gains in 1q, 15q, 7q, 8q, 5p have been noted to be recurrent aberrations. A brief description of the findings of past studies has been presented in Table 7.9. Our results closely resemble the previous studies in terms of the common chromosomal arms affected although losses of 7q, 16p and 19p and gains in 21q and 3q that have featured on the top losses and gains in our study have not been described in previous studies. The Oncoscan FFPE assay is a high throughput assay, able to assess a large number of loci simultaneously, it is therefore not surprising that we found a larger number and greater complexity of CNAs (3-866/sample) than previous CGH(1-8/sample)³⁶⁰ and aCGH (0-40/sample)³⁵⁵ based studies. We believe that this, along with the reasonably large sample size in our study has enabled us to uncover CNAs which occur in a significant proportion of MPM patients, could be important in the pathogenesis, diagnosis or treatment guidance yet are easily missed in assays with limited resolution done on a limited number of samples.

Table 7.9: Common copy number aberrations described in previous studies.

Authors	Year reported	Type of analysis	No. of samples	Type of sample	Commonest gains	Commonest losses
Bjorkqvist et al. ³⁶⁰	1997	CGH	18	patients	1q,10q,15q, 17q,19q	9p,4q,6q,13q,14q,22q
Balsara et al. ³⁶¹	1999	CGH	24	cell lines	5p,5q,7p,7q, 8q	22q,15q,1p,13q,14q, 6q,9p
Krismann et al. ³⁶²	2000	CGH	18	patients	1q,7q,15q	1p,4p,4q,6q,9p,14q, 22q
Kivipenas et al. ³⁵⁹	2001	CGH	11	patients	5p, 6p, 8q, 15q, 17q, and 20	1p, 8p, 14q, and 22q
Ascoli et al. ³⁶³	2001	CGH	4	patients		1p, 6q, 9p, 13q, and 14q.
Krismann et al. ³⁶⁴	2001	CGH	90	patients	8q,1q,7p,15q	9p,22q,4q,4p,14q,1p, 13q,3p,6q,10p,17p, 15q
Lindholm et al. ³⁵⁵	2007	aCGH	26	patients	17q	9p,1p,3p,6q,9p,13q, 14q,22q,12q
Taniguchi et al. ³⁵⁶	2007	aCGH	22	17 patient samples,9 cell lines	1q,5p,7p,8q, 20p	1p,3p,4q,6q,9p,10p, 13q,14q
Neragi-Miandoab et al. ³⁵⁷	2009	karyotyping	40	cell lines		1p,3p,6p,9p,6q,22q,
Takeda et al. ³⁸	2012	FISH	42	patients	5p, 7p, 8q	9p,1p,14q,22q
Klorin et al.	2013	aCGH, SKY	10	Cell lines	1q,5p,7p,8q, 9q,17q,20q	3p,4,6q,8p,9p,10p,1 1p,12p,13q,14q,15q, 16q,18q,18,19p,22q
Bueno et al. ⁵⁵	2016	SNP array/ whole genome	95	patients	RPTOR(17q), BRD4 (19p)	BAP1(3p), NF2(22q),CDKN2B(9 p), LATS2(13q)

A novel finding of our study was that based on the copy number profile, MPM samples could be divided into two distinct clusters. On account of small sample sizes and limited resolution assays, such analyses would not have been feasible in previous studies. We conducted the CNA clustering to try and identify subgroups among patients that could predict outcome, identify structure within the groups that was not evident a-priori, or influence the effect of PD-L1 status on survival. We found these clusters differed significantly in terms of their PGA with cluster one harbouring greater

genomic alterations than cluster two. Also, we found a significantly greater proportion of non-epithelioid MPMs in cluster two than in cluster one. The clusters however, did not significantly differ in terms of age, sex, history of asbestos exposure and PD-L1 expression. Although clustering did not identify informative subgroups, this may be due to lack of adequate power to detect the clinically relevant differences rather than absence of such differences. A similar consensus clustering on a larger number of samples may in fact uncover such differences. The success of clustering for identifying clinically important subgroups in previous studies^{375,376} suggests it is a worthwhile step in CNA analysis. Also, we think that the lack of such clusters is indeed an important negative result to communicate to the broad scientific community.

We used PGA as a surrogate for the genomic instability and to summarise CNA status for a given patient. In other cancer types, it is strongly predictive of disease outcome.³⁵⁸ The advantage of using PGA in addition to individual CNAs is that it allowed us to test the general effect of genome instability rather than the effect of only a CNA at a particular locus, and it is better powered since it does not require multiple testing corrections. It is also more informative than the count of CNAs in a patient as it takes into account the size of aberrations as well as the number. We conducted a manual calculation of PGA rather than using the metric “percentage of genome changed” provided by the Nexus express software. The manual calculation makes it more transparent and easier to adjust than the metric provided by Nexus Express. Nexus Express does not explicitly indicate how it calculated percent genome changed, and does not allow any customisation prior to calculation. An important advantage to calculating PGA ourselves is that prior to calculation we are able to exclude artefactual gains caused by the PAR region in males. We can also specify the events that contribute to PGA (eg copy number changes vs loss of heterozygosity), whereas the metric provided by Nexus Express does not specify the genomic events it incorporates. PGA is a well-established metric^{377,378} and other groups have used this metric to quantify copy number burden and examine its association with clinical covariates.³⁷⁹

In our analysis, we found PGA to be prognostic. In keeping with expectation, we found that patients with higher PGA had poorer outcome. This was true even when only epithelioid MPMs were included in the analysis. This has been demonstrated previously in prostate cancer.³⁵⁸ In MPM, a direct study of the correlation between the levels of genomic instability and patient survival in large cohorts has not been reported. However, a small CGH based study incorporating six cases of deciduoid mesothelioma did report a better survival in patients with lesser (<2/sample) losses.³⁶⁶ Our finding that PGA is in fact prognostic in MPM is important given the dearth of reliable prognostic markers in mesothelioma. It does however need to be further validated in independent cohorts in future studies.

An intriguing finding in our study was that non-epithelioid MPMs demonstrated lower PGA than epithelioid MPMs. This would be considered counterintuitive considering sarcomatoid MPMs are known to be more aggressive and also our own findings have suggested that PGA is prognostic. We found that the absolute numbers of CNAs were not different between histologies; but, the total proportion of the genome that had been altered was greater in epithelioid MPMs. Although there were differences in the relative frequencies of copy number changes in a large number of loci, none of them actually reached statistical significance after correction for multiple testing. A CGH based study has previously sought to explore the differences in CNA number and patterns between epithelioid and sarcomatoid MPMs.³⁶⁴ Evaluating 27 predominantly epithelioid, 25 sarcomatoid and 22 biphasic tumours, Krismann et al.³⁶⁴ found an average of 6.4, 6.4 and 5.8 copy number defects per sample in epithelioid, sarcomatoid and biphasic tumours respectively. They did however find that epithelioid tumours had greater numbers of losses in 3p21 (33%), 17p12 (26%) and 2p21 (15%) and gains in chromosome 7 (19%) relative to non-epithelioid tumours. Similarly sarcomatoid mesothelioma showed greater frequencies of loss at 7q31 (21%), 18p11 (21%) and a5q (18%) relative to other tumours. In a recent comprehensive analysis of the mesothelioma genome, Bueno et al.⁵⁵ using whole genome sequencing in 99 samples did not find any difference in somatic mutation rates between histotypes. Differences in our findings and those of Bueno et al. are likely

due to differences in our approaches and datasets. It is important to realise that Bueno et al. analysed transcriptomes and exomes using NGS on frozen tissues. As our tissues were largely FFPE samples, we utilised the Oncoscan array to determine genome wide instability through copy number. As copy number and point mutations arise from distinct mutational processes, it is not surprising that patterns observed in one mutation class would not necessarily reflect the other. If MPM is a class-C tumour driven more strongly by CNAs than point mutations as suggested by the low mutation rate,⁵⁵ our assessment of PGA would then be more likely to detect differences in genomic instability among subtypes than comparing point mutation rates. This is especially likely as the difference in genomic instability that we found was subtle (mean difference in PGA between epithelioid and non-epithelioid = 4.44 +- 4.34 (95% confidence interval)).

Our results seem to suggest the presence of differences in the copy number profiles (both numbers and patterns) between MPM histotypes. However, despite assessing a sizeable number of samples due to the large number of loci examined the power of the analysis was obviously not great enough to identify these subtle differences. Future larger studies or ones with coalesced data from multiple studies may be helpful in this regard. As to why the more aggressive non-epithelioid MPMs should have lesser PGA than epithelioid MPMs is a question that requires further study. One hypothesis could be that on account of the more indolent and prolonged course of growth, epithelioid MPMs may have had the time to acquire and accumulate more structural changes than the faster growing non-epithelioid variety.

Understanding the genomic landscape (both point mutations and CNAs) has become even more important in this the age of immunotherapy. This is especially highlighted by recent reports in lung cancer and melanoma linking response to check point inhibitors with the mutational landscape.^{235,236} Greater number of mutation generated neo-peptides leading to more visibility to the immune mechanism and therefore a more robust immune response is thought to be the reason of superior activity of check point inhibitors in tumours with higher mutation rates. We know that the

non-homologous recombination events that underlie changes in copy number allow generation of new combinations of exons between different genes by translocation, insertion or deletion, so that proteins might acquire new domains, and hence new or modified activities.³⁸⁰ A recent report from Swanton et al analysed the pattern of small insertion and deletions (indel mutations) across 19 solid tumour types (not including MPM) and found that renal clear cell carcinoma, renal papillary cell carcinoma, and chromophobe renal cell carcinoma have the highest indel rate as a proportion of their total mutational burden and the highest overall indel count and are enriched for mutant-specific neoantigens. They also observed that indel number is significantly associated with checkpoint inhibitor response in melanoma.³⁸¹ Some checkpoint inhibitors have demonstrated reasonable activity that in MPM^{170,172,268} despite the now proven low rates of somatic mutations in MPM. We therefore sought to find if indeed structural chromosomal aberrations, the more prominent genomic changes in the MPM genome show any correlation with the immune milieu of the tumour and therefore could be investigated prospectively for their ability to predict response to the immune based therapies in the future.

Our results of this analysis showed mixed results with the level of genomic instability (represented by PGA) not correlating with PD-L1 status but correlating with PD-L2 status. Levels of CD4+, CD8+infiltration, and positivity with TIM3 were higher in samples with lower PGA. These findings however need to be assessed with caution as both lower PGA and higher infiltration with CD+, CD8+ and TIM3+ cells correlate with non-epithelioid histology. This association therefore may be a spurious one and would need validation in future independent cohorts.

Our univariate analysis of the effect of copy number events in gene loci on OS suggests prognostic roles for some CNAs. Loss of *BAP1* was found to be associated with better survival and gain of *CDK6* together with loss of *MTAP* and *DMRT1A* were associated with poorer survival. Loss and/or inactivation by mutations of *BAP1* have been described extensively in MPM before^{28,87,89,90,351,382–385} (discussed at length in chapter 8, section 8.1.3). While most previous studies

investigating *BAP1* status (somatic mutations and copy number changes) have reported better prognosis for patients with *BAP1* loss/mutations, this has not been a universal findings with Zauderer et al⁹⁰ finding no effect on survival. However, almost all of these studies have been small scale. Our results on a relatively large cohort suggest *BAP1* loss is potentially important and could be used in MPM prognostication. Since *BAP1* expression status IHC has been shown to correlate with *BAP1* gene status,^{87,382} we sought to further investigate this using IHC on our MPM TMA. Results of this have been presented and discussed in the next chapter.

The cyclin dependent kinase 6 (*CDK6*) gene is located in chromosome 7q21 and codes CDK6 which is a member of the cyclin-dependent kinase, (CDK) family and are known to be important regulators of cell cycle progression.³⁸⁶ This kinase is important for the G1 phase progression and G1/S transition of the cell cycle and has been shown to phosphorylate, and thus regulate the activity of, tumour suppressor retinoblastoma protein (Rb) making CDK6 an important protein in cancer development.³⁸⁷ As such, CDK6 and other regulators of the G1 phase of the cell cycle are known to be unbalanced in more than 80-90% of tumours. Although no mutations in CDK6 have yet been linked to a particular neoplasm in humans or mice, CDK6 is expressed at dramatically enhanced levels in human leukemia and lymphoma.^{388,389} Amplification of this locus has been previously reported in glioblastoma and pancreatic cancer.^{390,391} CDK6 amplification has not been described before in mesothelioma. A study looking into the status of cell cycle associated genes in 4864 tumours found no amplifications in the mesothelioma samples (n=36%). We found CDK6 amplification in 45% of our samples. Also, CDK6 amplification was associated with poorer OS on univariate analysis. This is an interesting novel finding and one that could have implications on MPM therapeutics given that CDK6 inhibitors have been trialled in several human malignancies including in breast cancer.³⁹² We have therefore endeavoured to validate our findings regarding CDK6 amplification and to explore its correlation with clinicopathological covariates in chapter 8.

The *MTAP* gene is located at chromosomal locus 9p21, flanked by *CDKN2A* and miR-31. *MTAP* has been described to be frequently deleted in many different cancers either alone or in co-deletion with *CDKN2A* and *CDKN2B*. Loss of *MTAP* expression can also occur due to methylation of the *MTAP* promoter.³⁹³ *MTAP* deletion is seen in 40% of glioblastomas; 25% of melanomas, urothelial carcinomas, and pancreatic adenocarcinomas; and 15% of non-small cell lung carcinomas (NSCLC).³⁹⁴ We found loss of *MTAP* in 63% of our samples. In a FISH analysis of 95 fresh frozen MPM samples Illei et al.³⁹⁵ found co-deletion of *MTAP* and *CDKN2A* in 67% of the samples. While this previous study did not investigate the prognostic implication of *MTAP* loss, we found that in univariate analysis, *MTAP* loss was associated with poorer survival. This association of *MTAP* loss or loss of expression of *MTAP* on IHC with poor survival has been demonstrated in several other tumours like gastro-intestinal stromal tumours,³⁹⁶ carcinoma stomach.³⁹⁷

The cellular function of the gene product methylthioadenosinephosphorylase (*MTAP*) is to cleave methylthioadenosine (MTA) to generate precursor substrates for methionine and adenine salvage pathways. Cells lacking *MTAP* are unable to salvage adenine or methionine from endogenous MTA. As a consequence, they are more sensitive to inhibitors of de novo purine synthesis such as methotrexate (MTX), 6-mercaptopurine, azaserine (a potent inhibitor of the initial step in purine biosynthesis) and L-alanosine than cells with intact *MTAP*, and are also more sensitive to methionine starvation.³⁹⁸ Strategies to exploit *MTAP* loss with methionine starvation or by inhibiting de novo purine synthesis have been tried.³⁹⁹ In a multicentre phase II study of L-alanosine (an inhibitor of adenine biosynthesis), 65 patients who were negative for *MTAP* IHC with various malignancies including 16 with MPM were treated with L-alanosine at starting dose of 80mg/m² by continuous infusion for 5 days every 21 days. There were no objective responses but 5/13 (38%) of the evaluable mesothelioma patients had stable disease including two with prolonged stable disease lasting 7.5 and 15.2 months. Although this trial was largely considered negative, other avenues are being explored in therapy for *MTAP* deficient tumours. Given the increased susceptibility of *MTAP* negative tumours to thiopurines, combinations of 6-thioguanine (6-TG) -a well-studied purine

analogue that has both anticancer and immune-suppressive activities with MTA has been proposed.⁴⁰⁰

DMRT like family A1 (*DMRTA1*) is located in chromosome chr9p21.3. The gene product DMRTA1 is a transcription factor and along with DMRTA2 has been found to be highly expressed in telencephalon of rodent embryos. Studies show that *DMRTA1* is a downstream gene of PAX6, a potent regulator of proliferation and differentiation of neural stem/progenitor cells. Once expressed, *DMRTA1* promotes neuronal differentiation via regulation of NEUROG2.⁴⁰¹ DMRTA 1 loss has been demonstrated in bladder carcinoma⁴⁰² and astrocytoma.⁴⁰³ In patients with multiple myeloma, mutation in DMRTA1 has been associated with increased incidence of oral mucositis in those receiving stem cell treatment.⁴⁰⁴ No prior literature detailing the prognostic implications of DMRTA1 in cancers is available. The role (if any) of this novel CNA in the pathogenesis and prognostication of MPM may be an interesting research avenue in the future.

Our study of the copy number profile was extensive allowing us to investigate the status of a large number of gene loci. Optimum clinical annotation of the cohort enabled us to study the clinicopathological correlation of the aberrations discovered. However, there were several limitations of our study. The retrospective nature of the study meant that we did not have matched samples of normal pleura or blood accompanying the FFPE. A study of the CNAs in these samples would have enabled us to select out the truly somatic aberrations in the MPM genome. Also, given that our samples came from a very long time span, the methodologies of FFPE fixation would understandably differed between samples. This could potentially have impacted the results of our study. Unfortunately this was not something we could have controlled for.

High per sample cost of the assay and significant attrition of the samples due to poor quality FFPE derived data lead to restriction of the sample size for which genome wide copy number analysis data was available to 100. Our analyses of the differences of copy number profile amongst different MPM histotypes, association of CNAs with survival and PD-L1 status suffered from

significantly inadequate power to detect these differences. Larger studies in the future may be able to uncover them. An important advantage of our analysis was that although we did not have matched normal tissue or DNA, almost all (320/329) of our patients had not received prior chemo/radiotherapy prior to acquisition of the tissue sample included in the study.

In conclusion, our study of the copy number profile of a well annotated set of MPM patients demonstrated a large number of CNA events with significant variation between samples and MPM histotypes. We confirmed most previously described prominent CNAs but more importantly uncovered new ones like CDK6 amplifications and DMRTA1 loss which may be important in MPM prognostication and therapeutics. We found that greater degree of genomic instability confers a worse prognosis in MPM independent of histology but neither degree of genomic instability nor any specific CNA correlates with the immunological milieu.

Chapter 8: Investigating common CNAs in MPM and validation of the ONCOSCAN data

8.1 Introduction

Our assessment of the genome-wide copy number profile of MPM revealed many recurrent CNAs; some of which have been described before (loss of *BAP1*, *CDKN2A*, *NF2* etc.) and others that have not (gain in *CDK6*, loss of *DMRTA1*). Available and emerging literature suggests that these may be useful as diagnostic^{60,88,89,405} and prognostic^{60,87,406,407} markers for MPM and some (*CDK6*, *MTAP*) may represent potential objects for development and application of targeted therapy.^{392,399,408–410} These data on the genome-wide copy number profile are interesting, potentially important and possibly useful.

Reproducibility of whole-genome copy number data generated using the OncoScan assay has been demonstrated previously.³⁷² However, OncoScan is a high throughput technique querying the copy number status of a large number of genes. Therefore cross-validation of the findings and a more focused assessment of individual genes are important. Using the entire cohort of MPM patients on our TMA, we sought to validate our findings from the 100 cases profiled on OncoScan. These 100 cases were also included on the TMA enabling direct correlation of results using an independent method. As it was not possible to validate the large numbers of CNAs detected individually, we endeavoured to cross-validate key genes including the losses in *CDKN2A* and amplifications in *CDK6*. We used FISH assays to query the status of these genes. These particular genes were chosen based on the availability of high quality validated commercial probes for these genes and also on their prognostic implications seen on our CNA analysis.

Our findings on OncoScan with regards to alterations in *BAP1*, *CDKN2A* and *NF2* are in line with reported literature in MPM. They are in fact the most commonly altered genes in MPM. Although some studies have been conducted into these CNAs and their clinical implications, they are still

understudied. Assessment of protein expression of BAP1 and merlin using IHC has been a popular surrogate for analysis of the status of these genes; *CDKN2A* status has mostly been studied using FISH. Loss of BAP1 expression has been found to be associated with epithelioid histology and better survival.^{58,87,89,411} IHC evaluation for BAP1 loss has also been proposed as a specific marker to differentiate MPM from reactive pleuritis.^{88,89,412} Low expression of cytoplasmic merlin was found to be an independent prognosticator for shorter recurrence free survival.⁴⁰⁷ *CDKN2A* loss has been projected as a useful marker to differentiate MPM from atypical reactive pleural hyperplasia.^{405,413,414} However large scale studies into these markers and comprehensive assessment of their clinicopathological correlates have not been accomplished. To comprehensively explore the clinicopathological correlations of these common and important CNAs, in addition to the copy number analysis described in chapter 7 we conducted an IHC analysis of the expression of BAP1, *CDKN2A* (p16) and NF2 (merlin) and also a FISH assessment for *CDKN2A* and *CDK6*.

8.1 Commonly altered genes in MPM

8.1.1 Cyclin-dependent kinase inhibitor 2A (*CDKN2A*)/alternative reading frame (ARF) gene

CDKN2A is the most frequently inactivated TSG in human mesothelioma. *CDKN2A/ARF* is located at chromosome 9p21.3 and *CDKN2A* encodes p16INK4a with exon 1 α , 2 and 3, whereas ARF encodes p14ARF with exon 1 β , 2 and 3 with an alternative open reading frame. p16INK4a controls the cell cycle via the cyclin-dependent kinase 4/cyclin D retinoblastoma protein pathway, whereas p14ARF regulates p53 through inactivation of the human ortholog of mouse double minute 2 (MDM2), which is an upstream regulator of p53. Thus, homozygous deletions of *CDKN2A/ARF* indicate the inactivation of two major tumour suppressing pathways of retinoblastoma and p53 in the cell. Because the targeted deletion region of 9p21.3 is often large, other genes located in the same gene cluster such as *CDKN2B* (p15INK4b) and *MTAP* are also co-deleted, which are thought to be responsible for granting more malignant phenotype to MPM cells. Meanwhile, although *Tp53* is the

most frequently inactivated TSG in human malignancies, only a limited number of cases show a *Tp53* mutation. The inactivation of both p16INK4a and ARF has been suggested to cooperate to accelerate asbestos-induced tumorigenesis *in vivo*.⁴¹⁵ Gene therapy studies aimed at p16INK4a / p14ARF gene reactivation in order to restore the functions that are lost when this is mutated have shown that reactivating the gene in mesothelioma cells induces cell cycle arrest, an inhibition of pRb phosphorylation, and a decrease in cell growth. All of these modifications may therefore be related to an increase in survival, an increase in the levels of p53 protein, and a shift towards cellular apoptosis.^{416,417}

8.1.2 Neurofibromatosis 2 (*NF2*)

NF2 is a tumour suppressor gene located on chromosome 22q12 that code for the merlin protein (Moesin ezrin radixin like protein). Loss of *NF2* function occurs in about 40% of patients with MPM. The role of *NF2* loss/mutation in the pathogenesis of MPM was first described in 1995 by Sekido et al. and Bianchi et al.^{39,418} Recent studies have provided more evidence.^{38,40} This causes loss of contact inhibition and increased tumour cell proliferation and migration through interactions with a myriad of downstream effectors.⁴⁰ In studies with mouse models, heterozygous germline inactivation of one copy of *NF2* has been shown to consistently accelerate asbestos-induced MPM onset, providing experimental evidence implicating merlin loss as an important event in MPM igenesis.⁴¹⁹

8.1.3 *BRCA1*-associated protein 1 (*BAP1*)

BAP1 is a tumour suppressor gene located on chromosome 3p21 and encodes the BAP1, a deubiquitinating enzyme that seems to regulate DNA damage response, and the cell cycle. *BAP1* alterations have been shown to be important in several cancers besides MPM like metastasizing uveal melanoma and renal cell cancer.^{42,383} In 2011, two seminal papers described two putatively distinct cancer-related syndromes characterized predominantly by

melanocytic tumors or mesothelioma, along with uveal melanoma and linked them to germline *BAP1* mutations.^{351,420} The discovery of certain families in the Cappadocia region of Turkey with high preponderance of MPM and the presence of germline mutations in *BAP1* has led to the belief that it may represent genetic susceptibility to MPM especially when such individuals are exposed to asbestos or erionite.³⁵⁴ Somatic mutations too have been seen in up to 23% of sporadic mesothelioma and heterozygous/homozygous loss of *BAP1* gene containing 3p21 region have also been reported with a suggestion that these alterations may be specifically related to epitheloid rather than non epitheloid mesotheliomas.^{41,89,421} Despite the frequent alterations of the *BAP1* gene, the association with prognosis has not been conclusively proven with a study even suggesting that high level of expression of wild type *BAP1* actually correlated with poor prognosis.⁵⁸

8.2 Aims

The aims of the research described in this section were

- 1) To validate the CNAs seen in *CDKN2A* (loss) and *CDK6* (gain) using FISH.
- 2) To study the loss of *BAP1*, *CDKN2A* and *NF2* expression using IHC, corroborate IHC findings with copy number status and explore their correlations with clinicopathological covariates.

8.3 Specific methods.

8.3.1 IHC for *BAP1*, *CDKN2A* and *NF2*

The general methodology for IHC was as described previously in the methods chapter, section 2.6. A brief description is as presented in table 8.1. Scoring was done independently by me and Assoc. Prof Prue Russell with good interobserver agreement (Kappa scores depicted for individual stains)

Table 8.1: Brief description of the IHC used in this chapter

Antibody	Manufacturer	Catalogue number	Antigen Retrieval	Incubation time/temp	Controls	Assessment
BAP1	Santa Cruz (Santa Cruz biotechnologies, Dallas, Texas, USA)	sc-28383	Waterbath, 97°C for 45 minutes TRS buffer Ph 9	4°C overnight	Placenta, internal control, stromal cells	≥5% of tumour cells with nuclear staining were considered positive Exclusively cytoplasmic staining were disregarded and considered negative ⁸⁷
CDKN2A	Roche (Roche Holding AG, Basel, Switzerland)	725-4713	15 minutes in microwave TRS buffer Ph 9	4°C overnight	Ovary	>5% of tumour cells with nuclear and/or cytoplasmic staining were considered positive
NF2	Santa Cruz biotechnologies	Sc-331	15 minutes in microwave Citrate buffer Ph 6	4°C overnight	Testis	The staining intensity was semi-quantitatively scored 0 (negative), 0.5-1 (weak), 1.5-2 (moderate), or 2.5-3 (strong). The percentage of cells having any positivity was proportionally scored 0 (0%), 0.1 (1-9%), 0.5 (10-49%), or 1.0 (50% and more) as previously described ⁴⁰⁷

8.3.2 FISH analysis for CDKN2A and CDK6

Detailed description of the methods used has been described on the methods section. Brief overview is as presented in table 8.2.

Table 8.2: Brief description of methodology of FISH for CDKN2A and CDK6.

Gene	Catalogue no	Manufacturer of probes used	Probes	Examined under	Calling criteria
CDKN2A	Vysis probes (04N61-020)	Abbott Molecular (Des Plaines, IL, USA)	Spectrum green- Cep 9 Spectrum orange- locus specific probe for CDKN2A	Nikon Eclipse PS4-214	Ratio of average of orange/green signals was calculated ⁴²² no loss =>0.8-1.2 heterozygous loss = 0.1-0.8 homozygous loss = ≤0.1
CDK6	CDK6-20-OR	Empire genomics (Buffalo, NY, USA)	Spectrum green- Cep7 Spectrum orange- locus specific probe for 7q21.2	Nikon Eclipse PS4-214	Amplification was defined as CDK6:Cen7 (control) ratio of ≥ 1.2 ⁴²³ or >2.4 copies of CDK6 (independent of control locus) ⁴²² Average Cen7 ≥ 2.25 = polysomy Average Cen7 ≥ 5 = high polysomy

8.4 Results

8.4.1 BAP1 IHC

Of the 329 samples on the TMA, BAP1 IHC was evaluable in 317. There was good inter-observer correlation (Kappa score = 0.82). Taking nuclear staining in $\geq 5\%$ malignant cells as positive and disregarding purely cytoplasmic staining, we found loss of BAP1 expression in 126 (29%). Patients with loss of BAP1 expression were more likely to be younger age (63.95 ± 9.9 years vs 67.26 ± 10.26 years; $p = 0.006$) and of epithelioid histological subtype (chi-square test $p < 0.0001$). However, it was not associated with stage of the disease, sex, physiological status and PD-L1 expression status.

8.4.2 CDKN2A (p16) IHC

Expression of p16 was evaluable in 325 samples. Inter-observer correlation between BT and PR was good (Kappa = .80). Loss of p16 expression was found in 103 (23.8%). Loss of p16 expression was commoner in non-epithelioid MPM (Chi-square $p = 0.03$) but there was no relation with the age of the patient, sex, stage at presentation, physiological status and PD-L1 expression.

8.4.3 NF2 IHC

Merlin expression was evaluable in 328 samples. Low nuclear expression was seen in only 38 samples (8.8%) and low cytoplasmic expression was seen in 11 (2.5%). Expression of merlin in either location was not associated with age, sex, stage of the disease, physiological status and PD-L1 expression. Representative pictures of BAP1, CDKN2A (p16) and NF2 (merlin) IHC are presented in Figure 8.1.

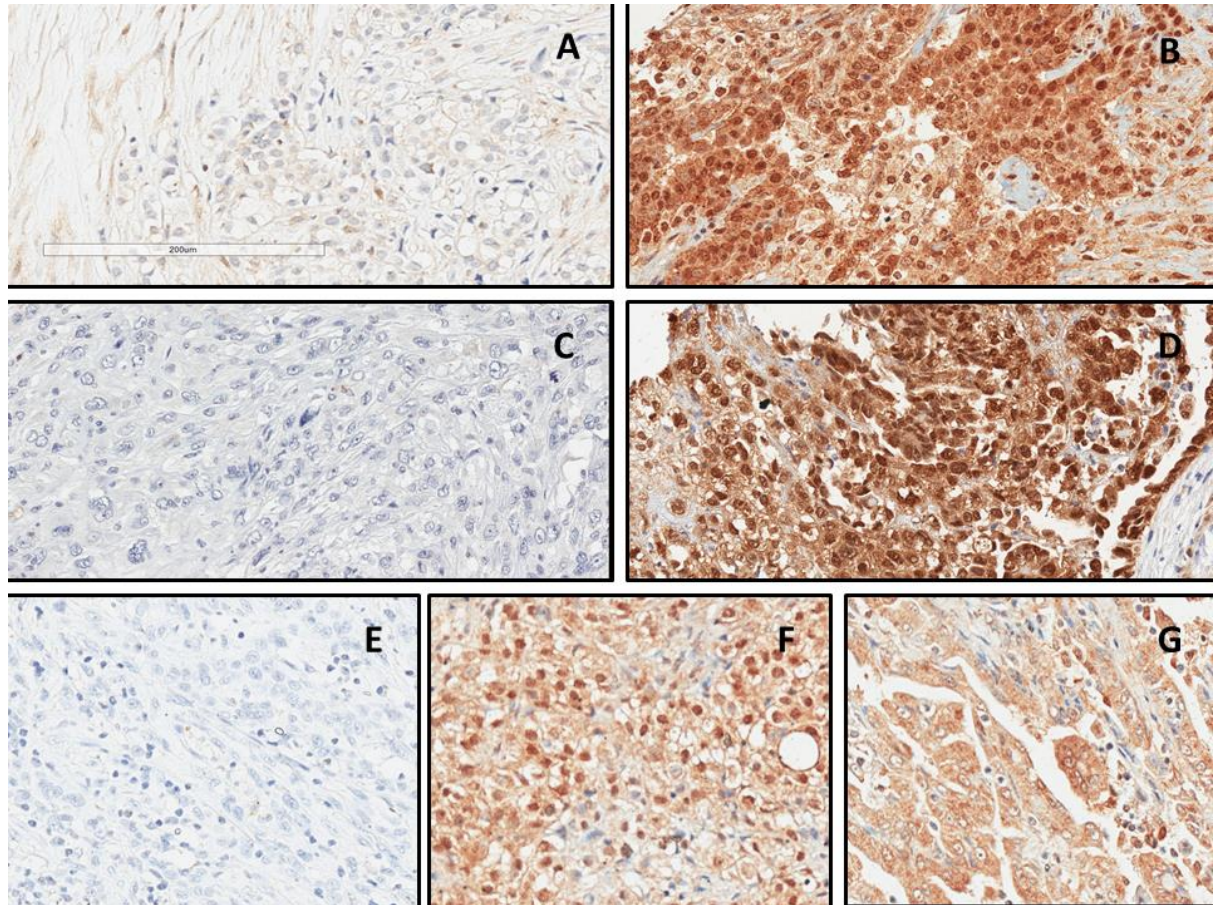


Figure 8.1: Representative pictures of the IHC assessment of BAP1, CDKN2A and NF2

A: BAP1 negative (some cytoplasmic staining, no nuclear staining) B: BAP1 positive C: CDKN2A negative D: CDKN2A positive E: NF2 negative F: NF2 staining mostly in the nucleus G: NF2 staining mostly in the cytoplasm

8.4.4 FISH assessment of *CDKN2A*

CDKN2A FISH was evaluable in 310 samples. Loss of *CDKN2A* gene (homozygous and heterozygous) was found in nearly 56% of our samples (Table 8.3). Representative pictures of the FISH assessment of *CDKN2A* are presented in Figure 8.2. There was a correlation between the p16 IHC and status of *CDKN2A* on FISH (spearman $r = 0.22$; CI 0.11-0.33; $p < 0.0001$). There was no correlation between the *CDKN2A* gene status FISH and age, sex, stage of disease, physiological status and PD-L1 expression status. There was good correlation between FISH and CNA by OncoScan for *CDKN2A* with 91% of the 97 cases in which had both FISH and OncoScan results available (Table 8.4)

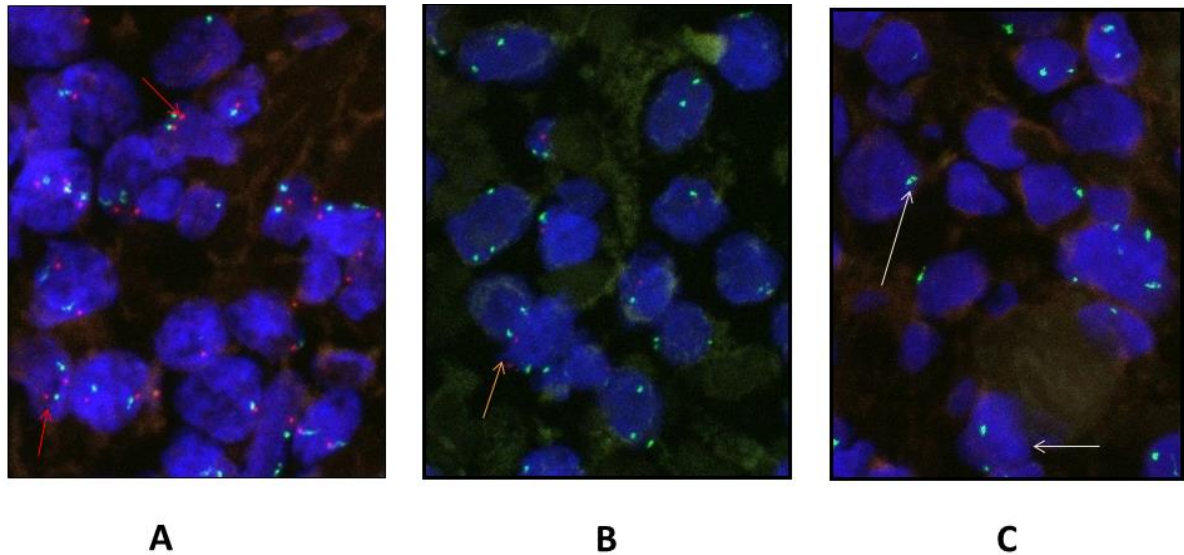


Figure 8.2: Representative pictures of the FISH for CDKN2A.

Blue colour (DAPI) delineating the nucleus. Green signals represent the centromere probe for chromosome 9 and the red (orange) signals represent the locus specific probe for CDKN2A.

A: Normal (2 green and 2 red signals- red arrows) B: Heterozygous loss (2 green and 1 red signals – brown arrows pointing to cell with heterozygous loss) C: Homozygous loss (2 green signals and no red signals – white arrows pointing to cells with homozygous loss)

Table 8.3: Status of CDKN2A in our cohort as assessed by FISH

	Number	Percentage
Homozygous loss	111	35.8
Heterozygous loss	61	19.6
No loss	138	44.5
Total	310	100

Table 8.4: Cross tabulation between the results of FISH and OncoScan on the status of CDKN2A

FISH result	OncoScan result	
	Loss	No loss
Loss (Heterozygous and Homozygous loss)	55	5
No loss	4	33
Total examined		97

The results of OncoScan and FISH were concordant in 88/97 (91%) of samples with Kappa score of 0.804

8.4.5 FISH assessment of *CDK6*

CDK6 status was evaluable in 320 samples. Representative pictures of the *CDK6* FISH assessment are presented in Figure 8.3. Abnormality in *CDK6* copy number was found in a total of 27.2% patients. However, in nearly half of the patients, gain in *CDK6* was also associated with polysomy of chromosome 7 (Table 8.5).

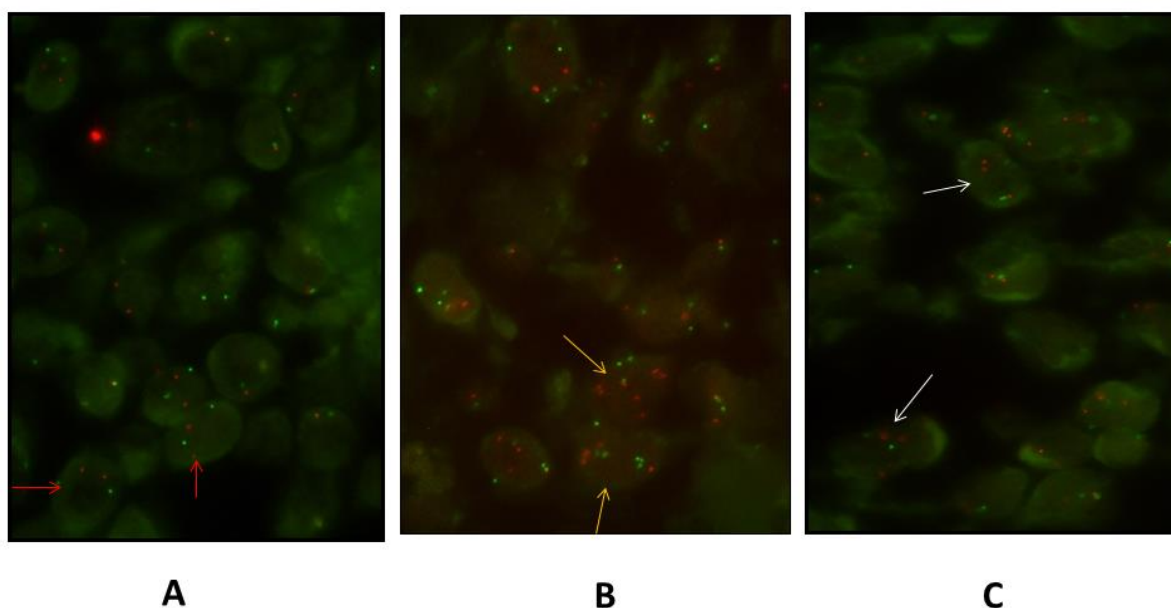


Figure 8.3: Representative pictures from the FISH analysis for *CDK6*.

Green signals represent the centromere probe for chromosome 7. Red signals represent the locus specific probe for *CDK6*

A: Normal (2 green and 2 red signals – red arrows) **B:** Polysomy (multiple green and multiple red signals – brown arrows showing cells with polysomy) **C:** Amplification (2 green and multiple red signals – white arrows showing cells with amplification)

Table 8.5: Status of the *CDK6* gene in our cohort

	Number	Percentage
Normal	230	71.8
Amplification only	47	14.6
Amplification +polysomy Chromosome 7	41	12.8
Polysomy only	2	0.006
Total evaluable	320	100

Concordance between FISH and OncoScan for *CDK6* was only 65% amongst the 97 cases where both results were available (Table 8.6). There was no relation between *CDK6* status and tumour histological type (Chi-square test $p = 0.23$).

Table 8.6: Concordance between the results of FISH and OncoScan on status of *CDK6*.

FISH result	OncoScan result	
	Gain	No Gain
Gain	27	13
No gain	20	37
Total examined		97

The results of OncoScan and FISH were discrepant in 29/97 samples i.e. the concordance rate was 65% ($\kappa 0.316$)

8.4.6 Relationship between status of *CDKN2A* and *CDK6*

Of the 304 samples in which FISH results for both *CDKN2A* and *CDK6* were available, there was no relation between the two CNAs (Fisher's exact test $p = 0.5$) (Table 8.7).

Table 8.7: Cross-tabulation of the status of *CDK6* and *CDKN2A* in our cohort.

CDK6	CDKN2A	
	Normal	Lost
Normal	103	124
Gained	31	46
Total evaluated	304	

8.4.7 Survival analysis

On univariate analysis, BAP1 loss on IHC was associated with improved OS than normal BAP1 expression (HR = 0.699; 95% CI = 0.55-0.87; Log Rank $p = 0.003$). *CDKN2A* loss on IHC was however associated with poorer survival (HR = 1.5; 95% CI = 1.2-1.6; Log Rank $p = 0.015$). Similarly, patients who had *CDKN2A* loss on FISH also had a worse OS (HR=1.6; 95%CI = 1.27-2.02; Log rank test $p < 0.0001$). Neither the nuclear nor cytoplasmic expression of NF2 (merlin) were prognostic. Patients with *CDK6* gain had an inferior OS than those who did not (HR= 1.33; 95% CI = 1.01-1.76; Log rank test $p = 0.04$) (Figure 8.4). Patients who had both *CDKN2A* loss and *CDK6* gain had poorer OS than those in which either or both of the genes were normal (Figure 8.5)

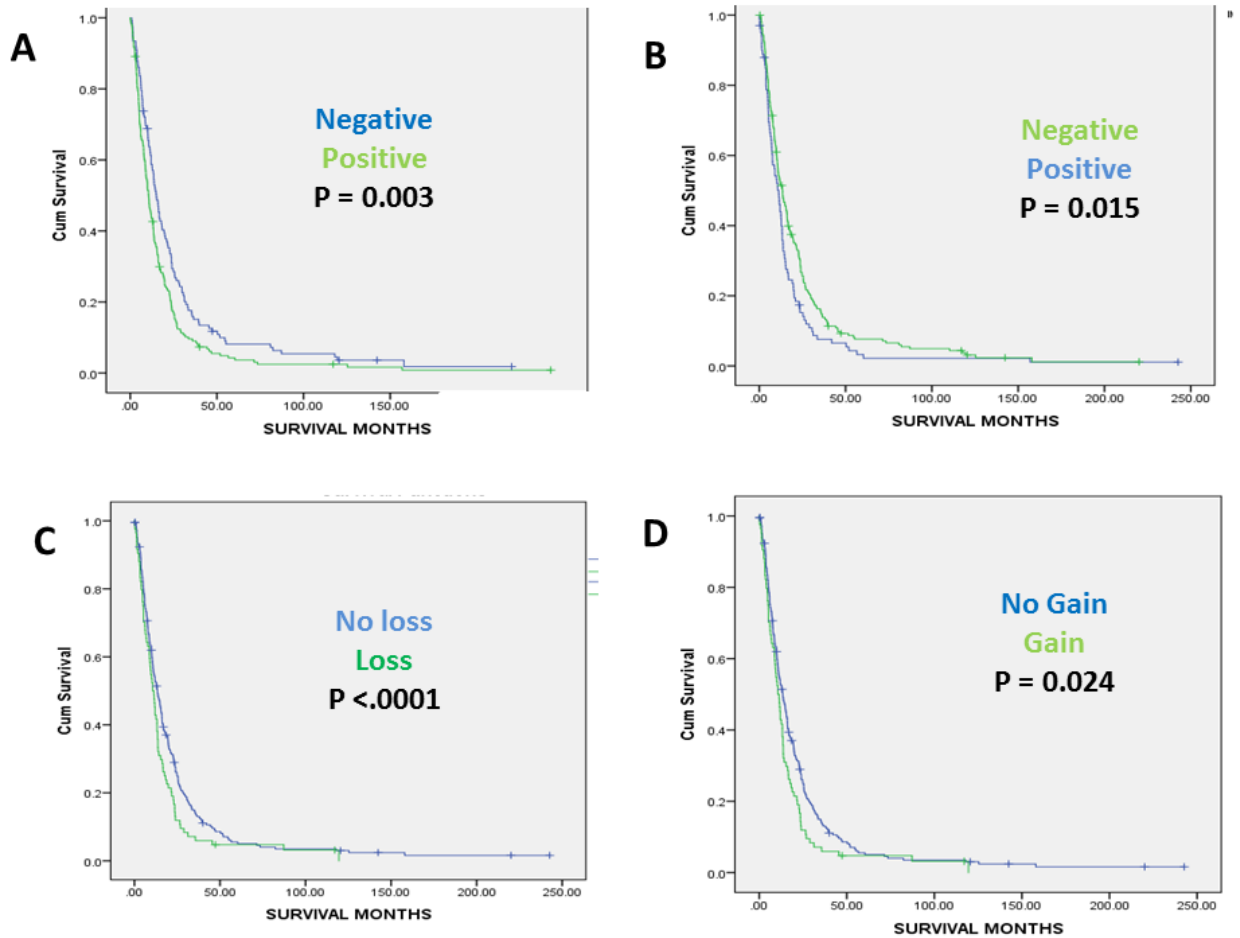


Figure 8.4: Prognostic significance of BAP1, CDKN2A and CDK6

- A) K-M curve comparing OS between patients who do/don't have BAP1 loss on IHC.
 - B) K-M curve comparing OS between patients who do/don't have CDKN2A loss on IHC.
 - C) K-M curve comparing OS between patients who do/don't have CDKN2A loss on FISH.
 - D) K-M curve comparing OS between patients who do/don't have CDK6 gain on FISH.
- P values from Log rank test

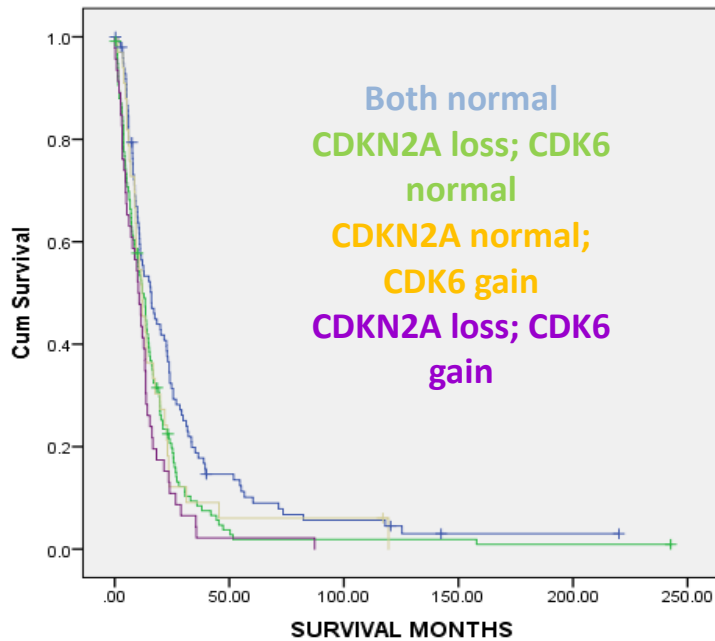


Figure 8.5: Prognostic implications of CDK6 and CDKN2A CNAs.
KM curve comparing the OS between patients with differing status of CDK6 and CDKN2A.

On multivariate analysis, loss of *CDKN2A* on FISH and gain of *CDK6* on FISH were found to remain significantly associated with poorer OS along with higher stage, non-epithelioid histology, and poorer physiological status on at presentation (Table 8.8).

Table 8.8: Multivariate analysis of survival.

Multivariate Analysis				
	P value	Hazard Ratio	95.0% CI for hazard ratio	
			Lower	Upper
Female sex	.029	.670	.467	.959
Higher ECOG score	.000	1.338	1.148	1.560
Non- epithelioid histological subtype	.000	1.806	1.474	2.214
Stage (I&II Vs III&IV)	.007	1.268	1.068	1.505
NLR (taken as a continuous variable)	.001	1.040	1.016	1.065
<i>CDKN2A</i> loss by FISH	.001	1.57	2.06	1.21
<i>CDK6</i> gain by FISH	.016	1.410	1.066	1.867

ECOG: Eastern co-operative oncology score, NLR: neutrophil to lymphocyte ratio

8.5 Discussion

We endeavoured to validate some of the CNAs demonstrated using the OncoScan platform detailed in chapter seven. Using FISH and IHC we also studied some commonly described MPM associated genes and studied their clinicopathological correlates. We demonstrated that while the losses in *CDKN2A* were easily validated by FISH, *CDK6* gains revealed by OncoScan were more difficult to validate. BAP1 loss of expression was found to be commoner in younger patients with epithelioid histological type. Loss of *CDKN2A* protein expression and *CDKN2A* loss by FISH were both more common in non-epithelioid histological type. Merlin expression had no clear clinicopathological correlates. *CDKN2A* loss and *CDK6* gain were found to be independently associated with poorer OS on multivariate analysis.

Using predefined cut offs for loss (homozygous & heterozygous) and gains, we found concordance between OncoScan and FISH data in 88/97 (91%) of our samples for loss of *CDKN2A* but only 64/97 (65%) for gain in *CDK6*. The results of the FISH and OncoScan in terms of the proportions of patients likely to harbour the CNAs also matched more closely for *CDKN2A* (55.4% of 310 patients evaluated by FISH and 65% of 100 patients evaluated by OncoScan) than it did for *CDK6* (26.5% of 320 patients evaluated by FISH and 45% of 100 patients evaluated by OncoScan). We therefore found it more difficult to validate the gains seen in OncoScan than the losses. While this is intriguing, several previous publications have also indicated limited concordance between OncoScan and FISH with respect to gene amplifications.^{424,425} Several factors relating to FISH, OncoScan and extent/position of the amplification may be responsible for such discrepancies. We used the OncoScan FFPE Express 2.0 which interrogates 335,000 markers for copy number changes. It has an increased density in the area of 200 tumour suppressor genes oncogenes with one probe per 0.5kb for the top 10 “actionable” tumour suppressor genes, a median spacing of one probe per 2kb for 190-plus actionable oncogenes but a median backbone spacing of one probe per 9kb.³⁷³ Also, a disadvantage of MIP technology on which OncoScan analyses are based is that it suffers from less

uniformity compared to other methods. This is because the probe design for each distinct genomic target is unique and thus the performance between individual probes may vary.

FISH allows detection of the real amount of gene copies in relation to the chromosome number and can discriminate between gene amplification from high gene copy number due to polysomy. As such it could be considered the gold standard assay for queries into copy number status of individual genes. However, a drawback from using FISH is that the results are based on a limited number of cells (50 cells in our study) in contrast to OncoScan which analyses 80 ng of DNA, equating to ~13 thousand diploid cells (1ng of DNA contains DNA from 167 diploid cells).⁴²⁵ *CDK6* status could possibly vary in different regions of the analysed tumour section and throughout the specimen due to heterogeneity thus leading to discrepancy in results. Additionally, there is also the potential bias of the assessor in focusing on areas with better/clearer staining. Increased infiltration with lymphocytes was demonstrated in a large proportion of our samples as described in chapter six. Increased cellular density in the TMA cores with overlapping of cells was in fact responsible for adding an additional layer of complexity to our FISH assay and although we tried to avoid these areas (Figure 8.6), potential errors introduced by this factor cannot be completely ruled out.

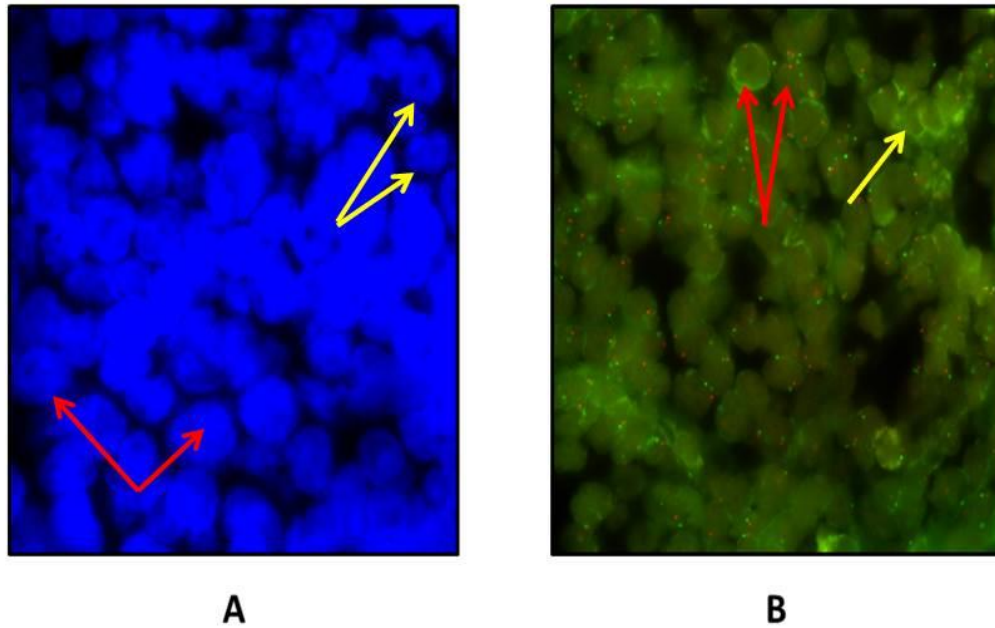


Figure 8.6: Heavy infiltration of MPM and high cellularity a potential source of errors in FISH analysis.

A: DAPI showing lymphocytes (smaller nuclei) packed amongst cancer cells (larger irregular nuclei). **B:** Lymphocytes intermingled amongst cancer cells making accurate counting of signals difficult. Larger cancer cells are marked with red arrows and closely placed lymphocytes masquerading as single large nuclei are shown with yellow arrows.

Another possible reason for the imperfect correlation between the FISH data and our genomic copy number analysis could be the tumour cellularity for the samples used for genomic copy number analysis. We cored areas of tumour marked by the pathologist but given the differing levels of lymphocytic infiltration seen in our samples, it is possible that the tumour purity levels were not uniform across all samples used for the genomic analysis.

Another challenge in trying to use FISH to validate the results of OncoScan is posed by the positions and the lengths of the segment of the chromosome that is amplified or lost. Such gains often involve large chromosomal segments sometimes including the centromere. This leads to increased number of both locus specific and centromere probe signals and may therefore mask amplifications.⁴²⁶ In our cohort, we did see patients with amplification of large segments of chromosome, which could be subject to this fallacy of FISH assessment. We also found samples with very short lengths of the genome amplified in this area (Figure 8.7). This could potentially mean that

not all amplifications in 7q21.2 were detected by the probe we used. A solution to this problem would be to use custom designed and potentially several different FISH assays to detect the different regions of amplifications. This approach however would be time consuming and costly while not guaranteeing the detection of all amplifications present.

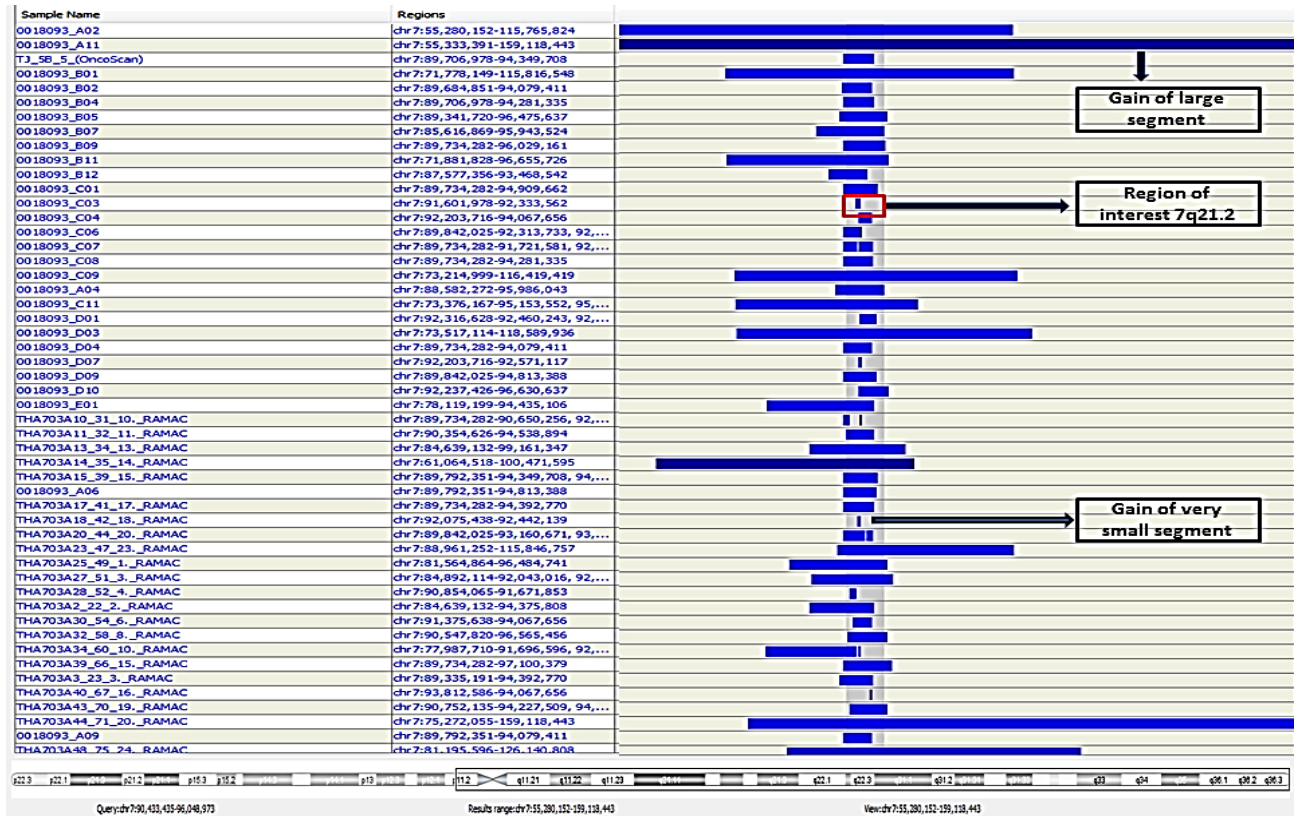


Figure 8.7: Extent and position of amplifications seen in 7q21.2 in our samples (position of CDK6-marked in grey bar).

There was great variation in the size and positions of the amplified chromosomal region.

We found loss of BAP1 protein expression to be associated with younger age, epithelioid histology and better survival. These findings are in complete agreement with previous reports.⁸⁷⁻⁸⁹

However our assessment of the loss of BAP1 on IHC was lower than reported in most previous series of smaller cohorts (46-66%).^{58,87,88} This may be because the previous studies have described BAP1 nuclear staining to be either uniformly positive or negative in cancerous cells and therefore have employed a binary system of positive/negative without a cut off. We often found focal positivity in cancer cells despite good staining in the stromal cells (internal positive control) and therefore

employed a previously described cut off ($\geq 5\%$).⁸⁷ This present study is the largest series to investigate BAP1 expression in MPM and validates findings of previous studies in terms of the favourable prognostic value of BAP1 loss. However, this association with a favourable prognosis may be more a function of BAP1 loss being more common in epithelioid MPMs.

Very little literature is available on the IHC assessment of NF2 (merlin) in MPM. In a study involving two separate MPM cohorts, one of which had patients who had undergone induction chemotherapy followed by EPP (cohort 1; n = 145) and the other with patients who underwent EPP followed by intrapleural chemotherapy or adjuvant chemo/radiotherapy (cohort 2; n = 59) looked at the prognostic implications of merlin expression. Low cytoplasmic labelling in cancer cells was found to be associated with significantly poorer OS and PFS in cohort 1 with a similar non-significant trend in cohort 2. Lo Iocano et al.³³ however, found no correlation of NF2 staining with any clinicopathological covariates in a study with 110 MPM patients. Our findings mirrored those of the latter investigators. Given that we have studied this in the largest cohort to date and also based on our findings from copy number analysis of *NF2* described in the previous chapter it looks unlikely that loss of *NF2* has any significant clinical correlates in MPM.

Several previous small scale studies have demonstrated the poor prognostic implications of both loss of p16 expression on IHC and loss of *CDKN2A* on FISH analysis.^{91,92} In a much larger cohort we were able to conclusively establish this not only in the whole cohort but also in the epithelioid sub-cohort. These findings assume additional importance in light of our findings of the presence of *CDK6* amplifications in a sizeable proportion of MPM patients. Both these genes are involved in cell cycle control. *CDK6/4* help to drive the progression of cells into the DNA synthetic (S) phase of the cell-division cycle and *CDKN2A* encodes for p16INKa which is an inhibitor of the CDKs. Our findings suggest that patients who have both *CDK6* amplification and *CDKN2A* loss represent an aggressive phenotype.

In conclusion, our finding of discordance between OncoScan and FISH for amplification in *CDK6* is concerning. While the problem may be specific to the locus studied here, the presence of previous studies reporting the same issue in different genes would suggest otherwise. FISH analysis being conducted into EGFR amplification by co-researchers in our group may also shed some more light on the issue. However, the presence of *CDK6* amplifications which we have been able to demonstrate either alone or in combination with *CDKN2A* loss may present an opportunity for trial of *CDK4/6* inhibitors in MPM. This is an avenue that needs to be explored by future studies. It may provide a potential for targeted therapy in MPM; a disease in which successful targeted therapy has been elusive.

Chapter 9: General discussion, limitations and future directions

MPM incidence continues to increase in many countries around the world.¹⁶ Numerous rapidly industrializing populous countries like India, Brazil, Russia and China continue to import and use asbestos.¹⁶ Even in countries which have banned import and use of asbestos, exposure during home renovations and 'bystander' exposures have ensured a new wave of MPM cases. Moreover, a lack of data for some of the world's most populous countries, among other factors, obscures the true risk of asbestos exposure worldwide.^{16,62} It is therefore very likely that the current world wide burden of MPM is much higher than current estimates and that it is going to remain a significant problem for the foreseeable future.

The diagnosis of MPM is still associated with dismal prognosis. The roles of surgery and radiotherapy in the treatment remain to be well defined. Standard of care is still chemotherapy with platinum derivate and anti-folate agents. Although the MAPS trial in front line setting showed improvement in OS in cisplatin and pemetrexed combined with bevacizumab compared to cisplatin and pemetrexed, there have been very few recent treatment paradigm changing advances in MPM therapeutics.⁴²⁷ Failure to identify oncogene driver mutations that may be responsive to targeted therapies has meant that targeted therapy is yet to emerge as an effective treatment modality in MPM. Reported trials of immunotherapy in MPM have shown some activity of checkpoint inhibitors. However, it now becoming clear that better predictive markers will be needed to choose patients who are likely to respond and also to tailor immunotherapy to individual patients.

Despite its worldwide prevalence and almost uniformly dreary outcomes, MPM remains an understudied disease. Lack of comprehensive knowledge of MPM molecular pathogenesis has no doubt been a contributor to the lack of effective targeted therapy options. Similarly, the limited understanding of the MPM tumour microenvironment has restricted the ability to effectively apply immunotherapeutic approaches to MPM treatment. This study was conducted with the objective to

comprehend the genomic changes in the MPM genome and also to define the tumour microenvironment. The endeavour was also to study any potential associations between them and to identify genomic changes that could affect the immunological milieu and possibly the suitability of individual patients to immunotherapeutic modalities.

During the course of this research we started out by assembling a large cohort of MPM patients. We reconfirmed the diagnosis of MPM of every patient by re-evaluation of the tumour morphology and also re-examination of the IHC evidence. We then conducted a retrospective audit of demographics, clinical, pathological and outcome data of these confirmed MPM patients to characterise our cohort. Given the relative rarity of MPM, large prospective cohorts although ideal, are incredibly difficult to build in a short period of time. Large retrospective cohorts which are clinically well annotated are therefore valuable resources. We were able to put together this cohort with good clinical annotation and adequate good quality FFPE tissue. Using this resource, we were able to study several biomarkers related to MPM.

Given that IHC plays a huge part in MPM diagnosis and characterisation, we used the tumour expression of calretinin which is a marker most widely used in MPM to characterize our cohort. We found the pattern and distribution of calretinin expression in our cohort to conform to previous reports with large cohorts.^{74,77} Additionally, we confirmed the positive prognostic implication of calretinin expression and also demonstrated a difference between histological subtypes with regards to expression. Our investigation into expression of caveolin-1 demonstrated it to be a reliable marker for MPM given its uniform expression in all histological subtypes. This finding is important as it could be helpful in the diagnosis of sarcomatoid MPMs which are known to often be negative for calretinin. Using a small cohort of lung adenocarcinomas, we were able to demonstrate very low positivity rates in these tumours therefore paving the path for potentially using caveolin as a marker to differentiate MPMs from lung adenocarcinomas metastatic to pleura.

Understanding the intricacies of the immunosuppressive mechanisms that tumours use to escape detection and elimination by the host immune system is now being recognised as the key to successful and precise application of immunotherapeutic modalities. Using IHC, we defined the immunological milieu in MPM. We found MPM tumours to vary widely in terms of their immunological profile. Immunologically 'hot' tumours were found to be associated with high expression of PD-L1 and PD-L2; they had more TILs but also higher expression of TIM3 on the TILs. Non-epithelioid MPMs were more likely to be 'hot' immunologically thus giving hope that this subgroup of MPM tumours with otherwise dismal prognosis may in fact be better targets for immunotherapy.

Our investigations revealed that besides PD-L1, MPM also expresses PD-L2 in a significant proportion. Although the expression of PD-L1 and PD-L2 mostly tracked together, in nearly a third of the patients, their expression was independent of each other. LAG3 expression was sparse. There was widespread expression of TIM3 in TILs. These findings may at least in part explain the difficulty in matching PD-L1 expression status to response to anti-PD-1/anti PD-L1 treatment. By no means is assessment of the immune microenvironment in MPM complete or even comprehensive. Yet our findings are enough to suggest that prediction of susceptibility to immune checkpoint therapy cannot be based on PD-L1 expression status alone. A broader assessment of the expression of multiple checkpoints and their ligands may be better able to predict responses and may also aid in choosing the optimum individual or combination checkpoint inhibition. Our comparison of the expression of PD-L1, PD-L2, TIM3 and LAG3 in MPM and NSCLC demonstrates difference in their expression rates between these tumours. This is again an important finding and raises the question of whether differences in the expression of these checkpoint receptors and their ligands can at least in part explain the differences in the rates of response to checkpoint inhibitors. This information may also be paramount in choosing checkpoint inhibitor combinations in different tumours.

TILs as an independent prognostic factor are known to be associated with good outcome in many cancers including breast and lung. The fact that we found high infiltration with TILs to be negatively prognostic in MPM is counter intuitive yet interesting. Widespread expression of lymphocyte exhaustion markers TIM3 in these TILs in our cohort probably suggests they are inactive and unable to mount an immune response. A similar analysis of TILs and TIM3 in cancers where TILs are found to be positively prognostic might help us understand why the effect of having high infiltration with TILs in MPM is contrary to that in most other cancers. Whether the level of TILs can act as a predictive marker for checkpoint inhibition would be an interesting and important study to conduct.

We conducted a comprehensive assessment of the copy number profile in a large number of patients. Other than confirming the frequent losses in *CDKN2A*, *NF2* and *BAP1*, our analyses unearthed some previously undescribed CNAs like gain in *CDK6* and loss in *DMRTA1* which could hold diagnostic, prognostic and possibly therapeutic implications. Contrary to expectations we did not find individual CNAs which were associated with any particular histology, with history of asbestos exposure or survival. However, we did find that despite being associated with worse prognosis, sarcomatoid MPMs showed lower PGA. High PGA was associated with worse prognosis in both epithelioid and non-epithelioid histological subtypes. These are very important findings but ones that need further exploration in dedicated studies.

In recent times the mutational burden has been linked to response to checkpoint inhibition. We looked for evidence of association of the copy number profile and individual CNAs with aspects of the tumour immune microenvironment specifically PD-L1 expression. Although the intuition was that tumours with greater PGA would have higher rates of PD-L1 positivity, we found no such association. We were unable to detect a significant association between any particular CNA and PD-L1 positivity. While it may be possible that this is because no such associations truly exist, it may just as well be because our study was not powered enough to detect these associations.

For the first time in MPM, we revealed *CDK6* amplification and also demonstrated its prognostic prowess. *CDK6* is important for the G1 phase progression and G1/S transition of the cell cycle and its inhibitor, *CDKN2A* is one of the most frequently lost genes in MPM. We think this makes for compelling argument in favour of preclinical studies into the activity of CDK6 inhibitors in MPM. Our inability to validate a significant proportion of copy number calls on *CDK6* made on OncoScan using FISH is concerning. Although, numerous factors related to FISH analysis in a morphologically difficult and diverse tumour such as MPM could be among the causes, we do think that there needs to be further interrogation and scrutiny of the ability of OncoScan to correctly identify CNgains.

9.1 Limitations

Retrospective studies are limited by a variety of important factors. Our study spans a total of 26 years. In this duration, there have been many changes in multiple aspects of health care. Just to enumerate a few that could have potentially affected our results:

- 1) Practices of collection, processing, fixation and storage of the FFPE samples have no doubt changed and improved over the years. The variation in how the tissue samples were initially handled could have affected the quality of the DNA obtained and therefore results of our copy number analysis. Additionally, whether there was any effect of this variable on IHC and its reading is not known. We assessed the age of the samples which had failed to yield satisfactory QC results for OncoScan but could not pin point any relation to age of the samples.
- 2) Treatment paradigms undoubtedly changed over the period. This would have an impact on the patient outcomes and as such we did demonstrate that the OS of patients treated after 2004 were better (likely coinciding with adoption of cisplatin + pemetrexed chemotherapy). This definitely means that the survival analysis needs to be interpreted cautiously.
- 3) Lack of adequate recorded data on a host of clinical and treatment parameters did make assessment of their effects on survival difficult. Prominent among these were lack of

adequate data on staging imaging and on the chemotherapy and radiotherapy received when they were performed outside of the Austin hospital.

A protocolled assessment and staging, protocol based treatment and follow up would probably have generated a more robust dataset. However, generation of a prospective cohort as large as the present one would be slow and difficult at best given the relative rarity of MPM.

Our analysis of CNAs was performed solely on the tumour tissue cores. Being archival samples, matching normal tissues were not available to assess and compare the copy number profiles. This would have allowed us to select out the CNAs selectively seen in tumour. We have commenced prospective collection of tumour and normal tissue and this would enable us to do such comparative studies in the future.

We conducted a large number of IHC evaluations in the course of these studies. Almost all were done on TMAs. Although we did take 1 mm cores in triplets from each sample, it is easy to see that IHC assessment from TMAs could yield different results compared to those from full face sections especially when the staining can be focal and sparse. This is an accepted limitation of use of TMAs and one that has to be balanced against the advantage it provides in terms of expedient and cost effective analysis of these IHC markers. In a cohort as large as ours, trying to do all markers on full sections would be very difficult, costly and slow.

9.2 Future directions

Targeted therapy and immunotherapy are now slowly being established as viable and effective treatment modalities in several cancers. It would be fair to say that these are the modalities which need to be explored further in an endeavour to develop newer treatment options in MPM. The focus in this thesis was therefore to conduct an explorative study of these two aspects of MPM. Our assessment of CNAs in MPM was comprehensive and yielded findings that could be of importance. However, contrary to expectation our analysis was not able to demonstrate cross links between CNAs and the immunological milieu. We do believe that such links exist. We have not been able to

study the difference in the levels or profile of somatic/germ line mutations between patients who have a “hot” immunological milieu from those who have a “cold” immunological milieu. We did try to do a targeted search for mutations in 50 genes that have been previously described in MPM. However, the DNA samples extracted from our FFPE samples were found to be of sub-optimal quality to reliably yield credible sequencing results using Hi-seq panel from Illumina. Such evaluations might be easier and more credible if done on DNA from fresh frozen tissue with accompanying plasma or normal pleura. We have in the duration of this study also managed to prospectively collect 17 such samples from consented patients with MPM operated at the Austin, Warrigal and Geelong hospitals. A whole genome/exome sequencing of these samples utilising the next generation sequencing platforms may in fact yield more results that further elucidate differences in genomic changes between patients who do and do not have an immunologically active tumour.

Our assessment of the immunological milieu in MPM is extensive but by no means comprehensive or complete. As our knowledge of the immunological mechanisms used by cancer cells to escape immunological surveillance and destruction grows, it is becoming clear that we need to have a much broader understanding of the roles of these multiple immunosuppressive mechanisms and their interplay. The roles of the other check points, their ligands and macrophages are yet to be defined. In generating the large cohort with good quality tissue, we have established the platform on which these studies can be conducted.

Some CNAs revealed to frequent and be of prognostic importance in MPM represent potential targets which would definitely merit further investigation and functional studies. One such investigation into *CDK6* and the potential to use *CDK4/6* inhibitors is currently being investigated in our lab. Similar studies need to be done to probe the possibilities of using *DMRTA1*, *MTAP* as targets.

In summary, during the course of our study, we generated and used a large well annotated, biopsy proven cohort of patients to study genomic alterations and immunological profile in MPM.

Our effort was to explore the potential associations between the extent and pattern of copy number changes in MPM and the immunological characteristics of individual tumours. We also sought to explore differences in copy number profiles between MPM histological subtypes and to identify individual alterations that may have prognostic and potentially therapeutic implications

We found MPM to be immunogenic with varying degrees of tumour infiltration. The immune microenvironment appeared to vary amongst tumours with heavier infiltration with lymphocytes in sarcomatoid histological subtype. This subtype was however also associated with greater immunosuppressive environment with greater PD-L1 and PD-L2 expression. Despite its association with sarcomatoid histological subtype, increased level of TILs was found to be an independent negative prognostic marker contrary to most other cancers studied. Varying numbers of CNAs were found in our genome-wide copy number analysis with losses of genomic regions outnumbering gains. Although PGA was surprisingly lower in non-epithelioid histological subtype, patients with higher PGA were found to have a worse OS. The copy number profile did not significantly differ amongst histological subtypes, and importantly, we were not able to demonstrate any association of PGA, copy number profile or individual CNAs with PD-L1 expression. We found *BAP1* loss to be associated with better OS while loss of *CDKN2A*, *MTAP* and *DMRTA1* along with *CDK6* gain with poorer OS. We found that patients who had both *CDKN2A* loss and *CDK6* gain on FISH did worse than those who had either or none of these aberrations. On endeavouring to validate our copy number results from using FISH, we found good concordance for losses but the concordance for gains was lower.

MPM has lagged behind most other cancers in terms of development of new and effective treatment options. Drastic improvement in outlook seen in some cancers has been illusive in MPM. However, recent clinical studies do suggest a potential to improve outcomes especially with immunotherapeutic modalities and targeted therapy. If immunotherapy and targeted therapy are going to be the innovations most likely to generate effective treatment options for MPM in the near

future, understanding the common genomic changes, the immunological milieu, their interactions and clinicopathological correlates is paramount. During the course of the studies described in the presented thesis, we have been able to shed considerable light on these issues. Our findings have highlighted aspects of MPM micro-environment (especially non-epithelioid histological subtype) that could potentially better direct checkpoint inhibition therapy or combinations thereof. Some genomic changes identified in our analysis could be potentially targetable. We would hope that further continued research into the leads derived from these findings could lead to treatment options that could potentially change MPM from an aggressive incurable malignancy to one that can be reasonably controlled or at some time even cured.

Of the many aspects that set MPM apart from other cancers an important one is the fact there is an avoidable cause in at least 80% of the cases. As such prevention of MPM at least at present seems to be much more realistic goal than its cure. Completely stopping the mining, selling and use of asbestos along with optimum precautions in handling asbestos products in older installations could in the future radically decrease MPM incidence. This would however need great public awareness and strong political will not only in the developed countries but also in the developing economies which continue to buy and use asbestos.

References:

- Roggli VL, Sharma A, Butnor KJ, Sporn T, Vollmer RT. Malignant Mesothelioma and Occupational Exposure to Asbestos : A Clinicopathological Correlation of 1445 Cases. *Ultrastruct Pathol.* 2002 Mar-Apr;26(2):55-65.
2. Rake C, Gilham C, Hatch J, Darnton A, Hodgson J, Peto J. Occupational, domestic and environmental mesothelioma risks in the British population: a case-control study. *Br J Cancer.* 2009;100(7):1175-1183. doi:10.1038/sj.bjc.6604879.
3. Goodman JE, Nascarella MA, Valberg PA. Ionizing radiation: a risk factor for mesothelioma. *Cancer Causes Control.* 2009;20(8):1237-54. doi:10.1007/s10552-009-9357-4.
4. Ortega-Guerrero MA, Carrasco-Núñez G, Barragán-Campos H, Ortega MR. High incidence of lung cancer and malignant mesothelioma linked to erionite fibre exposure in a rural community in Central Mexico. *Occup Environ Med.* 2015;72(3):216-8. doi:10.1136/oemed-2013-101957.
5. Demirer E, Ghattas CF, Radwan MO, Elamin EM. Clinical and Prognostic Features of Erionite-Induced Malignant Mesothelioma. *Yonsei Med J.* 2015 Mar;56(2):311-23. doi:10.3349/ymj.2015.56.2.311.
6. Pershouse MA, Heivly S, Girtsman T. The role of SV40 in malignant mesothelioma and other human malignancies. *Inhal Toxicol.* 2006;18(12):995-1000. doi:10.1080/08958370600835377.
7. Abdul-ghafar MEJ, Seop W, Seung K, Ha Y. No Detection of Simian Virus 40 in Malignant Mesothelioma in Korea. *Korean J Pathol.* 2013 Apr;47(2):124-9. doi:10.4132/KoreanJPathol.2013.47.2.124.
8. Mohammad-taheri Z, Nadji ĀSA, Raisi F. No Association Between Simian Virus 40 and Diffuse Malignant Mesothelioma of the Pleura in Iranian Patients : A Molecular and Epidemiologic Case – Control Study of 60 Patients. *Am J Ind Med.* 2013 Oct;56(10):1221-5. doi:10.1002/ajim.22160.
9. Sekido Y. Molecular pathogenesis of malignant mesothelioma. *Carcinogenesis.* 2013;34(7):1413-9. doi:10.1093/carcin/bgt166.
10. Røe OD, Stella GM. Malignant pleural mesothelioma: history, controversy and future of a manmade epidemic. *Eur Respir Rev.* 2015;24(135):115-131. doi:10.1183/09059180.00007014.
11. Luus K. Asbestos : mining exposure , health effects and policy implications. *McGill J Med.* 2007;10(2):121-126.
12. Ribak J, Lilis R, Suzuki Y, Penner L, Selikoff IJ. Malignant mesothelioma in a cohort of asbestos insulation workers : clinical presentation , diagnosis , and causes of death. *Br J Ind Med.* 1988:182-187.
13. Wagner JC, Sleggs CA, Marchand P. Diffuse pleural mesothelioma and asbestos exposure in the north western cape province. *Br J Ind Med.* 1960:260-271.

14. Virta RL. Asbestos from report of US Geological Survey, Mineral Commodity Services [Internet]. 2010 [cited date accessed 20th May 2017]. Available from https://pubs.usgs.gov/circ/2005/1255/kk/Circ_1255KK.pdf.
15. Health and safety executive. Mesothelioma in Great Britain 2014 - Mesothelioma mortality in Great Britain 1968-2015 [Internet]. 2016 [cited date accessed 25th May 2017]. Available from <http://www.hse.gov.uk/statistics/causdis/mesothelioma/mesothelioma.pdf>.
16. Bianchi C, Bianchi T. Global mesothelioma epidemic: Trend and features. *Indian J Occup Environ Med*. 2014;18(2):82-88. doi:10.4103/0019-5278.146897.
17. Australian Mesothelioma registry. Mesothelioma in Australia 2015- Annual report [Internet]. 2016 [cited date accessed 25th May 2017]. Available from: <https://www.mesothelioma-australia.com/media/12513/mesothelioma-in-2015-final.pdf>
18. Olsen NJ, Franklin PJ, Reid A, et al. Increasing incidence of malignant mesothelioma after exposure to asbestos during home maintenance and renovation. *Med J Aust*. 2011;195(5):271-274. doi:10.5694/mja11.10125.
19. Benedetti S, Nuvoli B, Catalani S, Galati R. Reactive oxygen species a double-edged sword for mesothelioma. *Oncotarget*. 2015 Jul 10;6(19):16848-65.
20. Okayasu R, Takahashi S, Yamada S, Hei TK, Ullrich RL. Advances in Brief Asbestos and DNA Double Strand Breaks . *Cancer Res*. 1999 Jan 15;59(2):298-300.
21. Upadhyay D KD. Asbestos-induced pulmonary toxicity: role of DNA damage and apoptosis. *Exp Biol Med (Maywood)*. 2003;228(6):650-9.
22. Agency for Toxic Substances and Disease Registry. ATSDR Case Studies in Environmental Medicine- Asbestos Toxicity [Internet]. 2018 [cited date accessed 3/03/2018]. Available from: https://www.atsdr.cdc.gov/csem/asbestos_2014/docs/asbestos.pdf
23. Yang H, Bocchetta M, Kroczyńska B, et al. TNF- α inhibits asbestos-induced cytotoxicity via a NF- κ B-dependent pathway , a possible mechanism for asbestos-induced oncogenesis. *Proc Natl Acad Sci* 2006;103(27).10397-402.
24. Carbone M, Yang H. Molecular Pathways : Targeting Mechanisms of Asbestos and Erionite Carcinogenesis in Mesothelioma. *Clin Cancer Res*. 2012 Feb 1;18(3):598-604. doi: 10.1158/1078-0432.CCR-11-2259.
25. Klorin G, Rozenblum E, Glebov O, et al. Integrated high-resolution array CGH and SKY analysis of homozygous deletions and other genomic alterations present in malignant mesothelioma cell lines. *Cancer Genet*. 2013;206(5):191-205. doi:10.1016/j.cancergen.2013.04.006.
26. Hylebos M, Van Camp G, Van Meerbeeck JP, De Beeck KO. The genetic landscape of malignant pleural mesothelioma: Results from massively parallel sequencing. *J Thorac Oncol*. 2016;11(10):1615-1626. doi:10.1016/j.jtho.2016.05.020.
27. Bueno R, De Rienzo A, Dong L, et al. Second generation sequencing of the mesothelioma tumor genome. *PLoS One*. 2010;5(5):e10612. doi:10.1371/journal.pone.0010612.

28. Guo G, Chmielecki J, Goparaju C, et al. Whole-exome sequencing reveals frequent genetic alterations in BAP1, NF2, CDKN2A, and CUL1 in malignant pleural mesothelioma. *Cancer Res.* 2015;75(2):264-9. doi:10.1158/0008-5472.CAN-14-1008.
29. Mäki-Nevala S, Sarhadi VK, Knuutila A, et al. Driver Gene and Novel Mutations in Asbestos-Exposed Lung Adenocarcinoma and Malignant Mesothelioma Detected by Exome Sequencing. *Lung.* 2016;194(1):125-135. doi:10.1007/s00408-015-9814-7.
30. Rodriguez-Paredes M, Martinez de Paz a, Simó-Riudalbas L, et al. Gene amplification of the histone methyltransferase SETDB1 contributes to human lung tumorigenesis. *Oncogene.* 2014;33(21):2807-13. doi:10.1038/onc.2013.239.
31. Kang HC, Kim HK, Lee S, et al. Whole exome and targeted deep sequencing identify genome-wide allelic loss and frequent SETDB1 mutations in malignant pleural mesotheliomas. *Oncotarget.* 2016;7(7):11-14. doi:10.18632/oncotarget.7032.
32. Sugarbaker DJ, Richards WG, Gordon GJ, et al. Transcriptome sequencing of malignant pleural mesothelioma tumors. *Proc Natl Acad Sci U S A.* 2008;105(9):3521-6. doi:10.1073/pnas.0712399105.
33. Lo Iacono M, Monica V, Righi L, et al. Targeted next-generation sequencing of cancer genes in advanced stage malignant pleural mesothelioma: a retrospective study. *J Thorac Oncol.* 2015;10(3):492-9. doi:10.1097/JTO.0000000000000436.
34. Melaiu O, Melissari E, Mutti L, et al. Expression status of candidate genes in mesothelioma tissues and cell lines. *Mutat Res.* 2015;771:6-12. doi:10.1016/j.mrfmmm.2014.11.002.
35. Alkan C, Coe BP, Eichler EE. Genome structural variation discovery and genotyping. *Nat Rev Genet.* 2011 May;12(5):363-76. doi:10.1038/nrg2958.
36. Li W, Olivier M. Current analysis platforms and methods for detecting copy number variation. *Physiol Genomics.* 2013;45(1):1-16. doi:10.1152/physiolgenomics.00082.2012.
37. Ivanov S V, Miller J, Lucito R, et al. Genomic events associated with progression of pleural malignant mesothelioma. *Int J Cancer.* 2009 Feb 1;124(3):589-99. doi:10.1002/ijc.23949.
38. Takeda M, Kasai T, Enomoto Y, et al. Genomic gains and losses in malignant mesothelioma demonstrated by FISH analysis of paraffin-embedded tissues. *J Clin Pathol.* 2012;65(1):77-82. doi:10.1136/jclinpath-2011-200208.
39. Bianchi AB, Mitsunaga SI, Cheng JQ, et al. High frequency of inactivating mutations in the neurofibromatosis type 2 gene (NF2) in primary malignant mesotheliomas. *Proc Natl Acad Sci USA.* 1995 Nov 21;92(24):10854-8.
40. Sekido Y. Inactivation of Merlin in malignant mesothelioma cells and the Hippo signaling cascade dysregulation. *Pathol Int.* 2011;61(6):331-44. doi:10.1111/j.1440-1827.2011.02666.x.
41. Yoshikawa Y, Sato A, Tsujimura T, et al. Frequent inactivation of the BAP1 gene in epithelioid-type malignant mesothelioma. *Cancer Sci.* 2012;103(5):868-74. doi:10.1111/j.1349-7006.2012.02223.x.

42. Harbour JW, Onken MD, Roberson EDO, et al. Frequent mutation of BAP1 in metastasizing uveal melanomas. *Science*. 2010 Dec 3;330(6009):1410-3 doi:10.1126/science.1194472.Frequent.
43. De Assis LVM, Locatelli J, Isoldi MC. The role of key genes and pathways involved in the tumorigenesis of Malignant Mesothelioma. *Biochim Biophys Acta*. 2014;1845(2):232-47. doi:10.1016/j.bbcan.2014.01.008.
44. Zucali P A, Ceresoli GL, De Vincenzo F, et al. Advances in the biology of malignant pleural mesothelioma. *Cancer Treat Rev*. 2011;37(7):543-58. doi:10.1016/j.ctrv.2011.01.001.
45. Prives C and Hall PA. The P53 Pathway. *J. Pathol*. 1999;187:112-126.
46. Stott FJ, Bates S, James MC, et al. The alternative product from the human CDKN2A locus, p14(ARF), participates in a regulatory feedback loop with p53 and MDM2. *EMBO J*. 1998;17(17):5001-5014. doi:10.1093/emboj/17.17.5001.
47. Ladanyi M, Zauderer MG, Krug LM, et al. New strategies in pleural mesothelioma: BAP1 and NF2 as novel targets for therapeutic development and risk assessment. *Clin Cancer Res*. 2012;18(17):4485-4490. doi:10.1158/1078-0432.CCR-11-2375.
48. Ouelle DE, Zindy F, Ashmun R a., Sherr CJ. Alternative reading frames of the INK4a tumor suppressor gene encode two unrelated proteins capable of inducing cell cycle arrest. *Cell*. 1995;83(6):993-1000. doi:10.1016/0092-8674(95)90214-7.
49. Petroski MD, Deshaies RJ. Function and regulation of cullin-RING ubiquitin ligases. *Nat Rev Mol Cell Biol*. 2005;6(1):9-20. doi:10.1038/nrm1547.
50. Dhillon A S, Hagan S, Rath O, Kolch W. MAP kinase signalling pathways in cancer. *Oncogene*. 2007;26(22):3279-90. doi:10.1038/sj.onc.1210421.
51. Tsuruta F, Masuyama N, Gotoh Y. The phosphatidylinositol 3-kinase (PI3K)-Akt pathway suppresses Bax translocation to mitochondria. *J Biol Chem*. 2002;277(16):14040-14047. doi:10.1074/jbc.M108975200.
52. López-Lago M A, Okada T, Murillo MM, Socci N, Giancotti FG. Loss of the tumor suppressor gene NF2, encoding merlin, constitutively activates integrin-dependent mTORC1 signaling. *Mol Cell Biol*. 2009;29(15):4235-49. doi:10.1128/MCB.01578-08.
53. Brims FJ, Lee YCG, Creaney J. The continual search for ideal biomarkers for mesothelioma: the hurdles. *J Thorac Dis*. 2013;5(3):364-6. doi:10.3978/j.issn.2072-1439.2013.04.19.
54. Chernova T, Murphy FA, Galavotti S, et al. Long-Fiber Carbon Nanotubes Replicate Asbestos-Induced Mesothelioma with Disruption of the Tumor Suppressor Gene Cdkn2a (Ink4a / Arf). *Curr Biol*. 2017;27(21):3302-3314.e6. doi:10.1016/j.cub.2017.09.007.
55. Bueno R, Stawiski EW, Goldstein LD, et al. Comprehensive genomic analysis of malignant pleural mesothelioma identifies recurrent mutations, gene fusions and splicing alterations. *Nat Genet*. 2016;(October 2015):1-13. doi:10.1038/ng.3520.

56. Carbone M, Gaudino G, Yang H. Recent insights emerging from malignant mesothelioma genome sequencing. *J Thorac Oncol*. 2015;10(3):409-11. doi:10.1097/JTO.0000000000000466.
57. Altomare DA, Vaslet CA, Skele KL, et al. A mouse model recapitulating molecular features of human mesothelioma. *Cancer Res*. 2005;65(18):8090-5. doi:10.1158/0008-5472.CAN-05-2312.
58. Arzt L, Quehenberger F, Halbwedl I, Mairinger T, Popper HH. BAP1 protein is a progression factor in malignant pleural mesothelioma. *Pathol Oncol Res*. 2014;20(1):145-51. doi:10.1007/s12253-013-9677-2.
59. Szymiczek A, Carbone M, Pastorino S, et al. Inhibition of the spindle assembly checkpoint kinase Mps-1 as a novel therapeutic strategy in malignant mesothelioma. *Oncogene*. 2017 Nov 16;36(46):6501-6507. doi: 10.1038/onc.2017.
60. Husain AN, Colby T, Ordonez N, et al. Guidelines for pathologic diagnosis of malignant mesothelioma: 2012 update of the consensus statement from the International Mesothelioma Interest Group. *Arch Pathol Lab Med*. 2013;137(5):647-667. doi:10.5858/arpa.2012-0214-OA.
61. Arif Q, Husain AN. Malignant mesothelioma diagnosis. *Arch Pathol Lab Med*. 2015;139(8):978-980. doi:10.5858/arpa.2013-0381-RA.
62. John T, Russell PA., Thapa B. Is Mesothelioma in China Rare or Misdiagnosed? *J Thorac Oncol*. 2017;12(4):607-609. doi:10.1016/j.jtho.2017.02.004.
63. Comertpay S, Pastorino S, Tanji M, et al. Evaluation of clonal origin of malignant mesothelioma. *J Transl Med*. 2014 Dec 4;12:301. doi: 10.1186/s12967-014-0301-3.
64. Herrick SE, Mutsaers S. Mesothelial progenitor cells and their potential in tissue engineering. *Int J Biochem Cell Biol*. 2004;36(4):621-42.
65. Rusch VW. A proposed new international TNM staging system for malignant pleural mesothelioma from the International Mesothelioma Interest Group. *Lung Cancer*. 1996;14(1):1-12.
66. Nowak AK, Chansky K, Rice DC, et al. The IASLC Mesothelioma Staging Project: Proposals for Revisions of the T Descriptors in the Forthcoming Eighth Edition of the TNM Classification for Pleural Mesothelioma. *J Thorac Oncol*. 2016;11(12):2089-99.
67. Rice D, Chansky K, Nowak A, et al. The IASLC Mesothelioma Staging Project: Proposals for Revisions of the N Descriptors in the Forthcoming Eighth Edition of the TNM Classification for Pleural Mesothelioma. *J Thorac Oncol*. 2016;11(12):2100-111.
68. Linton a, Pavlakis N, O'Connell R, et al. Factors associated with survival in a large series of patients with malignant pleural mesothelioma in New South Wales. *Br J Cancer*. 2014;111(9):1860-1869. doi:10.1038/bjc.2014.478.

69. Curran D, Sahmoud T, Therasse P, van Meerbeeck J, Postmus PE GG. Prognostic factors in patients with pleural mesothelioma: the European Organization for Research and Treatment of Cancer experience. *J Clin Oncol*. 1998;16(1):145-52.
70. Fennell DA, Parmar A, Shamash J, et al. Statistical validation of the EORTC prognostic model for malignant pleural mesothelioma based on three consecutive phase II trials. *J Clin Oncol*. 2005;23(1):184-9.
71. Edwards JG, Abrams KR, Leverment JN, Spyt TJ, Waller DA, O'Byrne KJ. Prognostic factors for malignant mesothelioma in 142 patients: validation of CALGB and EORTC prognostic scoring systems. *Thorax*. 2000;55(9):731-5. doi:10.1136/thorax.55.9.731.
72. Meniawy TM, Creaney J, Lake RA, Nowak AK. Existing models, but not neutrophil-to-lymphocyte ratio, are prognostic in malignant mesothelioma. *Br J Cancer*. 2013;109(7):1813-20. doi:10.1038/bjc.2013.504.
73. Murphy S, Probert G, Anderson J, Pollock S, Taylor I, Clague H SK. Malignant mesothelioma, hypoalbuminaemia and the effect of carboplatin/pemetrexed on survival. *Clin Oncol Coll Radiol*. 2013;25(12):713-8. doi:doi: 10.1016/j.clon.2013.08.009.
74. Kao SC, Klebe S, Henderson DW, et al. Low Calretinin Expression and High Neutrophil-To-Lymphocyte Ratio Are Poor Prognostic Factors in Patients with Malignant Mesothelioma Undergoing Extrapleural Pneumonectomy. 2011;6(11):1923-9.
75. Kao SCH, Pavlakis N, Harvie R, et al. High blood neutrophil-to-lymphocyte ratio is an indicator of poor prognosis in malignant mesothelioma patients undergoing systemic therapy. *Clin Cancer Res*. 2010;16(23):5805-13. doi:10.1158/1078-0432.CCR-10-2245.
76. Kao SC, Lee K, Armstrong NJ, et al. Validation of tissue microarray technology in malignant pleural mesothelioma. *Pathology*. 2011;43(2):128-32. doi:10.1097/PAT.0b013e328342016c.
77. Kao SC, Vardy J, Chatfield M, et al. Validation of prognostic factors in malignant pleural mesothelioma: a retrospective analysis of data from patients seeking compensation from the New South Wales Dust Diseases Board. *Clin Lung Cancer*. 2013;14(1):70-7. doi:10.1016/j.clcc.2012.03.011.
78. Cedrés S, Montero MA, Martinez P, et al. Exploratory analysis of activation of PTEN-PI3K pathway and downstream proteins in malignant pleural mesothelioma (MPM). *Lung Cancer*. 2012;77(1):192-8.
79. Pinato DJ, Mauri FA., Ramakrishnan R, Wahab L, Lloyd T, Sharma R. Inflammation-Based Prognostic Indices in Malignant Pleural Mesothelioma. *J Thorac Oncol*. 2012;7(3):587-594. doi:10.1097/JTO.0b013e31823f45c1.
80. Meniawy TM, Creaney J, Lake RA, Nowak AK. Existing models, but not neutrophil-to-lymphocyte ratio, are prognostic in malignant mesothelioma. *Br J Cancer*. 2013;109(7):1813-1820. doi:10.1038/bjc.2013.504.
81. Chen N, Liu S, Huang L, Li W, Yang W, Cong T. Prognostic significance of neutrophil-to-lymphocyte ratio in patients with malignant pleural mesothelioma : a meta-analysis. *Oncotarget*. 2017 Feb 16;8(34):57460-57469. doi: 10.18632/oncotarget.15404.

82. Pass HI. Biomarkers and prognostic factors for mesothelioma. *Ann Cardiothorac Surg*. 2012;1(4):449-56. doi:10.3978/j.issn.2225-319X.2012.10.04.
83. Gordon GJ, Jensen RV, Hsiao LL, et al. Using gene expression ratios to predict outcome among patients with mesothelioma. *J Natl Cancer Inst*. 2003;95(8):595-605.
84. Gordon GJ, Dong L, Yeap BY, et al. Four-gene expression ratio test for survival in patients undergoing surgery for mesothelioma. *J Natl Cancer Inst*. 2009;101(9):678-86.
85. Pass HI, Liu Z, Wali A, et al. Gene expression profiles predict survival and progression of pleural mesothelioma. *Clin Cancer Res*. 2004;10(3):849-59.
86. López-Ríos F, Chuai S, Flores R, et al. Global gene expression profiling of pleural mesotheliomas: Overexpression of aurora kinases and P16/CDKN2A deletion as prognostic factors and critical evaluation of microarray-based prognostic prediction. *Cancer Res*. 2006;66(6):2970-2979. doi:10.1158/0008-5472.CAN-05-3907.
87. Farzin M, Toon CW, Clarkson A, et al. Loss of expression of BAP1 predicts longer survival in mesothelioma. *Pathology*. 2015;47(4):302-307. doi:10.1097/PAT.0000000000000250.
88. Cigognetti M, Lonardi S, Fisogni S, et al. BAP1 (BRCA1-associated protein 1) is a highly specific marker for differentiating mesothelioma from reactive mesothelial proliferations. *Mod Pathol*. 2015;28(8):1043-1057. doi:10.1038/modpathol.2015.65.
89. McGregor SM, Dunning R, Hyjek E, Vigneswaran W, Husain AN, Krausz T. BAP1 facilitates diagnostic objectivity, classification, and prognostication in malignant pleural mesothelioma. *Hum Pathol*. 2015;46(11):1670-1678. doi:10.1016/j.humpath.2015.06.024.
90. Zauderer MG, Bott M, McMillan R, et al. Clinical characteristics of patients with malignant pleural mesothelioma harboring somatic BAP1 mutations. *J Thorac Oncol*. 2013;8(11):1430-3. doi:10.1097/JTO.0b013e31829e7ef9.
91. Kobayashi N, Toyooka S, Yanai H, Soh J, et al. Frequent p16 inactivation by homozygous deletion or methylation is associated with a poor prognosis in Japanese patients with pleural mesothelioma. *Lung Cancer*. 2008;62(1):120-5.
92. Dacic S, Kothmaier H, Land S, et al. Prognostic significance of p16/cdkn2a loss in pleural malignant mesotheliomas. *Virchows Arch*. 2008;453(6):627-35. doi:10.1007/s00428-008-0689-3.
93. Cao C, Tian D, Manganas C, Matthews P, Yan TD. Systematic review of trimodality therapy for patients with malignant pleural mesothelioma. *Ann Cardiothorac Surg*. 2012;1(4):428-37. doi:10.3978/j.issn.2225-319X.2012.11.07.
94. Rintoul RC, Ritchie AJ, Edwards JG, et al. Efficacy and cost of video-assisted thoracoscopic partial pleurectomy versus talc pleurodesis in patients with malignant pleural mesothelioma (MesoVATS): an open-label, randomised, controlled trial. *Lancet*. 2014;384(9948):1118-27.
95. Flores RM, Pass HI, Seshan VE, et al. Extrapleural pneumonectomy versus pleurectomy/decortication in the surgical management of malignant pleural mesothelioma:

- results in 663 patients. *J Thorac Cardiovasc Surg.* 2008;135(3):620-6, 626.e1-3. doi:10.1016/j.jtcvs.2007.10.054.
96. Kostron A, Friess M, Inci I, et al. Propensity matched comparison of extrapleural pneumonectomy and pleurectomy/decortication for mesothelioma patients†. *Interact Cardiovasc Thorac Surg.* 2017;25(5):740-6.
 97. Wolf AS FR. Current Treatment of Mesothelioma: Extrapleural Pneumonectomy Versus Pleurectomy/Decortication. *Thorac Surg Clin.* 2016;26(3):359.
 98. Sharif S, Zahid I, Routledge T, Scarci M. Extrapleural pneumonectomy or supportive care: treatment of malignant pleural mesothelioma? *Interact Cardiovasc Thorac Surg.* 2011;12(6):1040-5. doi:10.1510/icvts.2010.256289.
 99. Treasure T, Waller D, Tan C, et al. The Mesothelioma and Radical Surgery Randomized. *J Thorac Oncol.* 2009 Oct;4(10):1254-8.
 100. Treasure T, Lang-Lazdunski L, Waller D, et al. Extra-pleural pneumonectomy versus no extra-pleural pneumonectomy for patients with malignant pleural mesothelioma: clinical outcomes of the Mesothelioma and Radical Surgery (MARS) randomised feasibility study. *Lancet Oncol.* 2011;12(8):763-72. doi:10.1016/S1470-2045(11)70149-8.
 101. Rusch V, Baldini EH, Bueno R, et al. The role of surgical cytoreduction in the treatment of malignant pleural mesothelioma: Meeting summary of the International Mesothelioma Interest Group Congress, September 11-14, 2012, Boston, Mass. *J Thorac Cardiovasc Surg.* 2013;145(4):909-910. doi:10.1016/j.jtcvs.2013.01.039.
 102. Waller DA, Dawson AG. Randomized controlled trials in malignant pleural mesothelioma surgery — mistakes made and lessons learned. *Ann Transl Med.* 2017 Jun;5(11):240. doi:10.21037/atm.2017.04.05.
 103. Cho BCJ, Feld R, Leigh N, et al. A Feasibility Study Evaluating Surgery for Mesothelioma After Radiation Therapy: The “SMART” Approach for Resectable Malignant Pleural Mesothelioma. *J Thorac Oncol.* 2014;9(3):397-402. doi:10.1097/JTO.0000000000000078.
 104. Van Zandwijk N, Clarke C, Henderson D, et al. Guidelines for the diagnosis and treatment of malignant pleural mesothelioma. *J Thorac Dis.* 2013;5(6). doi:10.3978/j.issn.2072-1439.2013.11.28.
 105. Rusch VW, Rosenzweig K, Venkatraman E, et al. A phase II trial of surgical resection and adjuvant highdose hemithoracic radiation for malignant pleural mesothelioma. *J Thorac Cardiovasc Surg.* 2001;122(4):788-795. doi:10.1067/mtc.2001.116560.
 106. Baldini H. Radiation therapy options for malignant pleural mesothelioma. *Semin Thorac Cardiovasc Surg.* 2009;21(2):159-63.
 107. Di Salvo M, Gambaro G, Pagella S, Manfreda I, Casadio C KM. Prevention of malignant seeding at drain sites after invasive procedures (surgery and/or thoracoscopy) by hypofractionated radiotherapy in patients with pleural mesothelioma. *Acta Oncol.* 2008;47(6):1094-8.

108. Bovolato P, Casadio C, Bille a, et al. Does surgery improve survival of patients with malignant pleural mesothelioma?: A multicenter retrospective analysis of 1365 consecutive patients. *J Thorac Oncol.* 2014;9(3):390-396. doi:10.1097/JTO.000000000000064.
109. Blomberg C, Nilsson J, Holgersson G, et al. Randomized Trials of Systemic Medically-treated Malignant Mesothelioma: A Systematic Review. *Anticancer Res.* 2015;35(5):2493-501..
110. Kondola S, Manners D NA. Malignant pleural mesothelioma: an update on diagnosis and treatment options. *Ther Adv Respir Dis.* 2016;10(3):275-88. doi:10.1177/1753465816628800.
111. Vogelzang NJ, Rusthoven JJ, Symanowski J, et al. Phase III study of pemetrexed in combination with cisplatin versus cisplatin alone in patients with malignant pleural mesothelioma. *J Clin Oncol.* 2003;21(14):2636-44.
112. Krug LM. An overview of chemotherapy for mesothelioma. *Hematol Oncol Clin North Am.* 2005;19(6):1117-36.
113. Zalcman G, Mazieres J, Margery J, et al. Bevacizumab for newly diagnosed pleural mesothelioma in the Mesothelioma Avastin Cisplatin Pemetrexed Study (MAPS): A randomised, controlled, open-label, phase 3 trial. *Lancet.* 2015;6736(15):1-10. doi:10.1016/S0140-6736(15)01238-6.
114. Katirtzoglou N, Gkiozos I, Makrilia N, et al. Carboplatin plus pemetrexed as first-line treatment of patients with malignant pleural mesothelioma: a phase II study. *Clin Lung Cancer.* 2010;11(1):30-5.
115. Arrieta O, López-Macías D, Mendoza-García VO, et al. A phase II trial of prolonged, continuous infusion of low-dose gemcitabine plus cisplatin in patients with advanced malignant pleural mesothelioma. *Cancer Chemother Pharmacol.* 2014;73(5):975-82. doi:10.1007/s00280-014-2429-5.
116. Santoro A, O'Brien ME, Stahel R a, et al. Pemetrexed Plus Cisplatin or Pemetrexed Plus Carboplatin for Chemo-naïve Patients with Malignant Pleural Mesothelioma: Results of the International Expanded Access Program. *J Thorac Oncol.* 2008;3(7):756-763. doi:10.1097/JTO.0b013e31817c73d6.
117. Bonelli MA, Fumarola C, La Monica S, Alfieri R. New therapeutic strategies for malignant pleural mesothelioma. *Biochem Pharmacol.* 2016;123:8-18. doi:10.1016/j.bcp.2016.07.012.
118. Lafave LM, Béguelin W, Koche R, et al. Loss of BAP1 function leads to EZH2-dependent transformation. *Nat Med.* 2015 Nov;21(11):1344-9. doi: 10.1038/nm.3947.
119. Kemp CD, Rao M, Xi S, et al. Polycomb Repressor Complex-2 Is a Novel Target for Mesothelioma Therapy. *Clin Cancer Res.* 2012 Jan 1;18(1):77-90. doi: 10.1158/1078-0432.CCR-11-0962.
120. Lim S, Chen XL, Lim Y, et al. Article Nuclear FAK Promotes Cell Proliferation and Survival through FERM-Enhanced p53 Degradation. *Mol Cell.* 2008 Jan 18;29(1):9-22. doi: 10.1016/j.molcel.2007.11.031.

121. Gabarra-Niecko V, Schaller MD, Dunty JM. FAK regulates biological processes important for the pathogenesis of cancer. *Cancer Metastasis Rev.* 2003;22(4):359-74.
122. Ding Q, Grammer JR, Nelson MA, Guan J, Stewart JE, Gladson CL. p27 Kip1 and Cyclin D1 Are Necessary for Focal Adhesion Kinase Regulation of Cell Cycle Progression in Glioblastoma Cells Propagated in Vitro and in Vivo in the Scid Mouse Brain *. *J Biol Chem.* 2005 Feb 25;280(8):6802-15. doi:10.1074/jbc.M409180200.
123. Golubovskaya VM, Finch R, Zheng M, Kurenova EV, Cance WG. The 7-amino-acid site in the proline-rich region of the N-terminal domain of p53 is involved in the interaction with FAK and is critical for p53 functioning. *Biochem J.* 2008;411(1):151-60.
124. Melkounian ZK, Peng X, Gan B, Wu X, Guan J. Mechanism of Cell Cycle Regulation by FIP200 in Human Breast Cancer Cells. *Cancer Res.* 2005 Aug 1;65(15):6676-84.
125. Poulidakos PI, Xiao GH, Gallagher R, Jablonski S, Jhanwar SC, Testa JR. Re-expression of the tumor suppressor NF2/merlin inhibits invasiveness in mesothelioma cells and negatively regulates FAK. *Oncogene.* 2006;25(44):5960-8.
126. Ou W, Lu M, Eilers G, et al. Co-targeting of FAK and MDM2 triggers additive anti-proliferative effects in mesothelioma via a coordinated reactivation of p53. *Br J Cancer.* 2016;115(10):1253-63. doi:10.1038/bjc.2016.331.
127. Shapiro IM, Kolev VN, Vidal CM, et al. Merlin deficiency predicts FAK inhibitor sensitivity: a synthetic lethal relationship. *Sci Transl Med.* 2014;6(237):237ra68.
128. Iyer G, Hanrahan AJ, Milowsky MI, et al. Genome sequencing identifies a basis for everolimus sensitivity. *Science.* 2012;338(6104):221.
129. Li W, You L, Cooper J, et al. Merlin / NF2 Suppresses Tumorigenesis by Inhibiting the E3 Ubiquitin Ligase CRL4 DCAF1 in the Nucleus. *Cell.* 2010;140(4):477-490. doi:10.1016/j.cell.2010.01.029.
130. Soucy TA, Smith PG, Milhollen MA, et al. An inhibitor of NEDD8-activating enzyme as a new approach to treat cancer. *Nature.* 2009;458(7239):732-6.
131. Cooper J, Xu Q, Zhou L, et al. Combined Inhibition of NEDD8-Activating Enzyme and mTOR Suppresses NF2 Loss – Driven Tumorigenesis. *Mol Cancer Ther.* 2017;16(8):1693-1704. doi:10.1158/1535-7163.MCT-16-0821.
132. Sarantopoulos J, Shapiro GI, Cohen RB, et al. Phase I Study of the Investigational NEDD8-Activating Enzyme Inhibitor Pevonedistat (TAK-924 / MLN4924) in Patients with Advanced Solid Tumors. *Clin Cancer Res.* 2016 Feb 15;22(4):847-57. doi: 10.1158/1078-0432.CCR-15-1338.
133. Ou SH, Moon J, Garland LL, et al. SWOG S0722 : Phase II Study of mTOR Inhibitor. *J Thorac Oncol.* 2015;10(2):387-391. doi:10.1097/JTO.0000000000000360.
134. Pache J-C, Janssen YMW, Walsh ES, et al. Increased epidermal growth factor-receptor protein in a human mesothelial cell line in response to long asbestos fibers. *Am J Pathol.* 1998;152(2):333-40.

135. Garland LL, Rankin C, Gandara DR, et al. Phase II study of erlotinib in patients with malignant pleural mesothelioma: a Southwest Oncology Group Study. *J Clin Oncol*. 2007;25(17):2406-13. doi:10.1200/JCO.2006.09.7634.
136. Govindan R, Kratzke RA, Herndon JE, et al. Gefitinib in patients with malignant mesothelioma: a phase II study by the Cancer and Leukemia Group B. *Clin Cancer Res*. 2005;11(6):2300-4. doi:10.1158/1078-0432.CCR-04-1940.
137. Barbieri F, Würth R, Favoni RE, et al. Receptor tyrosine kinase inhibitors and cytotoxic drugs affect pleural mesothelioma cell proliferation: Insight into EGFR and ERK1/2 as antitumor targets. *Biochem Pharmacol*. 2011;82(10):1467-1477. doi:10.1016/j.bcp.2011.07.073.
138. Kalra N, Zhang J, Yu Y, et al. Efficacy of anti-insulin-like growth factor I receptor monoclonal antibody cixutumumab in mesothelioma is highly correlated with insulin growth factor-I receptor sites/cell. *Int J Cancer*. 2012;131(9):2143-2152. doi:10.1002/ijc.27471.
139. Kanteti R, Dhanasingh I, Kawada I, et al. Met and PI3K/mTOR as a potential combinatorial therapeutic target in malignant pleural mesothelioma. *PLoS One*. 2014;9(9):1-16. doi:10.1371/journal.pone.0105919.
140. Hassan R, Bera T, Pastan I. Mesothelin : A New Target for Immunotherapy Mesothelin. *Clin Cancer Res*. 2004;10(301):3937-3942. doi:10.1158/1078-0432.CCR-03-0801.
141. Servais EL, Colovos C, Rodriguez L, et al. Mesothelin overexpression promotes mesothelioma cell invasion and MMP-9 secretion in an orthotopic mouse model and in epithelioid pleural mesothelioma patients. *Clin Cancer Res*. 2012;18(9):2478-2489. doi:10.1158/1078-0432.CCR-11-2614.
142. Hassan R, Kindler HL, Jahan T, et al. Phase II clinical trial of amatuximab, a chimeric antimesothelin antibody with pemetrexed and cisplatin in advanced unresectable pleural mesothelioma. *Clin Cancer Res*. 2014;20(23):5927-5936. doi:10.1158/1078-0432.CCR-14-0804.
143. Gol S, Kopitz C, Kahnert A, et al. Anetumab Ravtansine : A Novel Mesothelin-Targeting Antibody – Drug Conjugate Cures Tumors with Heterogeneous Target Expression Favored by Bystander Effect. *Mol Cancer Ther*. 2014;13(6):1537-1548. doi:10.1158/1535-7163.MCT-13-0926.
144. Hassan R, Sharon E, Thomas A, et al. Phase 1 study of the antimesothelin immunotoxin SS1P in combination with pemetrexed and cisplatin for front-line therapy of pleural mesothelioma and correlation of tumor response with serum mesothelin, megakaryocyte potentiating factor, and cancer antigen. *Cancer*. 2014;120(21):3311-3319. doi:10.1002/cncr.28875.
145. Zhang X, Tang N, Rishi AK, Pass HI, Wali A. Methylation profile landscape in mesothelioma: possible implications in early detection, disease progression, and therapeutic options. *Methods Mol Biol*. 2015;1238:235-47.
146. Vandermeers F, Neelature Sriramareddy S, Costa C, Hubaux R, Cosse JP, Williams L. The role of epigenetics in malignant pleural mesothelioma. *Lung Cancer*. 2013;81(3):311-8.

147. Mcloughlin KC, Kaufman AS, Schrupp DS. Targeting the epigenome in malignant pleural mesothelioma. *Transl Lung Cancer Res.* 2017 Jun;6(3):350-365. doi: 10.21037/tlcr.2017.06.06.
148. Pathania R, Ramachandran S, Elangovan S, et al. DNMT1 is essential for mammary and cancer stem cell maintenance and tumorigenesis. *Nat Commun.* 2015;6:1-11. doi:10.1038/ncomms7910.
149. Yogelzang NJ, Herndon JE 2nd, Cirrincione C, et al. Dihydro-5-azacytidine in malignant mesothelioma. A phase II trial demonstrating activity accompanied by cardiac toxicity. Cancer and Leukemia Group B. *Cancer.* 1997;79(11):2237-42.
150. Schrupp DS, Fischette MR, Nguyen DM, et al. Cancer Therapy : Clinical Phase I Study of Decitabine-Mediated Gene Expression in Patients with Cancers Involving the Lungs , Esophagus , or Pleura. *Clin Cancer Res.* 2006 Oct 1;12(19):5777-85.
151. Krug LM, Kindler HL, Calvert H, et al. Vorinostat in patients with advanced malignant pleural mesothelioma who have progressed on previous chemotherapy (VANTAGE-014): a phase 3, double-blind, randomised, placebo-controlled trial. *Lancet Oncol.* 2015;16(4):447-56.
152. Wolff F, Leisch M, Greil R, Risch A, Pleyer L. The double-edged sword of (re) expression of genes by hypomethylating agents : from viral mimicry to exploitation as priming agents for targeted immune checkpoint modulation. *Cell Commun Signal.* 2017 Mar 31;15(1):13. doi: 10.1186/s12964-017-0168-z.
153. Covre A, Coral S, Nicolay H, et al. Antitumor activity of epigenetic immunomodulation combined with CTLA-4 blockade in syngeneic mouse models Antitumor activity of epigenetic immunomodulation combined with CTLA-4 blockade in syngeneic mouse models. *Oncoimmunology.* 2015 Apr 2;4(8):e1019978.
154. Peng D, Kryczek I, Nagarsheth N, et al. Epigenetic silencing of TH1-type chemokines shapes tumour immunity and immunotherapy. *Nature.* 2015;527(7577):249-53.
155. Kim K, Skora AD, Li Z, et al. Eradication of metastatic mouse cancers resistant to immune checkpoint blockade by suppression of myeloid-derived cells. *Proc Natl Acad Sci U S A.* 2014 Aug 12;111(32):11774-9. doi: 10.1073/pnas.1410626111.
156. Husson A, Brasse-Lagnel C, Fairand A, Renouf S, Lavionne A. Argininosuccinate synthetase from the urea cycle to the citrulline-NO cycle. *Eur J Biochem.* 2003;270(9):1887-99.
157. Rabinovich S, Adler L, Yizhak K, et al. Diversion of aspartate in ASS1-deficient tumours fosters de novo pyrimidine synthesis. *Nature.* 2015;527(7578):379-83.
158. Huang H, Wu W, Wang Y, Wang J, Fang F, Tsai J. ASS1 as a Novel Tumor Suppressor Gene in Myxofibrosarcomas : Aberrant Loss via Epigenetic DNA Methylation Confers Aggressive Phenotypes , Negative Prognostic Impact , and Therapeutic Relevance. *Clin Cancer Res.* 2013;2861-2873. doi:10.1158/1078-0432.CCR-12-2641.
159. Ensor CM, Holtsberg FW, Bomalaski JS, Clark MA. Pegylated Arginine Deiminase (ADI-SS PEG 20 , 000 mw) Inhibits Human Melanomas and Hepatocellular Carcinomas in Vitro and in Vivo. *Cancer Res.* 2002 Oct 1;62(19):5443-50.

160. Cheng PN, Lam T, Lam W, et al. Inhibits the In vitro and In vivo Proliferation of Human Hepatocellular Carcinoma through Arginine Depletion. *Cancer Res.* 2007 Jan 1;67(1):309-17.
161. Izzo F, Marra P, Beneduce G, et al. Pegylated arginine deiminase treatment of patients with unresectable hepatocellular carcinoma: results from phase I/II studies. *J Clin Oncol.* 2004;22(10):1815-22.
162. Ascierto PA, Scala S, Castello G, et al. Pegylated arginine deiminase treatment of patients with metastatic melanoma: results from phase I and II studies. *J Clin Oncol.* 2005;23(30):7660-8.
163. Szlosarek PW, Klabatsa A, Pallaska A, et al. Cancer Therapy : Preclinical In vivo Loss of Expression of Argininosuccinate Synthetase in Malignant Pleural Mesothelioma Is a Biomarker for Susceptibility to Arginine Depletion. *Clin Cancer Res.* 2006 Dec 1;12(23):7126-31.
164. Szlosarek PW, Steele JP, Nolan L, et al. Arginine Deprivation With Pegylated Arginine Deiminase in Patients With Argininosuccinate Synthetase 1–Deficient Malignant Pleural Mesothelioma A Randomized Clinical Trial. *JAMA Oncol.* 2017 Jan 1;3(1):58-66. doi: 10.1001/jamaoncol.2016.3049.
165. Beddowes E, Spicer J, Chan PY, et al. Phase 1 Dose-Escalation Study of Pegylated Arginine Deiminase, Cisplatin, and Pemetrexed in Patients With Argininosuccinate Synthetase 1-Deficient Thoracic Cancers. *J Clin Oncol.* 2017;36(16):1778-85.
166. Thapa B, Watkins DN and JohnT. Immunotherapy for malignant mesothelioma: reality check. *Expert Rev Anticancer Ther.* 2016;Oct:1-10.
167. Calabrò L, Morra A, Fonsatti E, et al. Tremelimumab for patients with chemotherapy-resistant advanced malignant mesothelioma: an open-label, single-arm, phase 2 trial. *Lancet Oncol.* 2013;14(11):1104-11. doi:10.1016/S1470-2045(13)70381-4.
168. Calabrò L, Morra A, Fonsatti E, et al. Efficacy and safety of an intensified schedule of tremelimumab for chemotherapy-resistant malignant mesothelioma: an open-label, single-arm, phase 2 study. *Lancet Respir Med.* 2015;3(4):301-9. doi:10.1016/S2213-2600(15)00092-2.
169. Kindler HL, Scherpereel A, Calabrò L, et al. Tremelimumab as second- or third-line treatment of unresectable malignant mesothelioma (MM): Results from the global, double-blind, placebo-controlled DETERMINE study. *J Clin Oncol.* 2016;34(suppl):abstr 8502.
170. Alley EW, Molife LR, Santoro A, et al. Clinical safety and efficacy of pembrolizumab (MK-3475) in patients with malignant pleural mesothelioma: Preliminary results from KEYNOTE-028 [Abstract]. In: *Proceedings of the 106th Annual Meeting of the American Association for Cancer Research; 2015 Apr 18-22; Philadelphia(PA): AACR; 2015.* Abstract nr CT103.
171. Quispel-Janssen J, Zimmerman M, Buikhuisen W, Burgers S, Zago G BP. Nivolumab in malignant pleural mesothelioma (NIVOMES): An interim analysis. In: *13TH INTERNATIONAL CONFERENCE OF THE INTERNATIONAL MESOTHELIOMA INTEREST GROUP; 2016 May 1-4; Birmingham: iMig;2016.* Abstract nr Available at: <http://imig2016.org/wp-content/uploads/2016/04/iMig-2016-Abstract-Book.pdf>.

172. Hassan R, Thomas A, Patel MR, et al. Avelumab (MSB0010718C; anti-PD-L1) in patients with advanced unresectable mesothelioma from the JAVELIN solid tumor phase Ib trial: Safety, clinical activity, and PD-L1 expression. *J Clin Oncol*. 2016;34(suppl):abstr 8503
173. Mahoney KM, Atkins MB. Prognostic and predictive markers for the new immunotherapies. *Oncology*. 2014;28(Suppl 3):39-48.
174. Larkin J, Chiarion-Sileni V, Gonzalez R, et al. Combined Nivolumab and Ipilimumab or Monotherapy in Untreated Melanoma. *N Engl J Med*. 2015;373(1):23-34. doi:10.1056/NEJMoa1504030.
175. Hammers HJ, Plimack ER, Rini BI, et al. Expanded cohort results from CheckMate 016: A phase I study of nivolumab in combination with ipilimumab in metastatic renal cell carcinoma (mRCC). *J Clin Oncol* 33,2015 (suppl; abstr 4516)
79. Rizvi NA, Gettinger SN, Goldman JW, et al. Safety and Efficacy of First-Line Nivolumab (NIVO; Anti-Programmed Death-1 [PD-1]) and Ipilimumab in Non-Small Cell Lung Cancer (NSCLC). *J Thorac Oncol*;10(suppl2):p S176
177. Luana Calabro, Aldo Morra, Diana Giannarelli, Giovanni Amato, Erica Bertocci AD. Tremelimumab in combination with durvalumab in first or second-line mesothelioma patients: Safety analysis from the phase II NIBIT-MESO-1 study. *J Clin Oncol*. 2017;35(15_suppl):8558-8.
178. Arnaud Scherpereel, Julien Mazieres, Laurent Greillier, Pascal Dô, Olivier Bylicki IM. Second- or third-line nivolumab (Nivo) versus nivo plus ipilimumab (Ipi) in malignant pleural mesothelioma (MPM) patients: Results of the IFCT-1501 MAPS2 randomized phase II trial. *J Clin Oncol* 35,. 2017;35(18_suppl).
179. Jiang H, Hegde S, Knolhoff BL, et al. Targeting focal adhesion kinase renders pancreatic cancers responsive to checkpoint immunotherapy. *Nat Med*. 2016;22(8):851-60.
180. Symeonides SN, Anderton SM, Serrels A. FAK-inhibition opens the door to checkpoint immunotherapy in Pancreatic Cancer. *J Immunother Cancer*. 2017 Feb 21;5:17. doi: 10.1186/s40425-017-0217-6.
181. Jenkins RW, Barbie DA, Flaherty KT. Mechanisms of resistance to immune checkpoint inhibitors. *Br J Cancer*. 2018;118(1):9-16. doi:10.1038/bjc.2017.434.
182. Daille R, Roberti P, Yamazaki T, et al. in Cancer : Tumor-Intrinsic and -Extrinsic Factors. *Immunity*. 2016 Jun 21;44(6):1255-69. doi: 10.1016/j.immuni.2016.06.001.
183. Sharma P, Hu-lieskovan S, Wargo JA, Ribas A. Primary , Adaptive , and Acquired Resistance to Cancer Immunotherapy. *Cell*. 2017;168(4):707-723. doi:10.1016/j.cell.2017.01.017.
184. O'Donnell JS, Long GV, Scolyer RA, Teng MW, Smyth MJ. Resistance to PD1/PDL1 checkpoint inhibition. *Cancer Treat Rev*. 2017;52:71-81.
185. Turner EH, Ng SB, Nickerson DA SJ. Methods for genomic partitioning. *Annu Rev Genomics Hum Genet*. 2009.

186. Wang Y, Moorhead M, Karlin-Neumann G, et al. Analysis of molecular inversion probe performance for allele copy number determination. *Genome Biol.* 2007;8(11):R246. doi:10.1186/gb-2007-8-11-r246.
187. Hardenbol P, Banér J, Jain M, et al. Multiplexed genotyping with sequence-tagged molecular inversion probes. *Nat Biotechnol.* 2003;21(6):673-8. doi:10.1038/nbt821.
188. Jung H-S, Lefferts J a, Tsongalis GJ. Utilization of the oncoscan microarray assay in cancer diagnostics. *Appl Can Res.* 2017:1-8. doi:10.1186/s41241-016-0007-3.
189. Wang Y, Carlton VEH, Karlin-Neumann G, et al. High quality copy number and genotype data from FFPE samples using Molecular Inversion Probe (MIP) microarrays. *BMC Med Genomics.* 2009;2:8. doi:10.1186/1755-8794-2-8.
190. Loo P Van, Nordgard SH, Lingjærde OC, et al. Allele-specific copy number analysis of tumors. *Proc Natl Acad Sci.* 2010;107(39):16910-16915. doi:10.1073/pnas.1009843107.
191. Song S, Nones K, Miller D, et al. qpure: A Tool to Estimate Tumor Cellularity from Genome-Wide Single-Nucleotide Polymorphism Profiles. *PLoS One.* 2012;7(9):5-11. doi:10.1371/journal.pone.0045835.
192. Harrow J, Frankish A, Gonzalez JM, Frazer K a. GENCODE : The reference human genome annotation for The ENCODE Project. 2012:1760-1774. doi:10.1101/gr.135350.111.
193. Mermel CH, Schumacher SE, Hill B, Meyerson ML, Beroukheim R, Getz G. GISTIC2.0 facilitates sensitive and confident localization of the targets of focal somatic copy-number alteration in human cancers. *Genome Biol.* 2011;12(4):R41. doi:10.1186/gb-2011-12-4-r41.
194. Agostinis P, Berg K, Cengel KA, et al. Photodynamic therapy of cancer: an update. *CA Cancer J Clin.* 2011 Jul-Aug;61(4):250-81. doi: 10.3322/caac.20114.
195. Merritt N, Blewett CJ, Miller JD, Bennett WF, Young JE UJ. Survival after conservative (palliative) management of pleural malignant mesothelioma. *J Surg Oncol.* 2001;78(3):171-4.
196. Sugarbaker DJ, Richards WG BR. Extrapleural pneumonectomy in the treatment of epithelioid malignant pleural mesothelioma: novel prognostic implications of combined N1 and N2 nodal involvement based on experience in 529 patients. *Ann Surg.* 2014;260(4):577-80. doi:10.1097/SLA.0000000000000903.
197. Wolf AS FR. Current Treatment of Mesothelioma: Extrapleural Pneumonectomy Versus Pleurectomy/Decortication. *Thorac surg Clin.* 2016;26(3):359-75. doi:10.1016/j.thorsurg.2016.04.003.
198. Zahid I, Sharif S, Routledge T, Scarci M. Is pleurectomy and decortication superior to palliative care in the treatment of malignant pleural mesothelioma? *Interact Cardiovasc Thorac Surg.* 2011;12(5):812-7. doi:10.1510/icvts.2010.256271.
199. Munck C, Mordon SR, Scherpereel A, Porte H, Dhalluin X, Betrouni N. Intrapleural photodynamic therapy for mesothelioma: What place and which future? *Ann Thorac Surg.* 2015;99(6):2237-2245. doi:10.1016/j.athoracsur.2014.12.077.

200. Schouwink H, Rutgers ET, van der Sijp J, Oppelaar H, van Zandwijk N, van Veen R, Burgers S, Stewart FA, Zoetmulder F BP. Intraoperative photodynamic therapy after pleuropneumonectomy in patients with malignant pleural mesothelioma: dose finding and toxicity results. *Chest*. 2001;120(4):1167-74.
201. Pass HI, Delaney TF, Tochner Z, et al. Intrapleural Photodynamic Therapy : Results of a Phase I Trial. 1993;1(1):28-37.
202. Takita H, Mang TS, Loewen GM, Antkowiak JG, Raghavan D, Grajek JR DT. Takita H, Mang TS, Loewen GM. Operation and intracavitary photodynamic therapy for malignant pleural mesothelioma: a phase II study. *Ann Thorac Surg*. 1994;58(4):995-8.
203. Moskal TL, Dougherty TJ, Urschel JD, et al. Operation and Photodynamic Therapy for Pleural Mesothelioma : 6-Year Follow-up. 1998;4975(98):0-5.
204. Friedberg JS, Mick R, Stevenson J, Metz J, Zhu T, Buyske J, Serman DH, Pass HI, Glatstein E HS. A phase I study of Foscan-mediated photodynamic therapy and surgery in patients with mesothelioma. *Ann Thorac Surg*. 2003;75(3):952-9.
205. Friedberg JS, Mick R, Culligan M, et al. Photodynamic therapy and the evolution of a lung-sparing surgical treatment for mesothelioma. *Ann Thorac Surg*. 2011;91(6):1738-45. doi:10.1016/j.athoracsur.2011.02.062.
206. Bellera C a, MacGrogan G, Debled M, de Lara CT, Brouste V, Mathoulin-Pélissier S. Variables with time-varying effects and the Cox model: some statistical concepts illustrated with a prognostic factor study in breast cancer. *BMC Med Res Methodol*. 2010;10:20. doi:10.1186/1471-2288-10-20.
207. Klebe S, Brownlee NA, Mahar A, et al. Sarcomatoid mesothelioma : a clinical – pathologic correlation of 326 cases. *Mod Pathol*. 2010;23(3):470-479. doi:10.1038/modpathol.2009.180.
208. Righi L, Cavallo MC, Gatti G, et al. Tumor/stromal caveolin-1 expression patterns in pleural mesothelioma define a subgroup of the epithelial histotype with poorer prognosis. *Am J Clin Pathol*. 2014;141(6):816-27. doi:10.1309/AJCP0F6WYBXGVDHX.
209. Li D, Wang B, Long H, Wen F. Diagnostic Accuracy of Calretinin for Malignant Mesothelioma in Serous Effusions: a Meta-analysis. *Sci Rep*. 2015;5:9507. doi:10.1038/srep09507.
210. Yaziji H, Battifora H, Barry TS, et al. Evaluation of 12 antibodies for distinguishing epithelioid mesothelioma from adenocarcinoma: identification of a three-antibody immunohistochemical panel with maximal sensitivity and specificity. *Mod Pathol*. 2006;19:514-523. doi:10.1038/modpathol.3800534.
211. Powell G RH& RWR. Expression of calretinin by breast carcinoma and the potential for misdiagnosis of mesothelioma. *Histopathology*. 2011;59(5):950-956. doi:10.1111/j.1365-2559.2011.04031.x.
212. Comin CE, Novelli L, Cavazza A, Rotellini M, Cianchi F ML. Expression of thrombomodulin, calretinin, cytokeratin 5/6, D2-40 and WT-1 in a series of primary carcinomas of the lung: an immunohistochemical study in comparison with epithelioid pleural mesothelioma. *Tumori*. 2014;100(5):559-67. doi:10.1700/1660.18182.

213. NG O. Value of calretinin immunostaining in differentiating epithelial mesothelioma from lung adenocarcinoma. *Mod Pathol.* 1998;11(10):929-33.
214. Lucas DR, Pass HI, Madan SK, Adsay NV, Wali A, Tabaczka P LF. Sarcomatoid mesothelioma and its histological mimics: a comparative immunohistochemical study. *Histopathology.* 2003;42(3):270-3.
215. Amatya VJ, Takeshima Y, Kohno H, et al. Caveolin-1 is a novel immunohistochemical marker to differentiate epithelioid mesothelioma from lung adenocarcinoma. *Histopathology.* 2009;55(1):10-9. doi:10.1111/j.1365-2559.2009.03322.x.
216. Trimmer C, Sotgia F, Whitaker-Menezes D, et al. Caveolin-1 and mitochondrial SOD2 (MnSOD) function as tumor suppressors in the stromal microenvironment. *Cancer Biol Ther.* 2014;11(4):383-394. doi:10.4161/cbt.11.4.14101.
217. Goetz JG, Minguet S, Navarro-Lérida I, et al. Biomechanical remodeling of the microenvironment by stromal caveolin-1 favors tumor invasion and metastasis. *Cell.* 2011;146(1):148-63. doi:10.1016/j.cell.2011.05.040.
218. Cassoni P, Daniele L, Maldi E, et al. Caveolin-1 expression in lung carcinoma varies according to tumour histotype and is acquired de novo in brain metastases. *Histopathology.* 2009;55(1):20-7. doi:10.1111/j.1365-2559.2009.03326.x.
219. Steffens S, Schrader AJ, Blasig H, et al. Caveolin 1 protein expression in renal cell carcinoma predicts survival. *BMC Urol.* 2011;11(1):25. doi:10.1186/1471-2490-11-25.
220. Chanvorachote P, Pongrakhananon V, Halim H. Caveolin-1 regulates metastatic behaviors of anoikis resistant lung cancer cells. *Mol Cell Biochem.* 2015;399(1-2):291-302. doi:10.1007/s11010-014-2255-4.
221. Rossi S, Poliani PL, Missale C, Monti E, Fanzani A. Caveolins in rhabdomyosarcoma. *J Cell Mol Med.* 2011;15(12):2553-2568. doi:10.1111/j.1582-4934.2011.01364.x.
222. Sáinz-jaspeado M, Martín-liberal J, Lagares-tena L, Mateo- S, Garcia X, Tirado OM. Caveolin-1 in sarcomas : friend or foe ? *Oncotarget.* 2011;2(4):305-312.
223. Takeshima, Yukio; Inai, Kouki; Ishikawa, Yuichi; Oka T, Hiroshima K. The trial of differentiation grading of epithelioid mesothelioma with reference to its clinicopathological significance. In: *International Mesothelioma Interest Group Meeting.* Kyoto; 2010:175.
224. Thapa B, Walkiewicz M, Murone C, et al. Calretinin but not caveolin-1 correlates with tumour histology and survival in malignant mesothelioma. *Pathology.* 2016;48(7):660-65. doi:10.1016/j.pathol.2016.08.003.
225. Anwar SL, Wahyono A, Aryandono T, Samuel J. Caveolin-1 in Breast Cancer : Single Molecule Regulation of Multiple Key Signaling Pathways. *Asian Pac J Cancer Prev.* 2015;16:6803-6812.
226. Simpkins SA, Hanby AM, Holliday DL, Speirs V. Clinical and functional significance of loss of caveolin-1 expression in breast cancer-associated fibroblasts. *J Pathol.* 2012;227(4):490-498. doi:10.1002/path.4034.

227. Rozali EN, Hato SV, Robinson BW, Lake RA, Lesterhuis WJ. Programmed death ligand 2 in cancer-induced immune suppression. *Clin Dev Immunol*. 2012;2012. doi:10.1155/2012/656340.
228. Matsuzaki H, Maeda M, Lee S, et al. Asbestos-induced cellular and molecular alteration of immunocompetent cells and their relationship with chronic inflammation and carcinogenesis. *J Biomed Biotechnol*. 2012;2012:492608. doi:10.1155/2012/492608.
229. Bononi A, Napolitano A, Pass HI, Yang H, Napolitano A. Latest developments in our understanding of the pathogenesis of mesothelioma and the design of targeted therapies. *Expert Rev Respir Med*. 2015 Oct;9(5):633-54.. doi:10.1586/17476348.2015.1081066.
230. Anraku M, Cunningham KS, Yun Z, et al. Impact of tumor-infiltrating T cells on survival in patients with malignant pleural mesothelioma. *J Thorac Cardiovasc Surg*. 2008;135(4):823-9. doi:10.1016/j.jtcvs.2007.10.026.
231. Jackaman C, Cornwall S, Lew AM, Zhan Y, Robinson BWS, Nelson DJ. Local effector failure in mesothelioma is not mediated by CD4+ CD25+ T-regulator cells. *Eur Respir J*. 2009;34(1):162-75. doi:10.1183/09031936.00101008.
232. Robinson BWS, Robinson C, Lake RA. Localised spontaneous regression in mesothelioma — possible immunological mechanism. *Lung Cancer*. 2001;32:197-201.
233. Pilling JE, Nicholson AG, Harmer C, Goldstraw P. Prolonged survival due to spontaneous regression and surgical excision of malignant mesothelioma. *Ann Thorac Surg*. 2007;83(1):314-5. doi:10.1016/j.athoracsur.2006.05.070.
234. Donnem T, Hald SM, Paulsen E-E, et al. Stromal CD8+ T-cell Density—A Promising Supplement to TNM Staging in Non-Small Cell Lung Cancer. *Clin Cancer Res*. 2015;21(11):2635-43. doi:10.1158/1078-0432.CCR-14-1905.
235. Rizvi NA, Hellmann MD, Snyder A, et al. Cancer immunology. Mutational landscape determines sensitivity to PD-1 blockade in non-small cell lung cancer. *Science (80-)*. 2015;348(6230):124-8.
236. Snyder A, Makarov V, Merghoub T, et al. Genetic Basis for Clinical Response to CTLA-4 Blockade in Melanoma. *N Engl J Med*. 2014;2189-2199. doi:10.1056/NEJMoa1406498.
237. Manson G, Norwood J, Marabelle A, Kohrt H, Houot R. Biomarkers Associated with Checkpoint Inhibitors. *Ann Oncol*. 2016;33(0):1-8. doi:10.1093/annonc/mdw181.
238. Gibney GT, Weiner LM, Atkins MB. Predictive biomarkers for checkpoint inhibitor-based immunotherapy. *Lancet Oncol*. 2016;17(12):e542-e551. doi:10.1016/S1470-2045(16)30406-5.
239. Topalian SL, Hodi FS, Brahmer JR, et al. Safety, Activity, and Immune Correlates of Anti-PD-1 Antibody in Cancer. *N Engl J Med*. 2012;366(26):2443-2454. doi:10.1056/NEJMoa1200690.
240. Taube JM, Anders RA, Young GD, et al. Colocalization of inflammatory response with B7-h1 expression in human melanocytic lesions supports an adaptive resistance mechanism of immune escape. *Sci Transl Med*. 2012;4(127):127-37.

241. Garon EB, Rizvi NA, Hui R, et al. Pembrolizumab for the Treatment of Non-Small-Cell Lung Cancer. *N Engl J Med*. 2015. doi:10.1056/NEJMoa1501824.
242. Borghaei H, Paz-Ares L, Horn L, et al. Nivolumab versus Docetaxel in Advanced Nonsquamous Non-Small-Cell Lung Cancer. *N Engl J Med*. 2015;373(17):1627-39. doi:10.1056/NEJMoa1507643.
243. Muro K, Chung HC, Shankaran V GR, et al. Pembrolizumab for patients with PD-L1-positive advanced gastric cancer (KEYNOTE-012): a multicentre, open-label, phase 1b trial. *Lancet Oncol*. 2016;17(6):717-726.
244. Powles T, Eder JP, Fine GD, et al. MPDL3280A (anti-PD-L1) treatment leads to clinical activity in metastatic bladder cancer. *Nature*. 2014;515(7528):558-62. doi:doi: 10.1038/nature13904.
245. Weber JS, Kudchadkar RR, Yu B, et al. Safety, efficacy, and biomarkers of nivolumab with vaccine in ipilimumab-refractory or -naive melanoma. *J Clin Oncol*. 2013;31(34):4311-4318. doi:10.1200/JCO.2013.51.4802.
246. Weber JS, D'Angelo SP, Minor D, et al. Nivolumab versus chemotherapy in patients with advanced melanoma who progressed after anti-CTLA-4 treatment (CheckMate 037): a randomised, controlled, open-label, phase 3 trial. *Lancet Oncol*. 2015;16(4):375-84.
247. Motzer RJ, Rini BI, McDermott DF, et al. Nivolumab for metastatic renal cell carcinoma: Results of a randomized phase II trial. *J Clin Oncol*. 2015;33(13):1430-1437. doi:10.1200/JCO.2014.59.0703.
248. Robert C, Long G V., Brady B, et al. Nivolumab in previously untreated melanoma without BRAF mutation. *N Engl J Med*. 2015;372(4):320-30. doi:10.1056/NEJMoa1412082.
249. Herbst RS, Soria J-C, Kowanetz M, et al. Predictive correlates of response to the anti-PD-L1 antibody MPDL3280A in cancer patients. *Nature*. 2014;515(7528):563-567. doi:10.1038/nature14011.
250. Sasada T, Suekane S. Variation of tumor-infiltrating lymphocytes in human cancers : controversy on clinical significance. *Immunotherapy*. 2011;3:1235-1251.
251. Mlecnik B, Tosolini M, Kirilovsky A, et al. Histopathologic-based prognostic factors of colorectal cancers are associated with the state of the local immune reaction. *J Clin Oncol*. 2011;29(6):610-618. doi:10.1200/JCO.2010.30.5425.
252. Galon J, Costes A, Sanchez-Cabo F, et al. Type, density, and location of immune cells within human colorectal tumors predict clinical outcome. *Science (80-)*. 2006;313(5795):1960-4.
253. Shah W, Yan X, Jing L, Zhou Y, Chen H, Wang Y. A reversed CD4/CD8 ratio of tumor-infiltrating lymphocytes and a high percentage of CD4+FOXP3+ regulatory T cells are significantly associated with clinical outcome in squamous cell carcinoma of the cervix. *Cell Mol Immunol*. 2010;8(1):59-66. doi:10.1038/cmi.2010.56.
254. Yamada N, Oizumi S, Kikuchi E, et al. CD8+ tumor-infiltrating lymphocytes predict favorable prognosis in malignant pleural mesothelioma after resection. *Cancer Immunol Immunother*. 2010;59(10):1543-9. doi:10.1007/s00262-010-0881-6.

255. Gajewski TF, Schreiber H, Fu Y-X. Innate and adaptive immune cells in the tumor microenvironment. *Nat Immunol*. 2013;14(10):1014-22. doi:10.1038/ni.2703.
256. Tumeh PC, Harview CL, Yearley JH, et al. PD-1 blockade induces responses by inhibiting adaptive immune resistance. *Nature*. 2014;515(7528):568-71. doi:10.1038/nature13954.
257. Chen PL, Roh W, Reuben A, et al. Analysis of immune signatures in longitudinal tumor samples yields insight into biomarkers of response and mechanisms of resistance to immune checkpoint blockade. *Cancer Discov*. 2016;6(8):827-837. doi:10.1158/2159-8290.CD-15-1545.
258. Hamid O, Schmidt H, Nissan A, et al. A prospective phase II trial exploring the association between tumor microenvironment biomarkers and clinical activity of ipilimumab in advanced melanoma. *J Transl Med*. 2011;9(90404):204. doi:10.1186/1479-5876-9-204.
259. Taube JM, Klein A, Brahmer JR, et al. Association of PD-1, PD-1 Ligands, and Other Features of the Tumor Immune Microenvironment with Response to Anti-PD-1 Therapy. *Clin Cancer Res*. 2014;20(19):5064-5074. doi:10.1158/1078-0432.CCR-13-3271.
260. Francisco LM, Salinas VH, Brown KE, et al. PD-L1 regulates the development, maintenance, and function of induced regulatory T cells. *J Exp Med*. 2009;206(13):3015-29. doi:10.1084/jem.20090847.
261. Hou J, Yu Z, Xiang R, et al. Correlation between infiltration of FOXP3+ regulatory T cells and expression of B7-H1 in the tumor tissues of gastric cancer. *Exp Mol Pathol*. 2014;96(3):284-91. doi:10.1016/j.yexmp.2014.03.005.
262. Currie AJ, Prosser A, McDonnell A, et al. Dual control of antitumor CD8 T cells through the programmed death-1/programmed death-ligand 1 pathway and immunosuppressive CD4 T cells: regulation and counterregulation. *J Immunol*. 2009;183(12):7898-908. doi:10.4049/jimmunol.0901060.
263. Cedrés S, Ponce-Aix S, Zugazagoitia J, et al. Analysis of expression of programmed cell death 1 ligand 1 (PD-L1) in malignant pleural mesothelioma (MPM). *PLoS One*. 2015;10(3):e0121071. doi:10.1371/journal.pone.0121071.
264. Mansfield AS, Roden AC, Peikert T, Sheinin YM. B7-H1 Expression in Malignant Pleural Mesothelioma is Associated with Sarcomatoid Histology and Poor Prognosis. 2014;9(7):1036-1040.
265. Combaz-Lair C, Galateau-Sallé F, McLeer-Florin a., et al. Immune biomarkers PD-1/PD-L1 and TLR3 in malignant pleural mesotheliomas. *Hum Pathol*. 2016;52:9-18. doi:10.1016/j.humpath.2016.01.010.
266. Alley EW, Lopez J, Santoro A, Morosky A, Saraf, B. Piperdi SJ. Long-Term Overall Survival for Patients with Malignant Pleural Mesothelioma on Pembrolizumab Enrolled in KEYNOTE-028. In: *17th World Conference on Lung Cancer*. Vienna: IASLC; 2016.
267. Quispel-Janssen, Josine Zago, Guilia Schouten, Robert Buikhuisen, Wieneke Monkhorst, Kim Thunissen, Eric Baas P. A phase II study of Nivolumab in malignant pleural mesothelioma (NIVOMES): With translational research (TR) biopsies. In: *World Conference on Lung Cancer*. International Association of study of Lung Cancer; 2016:S149.

268. Kindler, H, Theodore CT, Yi-Hung R, et al. Phase II trial of Pembrolizumab in patients with malignant mesothelioma (MM): Interim analysis. In: *World Conference on Lung Cancer*. International Association of study of Lung Cancer; 2016:S149.
269. Thapa B, Salcedo A, Lin X, et al. The Immune Microenvironment, Genome-wide Copy Number Aberrations, and Survival in Mesothelioma. *J Thorac Oncol*. 2017;28:pil: S1556-0864(17)30124-7. doi:10.1016/j.jtho.2017.02.013..
270. Ameratunga M, Asadi K, Lin X, et al. PD-L1 and Tumor Infiltrating Lymphocytes as Prognostic Markers in Resected NSCLC. *PLoS One*. 2016;11(4):e0153954. doi:10.1371/journal.pone.0153954.
271. Garcia-Rojo M, Sanchez J, de la Santa E, et al. Automated image analysis in the study of lymphocyte subpopulation in eosinophilic oesophagitis. *Diagn Pathol*. 2014;9 Suppl 1(Suppl 1):S7. doi:10.1186/1746-1596-9-S1-S7.
272. Momtaz P. Immunologic checkpoints in cancer therapy : focus on the programmed death-1 (PD-1) receptor pathway. *Pharmgenomics Pers Med*. 2014;7:357-365.
273. Hamid O, Carvajal RD. Anti-programmed death-1 and anti-programmed death-ligand 1 antibodies in cancer therapy. *Expert Opin Biol Ther*. 2013;13(6):847-861.
274. Bigelow E, Bever KM, Xu H, et al. Immunohistochemical staining of B7-H1 (PD-L1) on paraffin-embedded slides of pancreatic adenocarcinoma tissue. *J Vis Exp*. 2013;1(71):1-6. doi:10.3791/4059
275. Unitt E, Marshall A, Gelson W, et al. Tumour lymphocytic infiltrate and recurrence of hepatocellular carcinoma following liver transplantation. *J Hepatol*. 2006;45(2):246-253. doi:10.1016/j.jhep.2005.12.027.
276. Freeman GJ, Long AJ, Iwai Y, et al. Engagement of the PD-1 Immunoinhibitory Receptor by a Novel B7 Family Member Leads to Negative Regulation of Lymphocyte Activation. *J Exp Med*. 2000;192(7).
277. Brahmer JR, Tykodi SS, Chow LQ, et al. Safety and Activity of Anti-PD-L1 Antibody in Patients with Advanced Cancer. *N Engl J Med*. 2012:2455-2465.
278. Zhang Y, Kang S, Shen J, et al. Prognostic significance of programmed cell death 1 (PD-1) or PD-1 ligand 1 (PD-L1) Expression in epithelial-originated cancer: a meta-analysis. *Medicine (Baltimore)*. 2015;94(6):e515. doi:10.1097/MD.0000000000000515.
279. Donnem T, Hald SM, Paulsen E-E, et al. Stromal CD8+ T-cell Density—A Promising Supplement to TNM Staging in Non-Small Cell Lung Cancer. *Clin Cancer Res*. 2015;21(11):2635-43. doi:10.1158/1078-0432.CCR-14-1905.
280. Mahalingam D, Brumlik MJ, Waehler R, Curiel DT, Curiel TJ. Cancer Immunotherapy. *Science*. 2013;342(December):377-396. doi:10.1007/978-1-4614-4732-0.
281. Attia P, Phan GQ, Maker A V., et al. Autoimmunity correlates with tumor regression in patients with metastatic melanoma treated with anti-cytotoxic T-lymphocyte antigen-4. *J Clin Oncol*. 2005;23(25):6043-6053. doi:10.1200/JCO.2005.06.205.

282. Robert C, Thomas L, Bondarenko I, et al. Ipilimumab plus dacarbazine for previously untreated metastatic melanoma. *N Engl J Med*. 2011;364(26):2517-2526. doi:10.1056/NEJMoa1104621.
283. Topalian SL, Sznol M, McDermott DF, et al. Survival, durable tumor remission, and long-term safety in patients with advanced melanoma receiving nivolumab. *J Clin Oncol*. 2014;32(10):1020-1030. doi:10.1200/JCO.2013.53.0105.
284. Lipson EJ, Sharfman WH, Drake CG, et al. Durable cancer regression off-treatment and effective reinduction therapy with an anti-PD-1 antibody. *Clin Cancer Res*. 2013;19(2):462-468. doi:10.1158/1078-0432.CCR-12-2625.
285. Hamid O, Robert C, Daud A, et al. Safety and tumor responses with lambrolizumab (anti-PD-1) in melanoma. *N Engl J Med*. 2013;369(2):134-44. doi:10.1056/NEJMoa1305133.
286. Brahmer JR, Tykodi SS, Chow LQM, et al. Safety and activity of anti-PD-L1 antibody in patients with advanced cancer. *N Engl J Med*. 2012;366(26):2455-65. doi:10.1056/NEJMoa1200694.
287. Pico de Coaña Y, Choudhury A, Kiessling R. Checkpoint blockade for cancer therapy: Revitalizing a suppressed immune system. *Trends Mol Med*. 2015;21(8):482-491. doi:10.1016/j.molmed.2015.05.005.
288. Marcq E, Pauwels P, van Meerbeeck JP, Smits ELJ. Targeting immune checkpoints: New opportunity for mesothelioma treatment? *Cancer Treat Rev*. 2015:1-11. doi:10.1016/j.ctrv.2015.09.006.
289. Ohigashi Y, Sho M, Yamada Y, et al. Clinical Significance of Programmed Death-1Ligand-1 and Programmed Death-1Ligand-2 Expression in Human Esophageal Cancer. *Clin Cancer Res*. 2005;11(17):2947-2953. doi:10.1158/1078-0432.CCR-04-1469290.
290. Jung H II, Jeong D, Ji S, et al. Overexpression of PD-L1 and PD-L2 is Associated with Poor Prognosis in Patients with Hepatocellular Carcinoma. *Cancer Res Treat*. 2016:1-9. doi:10.4143/crt.2016.066.
291. Hamanishi J, Mandai M, Iwasaki M, et al. Programmed cell death 1 ligand 1 and tumor-infiltrating CD8+ T lymphocytes are prognostic factors of human ovarian cancer. *Proc Natl Acad Sci*. 2007;104(9):3360-3365. doi:10.1073/pnas.0611533104.
292. Gao Q, Wang XY, Qiu SJ, et al. Overexpression of PD-L1 significantly associates with tumor aggressiveness and postoperative recurrence in human hepatocellular carcinoma. *Clin Cancer Res*. 2009;15(3):971-979. doi:10.1158/1078-0432.CCR-08-1608.
293. Kim MY, Koh J, Kim S, Go H, Jeon YK, Chung DH. Clinicopathological analysis of PD-L1 and PD-L2 expression in pulmonary squamous cell carcinoma: Comparison with tumor-infiltrating T cells and the status of oncogenic drivers. *Lung Cancer*. 2015;88(1):24-33. doi:10.1016/j.lungcan.2015.01.016.
294. Kim S, Kim MY, Koh J, et al. Programmed death-1 ligand 1 and 2 are highly expressed in pleomorphic carcinomas of the lung: Comparison of sarcomatous and carcinomatous areas. *Eur J Cancer*. 2015;51(17):2698-2707. doi:10.1016/j.ejca.2015.08.013.

295. Monney L, Sabatos CA, Gaglia JL, et al. Th1-specific cell surface protein Tim-3 regulates macrophage activation and severity of an autoimmune disease. *Nature*. 2002;415(6871):536-541. doi:10.1038/415536a.
296. Zhu C, Anderson AC, Schubart A, et al. The Tim-3 ligand galectin-9 negatively regulates T helper type 1 immunity. *Nat Immunol*. 2005;6(12):1245-1252. doi:10.1038/ni1271.
297. Sakuishi K, Apetoh L, Sullivan JM, Blazar BR, Kuchroo VK, Anderson AC. Targeting Tim-3 and PD-1 pathways to reverse T cell exhaustion and restore anti-tumor immunity. *J Exp Med*. 2010;207(10):2187-2194. doi:10.1084/jem.20100643.
298. Zhou Q, Munger ME, Veenstra RG, et al. Coexpression of Tim-3 and PD-1 identifies a CD8+ T-cell exhaustion phenotype in mice with disseminated acute myelogenous leukemia. *Blood*. 2011;117(17):4501-4510. doi:10.1182/blood-2010-10-310425.
299. Fourcade J, Sun Z, Benallaoua M, et al. Upregulation of Tim-3 and PD-1 expression is associated with tumor antigen-specific CD8 + T cell dysfunction in melanoma patients. *J Exp Med*. 2010;207(10):2175-2186. doi:10.1084/jem.20100637.
300. Gao X, Zhu Y, Li G, et al. TIM-3 expression characterizes regulatory T cells in tumor tissues and is associated with lung cancer progression. *PLoS One*. 2012;7(2):1-8. doi:10.1371/journal.pone.0030676.
301. Yan J, Zhang Y, Zhang J-P, Liang J, Li L, Zheng L. Tim-3 expression defines regulatory T cells in human tumors. *PLoS One*. 2013;8(3):e58006. doi:10.1371/journal.pone.0058006.
302. Dardalhon V, Anderson AC, Karman J, et al. Tim-3/galectin-9 pathway: regulation of Th1 immunity through promotion of CD11b+Ly-6G+ myeloid cells. *J Immunol*. 2010;185(3):1383-92. doi:10.4049/jimmunol.0903275.
303. Chiba S, Baghdadi M, Akiba H, et al. Tumor-infiltrating DCs suppress nucleic acid-mediated innate immune responses through interactions between the receptor TIM-3 and the alarmin HMGB1. *Nat Immunol*. 2012;13(9):832-42. doi:10.1038/ni.2376.
304. Ngiow SF, Von Scheidt B, Akiba H, Yagita H, Teng MWL, Smyth MJ. Anti-TIM3 antibody promotes T cell IFN- γ -mediated antitumor immunity and suppresses established tumors. *Cancer Res*. 2011;71(10):3540-3551. doi:10.1158/0008-5472.CAN-11-0096.
305. Anderson AC. Tim-3: An Emerging Target in the Cancer Immunotherapy Landscape. *Cancer Immunol Res*. 2014;2(5):393-398. doi:10.1158/2326-6066.CIR-14-0039.
306. Sabatos CA, Chakravarti S, Cha E, et al. Interaction of Tim-3 and Tim-3 ligand regulates T helper type 1 responses and induction of peripheral tolerance. *Nat Immunol*. 2003;4(11):1102-1110. doi:10.1038/ni988.
307. Waterhouse P, Penninger JM, Timms E, et al. Lymphoproliferative disorders with early lethality in mice deficient in Ctl α -4. *Science (80-)*. 1995;270(5238):985-8.
308. Nishimura H, Nose M, Hiai H, Minato N, Honjo T. Development of lupus-like autoimmune diseases by disruption of the PD-1 gene encoding an ITIM motif-carrying immunoreceptor. *Immunity*. 1999;11(2):141-151. doi:10.1016/S1074-7613(00)80089-8.

309. Awad MM, Jones RE, Liu H, et al. Cytotoxic T Cells in PD-L1-Positive Malignant Pleural Mesotheliomas Are Counterbalanced by Distinct Immunosuppressive Factors. *Cancer Immunol Res.* 2016;4(December):1-12. doi:10.1158/2326-6066.CIR-16-0171.
310. Marcq, Elly Siozopoulou, Vasiliki De Waele, et al. Characterization of the Tumor Microenvironment and Investigation of Immune Checkpoint Expression in Malignant Pleural Mesothelioma. In: *World Conference on Lung Cancer*. Vienna: International Association of study of Lung Cancer; 2016:S129.
311. Workman CJ, Rice DS, Dugger KJ, Kurschner C, Vignali DA. Phenotypic analysis of the murine CD4-related glycoprotein, CD223 (LAG-3). *Eur J Cancer.* 2002;223:1-9.
312. Sierro S, Romero P SD. The CD4-like molecule LAG-3, biology and therapeutic applications. *Expert Opin Ther Targets.* 2011;15(1):91-101. doi:10.1517/14712598.2011.540563.
313. Wherry EJ, Ha SJ, Kaech SM, et al. Molecular Signature of CD8+ T Cell Exhaustion during Chronic Viral Infection. *Immunity.* 2007;27(4):670-684. doi:10.1016/j.immuni.2007.09.006
314. Nguyen LT, Ohashi PS. Clinical blockade of PD1 and LAG3 — potential mechanisms of action. *Nat Rev Immunol.* 2014;15(1):45-56. doi:10.1038/nri3790.
315. Matsuzaki J, Gnjatic S, Mhawech-Fauceglia P, et al. Tumor-infiltrating NY-ESO-1-specific CD8+ T cells are negatively regulated by LAG-3 and PD-1 in human ovarian cancer. *Proc Natl Acad Sci U S A.* 2010;107(17):7875-7880. doi:10.1073/pnas.1003345107.
316. Baitsch L, Baumgaertner P, Devevre E, et al. Exhaustion of tumour-specific CD8+ T cells in metastases from melanoma patients. *J Clin Invest.* 2011;121(6):2350-2360. doi:10.1172/JCI46102DS1.
317. Grosso JF, Kelleher CC, Harris TJ, et al. LAG-3 regulates CD8+ T cell accumulation and effector function in murine self and tumor-tolerance systems. *J Clin Invest.* 2007;117(11):3383-3392. doi:10.1172/JCI31184DS1.
318. Woo SR, Turnis ME, Goldberg M V., et al. Immune inhibitory molecules LAG-3 and PD-1 synergistically regulate T-cell function to promote tumoral immune escape. *Cancer Res.* 2012;72(4):917-927. doi:10.1158/0008-5472.CAN-11-1620.
319. Goding SR, Wilson KA, Xie Y, et al. Restoring immune function of tumor-specific CD4+ T cells during recurrence of melanoma. *J Immunol.* 2013;190(9):4899-909. doi:10.4049/jimmunol.1300271.
320. Melancon MP, Lu W, Huang Q, et al. Targeted imaging of tumor-associated M2 macrophages using a macromolecular contrast agent PG-Gd-NIR813. *Biomaterials.* 2010;31(25):6567-6573. doi:10.1016/j.biomaterials.2010.05.001.
321. Hemon P, Jean-Louis F, Ramgolam K, et al. MHC class II engagement by its ligand LAG-3 (CD223) contributes to melanoma resistance to apoptosis. *J Immunol.* 2011;186(9):5173-5183. doi:10.4049/jimmunol.1002050.

322. Estornes Y, Toscano F, Virard F, et al. dsRNA induces apoptosis through an atypical death complex associating TLR3 to caspase-8. *Cell Death Differ.* 2012;19(9):1482-94. doi:10.1038/cdd.2012.22.
323. Salaun B, Coste I, Rissoan M-C, Lebecque SJ, Renno T. TLR3 Can Directly Trigger Apoptosis in Human Cancer Cells. *J Immunol.* 2006;176(8):4894-4901. doi:10.4049/jimmunol.176.8.4894.
324. Wang R-F, Miyahara Y, Wang HY. Toll-like receptors and immune regulation: implications for cancer therapy. *Oncogene.* 2008;27:181-189. doi:10.1038/sj.onc.1210906.
325. Vercammen E, Staal J, Beyaert R. Sensing of viral infection and activation of innate immunity by toll-like receptor 3. *Clin Microbiol Rev.* 2008;21(1):13-25. doi:10.1128/CMR.00022-07.
326. Salaun B, Zitvogel L, Asselin-Paturel C, et al. TLR3 as a biomarker for the therapeutic efficacy of double-stranded RNA in breast cancer. *Cancer Res.* 2011;71(5):1607-1614. doi:10.1158/0008-5472.CAN-10-3490.
327. Gonzalez-Reyes S, Fernandez JM, Gonzalez LO, et al. Study of TLR3, TLR4, and TLR9 in prostate carcinomas and their association with biochemical recurrence. *Cancer Immunol Immunother.* 2011;60(2):217-226. doi:10.1007/s00262-010-0931-0.
328. Rydberg C, Månsson A, Uddman R, Riesbeck K, Cardell LO. Toll-like receptor agonists induce inflammation and cell death in a model of head and neck squamous cell carcinomas. *Immunology.* 2009;128(1 PART 2). doi:10.1111/j.1365-2567.2008.03041.x.
329. Boes M, Meyer-Wentrup F. TLR3 triggering regulates PD-L1 (CD274) expression in human neuroblastoma cells. *Cancer Lett.* 2015;361(1):49-56. doi:10.1016/j.canlet.2015.02.027.
330. Schalper KA, Velcheti V, Carvajal D, et al. In situ tumor PD-L1 mRNA expression is associated with increased tils and better outcome in breast carcinomas. *Clin Cancer Res.* 2014;20(10):2773-2782. doi:10.1158/1078-0432.CCR-13-2702.
331. Tian T, Ruan M, Yang W, et al. Evaluation of the prognostic value of tumor-infiltrating lymphocytes in triple-negative breast cancers. *Oncotarget.* 2016;7(28):44395-44405. doi:10.18632/oncotarget.10054.
332. Di Caro G, Bergomas F, Grizzi F, et al. Occurrence of tertiary lymphoid tissue is associated with T-cell infiltration and predicts better prognosis in early-stage colorectal cancers. *Clin Cancer Res.* 2014;20(8):2147-2158. doi:10.1158/1078-0432.CCR-13-2590.
333. Piersma SJ, Jordanova ES, Van Poelgeest MIE, et al. High number of intraepithelial CD8+ tumor-infiltrating lymphocytes is associated with the absence of lymph node metastases in patients with large early-stage cervical cancer. *Cancer Res.* 2007;67(1):354-361. doi:10.1158/0008-5472.CAN-06-3388.
334. Brambilla E, Le Teuff G, Marguet S, et al. Prognostic effect of tumor lymphocytic infiltration in resectable non-small-cell lung cancer. *J Clin Oncol.* 2016;34(11):1223-1230. doi:10.1200/JCO.2015.63.0970.
335. Salgado R, Denkert C, Campbell C, et al. Tumor-Infiltrating Lymphocytes and Associations With Pathological Complete Response and Event-Free Survival in HER2-Positive Early-Stage

- Breast Cancer Treated With Lapatinib and Trastuzumab: A Secondary Analysis of the NeoALTTO Trial. *JAMA Oncol.* 2015;1(4):448-454. doi:10.1001/jamaoncol.2015.0830.
336. Dieu-Nosjean MC, Giraldo N A, Kaplon H, Germain C, Fridman WH, Sauts-Fridman C. Tertiary lymphoid structures, drivers of the anti-tumor responses in human cancers. *Immunol Rev.* 2016;271(1):260-275. doi:10.1111/imr.12405.
337. Yu P, Lee Y, Liu W, Chin RK, et al. Priming of naive T cells inside tumors leads to eradication of established tumors. *Nat Immunol.* 2004;5(2):141-9.
338. Lutz ER, Wu A, Bigelow E, et al. Immunotherapy Converts Nonimmunogenic Pancreatic Tumors into Immunogenic Foci of Immune Regulation. *Cancer Immunol Res.* 2014;2(7):616-631. doi:10.1158/2326-6066.CIR-14-0027.
339. Maldonado L, Teague JE, Morrow MP, Jotova I, Wu TC, Wang C, Desmarais C, Boyer JD, Tycko B, Robins HS, Clark RA TC. Intramuscular therapeutic vaccination targeting HPV16 induces T cell responses that localize in mucosal lesions. *Sci Transl Med.* 2014;JAN 29;6(221):221RA13.
340. Sridharan V, Gjini E, Liao X, et al. Immune Profiling of Adenoid Cystic Carcinoma: PD-L2 Expression and Associations with Tumor-Infiltrating Lymphocytes. *Cancer Immunol Res.* 2016;(33):679-688. doi:10.1158/2326-6066.CIR-16-0031.
341. Baksh K, Weber J. Immune checkpoint protein inhibition for cancer: Preclinical justification for CTLA-4 and PD-1 blockade and new combinations. *Semin Oncol.* 2015;42(3):363-377. doi:10.1053/j.seminoncol.2015.02.015.
342. Goldberg SB. PD-1 and PD-L1 Inhibitors : Activity as Single Agents and Potential Biomarkers in Non-Small Cell Lung Cancer. *Immunotherapy.* 2015;11(9):10-13.
343. H.L. Kindler, T. Karrison, Y.C. Tan, B. Rose, M.I. Ahmad, C.M. Straus, R.M. Sargis TS. Phase II Trial of Pembrolizumab in Patients with Malignant Mesothelioma (MM): Interim Analysis. In: *17th World Conference on Lung Cancer.*; 2016.
344. Pardoll DM. The blockade of immune checkpoints in cancer immunotherapy. *Nat Rev Cancer.* 2012;12(4):252-264. doi:10.1038/nrc3239.
345. Noy R, Pollard JW. Tumor-associated macrophages : from mechanisms to therapy. *Immunity.* 2015;41(1):49-61. doi:10.1016/j.immuni.2014.06.010.Tumor-associated.
346. Lizotte PH, Robert EJ, Keogh L, et al. Fine needle aspirate flow cytometric phenotyping characterizes immunosuppressive nature of the mesothelioma microenvironment. *Sci Rep.* 2016 Aug 19;6:31745. doi: 10.1038/srep31745.
347. Schelker M, Feau S, Du J, et al. Estimation of immune cell content in tumour tissue using single-cell RNA-seq data.. *Nat Commun.*:1-12. doi:10.1038/s41467-017-02289-3.
348. Newman AM, Liu CL, Green MR, et al. Robust enumeration of cell subsets from tissue expression profiles. *Nat Methods.* 2015 May;12(5):453-7. doi: 10.1038/nmeth.3337.

349. Remon J, Reguart N, Corral J, Lianes P. Malignant pleural mesothelioma: New hope in the horizon with novel therapeutic strategies. *Cancer Treat Rev.* 2015;41(1):27-34. doi:10.1016/j.ctrv.2014.10.007.
350. Dong L, Jensen R V, De Rienzo A, et al. Differentially expressed alternatively spliced genes in malignant pleural mesothelioma identified using massively parallel transcriptome sequencing. *BMC Med Genet.* 2009;10:149. doi:10.1186/1471-2350-10-149.
351. Bott M, Brevet M, Taylor BS, et al. The nuclear deubiquitinase BAP1 is commonly inactivated by somatic mutations and 3p21.1 losses in malignant pleural mesothelioma. *Nat Genet.* 2011;43(7):668-672. doi:10.1038/ng.855.
352. Cheng JQ, Jhanwar S, Klein W, et al. p16 Alterations and Deletion Mapping of 9p21 - p22 in Malignant Mesothelioma'. *Cancer Res.* 1994 Nov 1;54(21):5547-5551.
353. Alexandrov LB, Nik-Zainal S, Wedge DC, Campbell PJ, Stratton MR. Deciphering Signatures of Mutational Processes Operative in Human Cancer. *Cell Rep.* 2013;3(1):246-259. doi:10.1016/j.celrep.2012.12.008.
354. Xu J, Kadariya Y, Cheung M, et al. Germline mutation of Bap1 accelerates development of asbestos-induced malignant mesothelioma. *Cancer Res.* 2014;74(16):4388-97. doi:10.1158/0008-5472.CAN-14-1328.
355. Lindholm PM, Salmenkivi K, Vauhkonen H, et al. Gene copy number analysis in malignant pleural mesothelioma using oligonucleotide array CGH. *Cytogenet Genome Res.* 2007;119(1-2):46-52. doi:10.1159/000109618.
356. Taniguchi T, Karnan S, Fukui T, et al. Genomic profiling of malignant pleural mesothelioma with array-based comparative genomic hybridization shows frequent non-random chromosomal alteration regions including JUN amplification on 1p32. *Cancer Sci.* 2007;98(3):438-446. doi:10.1111/j.1349-7006.2006.00386.x.
357. Neragi-Miandoab S, Sugarbaker DJ. Chromosomal deletion in patients with malignant pleural mesothelioma. *Interact Cardiovasc Thorac Surg.* 2009;9(1):42-4. doi:10.1510/icvts.2008.201509.
358. Lalonde E, Ishkanian AS, Sykes J, et al. Tumour genomic and microenvironmental heterogeneity for integrated prediction of 5-year biochemical recurrence of prostate cancer: A retrospective cohort study. *Lancet Oncol.* 2014;15(13):1521-1532. doi:10.1016/S1473-2045(14)71021-6.
359. Kivipensas P, Björkqvist AM, Karhu R, et al. Gains and losses of DNA sequences in malignant mesothelioma by comparative genomic hybridization. *Cancer Genet Cytogenet.* 1996;89(1):7-13.
360. Björkqvist a M, Tammilehto L, Anttila S, Mattson K, Knuutila S. Recurrent DNA copy number changes in 1q, 4q, 6q, 9p, 13q, 14q and 22q detected by comparative genomic hybridization in malignant mesothelioma. *Br J Cancer.* 1997;75(4):523-7.

361. Balsara BR, Bell DW, Sonoda G, et al. Comparative Genomic Hybridization and Loss of Heterozygosity Analyses Identify a Common Region of Deletion at 15q11 . 1 – 15 in Human Malignant Mesothelioma. *Cancer Res.* 1999;59(2):450-454.
362. Krismann M, Müller KM, Jaworska M, Johnen G. Severe chromosomal aberrations in pleural mesotheliomas with unusual mesodermal features. Comparative genomic hybridization evidence for a mesothelioma subgroup. *J Mol Diagn.* 2000;2(4):209-16. doi:10.1016/S1525-1578(10)60639-3.
363. Ascoli V, Aalto Y, Carnovale-Scalzo C, Nardi F, Falzetti D, Mecucci C KS. DNA copy number changes in familial malignant mesothelioma. *Cancer Genet Cytogenet.* 2001;127(1):80-2.
364. Krismann M, Müller KM, Jaworska M, Johnen G. Molecular cytogenetic differences between histological subtypes of malignant mesotheliomas: DNA cytometry and comparative genomic hybridization of 90 cases. *J Pathol.* 2002;197(3):363-371. doi:10.1002/path.1128.
365. Serio G, Scattone A, Gentile M, et al. Familial pleural mesothelioma with environmental asbestos exposure: Losses of DNA sequences by comparative genomic hybridization (CGH) [2]. *Histopathology.* 2004;45(6):643-645. doi:10.1111/j.1365-2559.2004.01941.x.
366. Scattone A, Pennella A, Gentile M, et al. Comparative genomic hybridisation in malignant deciduoid mesothelioma. *J Clin Pathol.* 2006 Jul;59(7):764-9. doi:10.1136/jcp.2005.026435.
367. Haraksingh RR, Abyzov A, Gerstein M, Urban AE, Snyder M. Genome-Wide Mapping of Copy Number Variation in Humans : Comparative Analysis of High Resolution Array Platforms. *PLoS One.* 2011;6(11). doi:10.1371/journal.pone.0027859.
368. Forozan F, Karhu R, Kononen J, Kallioniemi A KO. Genome screening by comparative genomic hybridization. *Trends Genet.* 1997;13(10):405-9.
369. Craig JM, Vena N, Ramkissoon S, et al. DNA fragmentation simulation method (FSM) and fragment size matching improve aCGH performance of FFPE tissues. *PLoS One.* 2012;7(6). doi:10.1371/journal.pone.0038881.
370. Van Beers EH, Joosse S a, Ligtenberg MJ, et al. A multiplex PCR predictor for aCGH success of FFPE samples. *Br J Cancer.* 2006;94:333-337. doi:10.1038/sj.bjc.6602889.
371. Miething F, Hering S, Hanschke B, Dressler J. Effect of fixation to the degradation of nuclear and mitochondrial DNA in different tissues. *J Histochem Cytochem.* 2006;54(3):371-4. doi:10.1369/jhc.5B6726.2005.
372. Foster JM, Oumie A, Togneri FS, et al. Cross-laboratory validation of the OncoScan® FFPE Assay, a multiplex tool for whole genome tumour profiling. *BMC Med Genomics.* 2015;8(1):5. doi:10.1186/s12920-015-0079-z.
373. Wang Y, Cottman M, Schiffman JD. Molecular inversion probes: a novel microarray technology and its application in cancer research. *Cancer Genet.* 2012;205(7-8):341-55. doi:10.1016/j.cancergen.2012.06.005.
374. Albert TJ, Molla MN, Muzny DM, et al. Direct selection of human genomic loci by microarray hybridization. *Nat Methods.* 2007;4(11):903-905. doi:10.1038/nmeth1111.

375. Curtis C, Shah SP, Chin S-F, et al. Europe PMC Funders Group The genomic and transcriptomic architecture of 2,000 breast tumours reveals novel subgroups. *Nature*. 2012;486(7403):346-352. doi:10.1038/nature10983.
376. Verhaak RGW, Hoadley K a., Purdom E, et al. Integrated Genomic Analysis Identifies Clinically Relevant Subtypes of Glioblastoma Characterized by Abnormalities in PDGFRA, IDH1, EGFR, and NF1. *Cancer Cell*. 2010;17(1):98-110. doi:10.1016/j.ccr.2009.12.020.
377. Lalonde E, Alkallas R, Chua ML, et al. Translating a Prognostic DNA Genomic Classifier into the Clinic: Retrospective Validation in 563 Localized Prostate Tumors. *Eur Urol*. 2016;16:S0302-2838(16)30716-3. doi:10.1016/j.eururo.2016.10.013.
378. Fraser M, Sabelnykova VY, Yamaguchi TN, et al. Genomic hallmarks of localized, non-indolent prostate cancer. *Nature*. 2017;541(7637):359-364. doi:10.1038/nature20788.
379. Hieronymus H, Schultz N, Gopalan A, et al. Copy number alteration burden predicts prostate cancer relapse. *Proc Natl Acad Sci U S A*. 2014;111(30):11139-44. doi:10.1073/pnas.1411446111.
380. Hastings P, Lupski JR, Rosenberg SM, Ira G. Mechanisms of change in gene copy number. *Nat Rev Genet*. 2009;10(8):551-564. doi:10.1038/nrg2593.
381. Turajlic S, Litchfield K, Xu H, et al. Articles and the immunogenic phenotype : a pan-cancer analysis. *Lancet Oncol*. 18(8):1009-1021. doi:10.1016/S1470-2045(17)30516-8.
382. Murali R, Wiesner T, Scolyer R a. Tumours associated with BAP1 mutations. *Pathology*. 2013;45(2):116-26. doi:10.1097/PAT.0b013e32835d0efb.
383. Nasu M, Emi M, Pastorino S, et al. High Incidence of Somatic BAP1 Alterations in Sporadic Malignant Mesothelioma. *J Thorac Oncol*. 2015;10(4):565-76. doi:10.1097/JTO.0000000000000471.
384. Yoshikawa Y, Sato A, Tsujimura T, et al. Frequent inactivation of the BAP1 gene in epithelioid-type malignant mesothelioma. *Cancer Sci*. 2012;103(5):868-874. doi:10.1111/j.1349-7006.2012.02223.x.
385. Carbone M, Yang H, Pass HI, Krausz T, Testa JR, Gaudino G. BAP1 and cancer. *Nat Rev Cancer*. 2013;13(3):153-9. doi:10.1038/nrc3459.
386. Tigan A-S, Bellutti F, Kollmann K, Tebb G, Sexl V. CDK6-a review of the past and a glimpse into the future: from cell-cycle control to transcriptional regulation. *Oncogene*. 2015;35(July):1-9. doi:10.1038/onc.2015.407.
387. Lim S, Kaldis P. Cdks, cyclins and CKIs: roles beyond cell cycle regulation. *Development*. 2013;140(15):3079-93. doi:10.1242/dev.091744.
388. Chilosi M, Doglioni C, Yan Z, et al. Differential expression of cyclin-dependent kinase 6 in cortical thymocytes and T-cell lymphoblastic lymphoma/leukemia. *Am J Pathol*. 1998;152(1):209-17.

389. Nagel S, Leich E, Quentmeier H, et al. Amplification at 7q22 targets cyclin-dependent kinase 6 in T-cell lymphoma. *Leukemia*. 2008 Feb;22(2):387-92.
390. Wiedemeyer WR, Dunn IF, Quayle SN, et al. Pattern of retinoblastoma pathway inactivation dictates response to CDK4/6 inhibition in GBM. *Proc Natl Acad Sci U S A*. 2010;107(25):11501-11506. doi:10.1073/pnas.1001613107.
391. Waddell N, Pajic M, Patch A, et al. Whole genomes redefine the mutational landscape of pancreatic cancer. *Nature*. 2015;518(7540):495-501. doi:10.1038/nature14169.
392. Sherr CJ, Beach D, Shapiro GI. Targeting CDK4 and CDK6: From discovery to therapy. *Cancer Discov*. 2016;6(4):353-367. doi:10.1158/2159-8290.CD-15-0894.
393. Ishii M, Nakazawa K, Wada H, et al. Methylthioadenosine phosphorylase gene is silenced by promoter hypermethylation in human lymphoma cell line DHL-9: another mechanism of enzyme deficiency. *Intern J Oncol*. 2005;26(4):985-91.
394. Cerami E, Gao J, Dogrusoz U, et al. The cBio Cancer Genomics Portal: An open platform for exploring multidimensional cancer genomics data. *Cancer Discov*. 2012;2(5):401-404. doi:10.1158/2159-8290.CD-12-0095.
395. Illei PB, Rusch VW, Zakowski MF, Ladanyi M. Homozygous deletion of CDKN2A and codeletion of the methylthioadenosine phosphorylase gene in the majority of pleural mesotheliomas. *Clin Cancer Res*. 2003;9(6):2108-2113.
396. Huang HY, Li SH, Yu SC, et al. Homozygous deletion of MTAP gene as a poor prognosticator in gastrointestinal stromal tumors. *Clin Cancer Res*. 2009;15(22):6963-6972. doi:10.1158/1078-0432.CCR-09-1511.
397. Kim J, Kim MA, Min SY, Jee CD, Lee HE KW. Downregulation of methylthioadenosin phosphorylase by homozygous deletion in gastric carcinoma. *Genes Chromosom Cancer*. 2011;50(6):421-33. doi:10.1002/gcc.20867.
398. Chen ZH, Olopade OI, Savarese TM. Expression of methylthioadenosine phosphorylase cDNA in p16-, MTAP- malignant cells: restoration of methylthioadenosine phosphorylase-dependent salvage pathways and alterations of sensitivity to inhibitors of purine de novo synthesis. *Mol Pharmacol*. 1997;52:903-911.
399. Bertino JR, Waud WR, Parker WB, Lubin M. Targeting tumors that lack methylthioadenosine phosphorylase (MTAP) activity: Current strategies. *Cancer Biol Ther*. 2011;11(7):627-632. doi:10.4161/cbt.11.7.14948.
400. Munshi PN, Lubin M, Bertino JR. 6-Thioguanine: a Drug With Unrealized Potential for Cancer Therapy. *Oncologist*. 2014;19(7):760-765. doi:10.1634/theoncologist.2014-0178.
401. Kikkawa T, Obayashi T, Takahashi M, Fukuzaki-Dohi U, Numayama-Tsuruta K, Osumi N. Dmrta1 regulates proneural gene expression downstream of Pax6 in the mammalian telencephalon. *Genes to Cells*. 2013;18(8):636-649. doi:10.1111/gtc.12061.

402. Nickerson ML, Witte N, Im KM, et al. Molecular analysis of urothelial cancer cell lines for modeling tumor biology and drug response. *Oncogene*. 2016;(November 2015):1-12. doi:10.1038/onc.2016.172.
403. Bidinotto LT, Torrieri R, Mackay A, et al. Copy Number Profiling of Brazilian Astrocytomas. *G3 (Bethesda)*. 2016;6(7):1867-1878. doi:10.1534/g3.116.029884.
404. Coleman EA, Lee JY, Erickson SW, et al. GWAS of 972 autologous stem cell recipients with multiple myeloma identifies 11 genetic variants associated with chemotherapy-induced oral mucositis. *Support Care Cancer*. 2014;23(3):841-849. doi:10.1007/s00520-014-2406-x.
405. Wu D, Hiroshima K, Yusa T, et al. Usefulness of p16/CDKN2A fluorescence in situ hybridization and BAP1 immunohistochemistry for the diagnosis of biphasic mesothelioma. *Ann Diagn Pathol*. 2017;26:31-37. doi:10.1016/j.anndiagnpath.2016.10.010.
406. Arzt L, Quehenberger F, Halbwedl I, Mairinger T, Popper HH. BAP1 protein is a progression factor in malignant pleural mesothelioma. *Pathol Oncol Res*. 2014;20(1):145-151. doi:10.1007/s12253-013-9677-2.
407. Meerang M, Bérard K, Friess M, et al. Low Merlin expression and high Survivin labeling index are indicators for poor prognosis in patients with malignant pleural mesothelioma. *Mol Oncol*. 2016;10(8):1255-1265. doi:10.1016/j.molonc.2016.06.005.
408. Tadesse S, Yu M, Kumarasiri M, Le BT, Wang S. Targeting CDK6 in cancer: State of the art and new insights. *Cell Cycle*. 2015;14(20):3220-3230. doi:10.1080/15384101.2015.1084445.
409. Kindler HL, Burris HA, Sandler AB, Oliff IA. A phase II multicenter study of L-alanosine, a potent inhibitor of adenine biosynthesis, in patients with MTAP-deficient cancer. *Invest New Drugs*. 2009;27(1):75-81. doi:10.1007/s10637-008-9160-1.
410. Marjon K, Cameron MJ, Quang P, et al. MTAP Deletions in Cancer Create Vulnerability to Targeting of the MAT2A/PRMT5/RIOK1 Axis. *Cell Rep*. 2016;15(3):574-587. doi:10.1016/j.celrep.2016.03.043.
411. Righi L, Duregon E, Vatrano S, et al. BRCA1-Associated protein 1 (BAP1) immunohistochemical expression as a diagnostic tool in malignant pleural mesothelioma classification: A large retrospective study. *J Thorac Oncol*. 2016;11(11):2006-2017. doi:10.1016/j.jtho.2016.06.020.
412. Churg A, Sheffield BS, Galateau-Salle F. New markers for separating benign from malignant mesothelial proliferations: Are we there yet? *Arch Pathol Lab Med*. 2016;140(4):318-321. doi:10.5858/arpa.2015-0240-SA.
413. Walts AE, Hiroshima K, McGregor SM, et al. BAP1 Immunostain and CDKN2A (p16) FISH Analysis: Clinical Applicability for the Diagnosis of Malignant Mesothelioma in Effusions. *Diagn Cytopathol*. 2016;44(7):599-606. doi: 10.1002/dc.23491.
414. Nabeshima K, Matsumoto S, Hamasaki M, et al. Use of p16 FISH for differential diagnosis of mesothelioma in smear preparations. *Diagn Cytopathol*. 2016;44(9):774-80. doi:10.1002/dc.23501.

415. Altomare DA, Menges CW, Xu J, et al. Losses of both products of the Cdkn2a/Arf locus contribute to asbestos-induced mesothelioma development and cooperate to accelerate tumorigenesis. *PLoS One*. 2011;6(4):e18828. doi:10.1371/journal.pone.0018828.
416. Frizelle SP, Rubins JB, Zhou JX, Curiel DT, Kratzke R a. Gene therapy of established mesothelioma xenografts with recombinant p16INK4a adenovirus. *Cancer Gene Ther*. 2000;7(11):1421-1425. doi:10.1038/sj.cgt.7700241.
417. Yang CT, You L, Yeh CC, Chang JW, Zhang F, McCormick F JD. Adenovirus-mediated p14(ARF) gene transfer in human mesothelioma cells. *J Natl Cancer Inst*. 2000;1(19):636-41.
418. Sekido Y, Pass HI, Bader S, et al. Neurofibromatosis Type 2 (NF2) Gene Is Somatic Mutated in Mesothelioma but not in Lung Cancer. *Cancer Res*. 1995;2(22):1227-1231.
419. Altomare DA, You H, Xiao G-H, et al. Human and mouse mesotheliomas exhibit elevated AKT/PKB activity, which can be targeted pharmacologically to inhibit tumor cell growth. *Oncogene*. 2005;24(40):6080-9. doi:10.1038/sj.onc.1208744.
420. Testa JR, Cheung M, Pei J, et al. Germline BAP1 mutations predispose to malignant mesothelioma. *Nat Genet*. 2011 Aug 28;43(10):1022-5. doi: 10.1038/ng.912.
421. Yoshikawa Y, Sato A, Tsujimura T, et al. Biallelic germline and somatic mutations in malignant mesothelioma: Multiple mutations in transcription regulators including mSWI/SNF genes. *Int J Cancer*. 2014:1-12. doi:10.1002/ijc.29015.
422. Young RJ, Waldeck K, Martin C, et al. Loss of CDKN2A expression is a frequent event in primary invasive melanoma and correlates with sensitivity to the CDK4/6 inhibitor PD0332991 in melanoma cell lines. *Pigment Cell Melanoma Res*. 2014;27(4):590-600. doi:10.1111/pcmr.12228.
423. Yang C, Li Z, Bhatt T, et al. Acquired CDK6 amplification promotes breast cancer resistance to CDK4/6 inhibitors and loss of ER signaling and dependence. *Oncogene*. 2016;(August):1-10. doi:10.1038/onc.2016.379
424. Geiersbach KB, Willmore-Payne C, Pasi A V, et al. Genomic Copy Number Analysis of HER2-Equivocal Breast Cancers. *Am J Clin Pathol July*. 2016;0:1-9. doi:10.1093/AJCP/AQW130.
425. Gray PN, Vuong H, Tsai P, et al. TumorNext: A comprehensive tumor profiling assay that incorporates high resolution copy number analysis and germline status to improve testing accuracy. *Oncotarget*. 2016;7(42). doi:10.18632/oncotarget.11910.
426. Casorzo L, Corigliano M, Ferrero P, Venesio T, Risio M. Evaluation of 7q31 region improves the accuracy of EGFR FISH assay in non small cell lung cancer. *Diagn Pathol*. 2009;4:36. doi:10.1186/1746-1596-4-36.
427. Maggioni C, Barletta G, Rijavec E, Biello F, Gualco E, Grossi F. Advances in treatment of mesothelioma. *Expert Opin Pharmacother*. 2016;6566(May):1-9. doi:10.1080/14656566.2016.1176145.



Minerva Access is the Institutional Repository of The University of Melbourne

Author/s:

Thapa, Bibhusal

Title:

Tumour immune microenvironment, genomewide copy number aberrations and their interactions in malignant pleural mesothelioma

Date:

2017

Persistent Link:

<http://hdl.handle.net/11343/208836>

File Description:

thesis

Terms and Conditions:

Terms and Conditions: Copyright in works deposited in Minerva Access is retained by the copyright owner. The work may not be altered without permission from the copyright owner. Readers may only download, print and save electronic copies of whole works for their own personal non-commercial use. Any use that exceeds these limits requires permission from the copyright owner. Attribution is essential when quoting or paraphrasing from these works.